SLSTR: Algorithm Theoretical Basis Definition Document for Level 1 Observables

Prepared by:	**Caroline Cox**	Date Caroline Cox Digitally signed by Caroline Cox DN: cn=Caroline Cox, o, ou, email=caroline.cox@stfc.ac.uk, c=GB Date: 2017.07.24 11:59:52 +01'00'
Checked By:	**Dave Smith**	Date Dave Smith 2017.07.24 12:16:24 +01'00'
Project Manager:	**Brian Maddison**	Date
PA Approval:	**Peter Hiscock**	Date Digitally signed by Eric Clark Date: 2017.07.24 13:00:54 +01'00'

Distribution List

RAL	C. Cox T.J. Nightingale
	C.T. Mutlow D. Dawson B.J. Maddison
Thales Alenia	D. Lebedeff J. L. Palmade
ESA	J. Nieke H. Rehban
ACRI	L. Bourg

Change Record

Issue	Date	Changes
Draft A	13/10/06	Original Version (Outline only)
1.0	20/12/06	New Revision
1.1	05/03/08	Overview revised
1.2	18/06/08	Revised draft: Section 2.4.5 outlining the theory of the geolocation added.
		Geolocation equations revised to respect SLSTR scan geometry in Section 3.2.
		Additional material added to cloud clearing sections. Page and equation
		Numbering revised; various minor corrections
1.3	17/07/08	Revised; Sections on regridding, cosmetic fill and conversion to radiance
		added. Various minor corrections.
1.4	16/12/08	1.6 micron cloud test added. Placeholders added for tests based on the new
		1.375 and 2.25 micron SLSTR channels.
1.5	13/03/09	Various comments on v1.4 incorporated Document format changed to reflect common project style Sections renumbered Equations Renumbered L0 Processing Section included in section 5.1 Scope of TDI processing described in section 5.3.3.10 Conversion from reflectance to radiance added 5.5.3.8
1.6	12/06/09	Housekeeping packet unpacking added. Infrared calibration updated.
		Infrared histogram cloud test details added and new 1.375 micron cloud test defined.
1.7	15/12/09	TDI Section removed since this is not performed at L1. Instead simple average of a and b pixels will be performed. Stage 18 of L1b processing updated accordingly. (Section 5.2.2) Updated reference RD-2, RD-3 and RD-13 (Section 2.2) Acronym List Updated (Section 3.2) Expanded description of L1b geolocation (Section 4.4.4) Scan jitter test updated for SLSTR (Section 5.4.3.1.7.2) BBEU and TAEO conversion algorithms updated although these are still pending information from the supplier. (Section 5.4.3.1.7) Description of science data (L0) processing (Section 5.4.3.2) Surface classification added (Section 5.5.3.6) Various Claifications and Typographical Corrections (All) Breakpoint Table Added (Appendix A)

1.8	08-July-2010	Update in response to numerous comments from ACRI, TAS-F and ESA. Consistent terms in calibration equations. Offset and slope used for calibration equations. Other edits made to calibration section Added sub-sections on Meteo annotation fields to the relevant sections (5.5..5 L1b processing, 5.5.2 processing objective and 5.5.3 mathematical description) based on OLCI descriptions. Scene classification reverted to simple 'centre of pixel' scheme. Solar channel calibration clarifications added Nomenclature of conversion from reflectance to radiance modified for consistency with previous sections. Purge of AATSR processing internal variables. Exception values defined explicitly. Figure numbers in section 4 corrected Reordering of Anciliary conversion functions to be compliant with SY-4
1.9	13/07/2010	Section 5.4.3.1.6 - Additional ancilliary conversion function 'f20: Look-Up Table' inserted on request from TAS-F.
2.0	14/01/2011	Changes implemented from S3-MO-RAL-SL-2010-01 - Issue 9 - Change Sheet for SLSTR ATBD.
2.1	14/06/2011	Changes implemented following satellite CDR from S3-MO-RAL-SL-2011-01 - Issue 3 - Change Sheet for SLSTR ATBD.
3.0	29/03/2012	Updates in response to change requests S3-CR-TAF-SC-00381 and S3-CR-TAF-SC-00382 Addition of processing switch to select or disable TDI processing Modification to geolocation processing to address problems with missing solar and view geometry in image borders. This is to reduce the processing time for ortho-geolocation and for using cosmetic filling to provide these border values. The revised geolocation algorithm follows the AATSR method of geolocating tie-point pixels to the geoid and bilinear interpolation for the intermediate pixels. Ortho-geolocation is still performed for each instrument pixel using the scan position telemetry. Specific BB and TAEO conversion algorithms removed since these are now using

		LUTs for the conversion from DN to Temperature. Following update of IMDD issue 3 and additional processing step has been included to ensure that detectors are in the correct position relative to the direction cosines provided in the geometry characterisation ADF. Processing step for detector nonlinearity correction added Section added to provide method to derive all variables to be written in the Summary Quality ADS Processing step added to provide a calibration correction for drift and bias derived from vicarious calibration results. Clarification added to ensure solar channel offsets are computed for full orbit as for TIR channels. Platform mode replicated for each scan Algorithm for identification of "Duplicate", "Day" and "Twilight" pixels needs added TBD, TBCs and assumptions removed. Clarification that vis offsets and dark noise is computed for full orbit as a scan indexed variable. Clarification that the surface classification is performed on the instrument grid. Clarification that when both hot and cold BBs are the same, the exception flag 'no_parameters' must be set, and that the data for that calibration interval remain un-calibrated
3.1	19/08/2013	Number of PIX10SYNC periods per scan cycle normalised to 3670 throughout document Corrections to ancillary ISP fields (page 98) Note added to clarifiy that ATBD applies to a fixed configuration concerning pixel timing (page 98) Corrected definition of scan value (page 105/106) Updated VIS gain settings (page 111) Clarifications added to non-linearity correction algorithm (page 112)

		Typo correction for SLSTR channel (page 114, 118) Correction to definition of scan window for consistency with SY-4 (page 120) Clarification added that BB radiance for VIS-SWIR channels = 0 (page 124) Clarification on the use of the photodiode monitor (page 125) Algorithm for identification of "Day", “Night” and "Twilight" pixels (page 149) Time offset adjustment for B stripe pixels removed since this is no longer required. (page 92) Swath widths of the along and across track stated on p19 are corrected so they are consistent with the rest of this document and the product definition document. Scan angle correction in equation 5.3-56 (page 80) Corrected scan angles added to account for the scan encoder positions giving the scan angle at the start of the pixel integration time and needing to be adjusted to account for the pixel centres. (page 96)
3.2		Modified BB temperature averaging algorithm to produce weighted average temperature Clarifications on interpolation of parameters computed on the tie-point grid TDI_Processing – configurable parameter added ‘TDI_Direction’ to account for the orientation of the SWIR detectors wrt. Ground track and scan direction.
4.0	31/03/2015	Document number changed to Issue 4.0 to coincide with V3 of O-GPP
5.0	19/02/2016	Update section 5.4.3.2.1.2: NL offset correction depends on t and k. To coincide with O-GPP V4.
6.0	09/06/2016	Update for Sentinel-3A In-Orbit-Commissioning-Review Section on stray light correction added with reference to stray-light ATBD
7.0	24/07/2017	Update for alignment with O-IPFP v3.3 -inclusion of pixel positional offset for VIS chanels -alignment of cloud algorithms (1.6 histogram test and 11um SCT) and statement regarding summary_cloud -inclusion of absolute function in noise calculations

		Updates to line of sight model to account for geometry of the PFMr instrument. Updates to relevant references.

Contents

1 INTRODUCTION

1.1 OVERVIEW

The main scope of the S3 mission is to serve research relating to the marine environment, with the main objective being to determine such parameters as sea surface topography, sea and land surface temperature and ocean colour. However, the mission will also support various land, atmospheric and cryospheric applications. The first S3 satellite is expected to launch in 2013, followed by a second launch in order to provide maximum coverage.

The Sea and Land Surface Temperature Radiometer (SLSTR) forms part of the S3 payload and is an infrared and visible radiometer for ocean and land monitoring. The instrument is described in more detail in section 4.2.1.

1.2 DOCUMENT CONTEXT AND SCOPE

This Algorithm Theoretical Basis document (ATBD) describes the algorithms used to produce the SLSTR Level 1 Radiometric Product and accompanying geo-location and environment data. In particular the document is concerned with the algorithms to be implemented in the SLSTR O-GPP.

2 DOCUMENTS

2.1 APPLICABLE DOCUMENTS

AD-1	Deleted reference – no longer applicable		
AD-2	Deleted reference – no longer applicable		
AD-3	GMES Sentinel-3 System Requirements Document	S3-RS-ESA-SY-0010	Issue 4.0, 13-Nov-09
AD-4	Earth Explorer Mission Software. EXPLORER_POINTING Software User Manual	EE-MA-DMS-GS-0005	Issue 4.1, 07-May-10

2.2 REFERENCE DOCUMENTS

RD-1	Contributions to Ground Segment Service Segment Requirements	SENS3-RAL-TN-31	24-Aug-2006
RD-2	SLSTR Design Description	IN-2 S3-RP-GA-SL-00008	07-Nov-2008
RD-3	SLSTR L1 Products Calibration and Validation Plan	S3-PL-RAL-SL-008	18-Jul-2008
RD-4	Sentinel-3 S3 Geometrical Performance Budgets Part 1 : General rules and contributors	SY-6 c, Issue 1, S3-TN-TAF-SY-01874	20-Dec-2010
RD-5	SLSTR: Science data Software Interface Requirement Document	S3-IS-GA-SL-00003	11-Nov-2008
RD-6	SLSTR Instrument Measurement Data Definition Document	S3-RP-GA-SL-00019 Issue 8	14-Nov-2016
RD-7	Zavody, A.M., Mutlow, C.T., and Llewellyn-Jones, D.T. Cloud Clearing over the Ocean in the Processing of Data from the Along-Track Scanning Radiometer (ATSR). J. Atmos. Oceanic Technol., 17, 595 – 615, 2000.		
RD-8	Space Packet Protocol	CCSDS 133.0-B-1	
RD-9	Deleted reference – no longer applicable		
RD-10	GPP Perimeter and Mission Products Format	S3-MO-TAF-00424/2008	
RD-11	SLSTR L1 Products Definition	S3-RS-RAL-SY-003	Issue 10, 12-Jul-

			2017
RD-12	Discriminating clear-sky from cloud with MODIS:Algorithm Theoretical Basis Document (MOD35)	MODIS Cloud Mask Team (Ackerman, s. et al)	Oct-2006
RD-13	Geodesy (4th Edition)	G. Bomford	Clarendon Press, Oxford
RD-14	NAVATT Packets Definition	S3-ID-TAF-SC-01890, Issue 1	07-Jan-2011
RD-15	ATBD for SLSTR Stray Light Correction	S3-TN-RAL-SL-104 Issue 1.0	19-Feb-2016

3 TERMS, DEFINITIONS AND ABBREVIATIONS

3.1 TERMS AND DEFINITIONS

Accuracy is defined as the difference between a result obtained and the 'true' value.

Channel- Spectral channel (S1-S9 + F1-F2)

Chain - Analogue channel of the signal processing chain

Detector - Pixel array at band N

Calibration is the process of quantitatively defining the system response to known, controlled system inputs.

Field-Of-View - is the angular extent of a given scene that is viewed by the instrument.

Infrared (IR) radiation is electromagnetic radiation of wavelengths between about 750nm and 1mm. This is broken down into 5 wavelength regions

Near-IR - 0.75-1.4 µm

Short-Wave IR - 1.4-3 µm

Medium-Wave IR - 3-8 µm

Long-Wave IR - 8–15 µm

Image swath - Maximum distance on ground between the positions of two spatial samples belonging to the same row.

Image sample - image element containing radiance measurements of co-registered pixels for all bands

Pixel - Detector single element, considering also fire elements (s7), blind and TDI ones
Detector 5 has 4x2 pixels (S5) + 2 reference pixels (blind) ,
Detector 7 has 2x1 pixels (S7) + 1 reference blind + 4x1 fire pixels (F1)

Precision is defined as the difference between one result and the mean of several results obtained by the same method, i.e. reproducibility (includes random errors only).

Traceability is the property of the result of a measurement or the value of a standard whereby it can be related to stated references, usually national or international standards, through an unbroken chain of comparisons all having stated uncertainties.

Visible light is electromagnetic radiation detectable by the human eye with a wavelength between approximately 400nm and 700nm.

Validation is the process of assessing by independent means the quality of the data products derived from the system outputs.

3.2 GLOSSARY OF ACRONYMS

(A)ATSR	(Advanced) Along Track Scanning Radiometer
ADC	Analog to Digital Converter
ADS	Annotation Data Set
AST	Averaged Surface Temperature (AATSR product)
ATSR-2	Along Track Scanning Radiometer-2
ATBD	Algorithm Theoretical Basis Document
BB	Black Body
BBEU	Black Body Electronics Unit
CCSPS	Consultative Committee for Space Data Systems
CFI	Customer Furnished Item
CPE	Control and Processor Electronics (component of the SLSTR)
DDT	Data Dictionary Tool
Defra	UK Department for Environment, Food and Rural Affairs
DEM	Digital Elevation Model
DPM	Detailed Processing Model
DS	Data Set
DSD	Data Set Descriptor
DSR	Data Set Record
ESA	European Space Agency
ESL	Expert Support Laboratory
FAT	Factory Acceptance Test
FEE	Front End Electronics (component of the SLSTR)
FEP	Front End Processor
FPA	Focal Plane Assembly
FOS	Flight Operations Segment
GBTR	Gridded Brightness Temperature / Reflectance (AATSR product)
GMES	Global Monitoring for Environment and Security
GST	Gridded Surface Temperature (AATSR product)
IFOV	Instantaneous Field of View
IODD	Input-Output Data Definition
IPF	Instrument Processing Facility
ISO	International Organisation for Standardisation
ISP	Instrument Source Packets
L1b	Level 1b
L2	Level 2
LBR	Low Bit Rate
LST	Land Surface Temperature
LUT	Look Up Table
LWIR	Long Wave InfraRed
MDS	Measurement Data Set
MDSR	Measurement Data Set Record
MERIS	MEdium Resolution Imaging Spectrometer
MPH	Main Product Header
MTF	Modulation Transfer Function
MUX	Mulitiplexor
MWIR	Medium Wave InfraRed
NRT	Near Real Time
OP	Operational Processor
O-GPP	Optical Ground Prototype Processor
OLCI	Ocean and Land Colour Instrument
PADD	Product Algorithm Detailed Documentation
PCAT	?
PCD	Product Confidence Data

PDS	Payload Data Segment
PP	Prototype Processor
PUS	Packet Utilisation Standard
QC	Quality Control
QWG	Quality Working Group
RFQ	Request for Quotation
RT	Radiative Transfer
SAFE	Standard Archive Format for Europe
SLSTR	Sea and Land Surface Temperature Radiometer
SOW	Statement of Work
SPH	Specific Product Header
SPS	System Performance Simulator
SST	Sea Surface Temperature
SUM	Software User Manual
SWIR	Short Wave InfraRed
TAEO	Temperature Acquisition Electronics Unit
TBC	To be confirmed
TD&P	Test Definition and Procedures
TDI	Time Domain Integration
TDS	Test Data Set[s]
USF	User Service Facility
WP	Work package
XML	eXtensible Markup Language

4 OVERVIEW AND BACKGROUND INFORMATION

4.1 OBJECTIVES OF SLSTR LEVEL 0 AND LEVEL 1 PROCESSING

4.1.1 Level 0 Processing

The SLSTR Level 0 product will consist of a SAFE container structure containing NAVATT and SLSTR data sets from the satellite telemetry, these data sets comprising Header, Annotation, and Data files. In particular the SLSTR data files will be binary files containing SLSTR Instrument Source Packets. The input to the Operational Processor will consist of the Level 0 product from the FEP. In the context of the OP, therefore, Level 0 processing will consist of unpacking the ISP and annotation data into suitable data structures from which it is available for onward processing.

It is not intended that the Optical SPS shall include any emulation of the FEP. Instead the O-GPP will receive simulated ISP and NAVATT packets from the SPS, stored in separate files. The principal objective of the O-GPP is to support the validation of the Operational Processor, and so in the case of the GPP Level 0 processing will be required to read the binary ISP files, unpack them in to the data structure as above, and assemble them into the Header, Annotation, and Data files of the Level 0 product proper for output.. At the same time, in order to allow two-way transport between the OP and GPP, the functionality to input and unpack the data as in the previous paragraph will be required.

It has been agreed that for transport between the O-GPP and the OP, it will not be a requirement that the component level 0 files will be included in the SAFE container (which is primarily required for archiving purposes).

4.1.2 Level 1 Processing

The objective of Level 1 processing is to derive, starting from the time-ordered and consolidated instrument source packets, a data product containing calibrated, geolocated brightness temperatures, for the thermal channels, and radiances for the short wave and visible channels, together with appropriate annotation data. These form the starting point of the Level 2 algorithms for retrieval of geophysical parameters such as SST.

4.2 INSTRUMENT OVERVIEW

4.2.1 The SLSTR instrument

A principal aim of the Sentinel SLSTR instrument mission is to maintain continuity with the (A)ATSR series of instruments, and the proposed design supports this by incorporating the basic functionality of AATSR, with the addition of some new, more advanced, features. These include a wider swath, new channels, and higher spatial resolution in some channels.

The proposed instrument will include the set of channels used by ATSR-2 and AATSR, thus ensuring continuity of data, together with two new channels at wavelengths of 2.25 and 1.375 microns in support of cloud clearing for SST retrieval. In total the instrument will have eleven channels as follows:

- 3 thermal infra-red channels at 3.7, 10.8 and 12 micron wavelengths;
- 2 fire channels at 3.7, and 10.8 micron wavelengths;
- 6 short-wave and visible channels at 2.25, 1.6, 1.375, 0.87, 0.67 and 0.55 micron wavelengths.

Like AATSR, the Sentinel SLSTR instrument will measure a nadir and an oblique view scan, each of which will also intersect the calibration black bodies and the visible calibration unit. The requirement for a wider nadir swath, and for enhanced resolution in coastal regions, means that the number of instrument pixels to be measured per scan will exceed the corresponding figure for AATSR. The baseline design, presented at the PRR, accomplishes this while reducing the scan rate.
AATSR scans at a rate of 400 scans per minute, corresponding to the along track resolution of 1 km. The SLSTR instrument will use two independent scan mirrors each scanning at 200 scans per minute, but each scan will measure 2 along-track pixels of 1 km (and 8 pixels at 500 m resolution) simultaneously. This configuration increases the swath width in both views, as well as providing 500 metre resolution in the reflectance channels.

Each scan mirror is mounted at an oblique angle to its axis of rotation, and directs radiation into a telescope assembly the optical axis of which is aligned parallel to the rotation axis. As the scan mirror rotates, the line of sight traces out a cone whose intersection with the Earth traces out the measurement swath of the instrument. The scan cone will intersect the Earth view, the two calibration black bodies, and the Visible Calibration (VISCAL) Unit, so that the line of sight will encounter each of these once during a complete rotation.

Radiation incident along the line of sight enters the focal plane assembly, where it is split into frequency bands corresponding to the different channels. Radiation in each channel is focussed onto a small array of detector elements which correspond to pixels.

4.2.2 The measurement cycle

The two scan mechanisms rotate in synchronism at a frequency of 200 cycles per minute. The basic timing relationships are described in reference [RD-6], and are as follows. The scan cycle has a period of 300 ms (200 rotations per minute). There is also a readout cycle or acquisition sequence of 2 scan periods (600 ms), because the black body and VISCAL targets for a given view are only sampled on alternate scans. These timing cycles are identified in reference [RD-6] as SCANSYNC and CYCLESYNC respectively.

Within these envelopes we have two sampling frequencies which govern the sampling of the individual detectors. In the terminology of [RD-6] these are:

- PIX10SYNC: There will be exactly 3670 PIX10SYNC periods in the 300 ms SCANSYNC period, so its duration is 81.7 μs. This is the rate at which the thermal (1 km resolution) channels are sampled.
- PIX05SYNC: This corresponds to a period which is exactly one-half of PIX10SYNC, or 40.9 μs. This defines the frequency at which the reflectance channels, having 0.5 km ground resolution, are sampled.

As the acquisition cycle proceeds the detectors are sampled simultaneously and synchronously at these frequencies. The thermal infra-red (LWIR and MWIR) and fire channels are sampled once per PIX10SYNC interval. Since each detector in these channels has two detector elements, this process gives two samples per PIX10SYNC period in each channel.

The SWIR and visible channels are sampled twice per PIX10SYNC interval, on alternate PIX05SYNC pulses, to give a ground resolution of 0.5 km. In the tables of ISP structure in reference [RD-5] the odd and even PIX05SYNC intervals appear to be identified as ‘cycle 1’ and ‘cycle 2’ respectively. In the case of the SWIR channels each detector in the FPA will have 8 detectors arranged in an array of two columns by four rows (with the long side of the array parallel to the ground track), to give 0.5 km sampling in the along-track direction.

Not all of the samples within a scan cycle appear in the telemetry, since there is no point in including samples taken when the line of site is viewing the inside of the instrument enclosure. Only samples corresponding to the earth view or the calibration targets are transmitted to the ground. As previously noted, the black body and VISCAL targets for a given view are only sampled on alternate scans. Figure 4-1, derived from the description in [RD-6], indicates the target measurements that are recorded during each scan cycle, for the nadir and inclined views.

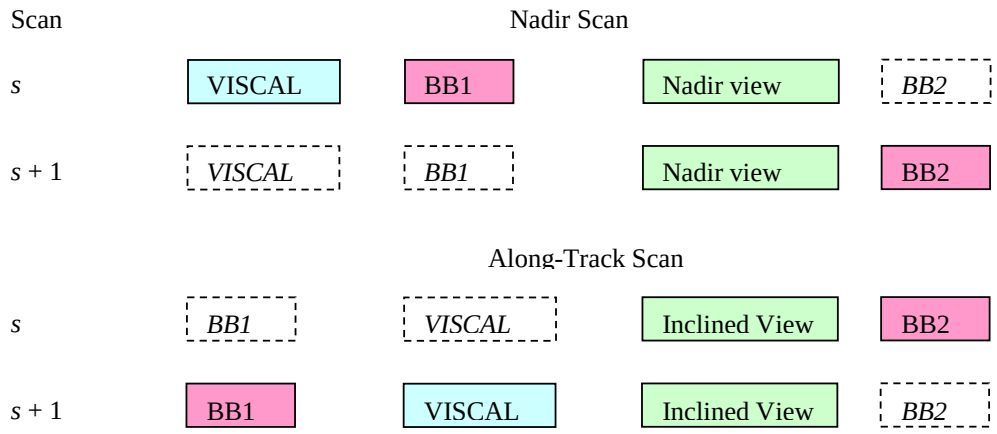

Figure 4-1: The SLSTR Measurement Cycle. Dashed boxes represent target encounters that are absent from the telemetry

4.2.3 Terminology and indexing

We define the following terminology

- A **scan** is defined as a complete rotation of the scan mirrors.
- A **scan cycle** comprises two consecutive scans (a CYCLESYNC period as defined above) during which a complete set of targets are sampled.
- A **target** is either the Earth view or one of the internal calibration targets (the VISCAL and the two black bodies); in the context of the telemetry data it refers to a section of the scan during which valid data is obtained, when the detectors are viewing the earth view or one of the calibration targets.
- A **pixel** is the IFOV of a single detector element; the projection of that detector element onto the ground at a given instant.
- A **scan trace**, or **scan locus** is the trace of a single detector element on the ground. Thus for example in the thermal channels each detector has two elements, and so a single scan will give two scan traces, displaced by 1 km in the along-track direction. Adjacent scan traces represent adjacent 'rows' of the instrument grid. We may use the term **instrument scan**, (as distinct from *scan*), as an alternative to *scan trace*.

During operation, the SLSTR Front End Electronics will transmit a packet of data to the CPE every PIX10SYNC interval, containing all the detector samples recorded during that interval, and these groupings are retained in the ISP transmitted to ground. This means that to uniquely identify a pixel in a given channel we may need the following indices:

S Scan number; a continuous count of scans, derived from the scan counter that we assume will be present in the telemetry, but with overflow corrected, and with an origin close to the start of the product.

p Pixel index; an index to the PIX10SYNC interval within which the sample was measured.

t An index to the PIX05SYNC interval within which the sample was measured; *t* = 0, 1 in the case of the 0.5 km (reflectance) channels,

k Detector index. *k* = 0, 1 for the 1 km channels, *k* = 0, … 7 for the 0.5 km channels. The detector index maps on to a two dimensional matrix of detectors, the row and column of which are aligned in the along-track and across-track directions respectively, and so the mapping between k and the two-dimensional row and column indices needs to be defined.

s Scan trace; for the thermal channels, $s = 2S + \text{row}(k)$, for the reflectance channels, for which the detector arrays have 4 rows, $s = 4S + \text{row}(k)$

4.3 CALIBRATION APPROACH

4.3.1 On-board calibration

On-board calibration of the Sentinel SLSTR will be based on the approach successfully implemented in the (A)ATSR series of instruments.

For the thermal infra-red channels, provision for their continuous on-board calibration is an integral part of the instrument design. The instrument includes two stable and high precision black-body targets, which are crossed by both the nadir and along-track scan cones. Thus each target is observed once per scan on each scan. One black body is held at a temperature lower than the expected range of surface brightness temperature, and the other at a temperature higher the expected range, so that the interval between the two black body temperatures covers the expected range of sea surface brightness temperature. The physical temperatures of the two black bodies are continuously monitored, and so for each scan the linear calibration relationship between the infra-red radiance and the measured signal counts can be determined from the measurements of the black body signals.

The use of two blackbodies in this way ensures that the calibration is optimised over the normal range of SST, and the effects of detector non-linearity over this range are minimised, thus maximising the accuracy of the SST measurement. The treatment of detector non-linearity is discussed further below.

The calibration scheme for the short-wave (near infra-red) and visible channels is based on a diffuse calibration target of accurately known reflectance which is illuminated by the sun over a short segment of the orbit, and which is intersected by the instrument scans. Measurements of this target when it is illuminated by the sun enable the linear calibration relationship between the measured signal in each channel and the surface reflectance to be determined. If applicable, corrections for any detector non-linearity measured during the pre-launch characterisation of the instrument may be applied based on look-up tables.

4.3.2 Vicarious Calibration and Validation

The concept of vicarious calibration (as distinct from validation) is not applicable to the calibration of the thermal infra-red channels of the SLSTR instrument.

Long-term drifts of the calibration of the visible and near-visible channels may be characterised by monitoring the signals from geophysical targets (e.g. certain desert regions) known to show stable reflectance characteristics, and by comparisons with other instruments. Drifts so

determined will be used to update the calibration files for the relevant channels. This, and instrument validation, are discussed in more detail elsewhere (reference [RD-3]).

4.4 LEVEL 1 PRODUCTS DEFINITION

Reference [RD-1] defines a single SLSTR Level 1 product, based on the AATSR Level 1B product. Note however that there is some ambiguity of terminology here, and the designation Level 1B does not have the same meaning in the context of Envisat as has been defined for Sentinel 3. In terms of the latter definition the product conforms to level 1c, since pixels in the two views are re-sampled and collocated onto a common grid

The product as defined in reference [RD-1] includes 34 measurement data sets, each representing the image for a particular channel and view combination as follows:

- 3 sets of calibrated nadir view brightness temperatures for the 3.74, 10.8 and 12 micron channels;
- 2 sets of calibrated nadir view brightness temperatures for the 3.74, and 10.85 micron fire channels
- 6 sets of calibrated nadir view radiances for the 2.25, 1.6, 1.375 (A-Stripe), 0.87, 0.67 and 0.55 micron channels;
- 3 sets of calibrated nadir view radiances for the 2.25, 1.6, 1.375 micron channels B-stripe detectors
- 3 sets of calibrated nadir view radiances for the 2.25, 1.6, 1.375 micron channels TDI (Average of A and B stripe). Note that the TDI MDS are optional outputs selected by a switch in the processing configuration ADF.
- 3 sets of calibrated oblique view brightness temperatures for the 3.7, 10.8 and 12 micron channels;
- 2 sets of calibrated obliqueview brightness temperatures for the 3.74, and 10.85 micron fire channels
- 6 sets of calibrated obliqueview radiances for the 2.25, 1.6, 1.375 (A-Stripe), 0.87, 0.67 and 0.55 micron channels.
- 3 sets of calibrated oblique view radiances for the 2.25, 1.6, 1.375 micron channels B-stripe detectors
- 3 sets of calibrated oblique view radiances for the 2.25, 1.6, 1.375 micron channels TDI (Average of A and B stripe). Note that the TDI MDS are optional outputs selected by a switch in the processing configuration ADF.

The brightness temperature and radiance values will be mapped onto a rectangular grid of resolution appropriate to the channel; this will be 1 km for the thermal IR channels, and 0.5 km for those channels that are measured at this resolution.

Following (A)ATSR practice, the 1 km grid will be defined with respect to the subsatellite track and the instrument swath projected onto the reference ellipsoid WGS84. The width of the nominal image swath will be 1470 km for the nadir view, and 775 km for the along-track view. The question of other possible grids will be discussed further in Section 4.4.4 below.

A further four measurement data sets will define, for each pixel at 1 km resolution, cloud and confidence flags:

- nadir view cloud clearing/land flagging;
- oblique view cloud clearing/land flagging;
- confidence words for nadir view pixels;
- confidence words for along-track view pixels.

Supplementary (annotation) data sets will provide, where appropriate on a low resolution grid of 16 by 16 km:

- latitude and longitude of tie point pixels;
- Cartesian (*x*, *y*) co-ordinates for tie point instrument pixels;
- Solar azimuth and elevation at the tie pixel;
- Satellite azimuth and elevation at the tie pixel;
- Topographic correction (over land)
- Scan and pixel number for each pixel (to retain the relationship between instrument and image pixels).

The Sentinel 3 System Requirements Document [AD-3] defines 3 processing levels for level 1 data, Level 1a, Level 1b and Level 1c. The relationship of these to the SLSTR product processing is discussed in the following sections.

4.4.1 Level 1a

Level 1a data is defined as 'Level 0 data with corresponding radiometric, spectral and geometric (i.e. Earth location) correction and calibration computed but not applied'.

This represents a very low processing level, and has no counterpart in the Envisat AATSR product set on which the definition of the SLSTR Level 1 product [RD-1] has been based. Nevertheless., a requirement for such a product has been identified, for long-term calibration and monitoring.

For the ATSR-1 and ATSR-2 instruments a product, the Ungridded Detector Count (UCOUNTS) Product, was defined that represented this level of processing. The product contained uncalibrated channel counts on the instrument grid, with geolocation data. The AATSR Prototype Processor also produces a UCOUNTS product, but no such product is generated by the AATSR ground segment.

4.4.2 Level 1b

Level 1b data is defined in reference [AD-3] as Level 1b data that is calibrated and geolocated but not resampled. However, it has subsequently been agreed that, in the case of the SLSTR, the Level 1b product will be relocated onto a specified quasi-Cartesian product grid defined in the following section. This is in order to fulfil the user requirement for a product that is consistent with, and shows continuity with, the AATSR heritage. (We prefer the term regridded rather than resampled to describe this, since resampling may imply an interpolation.)

This use of the term 'Level 1b' is similar to Envisat usage, and will be adopted in the following.

For the ATSR-1 and ATSR-2 instruments a product, the Ungridded Brightness Temperature / Reflectance (UBT) Product was defined at the level of processing corresponding to the SRD [AD-3] definition above. The product contained calibrated data on the same instrument grid as the UCOUNTS product defined above, along with geolocation data. The AATSR Prototype Processor

also produces a UBT product, but again no such product is generated by the AATSR ground segment.

4.4.3 The Level 1b product grid

For each view (nadir and along-track) the SLSTR data is measured on a curvilinear grid defined by the intersection of the instrument scan with the surface of the earth. Instrument samples are distributed at uniform angular intervals around a scan line that is the intersection of the relevant scan cone with the surface of the earth; these scan lines approximate to sections of an ellipse (if the Earth were flat, they would be arcs of ellipses). The two views are not collocated at this stage.

Level 1 processing calculates the geolocation with respect to this instrument grid. That is to say, for each instrument pixel, the latitude and longitude of the pixel are determined. Following AATSR practice, the X and Y co-ordinates of the instrument pixel are also calculated with respect to a quasi-Cartesian product grid that is defined with respect to the satellite ground track and instrument swath. These values are then used to resample the data onto the product grid; a nearest neighbour algorithm is used.

The definition of this product grid is as follows. Consider a point P in the SLSTR instrument swath. The X co-ordinate of the point is given by its distance from the instrument ground track, measured along the normal section PQ through P that intersects the satellite ground track at right angles; point Q is the intersection point of the normal curve with the ground track. The Y co-ordinate of P is then the distance of the intersection point Q measured along the ground track from an origin point. For consolidated products this origin is the ascending node of the ground track on the equator; for near real time products an arbitrary origin close to the start of the product will be used.

X and Y are then the co-ordinates of the point P in a quasi-Cartesian system whose Y axis is the local tangent to the ground track; we call it quasi-Cartesian because the ground track is curved (it is not a geodesic on the ellipsoid). This defines the ‘specified grid’ in the sense of the Level 1b definition above.

Given the Sentinel 3 orbit, the co-ordinates X and Y form a well-defined function of latitude and longitude on the reference ellipsoid (the WGS-84 ellipsoid in the case of Sentinel 3). The level 1b product grid is uniformly sampled in the X and Y co-ordinates.

Image points are sampled at uniform intervals of 1 km or 0.5 km, for the thermal and solar channels respectively, in the across-track (X) direction. In the along-track (Y) direction, following AATSR practice, an equal time interval sampling scheme will be adopted. That is to say, the sampling interval in Y will be equal to the distance moved by the sub-satellite point in (0.5 × SCANSYNC) intervals, for the thermal channels, or (0.25 × SCANSYNC) intervals for the solar channels. These distance increments approximately equal 1.0 (0.5) km, but will vary slightly around the orbit as the ground trace velocity changes.

This method of sampling has certain advantages, in particular it minimises the incidence of cosmetic fill pixels in the nadir view, and retains continuity with the AATSR algorithms. It has no adverse impact on Level 1c product generation.

The latitude and longitude corresponding to any given value of X and Y can be calculated provided the ground trace of the sub-satellite point is known. In practice Level 1b processing will compute these quantities at a series of tie points corresponding to the product grid sampling points, to populate the Image Pixel Geolocation ADS. Latitude and longitude of intermediate points can then be retrieved by interpolation. Details of how this grid is constructed are given in Section 4.4.3.1 below.

4.4.3.1 Calculation of Latitude and Longitude of grid (or image) Pixels

In order to permit the geolocation of the image pixels, Level 1b processing will compute a table of latitude and longitude at a series of tie points in X and Y corresponding to product grid sampling points. The table serves two purposes. Firstly, the column of points at x = 0 defines the ground track, for use by the geolocation algorithm for instrument pixels.

Secondly, the table is used to populate the Image Pixel Geolocation ADS. The latitude and longitude of any image pixel can then be retrieved by interpolation in the table.

The table is produced by the following steps.

Firstly, an auxiliary table is derived giving the latitudes and longitudes of a series of points on the ground track, spaced in time by a multiple of the SCANSYNC interval. This multiple is defined in the configuration ADF as cycles_per_tie_point (see section 6.8.3.1 of RD-11). If the time increment is chosen to be 8 SCANSYNC intervals (2.4 seconds) then the along-track sampling interval corresponds to 16 scan traces, or approximately 16 km. In the following this sampling interval will be denoted by Δt. The orbit propagator is used to calculate the latitude and longitude at each tie point, together with the azimuth of the ground track at the point. Adding 90° to this gives the azimuth of the normal section orthogonal to the ground track, which is the line of constant Y, through the point.

Then for each point in turn, a direct geodetic formula (Section 4.4.4.9.3) is used to compute the latitudes and longitudes of a series of points equally spaced X, along this normal section.

4.4.3.1.1 Along-track look-up tables

The look-up table defining points on the ground track at equal time interval spacing is generated as follows. We define a series of times t[i], i = 0, 1, 2, …

$t[0] = T_0$,

$t[i] = t[i-1] + \Delta t$, i = 1, 2, 3, ...

Here the time origin T_0 represents the start time of the output product, and will be the time of the ascending node crossing for consolidated products.

The orbit propagator is then used to calculate the position and velocity of the sub-satellite point at each time t[i]. If the latitude and longitude of the sub-satellite point at time t[i] are lat[i] and long[i] respectively, then given lat[i-1], long[i-1], lat[i] and long[i], the length of the line segment ds[i] between points i-1 and i can be derived (Section 4.4.4.9.3). Given ds[i], the along-track distance s[i] corresponding to the point at t[i] can be calculated by

s[0] = 0.0

s[i] = s[i-1] + ds[i], i = 1, 2, ...

This is by definition the Y co-ordinate of the tie point.

4.4.3.1.2 Reference Grid of Image Co-ordinates

Starting with these along-track latitudes and longitudes, the latitude and longitude of every set of across-track points corresponding to the along track grid points are calculated. In practice, so as to ensure that the derived co-ordinates faithfully represent true distance on the ellipsoid, we will use a direct geodetic formula (Section 4.4.4.9.3) for this calculation. However, to illustrate the principle of the calculation we will first show how it would be done for a spherical Earth. The full formulae will then be given in a later section.

Consider the point [i] on the ground track. If the velocity components of the sub-satellite point at this point in the Eastern (latuitude or lambda) and Northern (longitude or phi) directions are

velam[*i*] and vephi[*i*] respectively, then the azimuth (measured clockwise from North) of the ground track is

$\beta' = \text{atan2}\{\text{velam}[i], \text{vephi}[i]\}$.

(Note that because the orbit is retrograde β' will be a negative angle). The azimuth of the line orthogonal to the ground track is then $A = \beta' + \pi/2$. Now consider the spherical triangle NQG in Figure 4-2

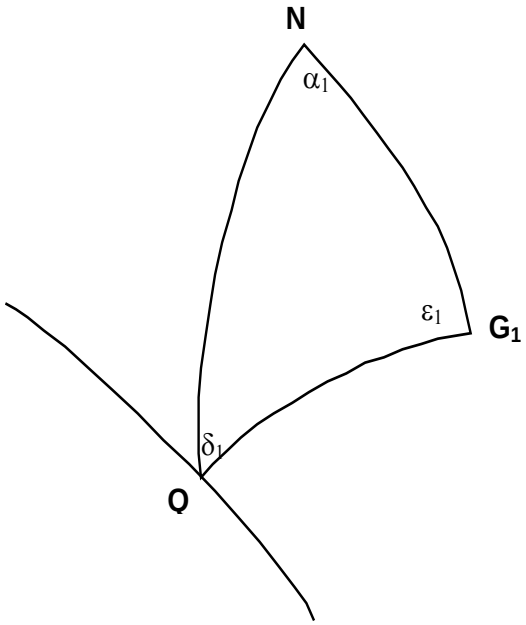

Figure 4-2.

In Figure 4-2, Q is the current ground track point indexed by i, N is the north pole, and G_1 is the next grid point, L km from Q along the great circle at azimuth $\delta_1 = \beta' + \pi/2$. In the triangle formed by these three points, the following quantities are known:

arc QN the co-latitude of Q)
The azimth angle δ_1
arc QG (L/R radians by definition, where R is the radius of the Earth.)

Thus two sides and an included angle are known, and the remaining quantities α_1, ε_1, and arc NG_1 can be calculated by standard techniques. Then the latitude of G_1 is given by 90° - arc NG_1, and its longitude by (longitude of Q + α_1). This process can be iterated to give further points G_j along the extended arc QG_1. The angle $\delta_{j+1} = \pi - \varepsilon_j$ is the azimuth of the great circle of constant Y at G_j. The procedure can then be repeated on the other side of the track. The along-track coordinate of all the points in the across-track direction is the same as that of the sub-satellite point through which the orthogonal great circle is drawn (by definition).

In practice the triangle NQG is drawn on the ellipsoid, and more complex methods are needed to solve it. However, this does not alter the basic principle of the method. The full equations are given in Section (4.4.4.9).

4.4.3.1.3 Comments

The process in which an off-track point G[i, j+1] is derived from the adjacent point G[i, j] could be replaced by one in which each point was derived directly from the on-track point. This would eliminate the possibility of cumulative errors. It would also generalise easily to the case of ellipsoidal geometry.

The process of generating the off-track grid points essentially reduces to the problem of determining the coordinates of the end-point of a line segment, of length *L* and azimuth *A*, given the starting co-ordinates (latitude and longitude). This is a standard problem in geodesy and surveying, and established techniques from these fields can be used to extend the computation to the ellipsoid.

4.4.4 Geo-referencing instrument samples

The process of geolocation aims to define the co-ordinates on the Earth's surface corresponding to the centre of each scan pixel. The required co-ordinates are the latitude and longitude of the pixel on the reference ellipsoid. Ortho-geolocation can then be derived from knowledge of the Digital Elevation Model.

The co-ordinates of the scan pixel correspond to the intersection with the reference ellipsoid of the line of sight for a given detector as it leaves the scan mirror. The problem, then, is to determine this point of intersection, given the satellite position and attitude and the orientation of the scan mirror.

The derivation proceeds in two main stages. First, from knowledge of the angle through which the scan mirror has rotated, we determine the direction cosines of the line of sight relative to a frame of reference fixed in the satellite; then we use the attitude steering law of the satellite and knowledge of its position in its orbit to relate the direction to the Earth-fixed frame of reference. In practice it is expected that the second stage will be accomplished using CFI software for orbit generation and target location similar to that used for AATSR processing. These calculations must be repeated for each pixel for which geolocation is required.

4.4.4.1 Frames of reference

First of all we define the reference frames used in the calculations. All the frames of reference are defined to be right-handed.

Reference [RD-4] defines a number of Sentinel-3 related frames of reference, in particular the Spacecraft Reference Frame and the SLSTR Reference Frame. In addition, we will require additional frames related to the SLSTR scan geometry, and these are also described below. The transformations between these reference frames will then be expressed as a series of elementary rotations.

In effect, relative to the (A)ATSR configuration, the SLSTR instrument flies backwards, with the inclined view following the nadir view. The active portions of the two scans retain opposite curvatures, so the nadir view is concave backwards rather than forwards.

The standard frames of reference defined in the Sentinel 3 [AD-3] and SLSTR [RD-2] documentation differ from those used for ENVISAT and AATSR. Frames of reference in the Sentinel documents are defined so that the *Y* axis points in the across-track direction, in contrast to the convention used for (A)ATSR, in which the *X* axis was directed across-track. Thus the equivalent AATSR and SLSTR reference frames are related by a rotation through 90 degrees about their common *Z* axes. Here we will adopt the Sentinel-3 definitions, at least as far as the orientation of each frame is concerned. Strictly we require the origin of each reference frame to coincide with the centre of the scan mirror, rather than the frame-specific origins defined in [RD-2]. In practice any error, in terms of displacement on the surface, is presumably negligible.

4.4.4.2 The yaw steering frame

This frame is defined in Appendix A of [AD-3]. It is a right-handed Cartesian reference frame having its origin at the centre of mass of the satellite. The Z axis points towards the local geodetic nadir, and the X axis is parallel to, and in the same direction as, the ground trace velocity of the

sub-satellite point. The Y axis then completes the right-handed set. This frame represents the nominal attitude of the satellite when in yaw steering mode; following [AD-3] co-ordinates in this system will be denoted by the subscript *yst*.

4.4.4.3 The spacecraft reference frame

This is defined in [RD-4] in terms of the spacecraft structure and the launch vehicle interface plane. However for our present purposes it can be defined as a Cartesian frame of reference, rigidly fixed in the spacecraft and oriented so that in the nominal flight configuration, the Z axis will point to geodetic nadir, and the X axis will be parallel to the satellite roll axis and directed backwards relative to the orbital velocity vector. The Y axis then completes the right-handed set. Co-ordinates in this system will be denoted by the subscript *s*.

4.4.4.4 The platform reference frame

This frame is fixed relative to the satellite, and is obtained from the spacecraft reference frame by a rotation about 180 degrees about the common *Z* axes so that the *X* axis points forward. It is defined for convenience in specifying line of site azimuth and elevation; it is nominally parallel to the yaw steering frame when the satellite is operating in yaw steering mode. Co-ordinates in this system will be denoted by the subscript *p*.

4.4.4.5 The instrument reference frame

The instrument frame of reference is then a Cartesian frame having the Z axis directed at nadir, in the normal flight configuration. The *X* axis is then orthogonal to this, in the plane containing the two scan axes, and directed from the centre point of the nadir scan towards the centre point of the oblique scan, that is to say, backwards relative to the direction of flight. The *Y* axis then completes the right-handed set. It will be denoted by the subscript *b*.

With this definition the *Y* axis points across-track, and corresponds to the *X* axis of the corresponding frame of reference used in discussion of the (A)ATSR instruments. In order to retain the algebraic link between the AATSR and SLSTR, we will measure scan angles from the *Y* axis.

For present purposes we can identify this frame with the SLSTR reference frame defined in [RD-2], apart from a small displacement in the origin which is not material to the geolocation precision. (We actually want the origin of the frame to correspond to the centre of the scan mirror).

4.4.4.6 The scan reference frames

We then define scan frames for the nadir and inclined views. In each case the scan frame is defined as the frame whose *Z* axis lies along the axis of the scan, and whose *Y* axis is identical to that of the instrument frame defined above. The *X* axis then completes the right-handed set.

With this definition, the nadir view scan frame is obtained from the instrument frame by a rotation about the common *Y* axes through the angle κ' necessary to bring the *Z* axis into line with the axis of the nadir scan. This frame will be denoted by the subscript *a*.

However, it is immediately clear that since the oblique scan rotates about a vertical axis, the oblique scan frame as we have defined it is identical to the instrument frame.

The viewing directions are initially defined with respect to these frames as follows. In each case we assume that the viewing direction rotates in a positive sense about the Z_a axis, to which it is inclined at angle κ. Thus the scan on the surface is traced in a clockwise direction, as seen from above.

We can then express the line of sight as a vector in the scan frame, and transform it into the instrument frame, and then into the satellite frame, taking into account any misalignment between the frames. The line of sight depends on the scan angle and, for the SLSTR design, on the position of the detector element relative to the focal point of the channel, as we will discuss in a later section.

4.4.4.7 Satellite transformations

We then define linear transformations $M_{ab}(-\kappa')$, $M_z(\zeta)$, $M_y(\zeta)$, $M_x(\xi)$, M_{ps} as follows:

$M_{ab}(-\kappa')$ converts the components of a vector defined in X_a, Y_a, Z_a to those of the same vector defined with respect to the baseplate axes X_b, Y_b, Z_b.

$M_z(\zeta)$, $M_y(\eta)$, $M_x(\xi)$, applied in turn, convert the components of a vector defined in X_b, Y_b, Z_b to those of the same vector defined with respect to the spacecraft axes X_S, Y_S, Z_S.

M_{ys} converts the components of a vector defined in X_S, Y_S, Z_S to those of the same vector defined with respect to the yaw steering frame X_{yst}, Y_{yst}, Z_{yst}.

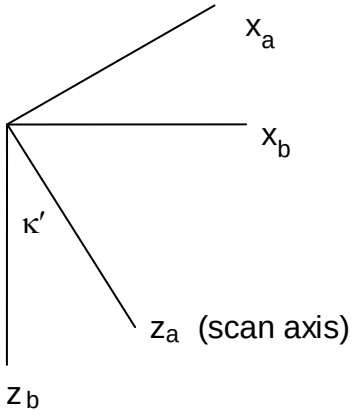

Figure 4-3

The equations of the transformations are as follows.

Suppose that x_a, y_a, z_a are the components of a vector **x** relative to the nadir scan reference frame, and that x_b, y_b, z_b are the components of the same vector relative to the baseplate reference frame. $M_{ab}(-\kappa')$ is a rotation of $-\kappa'$ about the common Y_a, Y_b axes (Figure 4-3), and so the components are related by [actually k-prime]

$$x_b = x_a \cos\kappa' + z_a \sin\kappa'$$
$$y_b = y_a$$
$$z_b = -x_a \sin\kappa' + z_a \cos\kappa'$$

eq 4.4-1

Therefore

$$M_{ab}(-\kappa') = \begin{pmatrix} \cos\kappa' & 0 & \sin\kappa' \\ 0 & 1 & 0 \\ -\sin\kappa' & 0 & \cos\kappa' \end{pmatrix} \qquad \text{eq 4.4-2}$$

Matrices $M_z(\zeta)$, $M_y(\eta)$, $M_x(\xi)$. represent elementary rotations of ζ, η, ξ about the *z*, *y* and *x* axes respectively. The transformation between the instrument and satellite frames is built up out of these elementary transformations. We adopt the convention that the rotations are to be applied in that order to give the total transformation to the platform frame. Strictly speaking the matrices representing elementary rotations about different axes do not commute, and so we should specify the order in which they are to be applied. In practice the angles are sufficiently small that any errors from this source are small in relation to the overall attitude error budget and the matrices can be regarded as commuting to a sufficient accuracy.

M_z represents a rotation about the axis Z_b to give a new intermediate frame of reference, in which the components of the vector **x** are x'_b, y'_b, z'_b. The components of **x** in the new basis are (Figure 4-4)

$$\begin{aligned} x'_b &= x_b \cos\zeta + y_b \sin\zeta \\ y'_b &= -x_b \sin\zeta + y_b \cos\zeta \\ z'_b &= z_b \end{aligned} \qquad \text{eq 4.4-3}$$

and so

$$M_z(\zeta) = \begin{pmatrix} \cos\zeta & \sin\zeta & 0 \\ -\sin\zeta & \cos\zeta & 0 \\ 0 & 0 & 1 \end{pmatrix} \qquad \text{eq 4.4-4}$$

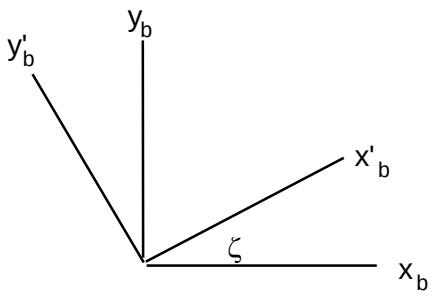

Figure 4-4

The matrix M_y represents a rotation about the transformed axis y'_b to give a new intermediate frame of reference (Figure 4-5) in which the components of **x** are x''_b, y''_b, z''_b given by

$$\begin{aligned} x''_b &= x'_b \cos\eta - z'_b \sin\eta \\ y''_b &= y'_b \\ z''_b &= x'_b \sin\eta + z'_b \cos\eta \end{aligned} \qquad \text{eq 4.4-5}$$

Therefore the matrix M_y is

$$M_y(\eta) = \begin{pmatrix} \cos\eta & 0 & -\sin\eta \\ 0 & 1 & 0 \\ \sin\eta & 0 & \cos\eta \end{pmatrix}$$ eq 4.4-6

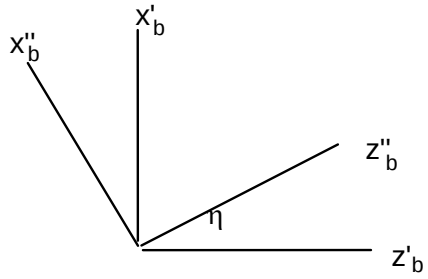

Figure 4-5

M_x represents the rotation about the transformed x''$_b$ axis to the satellite frame (Figure 4-6). The components of **x** in this basis are x_p, y_p, z_p given by

$$x_p = x_b''$$
$$y_p = y_b''\cos\xi + z_b''\sin\xi$$ eq 4.4-7
$$z_p = -y_b''\sin\xi + z_b''\cos\xi$$

and so

$$M_x(\xi) = \begin{pmatrix} 1 & 0 & 0 \\ 0 & \cos\xi & \sin\xi \\ 0 & -\sin\xi & \cos\xi \end{pmatrix}$$ eq 4.4-8

The above equations can be regarded as defining the misalignment angles.

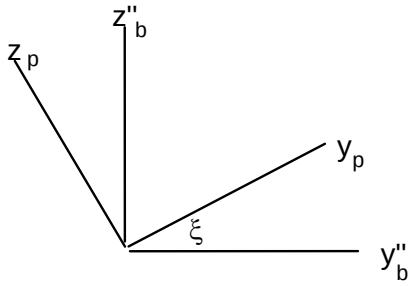

Figure 4-6

4.4.4.8 Treatment of multiple detectors

In general, the first stage of geolocation involves the application in turn of the above transformations to the line of sight vector expressed in the scan reference frame. This gives the vector expressed in the spacecraft reference frame; this is then used as a parameter of the CFI target function to define the instrument pixel position. We therefore need an expression for the initial line of sight.

In the case of the (A)ATSR instruments, the field stop at the prime focus of the telescope was imaged onto a single detector. Consequently the position of the pixel on the ground was given by the intersection with the surface of the line of sight from the focal point. It is very simple to write down the direction of the line of sight in this case.

Let the rotation angle of the scan mirror be φ, defined to be zero when the scan mirror normal lies in the *Y* - *Z* plane of its respective scan reference frame. With respect to the scan reference frame, the direction cosines of the line of sight are then

$$\lambda = -\sin\kappa \sin\varphi$$
$$\mu = \sin\kappa \cos\varphi \qquad \text{eq 4.4-9}$$
$$\nu = \cos\kappa$$

where κ is the apex semi-angle of the scan cone. (The negative sign appears because we have defined the scan angle in a way that is consistent with the definition used in the AATSR documentation.)

In the case of SLSTR, each channel will have more than one detector in the FPA, and these detectors will be displaced from the position of the focal point. More than one pixel will be imaged simultaneously (two in the case of the thermal channels, eight in the case of the short-wave and visible channels). For each detector element, the position of the corresponding pixel on the ground will be the intersection with the surface of the line of sight from the detector. In order to treat this case, we must replace the equations (4.4.9), which define the line of sight from the focus, by expressions which take account of the displacement of the detector from the focus. These will be different for each distinct detector element of a channel.

Let us suppose that the detector element under consideration is displaced from the focal point by a vector element (*dx*, *dy*) relative to the scan axes. (Strictly this refers to the point in the focal plane of the telescope that is imaged onto the detector element; we do not need to take account of the detailed geometry of the FPA optics).

If *F* represent s the focal length of the telescope, the direction in the scan frame, after reflection, from which rays will be focussed onto the detector element at (*dx*, *dy*) is given by the vector ***f*** = (*dx*, *dy*, *F*).

The corresponding unit vector is therefore given by $\boldsymbol{\tau} = col\{dx \quad dy \quad F\}/|\mathbf{f}|$, where

$|\mathbf{f}| = \sqrt{dx^2 + dy^2 + F^2}$ is the modulus of the vector ***f***. The relationship between this vector and the reflected ray direction follows from the equation of reflection

$$\boldsymbol{\tau}' + \boldsymbol{\tau} = \mathbf{2}(\boldsymbol{\tau}.\mathbf{n})\mathbf{n} \ . \qquad \text{eq 4.4-10}$$

This can be rewritten as

$$\boldsymbol{\tau}' = 2(\boldsymbol{\tau}.\mathbf{n})\mathbf{n} - \boldsymbol{\tau} = 2(\tau_x n_x + \tau_y n_y + \tau_z n_z)\mathbf{n} - \boldsymbol{\tau} \ . \qquad \text{eq 4.4-11}$$

This is a linear function of $\boldsymbol{\tau}$ and so can be expressed by a matrix transformation. In terms of the components of **n**, the expression becomes

$$\mathbf{T}' = \begin{pmatrix} 2n_x^2 - 1 & 2n_y n_x & 2n_z n_x \\ 2n_x n_y & 2n_y^2 - 1 & 2n_z n_y \\ 2n_x n_z & 2n_y n_z & 2n_z^2 - 1 \end{pmatrix} \mathbf{T} \qquad \text{eq 4.4-12}$$

The instantaneous direction of the mirror normal **n** is given by

$$\begin{aligned} n_x &= -\sin\varphi \sin i \\ n_y &= \cos\varphi \sin i \\ n_z &= \cos i \end{aligned} \qquad \text{eq 4.4-13}$$

In this equation φ is the scan angle as before, and i is the angle of incidence of the optical axis on the mirror. (Note this has the same form as (1), but with *i* in place of the cone angle κ.)

Substituting these expressions in the matrix equation we find

$$\mathbf{T}' = \begin{pmatrix} 2\sin^2\varphi\sin^2 i - 1 & -2\cos\varphi\sin\varphi\sin^2 i & -2\sin\varphi\sin i\cos i \\ -2\cos\varphi\sin\varphi\sin^2 i & 2\cos^2\varphi\sin^2 i - 1 & 2\cos\varphi\sin i\cos i \\ -2\sin\varphi\sin i\cos i & 2\cos\varphi\sin i\cos i & 2\cos^2 i - 1 \end{pmatrix} \mathbf{T} \qquad \text{eq 4.4-14}$$

This rather complicated-looking matrix can in fact be factorised into the following expression:

$$\mathbf{T}' = M_{ac}^{-1} M_{cm}^{-1} \begin{pmatrix} -1 & 0 & 0 \\ 0 & -1 & 0 \\ 0 & 0 & 1 \end{pmatrix} M_{cm} M_{ac} \mathbf{T} \qquad \text{eq 4.4-15}$$

In this expression the quantities M_{cm} and M_{ac} represent elementary rotations through φ and *i* respectively as follows:

$$M_{ac} = \begin{pmatrix} \cos\varphi & \sin\varphi & 0 \\ -\sin\varphi & \cos\varphi & 0 \\ 0 & 0 & 1 \end{pmatrix}; \; M_{cm} = \begin{pmatrix} 1 & 0 & 0 \\ 0 & \cos i & -\sin i \\ 0 & \sin i & \cos i \end{pmatrix} \qquad \text{eq 4.4-16}$$

It is easy if somewhat laborious to verify this factorisation.

Note that if the initial vector is a unit vector directed outward along the Z_a axis, i.e. if $\tau = col\{0, 0, 1\}$, then the outward line of sight from the mirror is

$$\tau' = \begin{pmatrix} -\sin\varphi\sin 2i \\ \cos\varphi\sin 2i \\ \cos 2i \end{pmatrix} \qquad \text{eq 4.4-17}$$

This represents the ATSR geometry, and is identical to (2.4.9) with $\kappa = 2i$.

In the case of the oblique scan, the above equations give the direction cosines of the line of sight relative to the common scan and instrument frames. In the case of the nadir scan, we must transform the line of sight vector into the instrument frame.

Given the direction of the line of sight as calculated above, the CFI software can be used to determine the location (latitude and longitude) of the pixel on the Earth.

4.4.4.9 Geometry on the Ellipsoid

We have seen above that the Level 1b output product grid is uniformly sampled in the co-ordinates X and Y. in order to relocate the pixels on this grid it is therefore necessary to transform the latitude and longitude of each pixel into the X and Y co-ordinate system. In order that the X - Y co-ordinate system gives a true representation of distances on the surface of the Earth, the transformation equations relating latitude and longitude to X and Y must take account of the geometry on the ellipsoid. Therefore before we present the transformation equations, we set out some relevant geodetic theory.

4.4.4.9.1 Some Relationships on the Ellipsoid

This section gives for reference a number of standard geometrical relationships relating to the ellipsoid. Some are given without proof, but can be found in texts such as References [RD-13].

The reference ellipsoid is the ellipsoid of revolution formed by rotating an ellipse about its semi-minor axis (which will coincide with the axis of rotation of the Earth). The cross-section of the surface in any plane containing the axis of rotation will be an ellipse. If we define axes x and y to coincide with, respectively, the semi-major and semi-minor axes of this ellipse, we can write its equation in the standard form

$$\frac{x^2}{a^2}+\frac{y^2}{b^2}=1 \qquad (4.4.18)$$

where *a* is the semi-major axis and *b* is the semi-minor axis. The ratio (a-b)/a is known as the flattening, *f*. It is related to the eccentricity *e* by

$$(1-f)^2 = (1-e^2) \qquad (4.4.19)$$

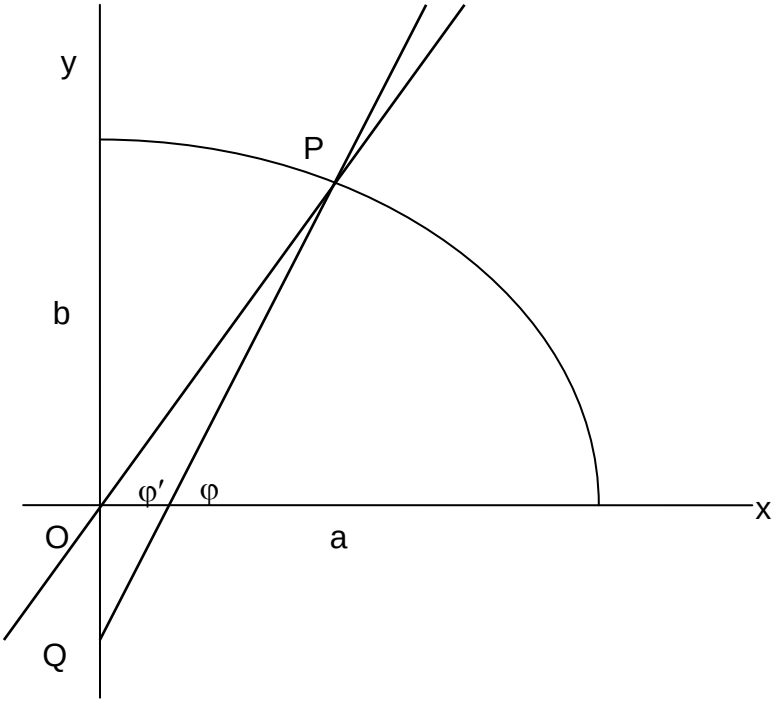

Figure 4-7

Figure 4-7 shows a point P (*x*', *y*') on the surface. The angle ϕ' is the geocentric latitude of P given by

$$\tan\varphi' = y'/x'$$
(4.4.20)

The line PQ is the normal to the surface at P. The angle ϕ that this makes with the *x* axis (or the equatorial plane) is the geodetic latitude of P;

$$\tan\varphi = 1\Big/\left(\frac{dy}{dx}\right)_P = \frac{y'}{(1-f)^2 x'}$$
(4.4.21)

Thus

$$\tan\varphi' = (1-f)^2 \tan\varphi = (1-e^2)\tan\varphi$$
(4.4.22)

The radius of curvature of the surface in the meridian plane at point P is given by

$$R = \frac{a(1-e^2)}{(1-e^2\sin^2\varphi)^{3/2}}$$
(4.4.23)

This equation can be derived fairly directly from the equation for the ellipse (Equation 4.4.18). The radius of curvature in the vertical plane normal to the meridian plane (in Figure 4-7, the plane containing PQ and normal to the plane of the diagram) is

$$N = \frac{a}{\sqrt{1-e^2\sin^2\varphi}}$$
(4.4.24)

This is sometimes termed the radius of curvature in prime vertical. The point Q is the common intersection of the surface normals at points on the parallel of latitude through P, and the length PQ can be shown to equal the normal radius of curvature *N*. Thus the centre of curvature in prime vertical lies on the minor axis of the ellipse. Note that the alternative notation ν, ρ is often used in the literature for the radii of curvature *N*, *R* respectively, and we shall use this notation below.

The equation of the line PQ is

$$(y-y') = (x-x')\tan\varphi$$
(4.4.25)

and its intercept Q at *x* = 0 is

$$y = y' - x'\tan\varphi = -y'e^2/(1-e^2)$$
(4.4.26)

Thus the projection of PQ onto the y axis is

$$N\sin\varphi = y' + y'e^2/(1-e^2) = y'/(1-e^2)$$
(4.4.27)

and finally we have an expression for the coordinates of P in terms of N and ϕ

$$x' = N\cos\varphi,\ y' = N(1-e^2)\sin\varphi \qquad (4.4.28)$$

Define a right-handed set of Cartesian axes *X*, *Y*, *Z* with origin at the centre of the Earth, with *Z* directed northwards along the axis of rotation, and with *X* in the plane of the prime meridian. The

XY plane is therefore the plane of the equator. If Figure 4-7 represents the meridian plane at longitude λ, the *X*, *Y*, *Z* coordinates of a point (*x*, *y*) in the plane are

$$X = x\cos\lambda$$
$$Y = x\sin\lambda \qquad (4.4.29)$$
$$Z = y$$

The geocentric Cartesian coordinates (*X*, *Y*, *Z*) of a point T at a height *h* vertically above P are therefore

$$X = (N+h)\cos\varphi\cos\lambda$$
$$Y = (N+h)\cos\varphi\sin\lambda \qquad (4.4.30)$$
$$Z = \left[N(1-e^2)+h\right]\sin\varphi$$

Length and azimuth on the ellipsoid

We also require formulae for the length and azimuth of the curves joining any two points P_1 and P_2 on the ellipsoid. Firstly it is necessary to be clear as to what is meant, since any of three different curves may be meant. The geodesic is the unique curve of shortest length between the two points P_1 and P_2; however, many of the standard formulae refer not to the geodesic but to one of the two normal sections between the points.

The geodesic does not lie in a plane, nor does its azimuth α coincide with the bearing of point P_2 that would be measured with a levelled theodolite at point P_1, although the deviations will be very small for short lines. There are an infinite number of plane sections through the ellipsoid including points P_1 and P_2. In particular we can consider two; the intersection of the ellipsoid with the plane containing point P_2 and the normal to the surface at point P_1, which we may call S_1, and the intersection with the plane containing point P_1 and the normal to the surface at point P_2, which we may call S_2. These are the normal sections, and their azimuths, measured at the points at which the plane section contains the normal to the surface, are the normal section azimuths. Thus the angle between the curve S_1 and the meridian plane through point P_1 is the normal section azimuth of point P_2 measured from point P_1, and this angle is the bearing of point P_2 that would be measured with a levelled theodolite at point P_1.

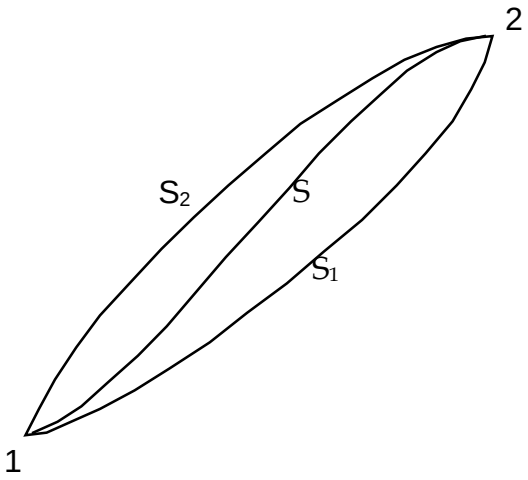

Figure 4-8

The geodesic S lies between these two arcs S_1 and S_2, somewhat as shown in Figure 4-8. The angles between the curves are very small; if we consider azimuths measured at point P_1 we have

$$\alpha_2 - \alpha_1 = 3(\alpha_2 - \alpha) \cong 00042 \text{ arc sec} \qquad (4.4.31)$$

for line lengths *L* = 10 km. The difference increases quadratically with *L*.

It is possible to give an exact expression for the normal section azimuth if the latitude and longitude of the two points are known. To simplify the notation, rename the two points P and Q, and let their geodetic latitude and longitude be (φ_1, λ_1) and (φ_2, λ_2) respectively. Consider the sphere of radius O'P centred at O', which is the intersection of the normal through P with the axis of rotation. This sphere is tangent to the ellipsoid at the parallel of latitude through P, but does not otherwise coincide with it. Consider the spherical triangle NPQ' drawn on this sphere (Figure 4-10), where N is the intersection of the axis with the sphere, and Q' is the intersection of the line O'Q with this sphere. As we have defined it, the plane O′PQ′, which also contains point Q, is the normal section at P containing Q, and so the desired normal section azimuth of Q measured from P is the angle at P (NPQ'). In the triangle, the angle at N is known, since it is given by the difference in the longitudes of Q and P, as are the sides NP and NQ', so that the triangle can be solved for angle P. NP is the geodetic co-latitude of point P. The calculation of the arc NQ' is more complicated.

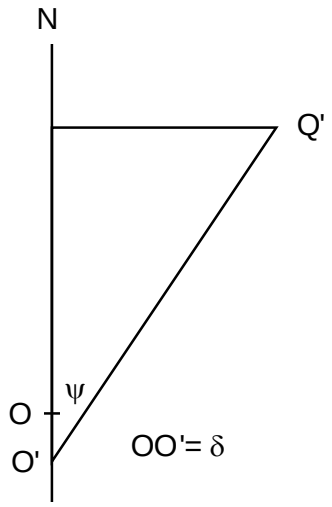

Figure 4-9

.

Suppose O is the centre of the Earth. We know that the z coordinate of O' is

$\delta = -e^2 N_1 \sin \varphi_1$.

At the same time the z coordinate of Q is (Equation 4.4.30)

$N_2 (1 - e^2) \sin \varphi_2$.

Thus in Figure 4-9, which shows the meridian plane through Q, the length O'Z (where Z is the projection of Q on the polar axis) is

$$N_2 (1 - e^2) \sin \varphi_2 + e^2 N_1 \sin \varphi_1 \qquad (4.4.32)$$

(The subscripts 1 and 2 refer to the points P and Q respectively.) The length ZQ is

$N_2 \cos \varphi_2$

and so we have

$$\tan \psi = \cos \varphi_2 / ((1 - e^2) \sin \varphi_2 + e^2 (N_1/N_2) \sin \varphi_1), \qquad (4.4.33)$$

from which the angle ψ can be determined.

In Section 4.4.4.9.4 we outline a general approach to the solution of a spherical triangle in which two sides and the included angle are known. By application of this method to the triangle PNQ' (Figure 4-10) we can obtain explicit expressions for sin *A* and cos *A* in terms of known quantities and of the unknown χ. Angle *A* is the azimuth of the normal section PQ at P.

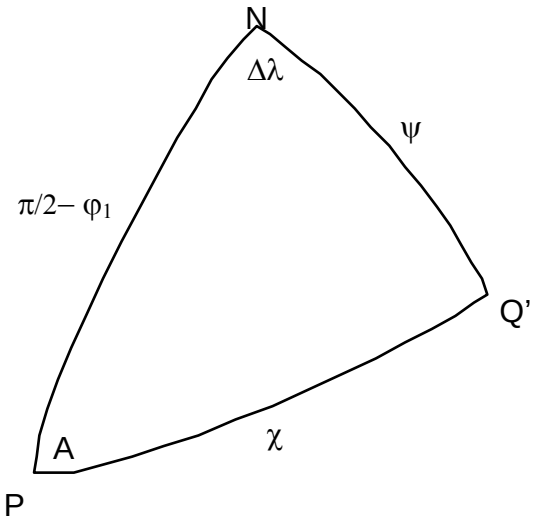

Figure 4-10

From the sine rule we get

$$\sin A = \sin \Delta\lambda \sin \psi \operatorname{cosec} \chi. \qquad (4.4.34)$$

Using two applications of the cosine formula, we can express both χ and ψ in terms of known quantities:

$$\cos\chi = \cos(\pi/2 - \varphi_1)\cos\psi + \sin(\pi/2 - \varphi_1)\sin\psi\cos\Delta\lambda$$
$$\cos\psi = \cos(\pi/2 - \varphi_1)\cos\chi + \sin(\pi/2 - \varphi_1)\sin\chi\cos A$$

We can now eliminate cos χ from these equations. Multiply the first equation by sin φ_1;

$$\cos\chi\sin\varphi_1 = \sin^2\varphi_1\cos\psi + \cos\varphi_1\sin\varphi_1\sin\psi\cos\Delta\lambda$$

and re-order the second;

$$\cos\chi\sin\varphi_1 = \cos\psi - \cos\varphi_1\sin\chi\cos A$$

The left-hand sides are equal, and so we can equate the right-hand sides. Therefore

$$\cos\varphi_1\sin\chi\cos A = \cos\psi(1 - \sin^2\varphi_1) - \cos\varphi_1\sin\varphi_1\sin\psi\cos\Delta\lambda$$

Divide this equation by $\cos\varphi_1\sin\chi$;

$$\cos A = [\cos\psi\cos\varphi_1 - \sin\varphi_1\sin\psi\cos\Delta\lambda]\operatorname{cosec}\chi.$$

Therefore

$$\cot A = \operatorname{cosec}\Delta\lambda\,[\cot\psi\cos\varphi_1 - \sin\varphi_1\cos\Delta\lambda]$$

$$= \sin\varphi_1\operatorname{cosec}\Delta\lambda\,[\cot\psi/\tan\varphi_1 - \cos\Delta\lambda] \qquad (4.4.35)$$

where

$$\cot\psi = \Lambda_{12}\tan\varphi_1$$

(4.4.36)

and

$$\Lambda_{12} = \left(1-e^2\right)\frac{\tan\varphi_2}{\tan\varphi_1} + e^2\left(\frac{\nu_1}{\nu_2}\right)\frac{\tan\varphi_2}{\tan\varphi_1}$$

(4.4.37)

from Equation (4.4.33). This is Cunningham's Azimuth formula (Bomford [RD-13]).

An exact equation for the length of the normal section is given by Bomford [RD-13]. Various approximate forms are also available, and will be discussed below.

4.4.4.9.2 Direct and Inverse Formulae

In order to define the SLSTR image grid (to determine the latitude and longitude of a general grid point), we will first define the latitudes and longitudes of a series of points on the Sentinel 3 ground track. The co-ordinates of the other grid points will then be defined on the assumption that each lies on a line through a ground track point, at a given azimuth and at a given distance (the grid X co-ordinate) from the ground track point.

This is an instance of a general problem that arises in surveying and geodesy, to find the co-ordinates of a point at a known distance, along a line at a known azimuth, from a point whose co-ordinates are known. If the two points are P_1 and P_2, and their geodetic latitude and longitude are respectively (φ_1, λ_1), (φ_2, λ_2), the problem is to find (φ_2, λ_2) given the distance *L* between P_1 and P_2, and the azimuth measured from North at P_1, together with the latitude and longitude of P_1. A formula that gives (φ_2, λ_2) in terms of the known quantities is known as a ‘direct formula’.

Conversely, to determine the *X* and *Y* co-ordinates of a point given its latitude and longitude, we require the inverse relationship, that gives the length and azimuth of the line between two points on the ellipsoid, as a function of the co-ordinates (latitude and longitude) of the two points.

Many geodetic formulae exist, of varying degrees of complexity and accuracy. Several are given by Bomford ([RD-13] and earlier editions of that work). Formulae differ according as whether they use geodesic or normal section distances and azimuths. Some formulae (e.g that of Vincenzy) are expressed in terms of the geodesic distance between the points, and the geodesic azimuths. For any modification of the AATSR regridding scheme, we desire to maintain consistency with other ENVISAT instruments, and in particular to ensure that the line of constant y should lie in the X-Z plane of the satellite, and this clearly defines a normal section at the sub-satellite point. We thus require normal section formulae. It is true that for sufficiently short lines the difference between the lengths of the geodesic and the normal section is negligible, but it might still be necessary to take account of the azimuth differences to maintain control of errors. Of the formulae cited by Bomford [RD-13], the two adopted for AATSR processing were those of Clarke and Robbins; Robbins’s formula is essentially the inverse of that of Clarke, and we consider it first.

Suppose that the co-ordinates (latitude and longitude) of two points P and Q are known. Given these quantities, the normal section azimuth of Q measured at P can be computed using Cunningham's azimuth formula (above). In the same spherical triangle (Figure 4-10) the angular distance χ (arc PQ measured at the centre of curvature in prime vertical at P, or O' in Figure 4-9) can also be derived from Equation (4.4.34 - 36). The corresponding length on the auxiliary sphere centred at O' is ($\nu_1\chi$). For small separations PQ it is clear that this length is very close to the desired length of the normal section PQ, so that the latter can be derived by the application of a small correction to χ. In effect this is what Robbins’s formula does.

The radii of curvature in prime vertical at the points P, Q are as follows:

$$\nu_1 = a/\left(1-e^2\sin(\varphi_1)\right)^{1/2} \quad (4.4.38)$$

$$\nu_2 = a/\left(1-e^2\sin(\varphi_2)\right)^{1/2} \quad (4.4.39)$$

where *a* is the semi-major axis (the equatorial radius) of the Earth; cf. Equation (4.4.24). We can then calculate the angle ψ as in equation (4.4.33):

$$S_\psi = (1-e^2)\sin\varphi_2 + (\nu_1/\nu_2)e^2\sin\varphi_1 \quad (4.4.40)$$

$$C_\psi = \cos\varphi_2 \quad (4.4.41)$$

$$\psi = \text{arc cot}\left(S_\psi / C_\psi\right) \quad (4.4.42)$$

Calculate the geodetic correction coefficients

$$g = \varepsilon\sin\varphi_1\cos\varphi_1\cos A \quad (4.4.43)$$

$$h = \varepsilon\cos^2\varphi_1\cos^2 A \quad (4.4.44)$$

where

$$\varepsilon = e^2/(1-e^2) \quad (4.4.45)$$

The line segment between points P and Q is then given as a function of the angle χ:

$$L = \nu_1\chi\left[1-\frac{\chi^2}{6}h(1-h)+\frac{\chi^3}{8}g(1-2h)+\ldots\right] \quad (4.4.46)$$

plus terms in higher powers of χ.

Clarke's direct formula, which we quote without proof, is then given as follows. Suppose we are given the latitude and longitude of point P (represented by subscript 1), and the length *L* of the arc PQ and the normal section azimuth *A* of point Q;

Calculate

$$r_2 = -\varepsilon\cos^2\varphi_1\cos^2 A \quad (4.4.47)$$

$$r_3 = 3\varepsilon(1-r_2)\cos\varphi_1\sin\varphi_1\cos A \quad (4.4.48)$$

Calculate the radius in prime vertical at latitude φ_1,

$$\nu_1 = a/\left(1-e^2\sin(\varphi_1)\right)^{1/2}. \quad (4.4.49)$$

Then

$$\vartheta = \frac{L}{\nu_1}\left[1-\frac{r_2(1+r_2)}{6}\left(\frac{L}{\nu_1}\right)^2-\frac{r_3(1+3r_2)}{24}\left(\frac{L}{\nu_1}\right)^3\right] \quad (4.4.50)$$

Refer again to Figure 4-10. The quantity just calculated is the angular distance PQ′ (χ in the diagram). Once this is known, the triangle can be solved by standard techniques for the longitude

difference $\Delta\lambda$ and for the angle ψ. Finally the latitude of Q can be determined from the latter as follows.

$$\rho = 1 - \tfrac{1}{2} r_2 \vartheta^2 - \tfrac{1}{6} r_3 \vartheta^3 \qquad (4.4.51)$$

$$S_2 = \cos\psi - e^2 \rho \sin\varphi_1 \qquad (4.4.52)$$

$$C_2 = (1 - e^2)\sin\psi \qquad (4.4.53)$$

$$\tan\varphi_2 = S_2 / C_2 \qquad (4.4.54)$$

Equations (4.4.51) to (4.4.54) are essentially a variant of Cunningham's formula, but adapted to the case that ν_2 (the radius of curvature at point Q) is not known.

How many terms is it necessary to take in the series (enclosed in square brackets) in Robbins's formula (4.4.46) to ensure a given degree of accuracy? Table 5.4.1 below gives an upper limit on the magnitude of each term, including some we have not quoted explicitly, for three different line lengths; 25 km (corresponding to the interval between along-track points used in computing the tables of along track distance), 32 km (ditto for a larger granule size) and 275 km, corresponding to the maximum across-track distance computed during the generation of the reference grid.

Table 5.4.1. Magnitude of terms in Robbins's Formula. (Terms in mm.)

Term	*L* = 25 km	32 km	275 km
χ^2	0.427 mm	0.895 mm	568.0 mm
χ^3	1.25 e-3	3.37 e-3	18.37
χ^4	6.57 e-7	2.25 e-6	0.106
χ^5	3.21 e-9	1.41 e-8	5.69 e-3

Clearly it is sufficient for our purposes to take only the first two terms. Table 5.4.2 shows the similar terms in Clarke's formula Equation (4.4.50).

Table 5.4.2. Magnitude of terms in Clarke's Formula. (Terms in mm.)

Term	*L* = 25 km	32 km	275 km
$(L/\nu_1)^2$	0.427 mm	0.895 mm	568.0 mm
$(L/\nu_1)^3$	1.25 e-3	3.37e-3	18.37

4.4.4.9.3 Solution of spherical triangles

In order to make use of these equations, it is necessary to be able to solve spherical triangles and triangles drawn on the ellipsoid. In this and the following sections we outline the equations for doing this. The implementation of this is described in section 5.3.3.2.1.

Suppose ABC is a spherical triangle, and suppose that its sides, in angular measure, are designated by a, b, c according to the usual convention. Thus *a* represents the length of the side BC, opposite the angle A, and so on. If the sides *b* and *c*are known, together with the included angle A, the remaining quantities *a*, B and C. may be determined. The relations between the sides and angles of the spherical triangle are well known, and can be found in standard references.

Using these, we can proceed as follows:

(i) Firstly, an application of the cosine rule gives us

cos a = cos b cos c + sin b sin c cos A

(ii) The sine rule can be written

sin A/ sin a = sin B /sin b = sin C /sin c

from which we can deduce, multiplying by sin a sin b sin c throughout

sin b sin c sin A = sin a sin c sin B = sin a sin b sin C.

The LHS is known, so we can write

sin a sin c sin B = sin b sin c sin A

sin a sin b sin C = sin b sin c sin A

(iii) Further applications of the cosine formula to the sides b an c respectively give after rearrangement

sin a sin c cos B = cos b - cos a cos c

sin a sin b cos C = cos c - cos a cos b

All the quantities on the RHS of (iii) are given apart from cos b, which is derived from (i).

Thus relations (ii) and (iii) give us expressions for the tangent or cotangent of the angles B and C, from which the angles themselves can be deduced.

B = atan2{sin a sin c sin B, sin a sin c cos B} = atan2{sin b sin c sin A, (cos b - cos a cos c)}
C = atan2{sin a sin b sin C, sin a sin b cos C} = atan2{sin b sin c sin A, (cos c - cos a cos b)}

The side a can be deduced directly from (i); but if its magnitude is small, there might be a loss of precision. In order to allow for this possibility, once B has been calculated it is possible to calculate sin *a* by a further application of the sine rule (ii);

sin a = sin b sin A / sin B

Thus using this equation the arctan function can be used.

a = atan2{(sin b sin A / sin B), (cos b cos c + sin b sin c cos A)}

4.4.4.9.4 Sign conventions

The algorithm to solve a spherical triangle just described is assumes that the sides of the triangle are less than 180° in magnitude. A triangle with this property, sometimes termed an Euler triangle, has the further property that its angles are also less than 180°. Thus the natural application of the algorithm is to the case that the sides a, b, c and angles A, B, C all have positive values between 0° and 180°.

In the application to the SLSTR processing, the algorithm is always applied to triangles whose sides are less than 180°, but it is not always the case that the included angle is positive. In particular, the routine is most frequently applied to triangles in which the apex at which the included angle (A) is defined coincides with the North pole of the Earth, and the angle A is defined by the difference of two longitudes. This longitude difference is always calculated so that its magnitude is less than 180°, but it may be negative. We should therefore discuss what happens if the algorithm is entered with the included angle A negative. This bears on the two questions of the sign convention of the azimuth, and of the consistency of the sign of azimuth angles defined at a point.

We assume throughout that the specified sides b and c are in the range 0° to 180°, so that sin b and sin c are positive. First suppose that A is specified as positive angle, in the range 0° < A < 180°. Then sin A is also positive, and the right-hand sides of the equations (ii) are positive. The angles B and C are unambiguously determined as to magnitude and quadrant by the equations (ii) and (iii) respectively on the assumption that the proportionality constant (sin a sin c) is positive; in the case under consideration this implies that the sines of B and C are positive . Thus B and C will lie in 0 to 180°. If a is then derived from the sine rule, a consistent positive value will be derived.

If now a negative value is substituted for A (i.e. if -180° < A < 0°), sin A is also negative and the right-hand sides, of the equations (ii) will be negative. Then both B and C will be found to have a negative sign (i.e. each will lie in -180° to 0°). If the sine rule is then used to determine sin a, it will be found to be positive, which is consistent with the implicit assumption that (sin a sin c) is positive. The resulting solution still satisfies the cosine law equations. Thus if the values a, b, c, A, B, C, satisfy the equations, so does the set a, b, c, -A -B, -C in which the sign of each angle is reversed. This is the solution that will be obtained if the subroutine is entered with a negative argument for a.

The sine rule is consistent if the sign of an angle and its opposite side are simultaneously reversed. The cosine rule equations are all unchanged if the signs of the angles A, B and C are reversed.

It might be noted that there is an alternative self-consistent solution of the equations. The angle -A is equivalent to 360° - A, and the triangle ABC might be interpreted as the non-Eulerian triangle of sides 2π - a, b, c. If we replace sin A by sin (360° - A) and sin a by sin(2π - a), the signs of both are reversed. The sine rule is then consistent if sin B and sin C are both unchanged, while to maintain consistency of the cosine rule equations it is necessary to reverse the signs of cos B and cos C since they appear multiplied by sin A. The corollary is that B and C must be replaced by 180 - B and 180 - C respectively, and these are the correct angles of the non-Eulerian triangle, measured inside the triangle. We do not get this solution if we enter the subroutine because it implicitly assumes that sin a is positive.

4.4.4.10 Calculation of Grid coordinates of Scan Pixel

The X and Y co-ordinates may in principle be calculated for any scan pixel, but in practice they are only directly calculated for a series of tie points, represented by every tenth pixel along each scan. The calculation makes use of the table of ground track point latitudes and longitudes described in Section 4.4.3.1.1.

Consider a pixel P. If a section is drawn through P to meet the ground track at a right angle in point X, the point X will lie between the tabular points Q[i] and Q[i+1], as shown schematically in Figure 4-11. The X co-ordinate of the pixel is then taken to be the distance PX of the pixel from the ground-track, measured along the section. The Y co-ordinate is determined from the distance, measured along the ground-track, between the i'th tabular point and the point X, which represents the difference between the y co-ordinate of X (and hence of P) and that of the i'th tabular point. Thus the distance Q[i]X is added to the Y co-ordinate of Q[i] (25i km) to give the y coordinate of P.

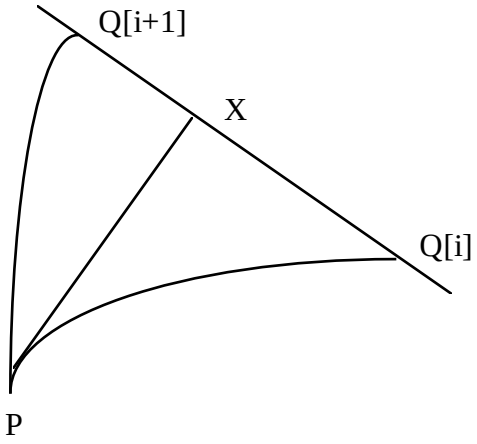

Figure 4-11

For the purposes of this calculation, the ground track between points Q[i] and Q[i+1] is regarded as approximated by the normal section between them. This is justified by the short length (16 km) of the segment; the ground track is not a geodesic, and cannot be approximated geodesic over long distances. The definition of the table of ground track points at 16 km intervals is essentially a means to by which the ground track is approximated by a piecewise continuous curve made up of 16 km segments.

4.4.4.10.1 Identification of the nearest tabular points

The first step is to identify the value of *i* corresponding to the interval within which the normal from P intersects the ground track. To be precise, this is the interval that contains a point X such that the normal section through X at right angles to the ground track contains the point P. The correct interval is determined by a test on the azimuths at the ground track points Q_i; the angle between the ground track and the PX varies continuously as the point X moves along the ground track, and therefore the correct interval is identified using the criterion that the angle of intersection passes through 90° within the interval.

Thus the intersection angle is calculated at the end-points of the interval. If the magnitude of angle PQ[i]Q[i+1] is less than 90°, and that of PQ[i+1]Q[i+2] is greater than 90°, then index *i* defines the correct interval.

To calculate the intersection angle at tabular point *i*, the azimuth of the ground track segment Q[i]Q[i+1] is first determined, then the azimuth of the great circle from Q[i] to point P. The intersection angle is given by the difference between the azimuths.

To determine the azimuth of the arc QP, the spherical triangle NPQ is solved, where N is the north pole of the Earth. If the general 'solve spherical triangle' routine (Section 5.3) is used, the length of the arc PQ and the azimuth of the arc at P are also determined as a by-product. The azimuth of the great circle segment is similarly determined by solution of the triangle NQ[i]Q[i+1].

Consider Figure 4-12. The latitudes and longitudes of the three points P, Q_1, Q_2 are known, and therefore an inverse formula can be used to derive the azimuths of P and Q_2 as seen from Q_1; in the diagram these are the angles ε and β respectively.

[One exceptional case may be accounted for; if the 180° meridian intersects the arc Q_1Q_2, the equation above for the longitude difference will give a negative value close to -360°. In this case 360° (2π) may be added to the angle (although its sine and cosine will not change, and the 'solve spherical triangle' routine will give the same answer; the issue is one of precision rather than of the form of the equations.)]

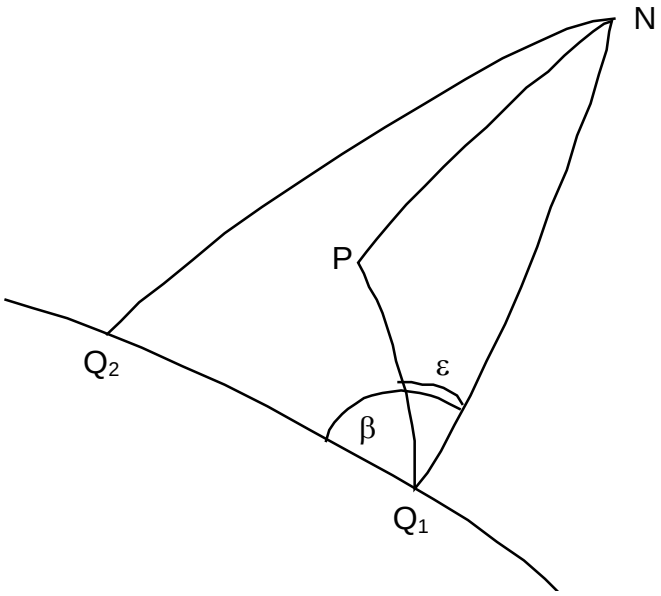

Figure 4-12

In accordance with the discussion of section 5.3.1.27, the angle β will come out in the range $0 \leq \beta < \pi$, and will represent the azimuth of the track at Q_1, measured anticlockwise from north. Similarly ε will represent the azimuth of P seen from at Q_1, according to the same sign convention. The difference $\beta - \varepsilon$ (reduced into the range $-\pi$ to π if necessary) represents the required intersection angle PQ_1Q_2.

Thus starting from a specific tabular point *i*, the intersection angle at point Q[i] is calculated. If its magnitude is less than 90°, the intersection angle at point Q[i+1] is then calculated. If this is greater than 90° the interval between *i* and *i* +1 is the required interval; otherwise the process steps in the direction of increasing *i* until the correct interval is found. If the magnitude of the intersection angle at the initial point *i* is greater than 90°, the intersection angle at point Q[i-1] is calculated. If this is less than 90° the interval between *i*-1 and *i* is the required interval; otherwise the process steps in the direction of decreasing *i*, still until the correct interval is found.

Although this process will work regardless of the initial value of *i*, a well-chosen initial value will improve the efficiency of the process by minimising the number of trials. For a given scan, an initial value for the first tie point pixel can be estimated from the known y coordinate of the sub-satellite point. Thereafter, as the tie point pixels are calculated regularly along the scan, the value of i found for one pixel can be used as the starting point for the next.

Once the correct interval has been found, the sign of the difference $\beta - \varepsilon$ (reduced into the range $-\pi$ to π if necessary), at either end-point, determines on which side of the ground track the pixel P lies, and therefore the sign of the x co-ordinate of P. If $(\beta - \varepsilon)$ is positive, then the point P is to the right (east) of the ground-track and its x co-ordinate will be positive. If $(\beta - \varepsilon)$ is negative, then the point P is to the left (west) of the ground-track and its x co-ordinate will be negative.

Some comments on the actual implementation of this test are appropriate here. Note first of all that the angle β will always be positive (i.e. $0 < \beta < 180°$) because the retrograde ground track always has a westwards component. The angle ε, however, may be negative. If ε is positive, then the difference $(\beta - \varepsilon)$ always lies in $-180° < \beta - \varepsilon < 180°$ and its sign and modulus give the required values.
If ε is negative, then $0° < (\beta - \varepsilon) < 360°$. If this is less than 180° it is already in the reduced range and we can return its sign and magnitude as before. If it is greater than 180° the angle should have 360° subtracted first. An equivalent approach is that the required magnitude is $360° - (\beta - \varepsilon)$ and the sign is negative. The table below summarises the situation. The algorithm explicitly tests these four cases.

	$(\beta - \varepsilon) > \pi$	$(\beta - \varepsilon) < \pi$
$\varepsilon < 0$	magnitude = $2\pi + (\varepsilon - \beta)$ sign negative	magnitude = $(\beta - \varepsilon)$ sign positive
	$\beta < \varepsilon$	$\beta > \varepsilon$
$\varepsilon > 0$	magnitude = $(\varepsilon - \beta)$ sign negative	magnitude = $(\beta - \varepsilon)$ sign positive

4.4.4.10.2 Calculation of the sides of the triangle

Once the correct interval Q_1Q_2 has been identified, the co-ordinates X, Y may be calculated. The latitude and longitude of each point P, Q_1 and Q_2 are known, and therefore the length of each side of the triangle PQ_1Q_2 can be determined by means of an inverse formula.

This process is applied in turn to each of the three sides of the triangle PQ_1Q_2. The triangle is then fully determined and any of its angles can be found. However, this is a triangle on the spheroid, .and if we are to base our computations on ellipsoidal geometry, we must use a self-consistent method for solving the triangles. The method adopted is described in the following section.

4.4.4.10.3 Solution of Ellipsoidal triangle.

There is no exact method for treating this case, and so the solution must be based on an approximation. The approximation adopted is based on Legendre's theorem, or more strictly on its extension to the spheroid.

Legendre's Theorem is a result relating to spherical triangles. It is well known, and is not difficult to prove, that the area of a spherical triangle is proportional to the spherical excess of the triangle; this is the amount by which the sum of its three angles exceeds π radians (180°). Thus, suppose ABC is a triangle drawn on a sphere of radius *R*. The sum of the angles A, B and C will exceed π by the amount

$$E = (A + B + C) - \pi.$$

Then the area of the triangle ABC is ER^2, where *E* is in radians. This result is exact.

Let the sides of the triangle ABC be *a*, *b*, *c* and consider the auxiliary plane triangle A'B'C' that has sides of the same length as ABC. The angles of A'B'C' will of course add up to π;

$$A' + B' + C' = \pi.$$

Legendre's theorem states that to a good approximation for sufficiently small triangles the area of the auxiliary plane triangle A'B'C' is the same as that of the spherical triangle ABC, and that each of its angles can be derived by reducing the corresponding angle of the spherical triangle by one-third of the spherical excess. Thus

$A' = A - E/3$

and similarly

$B' = B - E/3$

$C' = C - E/3$.

It follows that any problem in spherical trigonometry can be reduced to an equivalent problem in plane trigonometry by reducing the angles according to the above equations.

It can also be shown (Bomford [RD-13]) that Legendre's theorem can be extended to triangles on the ellipsoid. Thus the statements above are true (to an appropriate approximation) if the triangle ABC is drawn on the ellipsoid, where that the sides of the triangle are defined as the geodesics joining the vertices A, B, C. In this case the area of the triangle is given by the expression ER^2 as above provided a suitable value for the radius is given. Bomford [RD-13] gives the mean radius

$$R = \left\{\tfrac{1}{3}\left(1/(\rho_1\upsilon_1) + 1/(\rho_2\nu_2) + 1/(\rho_3\upsilon_3)\right)\right\}^{-1/2},$$

in which the subscripts 1, 2 and 3 refer to the three vertices A, B and C, and also gives higher order terms for this case. There are two consequences of this.

(1) Any trigonometric calculation on the spheroid may be reduced to a plane calculation by correcting the angles by $E/3$ as above.
(2) Because the relationship of the angles of the spheroidal triangle to those of the auxiliary plane triangle are the same as those of the angles of a spherical triangle having the same sides on a sphere of radius R, it follows that to the extent that the higher order terms are negligible, we may use the formulae of spherical trigonometry to solve the spheroidal triangle, if we work with the corrected angles.

4.4.4.10.4 The angle at Q

We now return to the solution of the triangle PQ_1Q_2. Thus far our calculation has been exact, to the extent that sufficient terms of the expansion in (equation 5.4.46) have been used, given that the lengths so determined will be normal section lengths. The next step is to compute the angle at Q_2.

The length of the normal section differs from that of the geodesic by a negligible amount for sufficiently short lines, and so we can regard the lengths calculated above as geodesic lengths, and can regard them as the lengths of the auxiliary plane triangle. We can therefore use Legendre's theorem to derive the angles of the geodesic triangle PQ_1Q_2.

The area of the auxiliary plane triangle is given exactly by a standard formula of plane trigonometry:

$$s = (s_{12} + s_{2p} + s_{p1})/2$$

$$A = \sqrt{s(s - s_{12})(s - s_{2p})(s - s_{p1})}$$

and so the spherical excess is $E = A/R^2$.

By plane trigonometry the angle at Q_2' in the plane triangle is

$$Q_2' = 2 \times \arctan\left\{\sqrt{\frac{(s - s_{12})(s - s_{2p})}{s(s - s_{p1})}}\right\}$$

hence the angle at Q_2 is this + E/3.

We now use the precept (2) above to use the formulae of spherical trigonometry to calculate the x and y co-ordinates. (Strictly this gives us geoid lengths to the point X" at which the geoid through P is orthogonal to the ground track, but the errors are small). It is this final stage that is the most difficult to quantify, but the errors are unlikely to be large in comparison with those due to the assumption that the ground track proper in an interval can be replaced by either the normal section or geodesic between the end-points.

4.4.4.10.5 The x and y co-ordinates

Given the side Q_2P (q_1) and the angle Q_2, the right-angled triangle PQ_2X (Figure 4-11) is fully determined, and the arcs PX and Q_2X can be calculated. The arc PX is determined by an application of the sine rule.

$$\sin (PX) = \sin (PQ_2) \sin Q_2. \qquad (4.4.55)$$

The side Q_2X is determined by an application of the cosine rule to the right-angled triangle.

$$\cos (PQ_2) = \cos (PX) \cos (Q_2X)$$

so

$$\cos (Q_2X) = \cos (PQ_2) / \cos (PX) \qquad (4.4.56)$$

The arc lengths ξ, η can be determined by multiplying the angular lengths PX and Q_2X respectively by the radius of the earth:

$$\xi = R (PX) \qquad (4.4.57)$$

$$\eta = R (Q_2X) \qquad (4.4.58)$$

The sign of the x co-ordinate of P is determined by inspecting the sign of the angle (β - ε) derived at the last value of i above. Then the x and y co-ordinates of P, expressed in km, are

$$x = (\text{sign of } x)\ \xi \qquad (4.4.59)$$

$$y = 25i + (25 - \eta) \qquad (4.4.60)$$

5 ALGORITHM DESCRIPTION

5.1 LEVEL 0 PROCESSING FOR THE SLSTR INSTRUMENT

5.1.1 The SLSTR Instrument Science Packet

The raw SLSTR instrument data are delivered in binary Instrument Source Packets (ISPs). There are 13 distinct types of ISP,

- Nine optical channel packets (S1 – S9),
- Two fire channel packets (F1, F2),
- One scan packet,
- One housekeeping packet.

All except the housekeeping packet are further differentiated by one of eight target IDs which identify the instrument view and scene from which the packet data is collected, giving a total of 97 distinct ISPs. A total of ten packets are generated for each optical channel and for the scan position in each “cycle”, corresponding to two complete revolutions (“scans”) of the scan mirrors. This is the shortest non-repeating instrument data cycle. One housekeeping packet is generated per scan, or two per cycle.

The ISPs for channels S1 – S9, F1 and F2, and for the scan ISP, may be of variable length, dependent on the pixel map loaded into the instrument processor, up to a well-defined maximum value.

Each ISP will be formatted as a Space Packet following the description given in the CCSPS Space Packet Protocol [RD-8]

The ISP will form the cargo of a SpaceWire packet [RD-8].

The information required to identify the source packet is contained in one of three contiguous headers:

- The Space Packet Primary Header,
- The Packet Utilisation Standard (PUS) Data Field Header,
- An Auxiliary Header which forms part of the packet content.

The primary header contains the PCAT (Table 5-1), a code with value 0 – 15 which identifies the packet type, and the number of packet bytes following the primary header, minus one.

PCAT	ISP Content	Band	Type
0	Channel S1	555nm	0
1	Channel S2	659nm	8
2	Channel S3	865nm	16
3	Channel S4	1.375µm	24
4	Channel S5	1.61µm	32
5	Channel S6	2.25µm	40
6	Channel S7	3.74µm	48
7	Channel S8	11.85µm	56
8	Channel S9	12µm	64
9	Channel F1 (fire)	3.74µm	72
10	Channel F2 (fire)	11.85µm	80
11	Scan position	–	88
12	Housekeeping	–	96

Table 5-1: Assignment of ISP PCAT codes (adapted from [RD-5]). Type is an index value assigned to the PCAT code to allow consistent ISP unpacking in the GPP.

The data field header contains a time stamp derived from the spacecraft clock. This time stamp is updated at cycle acquisitions 0 and 3670 (the first acquisition of each scan) and is identical for all packets associated with the scan.

The definition of the auxiliary header varies between packet types, but the first nine bytes are common to all packet types except for the housekeeping packet.

Content	Length (bytes)
DPM mode	1
Target ID	1
Target first acquisition	2
Target length	2
Validity	1
Scan sync counter	2

Table 5-2: ISP “common” auxiliary header (extracted from [RD-5]).

This “common” auxiliary header (Table 5-2) contains a target ID (Table 5-3) which identifies the instrument view from which the science content was collected. The first scan of each cycle contains the observation sequence D0h, B0h, A1h, C1h, A0h, and the second scan contains the observation sequence B1h, D1h, A1h, C0h, A0h.

Target ID	View	Scene	Type
A0h	Nadir	Swath	0
A1h	Oblique	Swath	1
B0h	Nadir	BB1	2
B1h	Oblique	BB1	3
C0h	Nadir	BB2	4
C1h	Oblique	BB2	5
D0h	Nadir	VISCAL	6
D1h	Oblique	VISCAL	7

Table 5-3: Assignment of ISP target IDs to instrument views (extracted from [RD-6]). Type is an index value assigned to the target ID to allow consistent ISP unpacking in the GPP.

Our understanding of the ISP content is summarised in

Figure 5-1 and Table 5-4. The first shows the derivation of the packet information and the associated naming conventions, while the second expands the information into a byte- and bit-ordered table.

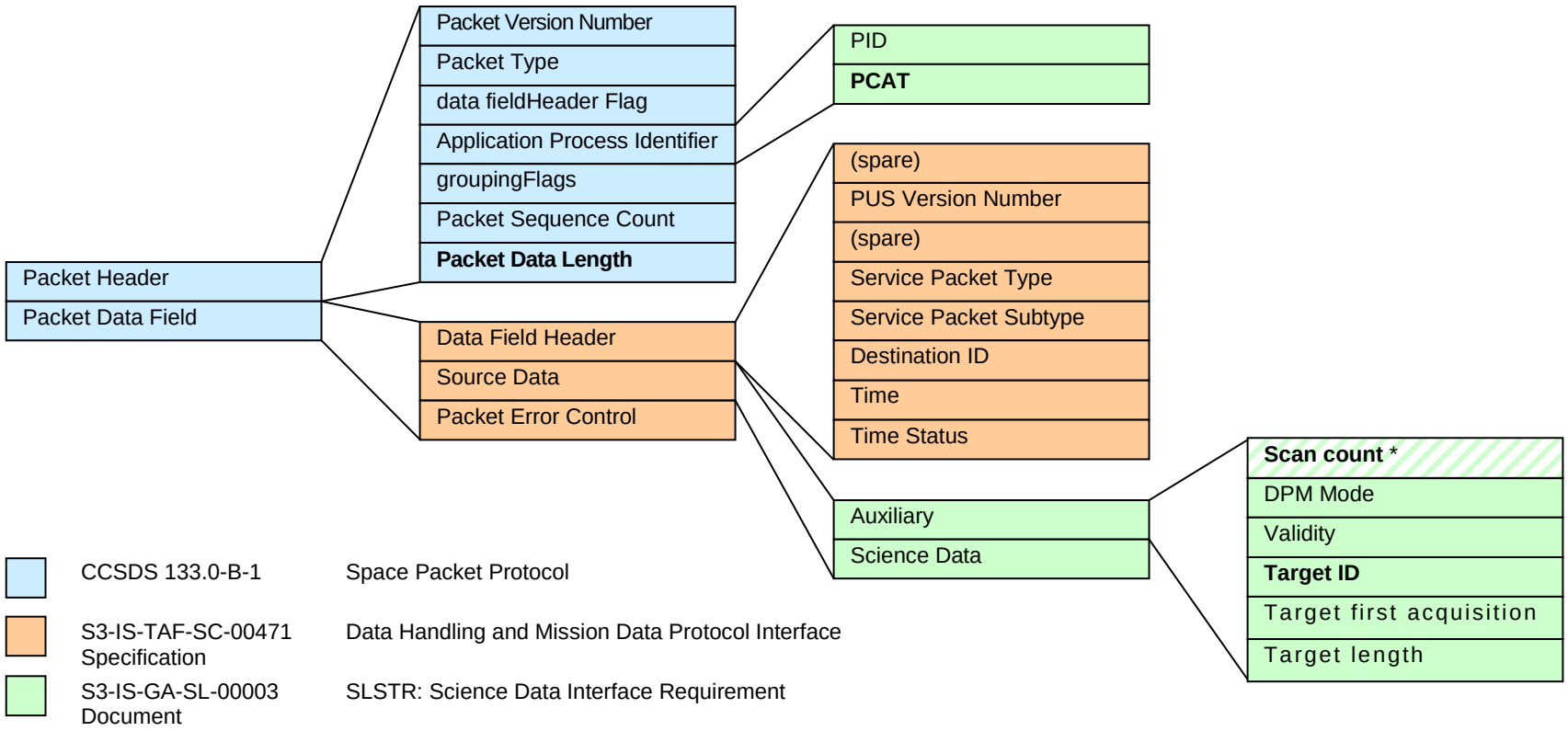

Figure 5-1: The provisional SLSTR Instrument Science Packet (ISP). Sources of information are indicated by colour. Information required to unpack the ISPs are highlighted with bold type. A scan count* is not yet defined in the auxiliary header.

Name	Size (byte.bit)	Value
Packet Version Number	0.3	000b
Packet Type	0.1	0b
Secondary data field Header Flag	0.1	1b
PID	0.7	4Ah
PCAT	0.4	0h – Ch
groupingFlags	0.2	11b
Packet Sequence Count	1.6	
Packet Data Length	2.0	(= n_{PDL})
(spare)	0.1	
PUS Version Number	0.3	001b
(spare)	0.4	
Service Packet Type	1.0	201dec
Service Packet Subtype	1.0	31 dec
Destination ID	1.0	0 dec
Time	7.0	
Time Status	1.0	0dec or 1dec
Scan count	2.0	0-65536
DPM Mode	1.0	0 or 1
validity	…	0 or 1
Target ID	1.0	00h-FEh
Target first acquisition		0-7339
Target length		0-1599
Science Data	n_{PDL} − 23	
Packet Error Control	2.0	

Table 5-4: Provisional SLSTR Instrument Science Packet (ISP). For sources of information, refer to Figure 5-1. Information required to unpack the ISPs are highlighted with bold type.

5.1.1.1 Comments

The content of the ISP is provisional. In particular, we have requested a scan counter (not currently defined) to order the packets and to disambiguate those packets which are generated every scan (housekeeping packet, S1 – S9, F1 and F2 nadir and oblique swath packets). We have also suggested that the housekeeping packet should be assigned the “common” anciliary data fields (including at least the scan count and a dummy target ID) so that, for all packet types, a single read can be used to extract all the header information required to unpack the packets.

5.1.2 The SLSTR Level 0 ISP Product

The SLSTR Level 0 ISP product will consist of:

- An ISP-specific XML header,
- Unaltered copies of the binary ISP file or files generated by the instrument or the instrument simulator,
- A searchable XML index to the positions of the ISPs within the binary files.

5.1.2.1 ISP File Unpacking

We presume that the raw binary ISP byte stream(s) will be contained in one or more binary files and that a list (XML or text) of these files will be provided. The following scheme can ingest, unpack and index any configuration of input files (including a single file) without modification.

1. Calculate the size of the unpacked data array:
    a. Extract the scan number of the first and last scan in the dataset and calculate the number of scans in the unpacked array:

        ```
        n_scan = last.scan_count – first.scan_count + 1
        ```

        Size `n_scan` must be calculated in unsigned integer arithmetic compatible with the definition of the scan counter to cope correctly with counter wrapping.

    b. Assign the number of distinct ISP types:

        ```
        n_type = 97
        ```

2. Create output arrays of dimension `array[n_scan][n_type]` to hold:
    a. the ISP headers,
    b. the ISP content,
    c. FEP annotations *,
    d. quality flags,
    e. file handles,
    f. file offsets.
3. Initialise all quality flags:

    ```
    quality[][].packet_absent = 1
    ```

4. Read in the names of the files containing the ISP data and for each ISP file, assign a unique file handle, `f` (this could just be the index to the file list).
5. For each file, step through the individual ISPs and for each ISP:
    a. Note the file pointer value, p
    b. Read the fixed-length file header(s), h
    c. Calculate the array indices:

        ```
        i = h.scan_count – first.scan_count
        j = ISP_type(h.PCAT, h.target_ID)
        ```

Index `i` must be calculated in unsigned integer arithmetic compatible with the definition of the scan counter to cope correctly with counter wrapping. ISP_type returns the sum of the type values in Table 5-1and Table 5-3.

d. Calculate the length of the remaining variable-length ISP content:

```
n = h.data_length + 5 – n_header
```

where `n_header` is the size of the fixed length header(s), and read n bytes of ISP content into the content array, `content[i][j][]`

e. Read the error control value, c

f. Copy the ISP header(s), file handle and offset to the out put arrays:

```
header[i][j] = h
handle[i][j] = f
offset[i][j] = p
```

g. Perform quality checks * and copy results into the quality flag array:

```
quality[i][j].packet_absent = 0
quality[i][j].CRC_failed = CRC_check(p, n, c)
  ...
```

At least the “packet absent” flag must be implemented to enable null entries to be interpreted correctly.

5.1.2.1.1 Comments

No additional annotation information is required to unpack the ISP files. As the L0 ISP content is identical to the raw ISP files, the unpacking scheme can be applied equally to raw ISP or Level 0 ISP files.

No FEP simulation is envisaged within the GPP perimeter [RD-10]. The L0 product description includes FEP annotations, but we are not aware of the content. We have included a notional annotation array in the unpacking scheme as a placeholder.

We have proposed that the simulator should forward the first and last packet headers as summary information and that in operation the FEP should do the same, but if these are not available, a modified approach will be required. Possibilities include:

1. Make a preliminary pass through the ISP files to identify the first and last packets,
2. Define an oversized “circular” scan array with the maximal number of entries (for a two-byte scan counter, this would be `n_scan = 65536`), and identify the first packet after unpacking,
3. Define a slightly oversized “circular” scan array (for one orbit, `n_scan ~ 20000`), begin filling from an arbitrary point (`i = 0`, say, for the first processed ISP) , and identify the first packet after unpacking.

Regardless of method, once the index of the first scan containing data has been identified, all subsequent processes are unchanged (with the exception of some minor indexing arithmetic).

The GPP perimeter document [RD-10] does not require quality checking, on the assumption that the input stream is perfect, but the following ISP checks are performed:

Set all flags for the ISP to 0 (i.e. all OK)

1. CRC check

   The CRC check will follow the scheme as defined in Annex A of ECSS--E--70--41A

   If error is present then

   CRC Error flag for ISP(i) = 1b

2. Consistency of the scan count with the time stamp,

   The test to be performed checks that the time interval between successive scans is nominally 301ms as follows.

   Note: Care has to be taken to account for the wrap around of the packet sequence counters and instrument scan counters that should occur every 2^16 scans. If a negative value is detected add 2^16 to the value before comparing.

   Δt = (time(scan_n)-time(scan_n-1))/(scan_count(scan_n)-scan_count(scan_n-1))

   IF($\Delta t \neq 301 \pm dt$) then

   scan_count_discontinuty flag for scan_n = 1b

   Where dt is the resolution of the on board clock

3. Valid fixed header information

   If(fixed_header_value(ISP(i)) ≠ expected_fixed_header_values) then

   Header_Error(ISP(i)) = 1b

4. Valid PCAT codes,

   This test checks that the Packet IDs contained in the ISPs fall within the expected range. Values outside this range could indicate a non standard instrument configuration.

   If(PCAT (ISP(i)) >Chex) then

   Invalid_PCAT(ISP(i)) = 1b

5. Valid target ID codes

This test checks that the target IDs contained in the ISPs fall within the expected range. According to RD-6, the baseline set of target ID's falls in the range A0h to D1h. Values outside this range could indicate a non standard instrument configuration.

If(Target_ID(ISP(i)) lies outside of range 0Fh to D2h) then

Invalid_Target_ISP(ISP(i)) = 1b

6. Consistent sequence counter values

This test checks that the packet counter is increasing monotonically. A difference between successive packets not equal to 1 could indicate a missing packet or data out of sequence.

Note: As with step 2, care are has to be taken to account for the wrap around of the packet sequence counters and instrument scan counters that should occur every 2^14 scans. If a negative value is detected add 2^14 to the value before comparing.

If(seq_count(isp(i))-seq_count (isp(i-1)) ≠ 1 then

Sequence_Error(isp(i)) = 1b

7. Duplicate packets.

This test checks that the packet is not a duplicate of one previously processed. The test compares the sequence_count, scan_count and crc_error, time of the ISP against the previous value. If all fields are identical then the packet shall be flagged as duplicate and is not to be used in the processing.

Duplicate_Packet(isp(i)) = 1b

5.1.2.2 ISP Index File

The ISP index file is a binary auxiliary file which contains an ordered and searchable list of references to the positions of the ISPs within the binary ISP files associated with the product and a limited amount of information about the individual ISPs, including the ISP size, APID (decoded to a channel), target ID (decoded to a view and scene) and time stamp. The product is described in [RD-11].

The ordering and hierarchy of the ISP entries in the cycle list is essentially the same as that of the ISP entries in the unpacked ISP array, so the contents of the index file can be built up by parsing the ISP array. We presume that the unpacked ISPs are organised in a two-dimensional array, ordered by type and scan, as described in the previous section. For each scan, there are 97 array elements corresponding to the 97 distinct combinations of channel (PCAT) and target (target ID). Reading by type and then by scan, they are ordered by target, then by channel (including scan position and housekeeping), then by scan, then by cycle.

5.1.2.2.1 Writing the ISP Index

The ISP index contains three principle elements: introductory metadata, a list of ISP files and a list of ISPs, including file references and a limited amount of information to allow the list to be searched. An XML entry is opened with a `<tag>` and closed with a `</tag>`.

1. Open the index entry.
2. Write any metadata entries (product name, processor version, generation time *etc*.).
3. Write the file list.
4. Write the ISP list.
5. Close the index entry.

5.1.2.2.2 Writing the File List

The purpose of the file list is to associate a file handle with each ISP file URL. This handle will then be used as a shorthand reference in the following ISP list. The only requirement on the handles is that they be unique for each ISP file associated with the product.

1. Open the file list entry.
2. For each file:
    a. Open the file entry,
    b. Write the file URL entry,
    c. Write the file handle entry,
    d. Close the file entry.
3. Close the file list entry.

5.1.2.2.3 Writing the ISP List

This section describes a parsing scheme to construct the ISP list from the array of unpacked ISPs.

1. Open the ISP list entry.
2. Step through the array elements in the order:

```
for (i = 0; i < n_scan; i++) for (j = 0; j < n_type; j++)
{...}
```

3. For each valid element, except for the first:
    a. Always close the current target entry.
    b. If the channel has changed from the previous array element, close the current channel entry.
    c. If the scan has changed from the previous array element, close the current scan entry.
    d. If the cycle has changed from the previous array element, close the current cycle entry.
4. For each valid element:
    a. If the cycle has changed from the previous array element:
        i. Open a new cycle entry,

ii. Write the cycle number entry, using the value of `header[i][j].scan_count >> 1`.

b. If the scan has changed from the previous element:

i. Open a new scan entry,

ii. Write the cycle number entry, using the value of `header[i][j].scan_count`,

iii. Write the time stamp entry, using the value of `header[i][j].time`.

c. If the channel has changed from the previous array element:

i. Open a new channel entry,

ii. Write the channel name entry, using one of: `"S1"`, `"S2"`, `"S3"`, `"S4"`, `"S5"`, `"S6"`, `"S7"`, `"S8"`, `"S9"`, `"F1"`, `"F2"`, `"scan"` or `"AUX"`, dependent on the value of `header[i][j].PCAT` (Table 5-1).

d. Always:

i. Open a new target entry,

ii. If not a housekeeping packet, write the instrument view, using one of: `"nadir"` or `"oblique"`, dependent on the value of `header[i][j].target_ID` (Table 5-3),

iii. If not a housekeeping packet, write the instrument scene, using one of: `"swath"`, `"BB1"`, `"BB2"` or `"VISCAL"`, dependent on the value of `header[i][j].target_ID` (Table 5-3),

iv. Write the file handle entry, using the value of `handle[i][j]`,

v. Write the ISP offset entry, using the value of `offset[i][j]`,

vi. Write the ISP size entry, using the value of `header[i][j].data_length + 7`.

5. After the last entry has been written, and if at least one entry has been written:

a. Close the current target entry

b. Close the current channel entry,

c. Close the current scan entry,

d. Close the current cycle entry.

6. Close the ISP list entry.

5.1.2.2.4 Comments

Most metadata will be placed in separate general and ISP-specific XML headers [RD-10]. Only minimal metadata information is envisaged for the XML index file.

It is in principle possible to extract additional information from the ISPs and the unpacking process and to include it as additional entries in each target entry. Possible candidates include the quality flags and FEP annotations, if available. However, it is assumed here that only the information required to distinguish and extract the different “flavours” of ISP (PCAT/target ID) is needed and that any further information will be taken directly from the ISPs themselves.

The beauty of the XML schema is that additional information can be introduced if required at a later stage with minimal modification to the existing XML writing process or to any reading tools, as the index is not format-dependent. It also copes straightforwardly with missing ISPs.

5.1.3 NAVATT File Processing

The structure of the NAVATT packets is described in RD-14. Assuming the simulator output includes a file containing NAVATT ISPs, the L0 processing scheme described in section 5.1.2 can be employed. Also refer to 5.4.3.2.2.

5.2 OVERVIEW OF LEVEL 1B PROCESSING FOR THE SLSTR INSTRUMENT

The following description of the expected SLSTR data processing is based on that used for the AATSR instrument processing facility, suitably modified. This is appropriate since the basic functionality of the SLSTR instrument is derived from that of AATSR, and so the necessary processing steps are largely unchanged. Moreover the algorithms are well-established and provide a robust baseline for the operational applications of the SLSTR instrument. The detailed algorithms will require amendment and possible enhancement to accommodate the higher ground sampling and wider swath widths of the SLSTR instrument.

Figure 5-2 and Figure 5-3 show an overview of the Level 1b processing.

The SLSTR Level 1 processor will operate on segments of Level 0 data of approximately one orbit. In the case of NRT data this may represent the data between downlinks to the ground station; for consolidated data it will be a segment of data slightly longer than the interval between consecutive ascending nodes. The data stream must exceed a single orbit because of the displacement of the nadir and oblique views and the curvature of the instrument scans; for example, if the oblique view is directed backwards, the oblique view at the end of the orbit is measured after the sub-satellite point has passed the ascending node.

The Level 0 data product will comprise a series of records presented in chronological sequence, each containing a single instrument source packet. It is assumed that each source packet represents the two scans (nadir and oblique) of a synchronous pair. With the exception of the determination of calibration parameters, which will be derived from the average across a range of scans, the data processing up to but not including the re-gridding stage will treat each source packet independently. For the visible channel calibration, the channel gains will be determined once per orbit by averaging over the block of scans for which the VISCAL target is visible.

In the following we give a brief description of each major processing stage, and an indication of the requirement for auxiliary data by that step.

5.2.1 Level 1a Processing

Figure 5-2 summarises these processing steps.

Source Packet Processing (Stages 1 - 6)

The purpose of these steps is to unpack and validate the source packet data and convert it to engineering units for the higher processing levels that generate the products and geolocate the data. The main functions of these steps can be summarised as follows:

1. Source Packet Quality Checks: Performs basic quality checks on each raw packet, ensuring that only those that pass the checks contribute to the product.
2. Unpack Anciliary Data: Unpacks all required anciliary and housekeeping data including the temperatures of the on-board black bodies and instrument health and status information.
3. Validate Unpacked Anciliary Data: validates the unpacked anciliary and housekeeping data.
4. Convert Unpacked Anciliary Data: Converts to engineering units those items of anciliary data, including the temperatures of the on-board black bodies and other instrument temperatures and data items, for which a conversion to engineering units is defined.
5. Validate Converted Anciliary Data: Validates those converted anciliary data items that are essential to the calibration.
6. Science Data Processing: Unpacks and validates the science data containing the earth view and black body pixel counts for all available channels from each packet. Correction for signal channel non-linearity is applied at this stage.

The inputs, outputs, and relationship between each Stage are summarised in Figure 5-2

The following auxiliary input data sets are required by these processing stages:

- Level 1B Processor Configuration File: defines processor configuration data, internal error codes and other items.
- SLSTR Instrument Data File: defines source packet data structures, validation parameters and engineering unit conversions for the SLSTR instrument.

Infra-Red Channel calibration (Stage 7)

7. Infra-red Channel Calibration: This step calculates the calibration offset and slope that describe the linear relationship between pixel count and radiance for the thermal IR channels. The parameters are determined from the black body pixels counts and the black body temperatures, and the process makes use of look-up tables for the conversion of temperature to radiance.

The following auxiliary input data set is required by this processing stage:

- SLSTR Calibration Data File: defines temperature to radiance look-up tables and non-linearity correction tables for the SWIR channels where required.

Solar Channel calibration (Stage 8)

8. Solar Channel Calibration: This step unpacks the VISCAL data once per orbit (if present), when it is detected that the VISCAL unit is in sunlight, and calculates calibration parameters for all visible channels. These calibration parameters may not be not used to calibrate the science data in the visible channels for the current orbit (which may make used of VISCAL

data from a previous orbit), but are written to the Visible Calibration Coefficients ADS in the GBTR product.

The following auxiliary input data set is required by this processing stage:

- Visible Calibration Data File: the Visible Calibration Coefficients ADS from a previous orbit.

Satellite Time Conversion (Stage 9)

9. Satellite Time Conversion: The OBT associated with each the SCANSYNC pulse of each source packet is GPS time in CCSDS standard format. This is converted to UTC using Earth Explorer CFI libraries using time correlations data in an ADF. The time of each pixel is also calculated.

Geolocation (Stages 10-18)

Stages 10 to 18 relate to establishing the product grid and geo-locating the tie-point pixels to the geoid. Note that these steps are independent of the information contained in the instrument source packets.

10. Generate the quasi-cartesian product grid. This stage, which is called only once in the processing computes the following tables for the later geolocation and regridding stages: (i) the latitude, longitude, and y co-ordinate of a series of sub-satellite points that define the satellite ground track and (ii) the latitudes and longitudes of a rectangular grid of tie points covering the satellite swath.
11. Determine Sentinel 3 Orbit: This Stage uses the CFI with the NAVATT to determine the position and orientation of the platform at the time of each pixel of every scan.
12. Calculate times for each tie point pixel.
13. Compute scan angles for each tie-point pixel in the scan.
14. Compute LoS for each tie-point pixel
15. Geolocate Tie-Point Pixels: Geolocation to the geoid is performed at the tie point pixels for each scan.
16. Calculate Tie Point pixel x and y coordinates: The x-y (across-track and along-track) coordinates of each tie point pixel are derived from the pixel latitude and longitude.
17. Interpolate x and y coordinates for each scan, pixel and detector element. These x and y coordinates will be used for the pixel regridding.
18. Calculate Solar and Viewing Angles: Solar and viewing angles required for cloud clearing are also determined at this stage. The angles are calculated using the CFI at the tie point pixels.

OrthoGeolocation (Stages 19-23)

Steps 19-23 define the steps for ortho-geolocating the instrument pixels and use the scan encoder telemetry to determine the pixel LoS.

19. Calculate times for each pixel in the ISPs
20. Get scan angles for each pixel in the ISPs
21. Compute LoS for Each Instrument Pixel
22. Geolocate Pixels: Orthogeolocation is performed on each pixel of each scan using the scan encoder telemetry and detector LoS.
23. Calculate Pixel *x* and *y* co-ordinates: The x-y (across-track and along-track) coordinates of each pixel are derived from the pixel latitude and longitude. These pixel x and y coordinates are retained on the measurement grid.

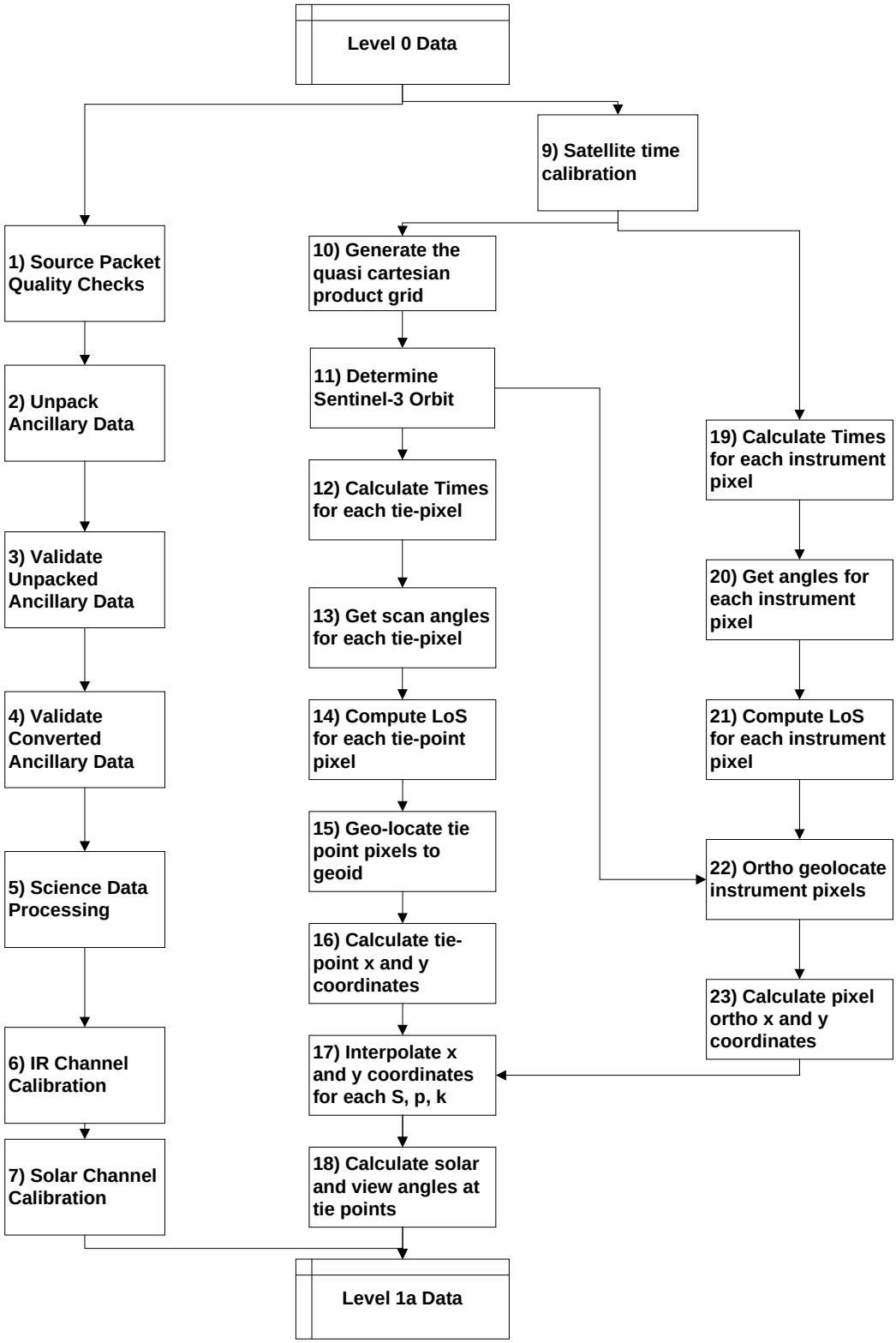

Figure 5-2: Level 1a Processing

5.2.2 Level 1b Processing

Figure 5-3 summarises these processing steps.

Signal Calibration (Stage 24)

24. Uncalibrated scan pixels are calibrated using calibration coefficients derived earlier. Pixel calibration uses these calibration coefficients to convert the pixel data to brightness temperature, in the case of the infra-red channels, or to radiance in the case of the visible and near-visible channels.

The following auxiliary input data set is required by this processing stage:

- SLSTR Calibration Data File: defines radiance to temperature look-up tables and non-linearity correction tables for the SWIR channels where required.

Time Domain Averaging (Stage 25)

25. In order to provide resolutions of 500 m in the SWIR channels, the design of the current FPA for these channels incorporates a 2 by 4 array of detectors, the long edge being aligned in the along-track direction. As a consequence, the swath is effectively scanned twice in the across-track direction, once by each column of the detector array, and so it is appropriate to perform averaging on these duplicate samples to reduce noise. Note that at the swath edge the pixels of the resultant averaged image will be distorted, but the individual plnes will be retained to support level 1c processing.

    Note that this step follows signal calibration so that the averaging is applied to calibrated reflectances. This is because the calibrations of the detectors in the two columns may differ.

Regrid Pixels (Stage 26)

26. Calibrated SLSTR pixels are regridded into co-located oblique and nadir images, onto a 1 km grid using the pixel positions derived previously. The process used in (A)ATSR processing has migrated instrument pixels to the nearest grid point. This is an input-driven process, in the sense that the process loops over input pixels, and is a highly efficient process in computational terms, but it has been suggested that an output-driven process (looping over image pixels) would present advantages. If such an algorithm were adopted, the next process (cosmetic fill) would not be required.

Cosmetic Fill (Stage 27)

27. Cosmetic filling of nadir/oblique view images is performed, to fill missing image pixels. Note that this step should only be used where there is an adjacent filled pixel and not for large areas of missing data.

Image Pixel Positions (Stage 28)

28. Linear interpolation is performed to determine the latitude and longitude coordinates of the grid pixels for use in the subsequent stages.

Determine Land-Sea Flag (Stage 29)

29. Given the image pixel latitude and longitude, the surface type for each instrument pixel is derived using the land/sea flagging algorithm.

The following auxiliary input data set is required by this processing stage:

- Land-Sea Mask Data File.

Cloud clearing (Stage 30)

30. The cloud-clearing algorithms are used to identify image pixels as cloudy or cloud-free. Baseline AATSR processing uses nine independent tests based on the AATSR suite of channels, and has recently been expanded by the addition of a new visible channel test. The additional channels proposed for SLSTR will permit additional tests yet to be specified.

The following auxiliary input data sets are required by this processing stage:

- Land-Sea Mask Data File.
- Cloud LUT Data File: contains look-up tables used by the cloud clearing tests.

Meteo annotations (stage 31)

This processing step aims to provide annotation data at a subset of the product pixels, referred to as the tie points grid. These annotations mainly concern acquisition geometry and meteorological data that are required by Level 2 processing.

Summary ADS (stage 32)

This processing step aims to provide annotation data at a subset of the product pixels, referred to as the tie points grid. These annotations mainly concern acquisition geometry and meteorological data that are required by Level 2 processing.

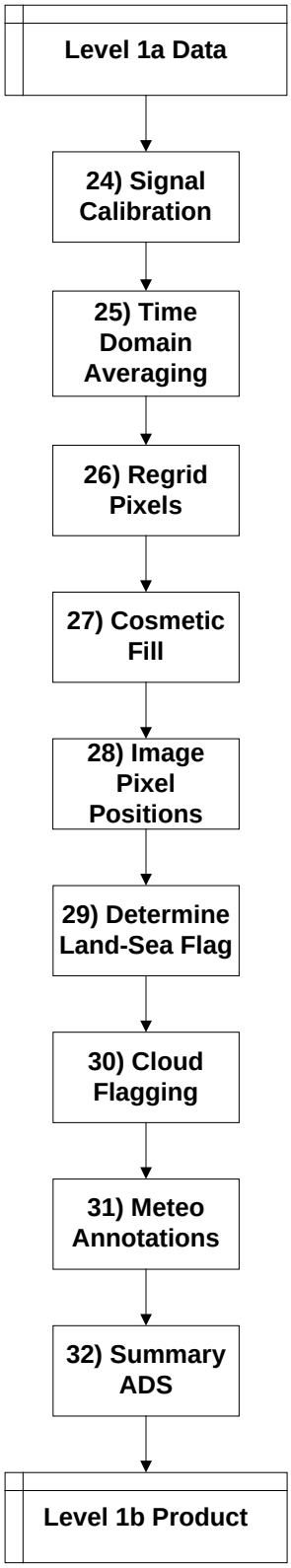

Figure 5-3: Level 1b Processing

5.3 GEO-REFERENCING

The processing modules described in this section, which are a sub-set of those classified as Level 1a processing algorithms, are concerned with aspects of geo-location.

Geo-referencing or geo-location determines the location on Earth of the instrument samples. Taking the satellite orbit data as given, the geo-location of a given pixel depends only on the scan position of the pixel and the measurement time, so that the geo-location is largely independent of the other processing, and can be applied as soon as these quantities have been decoded.

For each view (nadir and oblique) the SLSTR data is measured on a curvilinear grid defined by the intersection of the instrument scan with the surface of the earth. Instrument samples are distributed at uniform angular intervals around a scan line that is the intersection of the relevant scan cone with the surface of the earth; these scan lines approximate to sections of an ellipse (if the Earth were flat, they would be sections of ellipses). The two views are not collocated at this stage.

Note. In the product definitions we have assumed that the swath widths correspond to 1470 (2940) and 775 (1550) pixels at 1 km (0.5 km) resolution for the nadir and along-track swaths respectively. These values are based on the design values of the swath width with some margin added for orbit height variations.

Level 1A processing calculates the geo-location. That is to say, for each instrument pixel, the latitude and longitude of the pixel are determined. Following AATSR practice, the X and Y co-ordinates of the instrument pixel are also calculated with respect to a quasi-cartesian product grid that is defined with respect to the satellite ground track and instrument swath. These values are then used to resample the data onto the product grid; a nearest neighbour algorithm is used.

The definition of the Level 1b product grid is as follows. Consider a point P in the SLSTR instrument swath. The X co-ordinate of the point is given by its distance from the instrument ground track, measured along the normal section PQ through P that intersects the satellite ground track at right angles; point Q is the intersection point of the normal curve with the ground track. The Y co-ordinate of P is then the distance of the intersection point Q measured along the ground track from an origin point. For products generated by the O-GPP this is taken to be the first scan of data. X and Y are then the co-ordinates of the point P in a quasi-Cartesian system whose Y axis is the local tangent to the ground track; we call it quasi-Cartesian because the ground track is curved (it is not a geodesic on the ellipsoid).

Following AATSR practice, SLSTR channels are sampled at equal intervals of 1 km for the thermal channels or 0.5 km for the solar channels in the across-track direction, and at equal intervals corresponding to the interval between successive scans in the along-track direction.

The L1B product only provides the latitude and longitude of the image grid. To get the latitude and longitude of the MDS grid squares one has to perform the following steps.

(1) Look up the scan, pixel and detector number of origin of the MDS BTs and radiances. The measured pixel data in the MDS and the Scan, Pixel and Detector number ADS are provided as a function of full resolution grid position i_{grid},j_{grid}, and so simple look-up technique can be used to get the measured BTs and radiances in the spd instrument frame e.g.

$$BT(i_{grid},j_{grid}) \leftrightarrow SPD(i_{grid},j_{grid}) \leftrightarrow BT(s,p,d)$$

(2) Having found the scan, pixel and detector number of each of the image grid pixels, use the geodetic coordinates, provided as a function of scan, pixel and detector number, to look up the appropriate ortho-geolcated latitude and longitude of each grid square. The Cartesian coordinates can also be found in the same way.

In addition to the L1B image grid, there is a lower resolution grid, the tie point grid, onto which the meteorological, illumination and viewing geometry data is mapped. The tie point grid is at a reduced resolution of 16km and is aligned with the 0.5km and 1km image grids. The grid is regular in distance across track (16km) and regular in time along-track (8 SCANSYNC intervals (2.4 seconds)) which are approximately 16km. The oblique and nadir tie point grids have the same dimensions.

The relationship between the image grid and tie point grid is illustrated in Figure 5-4 and 5-5. Figure 5-4 shows the nadir tie point grid. The ground track of the satellite always has a full tie point grid square on each side. There are nominally 16x16 complete image grid squares (shown in orange) in each tie point grid square, except at the edges. The tie point grid has to be large enough to contain the entire nadir image and so at the edge of the swath, the first/last tie point grid square is not completely filled with image squares. In the oblique tie point grid, shown in figure 5-5, we see that there are many empty tie point grid squares at the edges of the grid due to the smaller swath width of the oblique view compared to the nadir view.

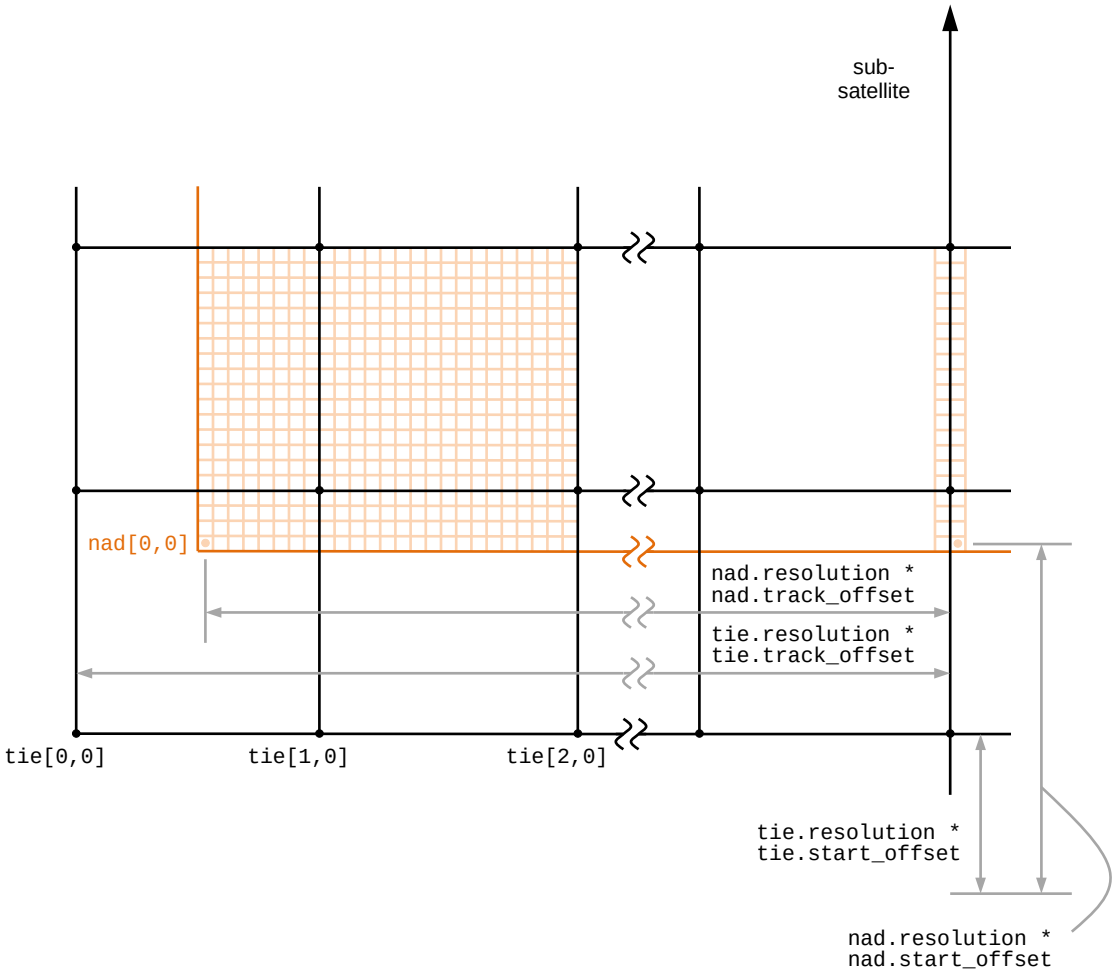

5-4: The relative alignments of generic 16km tie point and 1km nadir grids.

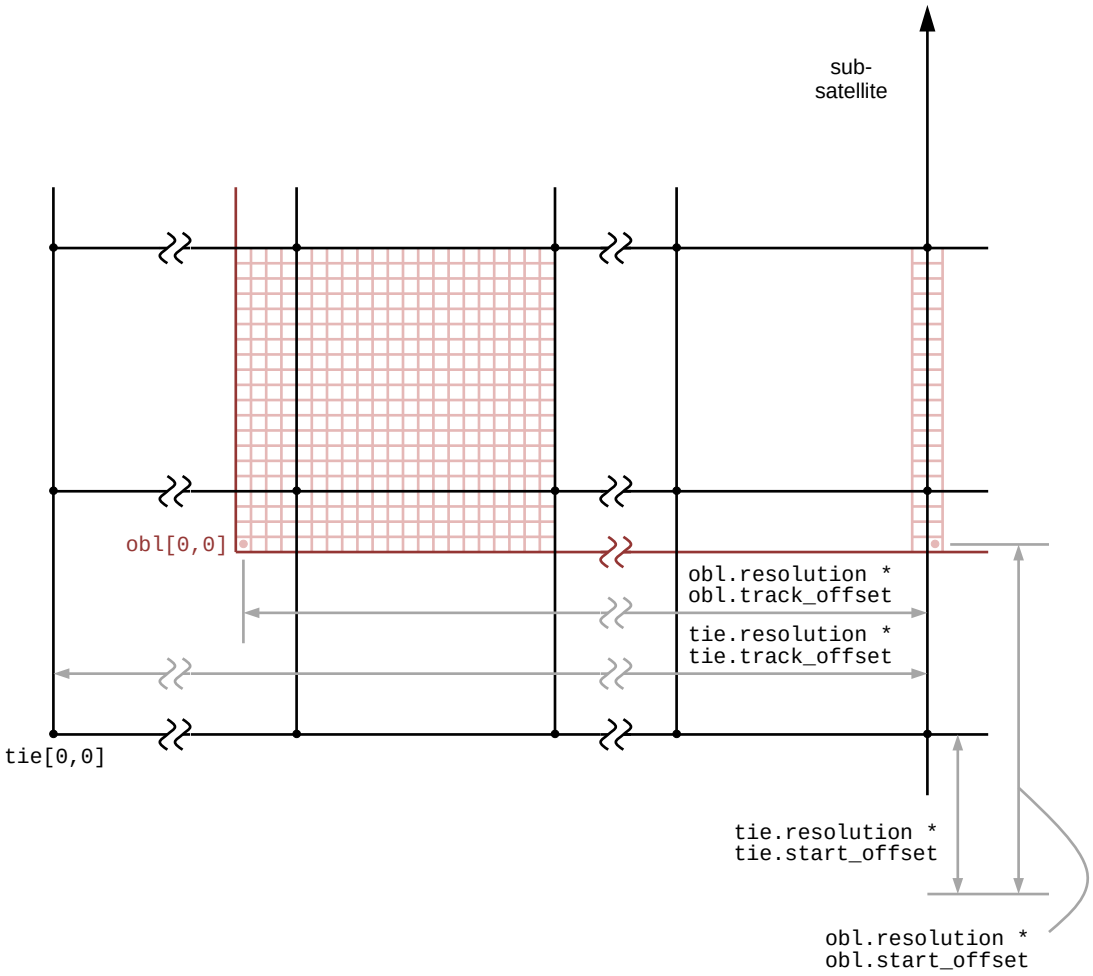

5-5: The relative alignments of generic 16km tie point and 1km oblique grids.

5.3.1 Algorithm Input

The following auxiliary input data sets are required by these processing stages:

- Satellite time correlation.
- Platform navigation and attitude data derived from the NAVATT data.
- The scan time and scan position of the instrument samples pointing vectors.
- Earth surface model (ellipsoid + DEM).
- Detector position offsets in the focal plane.

In the SLSTR instrument, the FPA of each channel includes multiple detector elements, each of which is sampled 3760 times per scan (although only those samples that correspond to genuine ground or calibration signals are retained in the telemetry). There are two such elements in the long-wavelength channels, four in the visible channels and eight in the short-wave infrared channels. Each

such element represents a single pixel. It is therefore necessary to account for their relative positions in the focal plane, and this is the purpose of the position offset data set.

Strictly, the arrays of detector elements may not be precisely aligned between the channels. We assume that the optical alignment is sufficiently good that the same set of position elements will apply to each channel group (2 element (TIR), 4 element (VIS) or 8 element (SWIR)) so that it is not necessary to specify different constants for each channel. Where more precise alignment is sought in the generation of the level 1c vegetation product, it is assumed that this is provided by the relative shift estimation of the Level 1c algorithm.

5.3.2 Processing Objective

The objective is to determine the co-ordinates of each instrument pixel. The positions of SLSTR pixels will be determined in two co-ordinate systems:

- The geodetic latitude and longitude will be determined with respect to the WGS 84 reference ellipsoid;
- The *x* and *y* co-ordinates of the pixel will be determined with respect to the quasi-Cartesian system described in Section 4.4.3. These co-ordinates are required to facilitate the regridding process by which the two views are co-located onto a common grid.

The stages of the calculation have already been summarised in Section5.2.1. The descriptions are repeated, with some additional detail, in the following.

5.3.2.1 Satellite Time Calibration (Stage 9)

The times associated with each instrument scan are converted to UTC. The objective of this stage is to provide a single UTC value associated with the scan for use as the argument of the ephemeris.

5.3.2.2 Geolocation (Stage 10-18)

Stages 10 to 18 relate to establishing the product grid and geo-locating the tie-point pixels to the geoid. Note that these steps are independent of the information contained in the instrument source packets.

10. Generate the quasi-cartesian product grid. This stage, which is called only once in the processing computes the following tables for the later geolocation and regridding stages: (i) the latitude, longitude, and y co-ordinate of a series of sub-satellite points that define the satellite ground track and (ii) the latitudes and longitudes of a rectangular grid of tie points covering the satellite swath.
11. Determine Sentinel 3 Orbit: This Stage uses the CFI with the NAVATT to determine the position and orientation of the platform at the time of each pixel of every scan.
12. Calculate times for each tie point pixel.
13. Compute scan angles for each tie-point pixel in the scan.
14. Compute LoS for each tie-point pixel
15. Geolocate Tie-Point Pixels: Geolocation to the geoid is performed at the tie point pixels for each scan.

16. Calculate Tie Point pixel x and y coordinates: The x-y (across-track and along-track) coordinates of each tie point pixel are derived from the pixel latitude and longitude.
17. Interpolate x and y coordinates for each scan, pixel and detector element. These x and y coordinates will be used for the pixel regridding.
18. Calculate Solar and Viewing Angles: Solar and viewing angles required for cloud clearing are also determined at this stage. The angles are calculated using the CFI at the tie point pixels.

5.3.2.3 Ortho-Geolocation (Stage 19-23)

Steps 19-23 define the steps for ortho-geolocating the instrument pixels and use the scan encoder telemetry to determine the pixel LoS.

19. Calculate times for each pixel in the ISPs
20. Get scan angles for each pixel in the ISPs
21. Compute LoS for Each Instrument Pixel
22. Geolocate Pixels: Orthogeolocation is performed on each pixel of each scan using the scan encoder telemetry and detector LoS.
23. Calculate Pixel *x* and *y* co-ordinates: The x-y (across-track and along-track) coordinates of each pixel are derived from the pixel latitude and longitude. These pixel x and y coordinates are retained on the measurement grid.

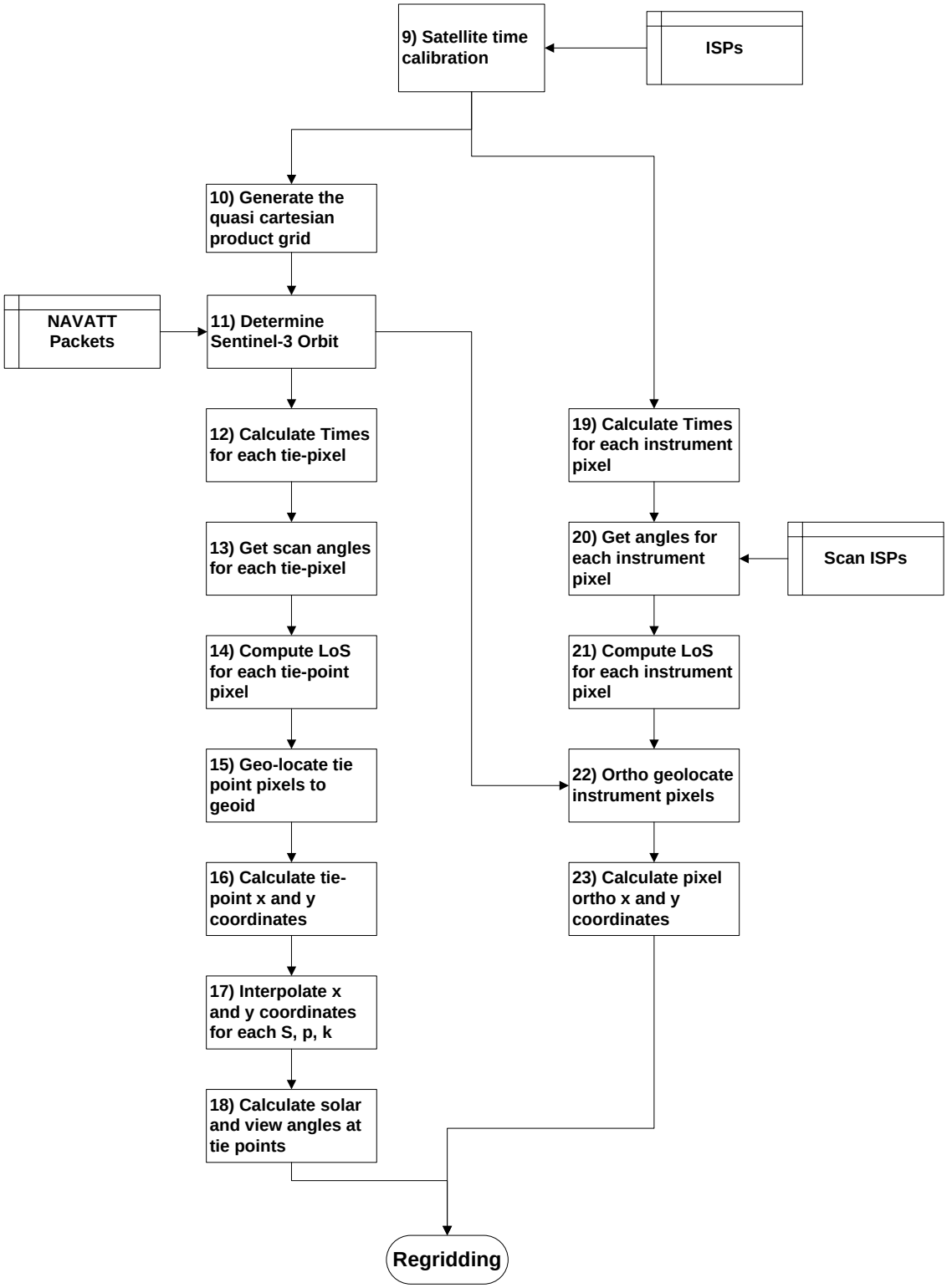

Figure 5-6: Geolocation Modules

5.3.3 Mathematical Description

5.3.3.1 Notation

Geolocation is applied to each measured instrument pixel. Pixels will be identified by a combination of scan number, *S*, pixel number *p*, and detector element index *k* (cf. Section 4.2.3).

The SLSTR includes two independent scan mirrors to generate the nadir and oblique scans. These will be synchronous, so that there is a one-to one correspondence between pairs of scans, and a single index will suffice to identify them. Each thermal infra-red detector element will be sampled *N_SAMPLE* = 3670 times per scan; reflectance channel detector elements will be sampled at twice this rate.

The Level 0 data will comprise instrument source packets each of which will contain instrument data measured during a single scan. Logically it would be possible to have all instrument data from a single pair of nadir and oblique scans in a single telemetry source packet. In practice the sentinel-3 design does not implement this option, and data from different channels may appear in different source packets (e.g. data from the visible and thermal channels may be placed in different packets. However, it should be possible to assemble packets corresponding to the same scan in ground processing, and so we define a logical source packet to be the aggregate of all data from a single pair of simultaneous instrument scans.

We assume that the channels are sampled synchronously, and that within each channel the detector elements $k = 1, \ldots k_{max}$ are sampled simultaneously. The absolute pixel number *p* will index the samples of a single detector element the scan. We will need to index the nadir and along-track samples independently, and will distinguish them by the suffixes *n* and *a* respectively. Then we have:

S	Scan number;
p^n	Absolute pixel number, nadir scan
p^o	Absolute pixel number, oblique (inclined) scan
k	Detector element index. k = 0, 1 for the thermal channels, k=0, 4 for the visible channels, k=0, … 7 for the SWIR channels.
t	acquisition cycle (relevant for 0.5km channels), t=0, 1

The telemetry does not contain every sample for a given scan; only those pixel samples that correspond to valid data are downlinked. Thus the downlinked pixels will comprise blocks corresponding to the black body, Earth view and VISCAL sections of the scan, selected according to the target position table.

5.3.3.2 Common Procedures

This section describes certain procedures which are used by subsequent processing on more than one occasion, and which can therefore be implemented as independent subroutines or procedures. They are presented separately here to simplify the presentation and to indicate how the algorithm may be made more modular. Three such procedures are described:

- solve spherical triangle
- Normal section length and azimuth
- Normal section endpoint

The procedures following make use of the atan2 function; this represents the arc tangent function of two arguments defined in the conventional way, atan2(y, x) being the angle whose tangent is (y/x) and whose quadrant is defined by the signs of x and y. Thus atan2(sin θ, cos θ) would return θ.

5.3.3.2.1 Solve spherical triangle

Purpose: to solve for the unknown side and angles of a spherical triangle, given two sides and an included angle. The basis of the method is described in Section 4.4.4.9.4.)

Notation: Suppose ABC is a spherical triangle. We denote by A, B, C the angles at the corresponding vertices, and according to the usual convention we denote by a, b and c the arc lengthsm, in radians, of the sides opposite the vertices A, B, C respectively. Thus a represents the side BC, and so on.

Input parameters; sides b, c and included angle A. (Units of radians)
Output parameters: the side a and the remaining angles B, C. (Units of radians)

Processing steps (See section 4.4.4.9.4 for the derivation of these equations):

cos a = cos b cos c + sin b sin c cos A

B = atan2{sin b sin c sin A, (cos b - cos a cos c)}
C = atan2{sin b sin c sin A, (cos c - cos a cos b)}

a = atan2{(sin b sin A / sin B), (cos b cos c + sin b sin c cos A)}

We denote this transformation by

Solve spherical triangle {A, b, c; B, C, a}

Here and in the following subsections we adopt the convention that the input parameters of the procedure call precede the semicolon, while the output parameters follow it.

5.3.3.2.2 Normal section length and azimuth

Purpose: given the geodetic latitude and longitude of two points P_1 and P_2 on the ellipsoid, to find the length and azimuth of the normal section through P_2 at P_1. The method is an implementation of Robbins's formula, described in Section 4.4.4.9.2

Input parameters:

φ_1	geodetic latitude of the point P_1	radians
λ_1	longitude of the point P_1	radians
φ_2	geodetic latitude of the point P_2	radians
λ_2	longitude of the point P_2	radians

Output parameters:

L	length of the normal section at P_1 through P_2	km
β	azimuth of the normal section at P_1 through P_2	radians

Calculate the radii of curvature in prime vertical at the points P_1, P_2 as follows:

$$\nu_1 = EARTH\_MAJOR\_AXIS/\left(1-e^2\sin^2(\varphi_1)\right)^{1/2} \quad \text{eq 5.3-1}$$

$$\nu_2 = EARTH\_MAJOR\_AXIS/\left(1-e^2\sin^2(\varphi_2)\right)^{1/2} \quad \text{eq 5.3-2}$$

$$S_\psi = (1-e^2)\sin\varphi_2 + (\nu_1/\nu_2)e^2\sin\varphi_1 \quad \text{eq 5.3-3}$$

$$C_\psi = \cos\varphi_2 \quad \text{eq 5.3-4}$$

$$\psi = \text{atan2}\left(S_\psi, C_\psi\right) \quad \text{eq 5.3-5}$$

(Note *e* is the eccentricity of the ellipsoid) Define the angles (expressed in radians)

$$b = \pi/2 - \varphi_1 \quad \text{eq 5.3-6}$$

$$c = \pi/2 - \psi \quad \text{eq 5.3-7}$$

$$\alpha_{12} = \lambda_1 - \lambda_2\,. \quad \text{eq 5.3-8}$$

It may be convenient to modify α_{12}, by adding or subtracting 2π, to bring it into the range $-180° \le \backslash\alpha_p < 180°$. This case arises if the 180° meridian intersects the arc P_1P_2.

Solve the following spherical triangle by the method of section 4.8.3.6.

Solve spherical triangle $\{A \leftarrow \alpha_{12}, b \leftarrow \psi_1, c \leftarrow \psi_2; \gamma, \beta, \sigma_{12}\}$

The angle β represents the azimuth of P_2 as measured at P_1. If only this azimuth is required, the following steps can be omitted. Otherwise correct the arc length to spheroidal length. Calculate

$$g = \varepsilon\sin\varphi_1\cos\varphi_1\cos\beta \quad \text{eq 5.3-9}$$

$$h = \varepsilon\cos^2\varphi_1\cos^2\beta \quad \text{eq 5.3-10}$$

Where $\varepsilon=e^2/(1-e^2)$

Calculate the line segment between the points:

$$s_{12} = \nu_1\sigma_{12}\left[1-\frac{\sigma_{12}^2}{6}h(1-h)+\frac{\sigma_{12}^3}{8}g(1-2h)\right] \quad \text{eq 5.3-11}$$

We denote this procedure by

Normal section length $\{\varphi_1, \lambda_1, \varphi_2, \lambda_2; L, \beta\}$

5.3.3.2.3 Normal section endpoint

Purpose: given the geodetic latitude and longitude of a point P_1 on the ellipsoid, to find the geodetic latitude and longitude of the point P_2 at a given distance from P_1 on the normal section through P_1 of azimuth β. The method is an implementation of Clarke's direct formula, described in Section 4.4.4.9.3.

Input parameters:

φ_1	geodetic latitude of the point P_1	radians
λ_1	longitude of the point P_1	radians
L	length of the normal section at P_1 through P_2	km
β	azimuth of the normal section at P_1 through P_2	radians

Output parameters:

φ_2	geodetic latitude of the point P_2	radians
λ_2	longitude of the point P_2	radians

Processing steps:

Calculate

$$r_2 = -\varepsilon \cos^2 \varphi_1 \cos^2 \beta \qquad \text{eq 5.3-12}$$

$$r_3 = 3\varepsilon(1-r_2)\cos\varphi_1 \sin\varphi_1 \cos\beta \qquad \text{eq 5.3-13}$$

where ε is as defined above. Calculate the radius in prime vertical at latitude φ,

$$\nu_1 = EARTH\_MAJOR\_AXIS/\left(1-e^2 \sin^2 \varphi_1\right)^{1/2} \qquad \text{eq 5.3-14}$$

$$\vartheta = \frac{L}{\nu_1}\left[1-\frac{r_2(1+r_2)}{6}\left(\frac{L}{\nu_1}\right)^2 - \frac{r_3(1+3r_2)}{24}\left(\frac{L}{\nu_1}\right)^3\right] \qquad \text{eq 5.3-15}$$

$$\psi_1 = \tfrac{1}{2}\pi - \varphi_1 \qquad \text{eq 5.3-16}$$

The quantities α and ψ_2 are given by the solution of a further spherical triangle:

Solve spherical triangle $\{\beta, \psi_1, \vartheta; \delta, \alpha, \psi_2\}$ eq 5.3-17

$$\rho = 1-\tfrac{1}{2}r_2\vartheta^2 - \tfrac{1}{6}r_3\vartheta^3 \qquad \text{eq 5.3-18}$$

$$S_j = \cos\psi_j = e^2 \rho \sin\varphi_1 \qquad \text{eq 5.3-19}$$

$$C_j = (1-e^2)\sin\psi_j \qquad \text{eq 5.3-20}$$

$$\varphi_2 = \text{atan2}\left(S_j, C_j\right) \qquad \text{eq 5.3-21}$$

$$\lambda_2 = \lambda_1 + \alpha \qquad \text{eq 5.3-22}$$

We denote this procedure by

Normal section end point{φ_1, λ_1, L, β; φ_2, λ_2}

5.3.3.3 Satellite Time Calibration

This step is performed for every ISP. The time is computed on four grids, the TIR grid, stripe A (VIS and SWIR) and stripe B (SWIR).

The OBT given in the ISP header is converted to UTC using the information in the NAVATT packets.

5.3.3.4 Generate Geolocation Grid

This section defines the look-up tables for use in later geolocation and image pixel co-ordinate calculations.

Notation

T_0 The start time of the output (Level 1b) product.
ΔT Along track sampling interval
ak Along-track index
y(*ak*) Along-track distance of sample *ak*. The calculation of this section is independent of the instrument geometry.
K is a constant offset that defines the number of samples prior to the ascending node prior to the start of the table, or output product start time if different. K=additional_scan_constant in the L1b processor ADF.

Step 5.3.3.4.1 Generate along-track time-distance LUT

A look-up table defining points on the ground track at time interval ΔT is generated using the NAVATT data. The time step ΔT is chosen to correspond to one tie point interval and calculated as follows:

ΔT= cycles_per_tie_point*scans_per_cycle*(cycle_period/2.0).

The sequence of times *t*(*k*) is defined by

$$t(ak) = T_0 + (ak - K)\Delta T,\ ak = 0, 1, 2, 3, ..., \quad \text{eq 5.3-23}$$

The scan number for the tie point is

$$S_t(ak) = ak*cycle\_per\_tie\_point*scans\_per\_cycle,\ ak=0,1,2,3,... \quad \text{eq 5.3-24}$$

The time T_0 represents the start time of the output product, which in the case of a consolidated orbit product we expect to be the ascending node of the orbit. Because the leading edge of the nadir scan precedes the sub-satellite point, instrument scans measured before T_0 are necessary to fill in the image at the start of the orbit, and the origin of the look-up tables must precede T_0 by the interval $K\Delta T$, where *K* is an auxiliary constant whose value is to be found in the additional_scan_constant in the L1b processor ADF.

An initialisation call to the CFI function xo_orbit_file_precise is required at this point, to initialise the orbit calculations.

status = xo_orbit_init_file_precise(input parameters, output parameters)

Input Parameters:

&sat_id	ID must be previously initialised.
&model_id	ID to be previously initialised; astronomical models etc
&time_id	ID to store time correlations. Should have been initialised as part of time correlation function
&orbit_file_mode	Flag to indicate type of orbit file(s) supplied
&n_files	Number of input files
input_files	String array of (I presume) input file names
&time_mode	Flag to indicate how time range is specified
&time_ref	Time reference ID
&time0	Start time of orbit calculation (if applicable)
&time1	End time of orbit calculation (if applicable)
&orbit0	Abs. orbit number of start orbit (if applicable)
&orbit1	Abs. orbit number of end orbit (if applicable)
&precise_conf	Configuration parameters if precise orbit used

Output parameters

&val_time0	Start of initialization validity range
&val_time1	Start of initialization validity range
&orbit_id	This is the output ID.
ierr	Status error vector

In addition to initialising the precursor IDs, we need to identify the correct orbit data to supply to this call. This should be in the same form as is defined for OLCI.

The CFI function xo_osv_compute is then used to find the latitude and longitude of the sub-satellite point at time t(*ak*) for each *ak*.

```
     status = xo_osv_compute (input parameters, output
parameters);
```

Input Parameters

(&orbit_id	From the initialisation above
&mode	Propagation model – dummy for current version
&time_ref	As above
&time	Reference time

Output parameters

pos_out	Osculating position vector at pixel time (Earth fixed CS)
vel_out	Osculating velocity vector at pixel time (Earth fixed CS)
acc_out	Osculating acceleration vector at pixel time (Earth fixed CS)
ierr	Status error vector

The output parameters generated by this call are not those required at this point. The required parameters are the latitude and longitude of the sub-satellite poiunt, and the ground trace velocity components. These require a call to xo_osv_compute_extra

```
     status = xo_osv_compute_extra(input parameters, output
parameters);
```

Input Parameters

&orbit_id	From the initialisation above
&extra_choice	Flag to allow an ancillary results choice

Output parameters;

model_out	Vector of model-dependent parameters
extra_out	Vector of model-independent parameters; depends upon extra choice
ierr	Status error vector

The required outputs are the latitude and longitude of the subsatellite point at *t*(*ak*):

`track_long[ak], track_lat[ak],`

and the corresponding velocity components:

`velam[ak], vephi[ak].`

These can be extracted from the model-dependent parameter vector.

The length of the line segment *ds*[*ak*] between points *ak* - 1 and *ak* is then derived by a call to the common function normal section length [and azimuth].

Convert the latitudes to radians:

$\varphi_1 = \pi$(track_lat[ak-1])/180.0 eq 5.3-25

$\varphi_2 = \pi$(track_lat[ak])/180.0 eq 5.3-26

$\lambda_1 = \pi$(track_long[ak-1])/180.0 eq 5.3-27

$\lambda_2 = \pi$(track_long[ak])/180.0 eq 5.3-28

Call the common procedure

Normal section length{φ_1, λ_1, φ_2, λ_2; *dy*(*ak*), β}

The required output is the line element *dy*(*ak*).

Calculate the along-track distance by

$y(0) = 0.0$ eq 5.3-29

$y(ak) = y(ak-1) + dy(ak),\ ak = 1, 2, \ldots.$ eq 5.3-30

Re-define origin of y

For all ak

track_y(ak) = y(ak) - y(K) eq 5.3-31

Step 5.3.3.4.2 Generate Geolocation Grids

Starting with the tabular along-track latitudes and longitudes, the latitude and longitude and x-coordinate of every across-track tie point corresponding to the along track grid points are calculated,

using spherical trigonometry. There are N1 + N2 + 1 tie points spaced by dL km. The following calculations are repeated for each value of i= ak-K, where 0<i<number of tie points in an orbit.

Step 5.3.3.4.2.1 Fill in central column of the grid

$\texttt{grid\_lat(i, N}_1\texttt{) = track\_lat[ak]}$ eq 5.3-32

$\texttt{grid\_long(i, N}_2\texttt{) = track\_long[ak]}$ eq 5.3-33

converted to lie in the range -180 to 180 by the subtraction (or addition) of 360 if required.

$\beta' = \pi + \text{atan2}\{\text{velam}[ak], \text{vephi}[ak]\}$. eq 5.3-34

(Note that the azimuth given by the atan2 function should be a negative angle at this point).

Step 5.3.3.4.2.2 Fill in grid points to the east of of ground track

The latitudes and longitudes of N_2 points to the right of the sub-satellite point are calculated, using an interval of *dL* km between the points. These points are in the across-track direction, and lie on the normal section locally orthogonal to the sub-satellite track. The azimuth of this normal section is $\beta' - \frac{1}{2}\pi$:

$\delta = \beta' - \frac{1}{2}\pi$ eq 5.3-35

$\varphi_1 = \pi(\texttt{track\_lat[ak]})/180.0$ eq 5.3-36

$\lambda_1 = \pi(\texttt{track\_long[ak]})/180.0$ eq 5.3-37

For $j = (N_1 + 1), (N_1 + N_2)$

$L = j*dL$ eq 5.3-38

Use the common procedure Normal section endpoint to determine the latitudes and longitudes of the tabular grid point correposonding to j.

Normal section endpoint$\{\varphi_1, \lambda_1, L, \delta; \varphi_j, \lambda_j\}$

$\text{grid\_lat}(i, j) = (180/\pi)\varphi_j$ eq 5.3-39

and their longitudes by

$\text{grid\_long}(i, j) = (180/\pi)\lambda_j$. eq 5.3-40

Each longitude should be converted to lie in the range -180 to 180 by the subtraction or addition of 360 if required.

Step 5.3.3.4.2.3 Fill in grid points west of ground track

$\tilde{\varepsilon} = \beta' + \frac{1}{2}\pi$ eq 5.3-41

$\varphi_1 = \pi$(track_lat[ak])/180.0 eq 5.3-42

$\lambda_1 = \pi$(track_long[ak])/180.0 eq 5.3-43

For j = 0, 1, ... N_1 - 1

$L = 25\ (N1 - j)$ eq 5.3-44

Use the common procedure Normal section endpoint to determine the latitudes and longitudes of the tabular grid point correposonding to j.

Normal section endpoint{φ_1, λ_1, L, δ; φ_j, λ_j}

The latitudes of the remaining tabular grid points are given by

grid_lat(i, j) = $(180/\pi)\varphi_j$ eq 5.3-45

and their longitudes by

grid_long(i, j) = $(180/\pi)\lambda_j$. eq 5.3-46

Each longitude should be converted to lie in the range -180 to 180 by the subtraction or addition of 360 if required.

Note that a consistent sign convention is being adopted for the azimuths, so that the sign of δ [j] will be positive for eastward displacements, negative for westward.

5.3.3.5 Satellite Navigation and Attitude

A call to the CFI function xo_osv_compute is used to determine the satellite position and velocity vector, relative to the geostationary frame of reference, at the time *t* of each instrument pixel. This assumes that the initialisation has already been performed in step 5.3.3.4.1.

The geolocation algorithm as currently defined assumes that the satellite attitude model corresponds to yaw steering mode, and the orbit initialisation should have included this.

```
status = xo_osv_compute(input parameters; output parameters);
```

Input Parameters

(&orbit_id	From the initialisation above
&mode	Propagation model – dummy for current version
&time_ref	As above
&time	Reference time

Output parameters

pos_out	Osculating position vector at pixel time (Earth fixed CS)
vel_out	Osculating velocity vector at pixel time (Earth fixed CS)
acc_out	Osculating acceleration vector at pixel time (Earth fixed CS)
ierr	Status error vector

The satellite position vectors so derived will be used as inputs to subsequent calls to the xp_targetinter function.

5.3.3.6 Tie pixel time calibration

To allow the image and tie point grids to extend beyond the range of pixels contained in the earth view ISPs we need to set up an instrument tie point grid from which the view and solar geometry can be computed.

The simplest approach would be to set up a grid for the full scan so that

p = 0, 10, 20, 30...3670.. eq 5.3-47

which gives 367 tie points per scan at 1km resolution. However, to avoid the situation where the nadir scan intercepts the oblique view, we need to make sure that only pixels appropriate to each earth view is used. Based on the tables in issue 2.0 of the IMDD for the nominal pixels, the range for each tie point array can be defined using

nadir_tie_start = 2144 eq 5.3-48
num_tie_nadir_pixels = 101 eq 5.3-49

for the nadir view, and

oblique_tie_start = 775 eq 5.3-50
num_tie_oblique_pixels = 40 eq 5.3-51

for the oblique view.

The important point to note is that the absolute pixel numbers of the tie points correspond directly to the target positions in the ISPs since all further computations will depend on this.

This should ensure that the nadir tie point swath extends to ~ 1080km east/west and the oblique tie point swath extends to ~450km east/west. i.e. extending beyond the image grid. The absolute pixel numbers on the tie points at intervals of *int_p* are given by

p_t^n = nadir_tie_start_pixel + (0, int_p, 2*int_p,...num_tie_nadir_pixels*int_p) eq 5.3-52

and for the oblique view

p_t^o = oblique_tie_start_pixel + (0, int_p, 2*int_p,...num_tie_oblique_pixels*int_p) eq 5.3-53

The baseline for SLSTR is to use *int_p* = 16.

The absolute times at the instrument tie point pixels for each scan are computed using t_scan_start. Here we only need to use the t_pix_10 calculation. So for each scan

t_pix_tie_nadir = $t(S_t)$ + (p_t^n + 0.5)*PIX10SYNC eq 5.3-54

and

t_pix_tie_oblique = $t(S_t)$ + (p_t^o + 0.5)*PIX10SYNC eq 5.3-55

where $t(S_t)$ is the time at each scan tie point computed in eq 5.3-23.

For the 0.5km pixels, a small adjustment to the time is needed to account for the 0.5km offset from the centres of the 1km pixels. So

t_pix_05km_offset = -0.25*PIX10SYNC

5.3.3.7 Compute scan angles at Tie-Point Pixels

Compute scan angles for nadir and oblique view tie point pixels.

For this we assume a constant rotation speed for the scan mechanisms. The scan angle for a given pixel is given by

$$\phi_p = ((p_t+0.5)*360/3670 + \text{Scan\_Offset} + 360) \bmod 360 \qquad \text{eq 5.3-56}$$

We apply the modulus to ensure that ϕ_p is in the range 0-360 degrees.

Where scan offset is the offset angle in degrees relative to the scan start so that the nadir pixel angle is at zero degrees.

As for the time, the 0.5km pixels require a small adjustment to the angle is needed to account for the 0.5km offset relative to the centres of the 1km pixels. So that

$$\phi_{p,0.5} = ((p_t+0.25)*360/3670 + \text{Scan\_Offset} + 360) \bmod 360 \qquad \text{eq 5.3-57}$$

5.3.3.8 Geolocate Tie Point Pixels

A pixel is represented by a single sample of a single detector element, and we shall refer to each set of near-simultaneous samples of the detector elements of a single channel as a pixel group.

For each tie pixel p_t in each tie point scan S_t the direction of the line of sight is determined in the scan reference frame. The corresponding direction cosines are determined, and transformed to the satellite reference frame, and thence to the geostationary reference frame.

Step 5.3.3.6.1 Determine line of sight and its direction cosines in the instrument reference frame.

Direction cosines of pixels relative to chief ray

The initial directions of the lines of sight to the detector elements k in the respective scan frames are defined by the direction cosines $\{\lambda_k, \mu_k, \nu_k\}$. Define the matrix whose columns are the initial line of sight vectors. This matrix has 3 rows and k_{max} columns:

$$M_{los} = \begin{pmatrix} \lambda_1 & \lambda_2 & \dots & \lambda_{k_{\max}} \\ \mu_1 & \mu_2 & \dots & \mu_{k_{\max}} \\ \nu_1 & \nu_2 & \dots & \nu_{k_{\max}} \end{pmatrix}. \qquad \text{eq 5.3-58}$$

Note that the there are two sets of vectors $\{\lambda_k, \mu_k, \nu_k\}$, one set containing two elements (k_{max} = 2) for the thermal channels at 1 km resolution, and one set containing eight elements (k_{max} = 8) for the short wave and visible channels. For the PFMr there will be two sets of direction cosines – one for nadir view and one for oblique.

Reflection at scan mirror

The matrix M_{cm} enables one to take into account the reflection of the scan mirror in the scan reference frame:

$$M_{cm}^{v} = \begin{pmatrix} 1 & 0 & 0 \\ 0 & \cos(\kappa_v / 2) & -\sin(\kappa_v / 2) \\ 0 & \sin(\kappa_v / 2) & \cos(\kappa_v / 2) \end{pmatrix} \qquad \text{eq 5.3-59}$$

The index *v* identifies the view (*v* = *n*|*a* = nadir | along-track).

Kv is the scan_cone_angle defined in Geometry ADF.

Rotation as function of scan angle

Let ϕ_p be the scan angle of the pixel.

Define the matrix M_{ac} which represents the scan angle corresponding to each pixel

$$M_{ac} = \begin{pmatrix} \cos\varphi_p & \sin\varphi_p & 0 \\ -\sin\varphi_p & \cos\varphi_p & 0 \\ 0 & 0 & 1 \end{pmatrix}. \qquad \text{eq 5.3-60}$$

Compute direction cosines in scan frame of reference

The direction cosines of the lines of sight to the ground pixels after reflection at the scan mirror are given by the columns of the matrix

$$M'_{los} = M_{ac}^{-1} M_{cm}^{-1} \begin{pmatrix} -1 & 0 & 0 \\ 0 & -1 & 0 \\ 0 & 0 & 1 \end{pmatrix} M_{cm} M_{ac} M_{los} \qquad \text{eq 5.3-61}$$

Computer direction cosines in instrument frame of reference

The matrix M_{ab} enables one to go from the scan reference frame to the instrument reference frame.

K' is the scan_inclination_nadir defined in Geometry ADF

$$M_{ab}(-\kappa') = \begin{pmatrix} \cos\kappa' & 0 & \sin\kappa' \\ 0 & 1 & 0 \\ -\sin\kappa' & 0 & \cos\kappa' \end{pmatrix} \qquad \text{eq 5.3-62}$$

For the oblique view, the model assumes that the scan axis is parallel to the instrument z axis as intended, so the corresponding rotation is

$$M_{ab}(0) = \begin{pmatrix} 1 & 0 & 0 \\ 0 & 1 & 0 \\ 0 & 0 & 1 \end{pmatrix}$$ eq 5.3 62a

Adjust for Misalignment

The matrices M_z, M_y and M_x are misalignement matrices enabling one to go from the instrument frame to the platform:

$$M_z(\zeta) = \begin{pmatrix} \cos\zeta & \sin\zeta & 0 \\ -\sin\zeta & \cos\zeta & 0 \\ 0 & 0 & 1 \end{pmatrix}$$ eq 5.3-63

$$M_y(\eta) = \begin{pmatrix} \cos\eta & 0 & -\sin\eta \\ 0 & 1 & 0 \\ \sin\eta & 0 & \cos\eta \end{pmatrix}$$ eq 5.3-64

$$M_x(\xi) = \begin{pmatrix} 1 & 0 & 0 \\ 0 & \cos\xi & \sin\xi \\ 0 & -\sin\xi & \cos\xi \end{pmatrix}$$ eq 5.3-65

The matrix M_{ps} enables to go from the satellite reference frame defined in the SRD to the reference one used in the CFI (old ENVISAT convention):

$$M_{ps} = \begin{pmatrix} 0 & 1 & 0 \\ 1 & 0 & 0 \\ 0 & 0 & -1 \end{pmatrix}$$ eq 5.3-66

The matrix M_{ps} represents a rotation of 180 degrees about the downward-pointing z axis to transform from the spacecraft reference frame to a frame (the platform frame) nominally aligned with the yaw steering frame and so having its x axis pointing forwards.

The direction cosines of the lines of sight relative to the platform reference frame are then given by the columns of the matrix

$$\begin{pmatrix} \lambda_1^p & \lambda_2^p & \dots & \lambda_{k_{max}}^p \\ \mu_1^p & \mu_2^p & \dots & \mu_{k_{max}}^p \\ \nu_1^p & \nu_2^p & \dots & \nu_{k_{max}}^p \end{pmatrix} = M_{ps} M_x(\xi) M_y(\eta) M_z(\zeta) M_{ab}(-\kappa') M'_{los}$$ eq 5.3-67

for the nadir view, or

$$\begin{pmatrix} \lambda_1^p & \lambda_2^p & \dots & \lambda_{k_{max}}^p \\ \mu_1^p & \mu_2^p & \dots & \mu_{k_{max}}^p \\ \nu_1^p & \nu_2^p & \dots & \nu_{k_{max}}^p \end{pmatrix} = M_{ps} M_x(\xi) M_y(\eta) M_z(\varsigma) M'_{los} \qquad \text{eq 5.3-68}$$

for the oblique view.

Here the nominal misalignment of the instrument to the spacecraft is a fixed value obtained from the pre-launch measurements of the instrument relative to the satellite. The default angular misalignments, ξ, η and ζ could be set to zero in which case there is no rotation. It shall be possible for the user to switch between the pre-flight fixed offsets as provided in the geometric characterisation ADF or use the geometric calibration model as given in the following step.

For the FM02 (SLSTR-A) instrument is was possible to use the same misalignment matrices for both nadir and oblique views. However, for the PFMr (SLSTR-B) we need to account for an offset in the scan rotation axis from their nominal orientations. The offsets will be different for both nadir and oblique views. To compensate for the different mis-alignments independently two separate sets of correction matrices Mz, My and Mx will be required for nadir and oblique views.

Step 5.3.3.6.2 Computation of the matrix to transforming the instrument frame to account for the pointing corrections from the geometric calibration model (see the TN "Geometric calibration model for SLST" (S3-MO-TAF-01054/2010) for an overview of the calibration principles).

For each view, there are N_{Qm} models (given as input), indexed by the date of the year, each being a quaternion LUT depending on a parameter X^v (v = a for along-track view and n for nadir view). X^v is a vector of several parameters:

- the On Orbit Position (OOP),
- the satellite position in the earth reference frame
- the sun position in the earth reference frame

For the first O-GPP issue, the model will only depend on OOP, but the process described here can easily be generalized to several parameters.
For each view:

1. the quaternion LUT corresponding to the current date is determined by linear interpolation between quaternion LUTs stored in the data base).
2. the parameters composing X^v must be computed, possibly using CFI functions.
3. Computation of the quaternion $Q^v(X^v)$ corresponding to X^v:
   a. SLERP interpolation at location X^v in the LUT obtained at step 1.
   b. Normalisation of the quaternion $Q^v(X^v)$ to unity.
4. Finally $Q^v(X^v)$ is converted into the equivalent rotation matrix $T^v_{calib}(X^v)$ (following standard formulae).

The corrected direction cosines of the lines of sight relative to the spacecraft reference frame are then given by the columns of the matrix

$$M^s_{los} = \begin{pmatrix} \lambda_1^s & \lambda_2^s & \dots & \lambda_{\kappa_{max}}^s \\ \mu_1^s & \mu_2^s & \dots & \mu_{\kappa_{max}}^s \\ \nu_1^s & \nu_2^s & \dots & \nu_{\kappa_{max}}^s \end{pmatrix} = T^v_{calib}(X^v) M'_{los} \qquad \text{eq 5.3-69}$$

for both views

The NAVATT packets also contain attitude quaternions (see section 5.4.3.2.2) and these can be treated in the same way described above.

Step 5.3.3.6.3 Use the CFI target subroutine to determine the latitudes and longitudes of the pixels

For the tie pixel in question, the outgoing line of sight direction corresponding to detector element *k* relative to the platform frame is given by column *k* of the above matrix, $\{\lambda_k^p, \mu_k^p, \nu_k^p\}$. We can derive a corresponding azimuth and elevation by inverting the equations

$$\lambda_k^p = \cos(elevation)\cos(azimuth) \qquad \text{eq 5.3-70}$$

$$\mu_k^p = \cos(elevation)\sin(azimuth) \qquad \text{eq 5.3-71}$$

$$\nu_k^p = \sin(elevation) \qquad \text{eq 5.3-72}$$

or therefore

$$azimuth = \text{atan2}\,(\mu_k^p, \lambda_k^p) \qquad \text{eq 5.3-73}$$

$$elevation = \text{atan2}\,(\nu_k^p, \sqrt{(\lambda_k^p)^2 + (\mu_k^p)^2}) \qquad \text{eq 5.3-74}$$

If *azimuth* < 0.0 then

$$azimuth = azimuth + 360.0. \qquad \text{eq 5.3-75}$$

In the above atan2 represents the arc tangent function of two arguments defined in the conventional way, atan2(y, x) being the angle whose tangent is (y/x) and whose quadrant is defined by the signs of x and y. Note that both azimuth and elevation are functions of detector index *k*.

For each tie pixel p_t and detector element index *k*, the azimuth and elevation just determined, together with the satellite position at the nominal time of the scan S_t as determined from the CFI orbit propagation subroutine and any attitude offset data, are used as parameters of a call to the CFI target subroutine to determine the latitude and longitude of the pixel.

This seems to need various stages of initialisation.

a) Create an empty attitude ID
status = xp_attitude_init(&attitude_id, ierr)

Input parameters: None.

Output parameters:

&attitude_id	New attitude structure
ierr	Status error vector

b) Populate it – this call uses the satellite position to define the attitude frame

status =xp_attitude_compute(parameters)
Input parameters:

&model_id	Model ID
&time_id	Structure that contains the time correlations
&sat_nom_trans_id	Structure that contains the Sat. Nom. Trans
&sat_trans_id	Structure that contains the Sat. Trans.
&instr_trans_id	Structure that contains the Instr. Trans.
&attitude_id	Structure that contains the Attitude (input/output)
&time_ref	Time reference ID
&time	Time in Processing Format
pos	Satellite position vector (Earth Fixed CS)
vel	Satellite velocity vector (Earth Fixed CS)
acc	Satellite acceleration vector (Earth Fixed CS)
&target_frame	Attitude FrameID

Output parameters:

&attitude_id	Modified input attitude structure
ierr	Status error vector

Call to xp_target_inter[section].

status = xp_target_inter(parameters)

Input Parameters:

&sat_id	Satellite ID
&attitude_id	Structure that contains the Attitude. (input/output)
&atmos_id	Structure that contains the atmosphere initialisation.
&dem_id	Structure that contains the DEM initialisation.
&deriv	Derivative ID - Allowed values: (0) XP_NO_DER (1) XP_DER_1ST (2) XP_DER_2ND
&inter_flag	Flag for first or second intersection point selection Allowed values: (1) XP_INTER_1ST (2) XP_INTER_2ND
&los_az	Azimuth of the LOS (Attitude Frame)
&los_el	Elevation of the LOS (Attitude Frame)
&geod_alt	Geodetic altitude over the Earth m
&los_az_rate	Azimuth-rate of the LOS (Attitude Frame)
&los_el_rate	Elevation-rate of the LOS (Attitude Frame)
&iray	Ray tracing model switch - Accepted values: (0) XP_NO_REF (1) XP_STD_REF (2) XP_USER_REF
&freq	Frequency of the signal Hz

Output parameters:

&num_user_target	Number of user defined targets calculated
&num_los_target	Number of LOS targets calculated
&target_id	Structure that contains the Target results

ierr	Status error vector

status = xp_dem_init(parameters)

Input parameters:

&mode	Digital Elevation Model initialization mode
&model	DEM initialization model (dummy in current implementation)
dem_file	File used for DEM initialization (See DEM Configuration file in [DAT_SUM])

Output parameters:

&dem_id	Structure that contains the DEM initialisation.
ierr	Status error vector

We call xp_target_inter with H = geod_ht = 0

We then call xp_target_extra_main with &target_type set to XP_USER_TARGET_TYPE to obtain the ellipsoid co-ordinates.

```
status = xp_target_extra_main (parameters)

Input parameters:
```

&target_id	Structure that contains the Target results
&choice	Flag to select the extra results to be computed. Even though derivatives could be requested by user, they will not be calculated if the target was computed without derivatives (a warning is raised in this case)
&target_type	Flag to select the type of target; XP_USER_TARGET_TYPE XP_LOS_TARGET_TYPE XP_DEM_TARGET_TYPE
&target_number	Target number

Output parameters:

main_results	See [AD-4] table 263
main_results_rate	See [AD-4] table 263
main_results_rate_rate	See [AD-4] table 263
ierr	Status error vector

The required parameters for each tie-point pixel are:

- Target geocentric latitude of tie-point pixels
- Target geodetic latitude of tie-point pixels
- Target geodetic longitude of tie-point pixels
- Target to satellite pointing Azimuth and Elevation

Then use the function xp_target_extra_target_to_sun function to obtain the solar geometry for each tie point pixel.

- Target to Sun (centre) azimuth of tie-point pixels
- Target to Sun (centre) elevation of tie-point pixels

5.3.3.9 Calculate Pixel x-y co-ordinates

The following steps (described in section 4.4.4.10) are carried out for every pixel. The ortho-geolocated latitudes and longitudes have been calculated for every pixel on the nadir and oblique scans.

Step 5.3.3.7.1 Co-ordinates of pixel

The ortho-geolocated latitude and longitude of the pixel are

$$\varphi_p = (\pi/180.0).nadir\_latitude(S, p^n) \quad \text{eq 5.3-76}$$

$$\lambda_p = (\pi/180.0).nadir\_longitude(S, p^n) \quad \text{eq 5.3-77}$$

for the nadir pixels, and

$$\varphi_p = (\pi/180.0).inclined\_latitude(S, p^o) \quad \text{eq 5.3-78}$$

$$\lambda_p = (\pi/180.0).inclined\_longitude(S, p^o) \quad \text{eq 5.3-79}$$

for the oblique pixels. The longitudes should be reduced to the range (-180.0, 180.0) if necessary.

Step 5.3.3.7.2 Identification of the nearest tabular points

First, choose an initial value of the index ig from which to start the iteration.

```
Set interval_not_found = TRUE
Set iteration_number = 1
If first entry of scan initialise ig:
ig = K + (source_packet_ut_time(s_t) + relative_scan_<view> - T0)/ΔT
```

where relative_scan is table 6-31 of SY-4

```
While (interval not found)
```

Where K, T0 and ΔT are defined in section 5.3.3.4

Step 5.3.3.7.3 Calculate azimuth of Q1Q2 (β_{12})

Calculate

$$\varphi_1 = (\pi / 180.0) \cdot track\_lat(i_g) \quad \text{eq 5.3-80}$$

$$\varphi_2 = (\pi / 180.0) \cdot track\_lat(i_g + 1) \quad \text{eq 5.3-81}$$

$$\lambda_1 = (\pi / 180.0) \cdot track\_long(i_g) \quad \text{eq 5.3-82}$$

$$\lambda_2 = (\pi / 180.0) \cdot track\_long(i_g + 1) \quad \text{eq 5.3-83}$$

Use the normal section length and azimuth procedure to compute the azimuth angle β_{12}. Note the length is not required.

Normal section length $\{\varphi_1, \lambda_1, \varphi_2, \lambda_2; s_{12}, \beta_{12}\}$

Note that s_{12} is an output of the procedure that is not used by subsequent processing.

The angle β_{12} will be in the range $0 \leq \beta_{12} < 180°$, and will represent the azimuth of the track at Q_1, measured anticlockwise from north.

Step 5.3.3.7.4 Calculate azimuth of Q1P (β_{1p})

Use the normal section length and azimuth procedure to compute the azimuth angle β_{1p} . Notepoint P as follows:

Normal section length $\{\varphi_1, \lambda_1, \varphi_p, \lambda_p; s_{1p}, \beta_{1p}\}$

Note that s_{1p} is an output of the procedure that is not used by subsequent processing.

Step 5.3.3.7.5 Iterate

This step describes how to locate the tabular interval in which the azimuthal angle between the ground track to the pixel changes through 90°

```
If abs (β12 - β1p) < π/2 then
      direction = +1
else
      direction = -1
endif
If iteration_number = 1 then prev_dir = direction
If prev_dir = direction then
      ig = ig + direction
else
      interval_not_found = FALSE
iteration_number = iteration_number + 1
prev_dir = direction
end while
If direction = -1 then ig = ig + direction
```

The difference

$$\beta_{12} - \beta_{1p}$$

(reduced into the range -π to π if necessary) represents the required intersection angle PQ_1Q_2.

In order that the tabular point specified be the earlier of the two, if in the last step of the iteration the value of i_g was increased by 1, it is now decremented by one.

Once the correct interval has been found, the sign of difference β_{12} - β_{1p} , reduced into the range -π to π if necessary, at either end-point determines on which side of the ground track the pixel P lies, and therefore the sign of the x co-ordinate of P. If β_{12} - β_{1p} is positive, then the point P is to the right (east) of the ground-track and its x co-ordinate will be positive. If β_{12} - β_{1p} is negative, then the point P is to the left (west) of the ground-track and its x co-ordinate will be negative.

Step 5.3.3.7.6 Calculation of the sides of the triangle

Once the correct interval has been identified, the co-ordinates are calculated by spherical trigonometry. Suppose that the point on the sphere whose co-ordinates are indexed by the final value of i_g from the iteration is Q_1 and that corresponding to i_g +1 is Q_2. The latitude and longitude of each point P, Q_1 and Q_2 are known, and therefore the length of each side of the triangle PQ_1Q_2 can be determined.

Update the co-ordinates of the ground track points:

$$\varphi_1 = (\pi / 180.0) \cdot track\_lat(i_g) \qquad \text{eq 5.3-84}$$

$$\lambda_1 = (\pi / 180.0) \cdot track\_long(i_g)\,. \qquad \text{eq 5.3-85}$$

$$\varphi_2 = (\pi / 180.0) \cdot track\_lat(i_g + 1) \qquad \text{eq 5.3-86}$$

$$\lambda_{12} = (\pi / 180.0) \cdot track\_long(i_g + 1) \qquad \text{eq 5.3-87}$$

Each of the remaining sides of the triangle PQ_1Q_2 are calculated in turn using this procedure, with subscripts replaced appropriately from the 3 indices {1, 2, p}.

Calculate the side Q_2P, s_{2p},

Normal section length $\{\varphi_2, \lambda_2, \varphi_p, \lambda_p; s_{2p}, \beta\}$

Calculate the side PQ_1, s_{p1},

Normal section length $\{\varphi_p, \lambda_p, \varphi_1, \lambda_1; s_{p1}, \beta\}$

Calculate the side Q_1Q_2, s_{12},

Normal section length $\{\varphi_1, \lambda_1, \varphi_2, \lambda_2; s_{12}, \beta\}$

The triangle is now fully determined and any of its angles can be found.

Step 5.3.3.7.7 The mean radius of curvature.

The remaining calculations will make use of Legendre's theorem. Compute a suitable mean radius of curvature.

$$\varphi_m = (\varphi_1 + \varphi_2 + \varphi_p)/3 \qquad \text{eq 5.3-88}$$

$$R = EARTH\_MAJOR\_AXIS \cdot (1-e^2)^{1/2} / (1-e^2 \sin^2 \varphi_m) \qquad \text{eq 5.3-89}$$

Calculate the area of the triangle, and the spherical excess *E*:

$$s = (s_{12} + s_{2p} + s_{p1})/2 \qquad \text{eq 5.3-90}$$

$$A = \sqrt{s(s-s_{12})(s-s_{2p})(s-s_{p1})} \qquad \text{eq 5.3-91}$$

$$E = A/R^2 \qquad \text{eq 5.3-92}$$

radians.

Step 5.3.3.6.8 The angle at Q

The next step is to compute the angle at Q_2. (The angle at Q_1 could be used instead; the choice is arbitrary.) The angle of the plane triangle having sides of the same length is computed, and then corrected by the spherical excess. Note that we do not use the procedure solve_spherical_triangle at this point because it is an ellipsoidal triangle and not a spherical triangle.

If (s_{2p} = 0) then
(trap the special case of a triangle of zero area, in which the angle is indeterminate)

$$Q_2 = 0.0 \qquad \text{eq 5.3-93}$$

else

$$s = (s_{12} + s_{2p} + s_{p1})/2 \qquad \text{eq 5.3-94}$$

$$Q_2 = 2.0 \cdot \arctan\left\{\sqrt{\frac{(s-s_{12})(s-s_{2p})}{s(s-s_{p1})}}\right\} + E/3 \qquad \text{eq 5.3-95}$$

(end if)

Step 5.3.3.7.9 The x and y co-ordinates

Given the side Q_2P and the angle Q_2, the right-angled triangle PQ_2X is fully determined, and the arcs PX and Q_2X can be calculated. The arc PX is determined by an application of the sine rule.

$$\sin PX = \sin (s_{2p}/R) \sin Q_2. \qquad \text{eq 5.3-96}$$

The side Q_2X is determined from the tangent formula

$$\tan Q_2X = \tan (s_{2p}/R) \cos Q_2. \qquad \text{eq 5.3-97}$$

The arc lengths ξ, ζ are determined by multiplying the angular lengths PX and Q2X respectively by the mean radius of curvature determined above.

$$\xi = R\ (PX) \qquad \text{eq 5.3-98}$$

$$\zeta = R\ (Q_2X) \qquad \text{eq 5.3-99}$$

The sign of the x co-ordinate of p is determined by inspecting the sign of the angle β_{12} - ε derived at the last value of i_g above, reduced if necessary into the range

$$-\pi < (\beta_{12} - \beta_{1p}) < \pi \qquad \text{eq 5.3-100.}$$

Then the x and y co-ordinates of the pixel, expressed in km, are

$$x = \mathrm{sgn}(\beta_{12} - \beta_{1p}) \cdot \xi \qquad \text{eq 5.3-101}$$

$$y = track\_y(i_g + 1) - \zeta \qquad \text{eq 5.3-102}$$

Assign the x and y co-ordinates to the relevant arrays:

$$x_t^v\{s, p^v, k\} = x$$
$$y_t^v\{s, p^v, k\} = y \qquad \text{eq 5.3-103}$$

where the superscript *v* represents *n* for nadir view or *o for oblique view* as appropriate.

5.3.3.10 Interpolate Pixel Positions

Geo-location has found the pixel co-ordinates, view and solar geometry of the tie point pixels. Now bi-linear interpolation with respect to pixel and scan number is used to define the co-ordinates, view and solar geometry of the intermediate pixels for each scan. The process is repeated for both nadir and oblique view scans.

For each scan S that is not a tie point:

$$0 \le S < MAX\_NADIR\_SCANS \qquad \text{eq 5.3-104}$$

$$S \notin \{S_t\}$$

we derive

$$i = \mathrm{int}(S / INT\_S) \qquad \text{eq 5.3-105}$$

and compute

$$w_s = (S - S_t(i))/(S_t(i+1) - S_t(i))$$

Similarly for the nadir view, for each pixel p^n that is not a tie point:

$$0 \le p^n < MAX\_NADIR\_PIXELS \qquad \text{eq 5.3-106}$$

$$p^n \notin \{p_t^n\} \qquad \text{eq 5.3-107}$$

we derive

$$j = \mathrm{int}(p^n / INT\_P) \qquad \text{eq 5.3-108}$$

and compute

$$w_p = (p^n - p_t^n(j))/(p_t^n(j+1) - p_t^n(j)) \qquad \text{eq 5.3-109}$$

Then we perform the bilinear interpolation for each detector element as follows:

First for x^n

$$nadir\_x\_geoid(S,p^n,k) = (1-w_s)(1-w_p)x_t^n(i,j,k) + w_s(1-w_p)x_t^n(i+1,j,k) + w_s w_p x_t^n(i+1,j+1,k) + (1-w_s)w_p x_t^n(i,j+1,k) \quad \text{eq 5.3-110}$$

then for y^n

$$nadir\_y\_geoid(S,p^n,k) = (1-w_s)(1-w_p)y_t^n(i,j) + w_s(1-w_p)y_t^n(i+1,j) + w_s w_p y_t^n(i+1,j+1) + (1-w_s)w_p y_t^n(i,j+1) \quad \text{eq 5.3-111}$$

Then repeat the process using the same equations but with the superscript *o,* to signify the oblique view, replacing the superscript *n*.

The result of this step should give arrays of x and y that are to be used in the regridding. The same method is later used to interpolate the latitudes, longitudes, solar and view geometry to the image tie points. I.e. we obtain values of

nadir_sza_geoid(S,p^n,k) from solar zenith angle at the tie points, sza^n_t
nadir_vza_geoid(S,p^n,k) from view zenith angles at the tie points vza^n_t
nadir_vaa_geoid(S,p^n,k) from view azimuth angles at the tie points vaa^n_t
nadir_lat_geoid(S,p^n,k) from latitudes at the tie points lat^n_t
nadir_lon_geoid(S,p^n,k) from longitudes at the tie points lon^n_t

and similarly for the oblique view.

5.3.4 Ortho-Geolocation

5.3.4.1 Pixel time calibration

The time given in the ISP header is the time at scan-sync, i.e. at the beginning of each scan (p=0) relating to the data contained in that ISP. This is denoted here as t_scan_start. The time of every pixel acquisition is calculated using the assumption of a constant scan speed. Due to differences in the detectors of some channels, the pixel time is not the same for all channels.

The time t_pix_10 of every pixel within a scan cycle for the 1km resolution channels are calculated using the following algorithm.

t_pix_10 = t_scan_start + (p*PIX10SYNC) + offset eq 5.3-112

where for all channels except S7F (F1),

offset = PIX10SYNC / 2 in units equivalent to t_scan_start eq 5.3-113

PIX10SYNC= 81.7μs, the period of the 1km resolution channel pixel acquisitions.

The absolute pixel number, p, of the pixel acquisition number in each ISP is determined using the modulo of the target first acquisition in the ISP header wrt. the total number of acquisitions during one scan so that

p = target_position = ((target_first_acquistion + pixel_acquisition_number) **mod** total number of acquisitions per scan) eq 5.3-114

Note that the offset is required because the exact time at which a pixel is measured is not at the beginning of a PIXSYNC period, but the centre of the cycle.

The FIRE channel on detector S7 differs from the other channels. The F2 channel uses the S8 detectors, but the F1 channel uses detector elements that are adjacent to the S7 detector and so the data which are acquired in the same PIX10SYNC period from the two fire channels are for different ground samples. The information relevant for the same ground sample will be at different times from these channels. F2 will have pixel times identical to the other channels as it shares the S8 detectors, but F1 pixel times will differ. In the oblique view, the acquisition from F1 taken at time i has to be compared with the acquisition from F2 taken in time i+1. In the nadir view the reverse statement is true. Therefore, the offset used for channel F1 must take account of this.

For S7F (F1),

offset = PIX10SYNC/2 + PIX10SYNC for the oblique view and eq 5.3-115

offset = PIX10SYNC/2 - PIX10SYNC for the nadir view eq 5.3-116

The time t_pix_05 of every pixel within a scan cycle for the 0.5km resolution channels are calculated in a similar fashion using the algorithm outlined below.

t_pix_05 = t_scan_start + ((2*p + t)*PIX10SYNC/2) + offset eq 5.3-117

where for all channels

offset = PIX10SYNC / 4 eq 5.3-118

t denotes the acquisition cycle (0 or 1)

In summary, there are therefore 3 different sets of pixel timings for SLSTR:

t_pix_10 pixel time associated with TIR channels S7-S9 and F2
t_pix_10F1 pixel time associated with F1
t_pix_05 pixel time associated with VIS channels and SWIR channels S4-S6

However the F1 channel is assigned the t_pix_10 pixel timings as the difference is negligible

5.3.4.2 Obtain Scan Angles for Each Pixel

The scan mirror encoder position taken from the spacecraft telemetry is converted into φ_p using the encoder_conversion_nadir and encoder_conversion_oblique parameters in the geometry ADF.

Note that the scan encoder positions give the scan angle at the start of the pixel integration time and need to be adjusted to account for the pixel centres. The corrected scan angle is given by

$\varphi'_p = \varphi_p + \Delta\varphi/2$ for 1km pixels
$\varphi'_p = \varphi_p + (2t+1)\Delta\varphi/4$ for 0.5km pixels

where $\Delta\varphi$ is the angle increment between successive 1km pixels. Since the variation over the PIX10SYNC interval should be negligible, $\Delta\varphi$ can assume a constant value of 360/3670 degrees.

If no scan ISP is present for a given flag then an exception flag is set and the ortho-geolocation for that scan is not performed. The checks on the scan and flip mirror encoder positions described in section 5.4.3.1.7 to generate the pointing confidence word.

5.3.4.3 Geolocate Instrument Pixels

We then call xp_target_extra_main with &target_type set to XP_DEM_TARGET_TYPE to obtain the co-ordinates for each pixel on the DEM.

The required outputs for each pixel are taken from the output array main-results:

- Target geocentric latitude (Earth Fixed CS)
- Target geodetic latitude (Earth Fixed CS)
- Target geodetic altitude (Earth Fixed CS)

5.3.4.4 Compute Pixel x and y coordinates

Assign the x and y co-ordinates to the relevant arrays:

$$< view > \_ x \_ ortho(s, p^v, k) = x$$
$$< view > \_ y \_ ortho(s, p^v, k) = y \qquad \text{eq 5.3-119}$$

where <*view*> = *nadir* | *along_track*, and where the superscript *v* represents *n* or *a*, as appropriate.

5.4 LEVEL 1A PROCESSING

Description of part 1 of the processing: the computation of the radiometric, spectral and geometric correction and calibration coefficients.

5.4.1 Algorithm Input

5.4.1.1 Level 0 Instrument Digital Numbers

5.4.1.2 Ancillary Radiometric Data

The following auxiliary input data sets are required by these processing stages:

1. Level 1B Processor Configuration File: defines processor configuration data, internal error codes and other items.
2. SLSTR Instrument Data File: defines source packet data structures, validation parameters and engineering unit conversions for the SLSTR instrument.
3. SLSTR Calibration Data File: defines temperature to radiance look-up tables and non-linearity correction tables for the SWIR channels where required.
4. Visible Calibration Data File: the Visible Calibration Coefficients ADS from a previous orbit.

Fuller details of the contents of these files are given in reference [RD-1] Annex A.

5.4.2 Processing Objective

5.4.2.1 Source Packet Processing (Stages 1 - 6)

The purpose of these steps is to unpack and validate the source packet data and convert it to engineering units for the higher processing levels that generate the products and geolocate the data. The main functions of these steps can be summarised as follows:

1. Source Packet Quality Checks: Performs basic quality checks on each raw packet, ensuring that only those that pass the checks contribute to the product.
2. Unpack Anciliary Data: Unpacks all required anciliary and housekeeping data including the temperatures of the on-board black bodies and instrument health and status information.
3. Validate Unpacked Anciliary Data: validates the unpacked anciliary and housekeeping data.
4. Convert Unpacked Anciliary Data: Converts to engineering units those items of anciliary data, including the temperatures of the on-board black bodies and other instrument temperatures and data items, for which a conversion to engineering units is defined.
5. Validate Converted Anciliary Data: Validates those converted anciliary data items that are essential to the calibration.
6. Science Data Processing: Unpacks and validates the science data containing the earth view and black body pixel counts for all available channels from each packet. Correction for signal channel non-linearity is applied at this stage.

5.4.2.2 Infra-Red Channel calibration (Stage 7)

7. Infra-red Channel Calibration: This step calculates the calibration offset and slope that describe the linear relationship between pixel count and radiance for the thermal IR channels. The parameters are determined from the black body pixels counts and the black body temperatures, and the process makes use of look-up tables for the conversion of temperature to radiance.

5.4.2.3 Visible Channel calibration (Stage 8)

8. Visible Channel Calibration: This step unpacks the viscal data once per orbit (if present), when it is detected that the viscal unit is in sunlight, and calculates calibration parameters for all visible channels. These calibration parameters may not be not used to calibrate the science data in the visible channels for the current orbit (which may make used of VISCAL data from a previous orbit), but are written to the Visible Calibration Coefficients ADS in the GBTR product.

5.4.3 Mathematical Description

5.4.3.1 Source Packet Processing

Section 5.1 has described the unpacking of the Level 0 product and/or the Instrument Simulator output into a data structure that essentially consists of a two-dimensional array of structures `ISP_data[i][j]`, indexed by scan number `i` and ISP type `j`. These data structures form the starting point for Level 1 processing. It should be noted that the index i is always incremented by the scan count, even if a scan has been missed for any reason and there is no L0 packet present.

We have identified the basic processing stages in Section 5.2.1 and Figure 5.2.

5.4.3.1.1 Source Packet Quality Checks (Stage 1)

Basic validation checks are performed on the source packets in order to identify major problems such as data corruption which would require the affected source packet to be excluded from subsequent processing. In the case of SLSTR it is also necessary to identify and flag missing source packets, since for example the calibration targets are only sampled once in every two scans, while the visible channels are not sampled at night.

In the present formulation, these tests have been performed during the stage of data input and unpacking described in Section 5.1.2, and their results can be found in the array of flag structures `quality[i][j]` described there.

A single overall validity flag for the ISP of type `j` corresponding to scan `i` can be defined as the union (logical OR) of the individual flags:

$$ISP\_invalid[i][j] = \bigcup_k quality[i][j][k] \qquad \text{eq 5.4-1}$$

5.4.3.1.2 Housekeeping Packet processing (Stages 2-5)

The housekeeping source packet (PCAT = F) contains a variety of parameters relating to the SLSTR subsystems, including quantities such as black body temperatures required for STSTR Level 1 processing. The contents of the packet are defined in RD-5.

Let us define the following notation for the ISP structures

ISP[i,][j].record[k]
HK_packet[i].record[k]

where both record structures are byte arrays indexed by k. Here i indexes the scan and J the ISP type.
Obviously HK_packet[i].record[k] = ISP[i,]['HK'].record[k], where 'HK' is the ISP type associated with the Housekeeping packet.

Individual parameters occupy fields of variable length in the record (and do not start on, say, even byte boundaries). For Level 1b processing, each relevant field must be unpacked and the contents verified and where relevant converted to engineering units. Each parameter should be identified by a unique parameter identifier to act as a cross-reference between the anciliary data tables used to control the processing. AATSR processing used a 5-character alphanumeric code for this purpose, and this method has been adopted in the tables here, but logically any unambiguous convention could be adopted.

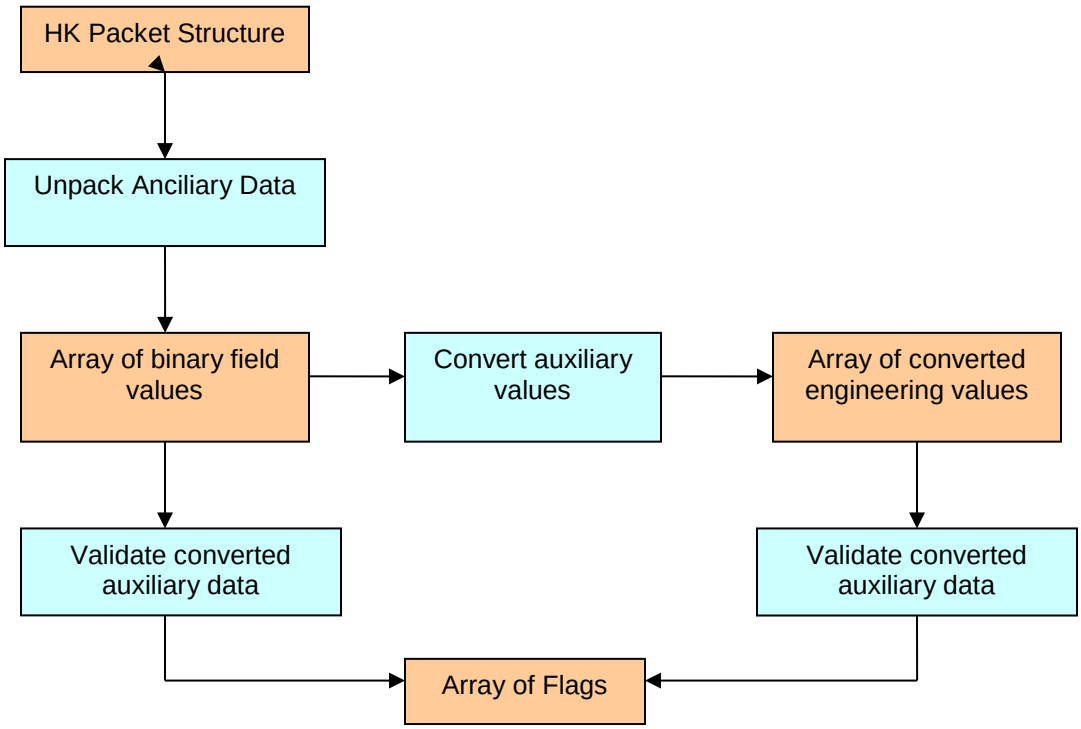

Figure 5-7

5.4.3.1.3 Ancillary Data Unpacking (Stage 2)

In order to accommodate the variable field lengths in which the parameters are stored, a generic table-driven algorithm (similar to those used for AATSR) is proposed to unpack these items and where necessary to convert them to engineering units.

For maximum generality we allow for the possibility that an item of data may occupy only part of a field, although there may be few if any such cases defined in RD-5.

The SLSTR telemetry specification will define the length and starting byte within the ISP of each field, and if applicable, the starting bit number and length of each item within the field. This information can be stored in the Ancillary Data ADF which defines the field in the source packet in which each variable can be found, and if applicable the mask required to extract the variable from the field, and the shift required to correctly justify it. This table is then read in at the start of processing and used to unpack each anciliary data item from the raw packet, storing the resultant integers in an array.

The table will contain one entry for each parameter from the House-keeping source packet that is required by the Level 1b processing algorithms. The total number of entries is defined by the anciliary parameter *anc_ tot*. Each entry will contain the following;

- Anciliary item identifier
- Start byte of field in ISP
- Length of field in bytes

- Mask to extract anciliary item from field
- Shift to justify extracted anciliary data item.

For each scan i, and for each anciliary data item l, the corresponding anciliary datum is then unpacked as follows.

```
ancdata(l) = HK_packet[i].record[offset:offset+item_length-1] AND
extraction_mask(i)

if bit_shift[l] ≠ 0 then shift ancdata(i) left by bit_shift[l] bits
```

For this version of the ATBD the relevant fields in the Ancilary ISP are

Byte 460 – FEE Gain S1-S3
Byte 461-481 – FEE Offset S1-S9
Byte 483-491 – FEE Bias for DU4-DU7
Byte 493-503 – Integration time for S4-S9, F1-F2
Byte 504-520 – Delay in start of integration/sampling times
Byte 522 - Over-sampling for S1, S2, S3 (2 bits each) 6.1.13.1.12
Byte 523 - Over-sampling for S4, S5, S6 (2 bits each) 6.1.13.1.13
Byte 524 - Over-sampling for S7, S8, S9 (2 bits each) 6.1.13.1.14
Byte 536-543 - Voltage reference on detector S4-S7
Byte 544 - Vdg S7
Byte 546-549 - Voltage bias S8 & S9
Byte 550-567 – Detector Temperatures
Byte 568-579 – Coarse Detector Temperatures
Byte 198-264 – BB PRTs and reference resistors
Byte 270-300 – TAEO PRTs
Bytes 330-456 – TAEO TH_1 to TH_32
Bytes 302-303 – TAEO Plus5V internal Reference Voltage value
Bytes 306-307 – TAEO VPRT internal Reference Voltage value
Bytes 310-311 – TAEO PlusVRTH internal Reference Voltage value
Byes 314-315 - TAEO MinusVRTH internal Reference Voltage value

Note that the design of SLSTR allows for an adjustable delay to the start of the sampling/integration time to ensure the correct co-registration of the pixel centres. The present ATBD and O-GPP design assumes a fixed instrument configuration for the mission. An update to the ATBD and O-GPP design would be required to account for adjustments in the flight configuration if needed.

5.4.3.1.4 Validation of Unpacked Anciliary Data (Stage 3)

The validation of the unpacked anciliary data consists of limit checks on the unconverted data. Limit checking is table driven; the upper and lower limits of all specified unpacked anciliary items are read in from a data file along, with the identifier with which they are associated. The result of each validation is loaded into the integer array anciliary_data_validation_result which is defined so that the same index is used to access corresponding values from ancdata and from anciliary_data_validation_result.

For each anciliary datum for which limit checks are defined, the corresponding data set will contain upper and lower limit values validation_lower[i], validation_upper[i] defined in the Ancillary data ADF. These will be provided in a data record tagged with the Anciliary item identifier.

Then for each k $\in$ {k: limit parameters for anciliary data item k are defined}

```
If ancdata[k] < validation_lower[k] or ancdata[k] >
validation_upper[k]
Then anciliary_data_validation_result[k] += 1 (Validation Error)
```

This error code indicates that the item is out of range. Note that it is assumed that the array anciliary_data_validation_result[k] is initialised to zero.

5.4.3.1.5 Conversion of Unpacked Anciliary Data (Stage 4)

Not all anciliary items can be converted to engineering units. For example, some items may be status flags for which no conversion is sensible. If a conversion is defined for an item, the conversion function will be specific to that item, and may not be known until ground characterisation of the instrument. For this reason, the conversion of the unpacked anciliary data is specified in the Anciliary Data ADF.

The ADF describes, for each variable that can be converted, which of a number of generic conversion functions to use, and the list of parameters to use for the conversion. A series of generic functions are defined to cater for each mathematical operation likely to be required in the conversion of SLSTR engineering data.

For each anciliary datum, the ADF entry will contain the following fields:

- the function identifier (function_ID): this specifies the function to be used to perform the conversion for this item.
- The number of parameters in the conversion function (num_param)
- the list of parameters (parameter) associated with the function.

For example, if the conversion function associated with a given parameter is

$$y = (z + a)/b$$

where *z* is the unconverted anciliary data value, then *a* and *b* are the parameters associated with the conversion of this datum. Note that the same function may be used for the conversion of different anciliary data values but with different parameters.

In some cases it may be necessary to specify other, unpacked telemetry items in the list of function parameters, as well as constants. These parameters may be distinguished from constants by the adoption of some suitable convention. For example, such items might occur first in the parameter list, and be distinguished from constants by an identifying prefix of “A”.

The values of the converted data items are loaded into a floating point array converted_anciliary_data. All anciliary items that are not eligible for conversion shall be cast to floating point and copied to this array, so that all anciliary items are accessible in a single array, rather than two.

The anciliary ADF of conversion parameters will contain n_conv records for each parameter,which we can index by k ($0 \le k < n\_anc$). Denote the contents of the record as follows:

item_ID[k]
function_ID[k]
a[k], b[k], …= conversion parameters

For each anciliary data item identify the conversion function function_ID[k] and corresponding parameters a[k], b[k], …

Then provided that the unpacked item is valid, that is if anciliary_data_validation_result[k] ≠1 then the item is conveted using the specified conversion function

```
conv_anc_data[k] = fn(unpacked_anciliary_data[k], a[k], b[k], ...)
```

5.4.3.1.6 The generic conversion algorithms

For each conversion algorithm, f0 to f14, Z is the integer value of the unpacked anciliary data item which is being converted, and a, b, c, d, e, f, g and h,...etc. are the values of parameters which are supplied specifically for each anciliary data item which uses that function. In more complex functions, “result” is the name of a local variable in which the result of the function is returned.

If a conversion is not necessary for a parameter, it has a function ID=f0.

```
f0:   float(Z)

f1:   if (Z=0) then 4
      else if (Z=1) then 8
      else if (Z=2) then 16
      else if (Z=4) then 32
      else if (Z=8) then 64
      else if (Z=9) then 128

f2:   a + bZ

f3:   a + bZ + cZ^2

f4:   a+ bZ^2 + cZ^2 + dZ^3

f5:   a^Z*b

f6:   aZ/b

f7:   (Z+a)/b

f8:   a+(Z/b)

f9:   a/(Z+b)

f10:  if (Z>=a) then b+cZ
      else d+eZ
```

```
f11:  ((aZ+b)^2)/c

f12:  if (Z<a) then
           cZ+d
      else if (a<=Z<=b) then
           eZ+f
      else
           gZ+h

<f13-f19> Spare functions


f20: Look-Up Table
```

Here 2 x Nparameter LUT is provided in the ADF giving converted values as a function of Z. The conversion from Z to anc_conv_data is performed by a polynomial interpolation function.

5.4.3.1.7 Validation of Converted Anciliary Data (Stage 5)

Further quality assurance is provided by tests on the converted values of selected parameters from the HK packet. There are two types of test; the first are general limit checks on appropriate values, the second are additional specific tests on those values that are particularly important for calibration, e.g. BB temps. The design of the instrument is not sufficiently advanced to enable these tests to be specified in detail. However, we here set out tests based on the equivalent AATSR tests to indicate the level of complexity involved. These specialised tests are performed principally on the data of each housekeeping packet which has passed the packet quality check.

5.4.3.1.7.1 General limit checks

This test is applied to all converted items for which maximum and minimum surveillance limits are specified in the anciliary data ADF. If no limit is specified, then no check is made. Limits are specified as the surveillance limits, which contains one record for each parameter. Denote the contents of the record as follows:

- anciliary identifier item_ID[k]
- surveillance lower bound - surveillance_lower[k]
- surveillance upper bound - surveillance_upper[k]

For each anciliary data item k the value is compared with the surveillance limits.

If((conv_anc_data[k] < surveillance_lower[k]) OR (conv_anc_data[j] > surveillance_upper[k]))

then

logical OR anciliary_data_validation_result array[k] with error_code

Where error_code = 4 if conv_anc_data[k] is one of the black body temperature values (BB Temp out of limit), otherwise error_code = 2.(TM Surveillance error)

5.4.3.1.7.2 Specific tests on critical parameters

As noted above, the design of the instrument is not sufficiently advanced to enable these tests to be specified in detail. Here we set out tests based on the equivalent AATSR tests.

Check of the parabaloid mirror temperatures and the black body PRT counts

This test is performed on the unconverted counts of the black body temperature sensors (BB PRTs and reference resistors) and of other critical temperature transducers (TAEO PRT and TAEO Th) to be specified.

For each count to be tested, if the value is either zero or max_count then

logical OR the anciliary_data_validation_results array with the error_code at the corresponding index. k, for that sensor.

Where error code = 8 (Indicates BB PRT raw value out of range)

The error code will ensure that the value is not included in the calibration calculations. The value max_count is the maximum count possible for the field (equal to $2^n - 1$ for an n-bit field).

Test of the Paraboloid mirror temperatures transducers

The test uses the converted values of the paraboloidal mirror temperatures transducers (TAEO PRTs). If none of the telemetry values have been flagged in the corresponding element of the anciliary_data_validation_results array, the arithmetic mean of the valid temperature values is calculated:

$$mean = \frac{1}{n}\sum_{k=1}^{n} T_k \qquad \text{eq 5.4-2}$$

where n is the number of temperature transducers contributing to the sum and T_k is the temperature of the k'th transducer.

The value of each sensor in turn is compared with the mean. If the absolute difference exceeds prt_max_difference (defined in the additional parameters in the Ancillary data ADF), the datum is flagged.

If $abs(T_k - mean) > prt\_max\_difference$ then flag this datum by a logical OR with the error_code into the corresponding field of the anciliary_data_validation_results array

Where error_code = 16 (Indicates rogue PRT sensor)

Check each black body sensor temperature

This test is carried out provided that the appropriate telemetry status flag is set to indicate that the heater is selected for one of the black bodies. If this is not the case, the black body data cannot be used to determine the calibration of the thermal channels; If this occurs then

logical OR the error_code into the corresponding element of the anciliary_data_validation_result array.

Where error_code = 64 (Indicates Rogue BB temperature sensor)

The heated black body is determined by comparing the temperatures of BB1 and BB2. The black body with the highest temperature is then the heated one.

If the heated black body is BB1 then

BB1_PRT_MAX_DIFF = (MAX_HBB_PRT _DIFF) eq 5.4-3
BB2_PRT_MAX_DIFF = (MAX_CBB_PRT _DIFF) eq 5.4-4

else

BB1_PRT_MAX_DIFF = (MAX_CBB_PRT _DIFF) eq 5.4-5
BB2_PRT_MAX_DIFF = (MAX_HBB_PRT _DIFF) eq 5.4-6

The following test is then applied to each black body separately. A weighted mean temperature is calculated for each black body and for each scanner (nadir/oblique), and the separate temperature values (BB PRT readings) are compared with this. Any that deviate by too large an amount are flagged as defective.

Step 1. Calculate the weighted mean temperature of both hot and cold black bodies.

Note. The purpose of the weighted mean algorithm is to incorporate redundancy and to account for temperature gradients, so that the weighted mean value can be derived, even if one (or more) sensors fail.

Denote the number of temperature sensors associated with the black body under consideration by n, and their outputs the by T_k, $0< k \leq n$. We define a valid value as one for which the error code in the corresponding element of the anc_data_validation_result array indicates a valid conversion. For each thermometer there is a corresponding weighting factor w_k (provided in the ancilliary ADF) in the range 0-1 that are different for each scanner (nadir, oblique) to account for the gradients across the blackbody baseplate. The weighted mean temperature is given by

$$\overline{T_{BB}} = \sum_{k=1}^{n} w_k T_k \Big/ \sum_{k=1}^{n} w_k \qquad \text{eq 5.4-7}$$

where n are the numbers of valid temperature sensor readings.

Note that if *n* = 0 no valid temperatures have been recorded and the calibration cannot proceed.

Step 2. Test each sensor value on the BB1.

For each sensor k on BB1 calculate the absolute difference

$$abs\_diff = abs(T_k - mean) \qquad \text{eq 5.4-8}$$

between the temperature of the sensor and the weighted mean BB temperature derived above. If *abs_diff* is greater than *BB1_PRT_MAX_DIFF* then

logical OR the error_code into the corresponding element of the anciliary_data_validation_result array.

Where error_code = 64 (Indicates Rogue BB temperature sensor)

to flag the sensor value as not to be used for the calibration.

Step 3. Test each sensor value on the BB2.

The test is then repeated for BB2.

Test on reference resistor.
The following test is to check that the BB reference resistor values measured by the BBEU are at the expected values. If the corresponding anciliary_data_validation_result indicates a valid conversion then if the corresponding element of the array conv_anc_data is outside the range *REFERENCE_RESISTOR_VAL* ± *REFERENCE_RESISTOR_VARIANCE*, then

logical OR the error_code into the corresponding element of the anciliary_data_validation_result array.

Where error_code = 128 (Indicates Reference Resistor Error)

Note. The error code added is here not enough on its own to qualify the temperature for exclusion from the calculation of the calibration parameters, but it may be added to an existing error code, the combined error may take the error value over the threshold for inclusion.

Test the Detector Temperature Values.
Step 1 Test the converted values of IR channel detector temperatures (S7-S9 detector temperatures). Derive the maximum difference *max_diff* between the temperatures converted from the IR channel detector temperatures (that is, the range spanned by the temperatures).
For each of the converted temperatures taken individually, if the corresponding anciliary_data_validation_result error code indicates a valid conversion and if max_diff is greater than *IR_DET_TEMP_DIFF* then

logical OR the error_code into the corresponding element of the anciliary_data_validation_result array.

Where error_code = 256 (Indicates Detector Temperature Error)

(Note. The error code added is not enough on its own to qualify the temperature for exclusion from the calculation of the calibration parameters, but since the error for this condition may be added to an existing error code, it is possible that the combined error may take the error value over the threshold for inclusion.)

Step 2 Test the visible channel detector temperatures

Repeat the test for the visible channel detector temperatures (S1-S6 detector temperatures), but replacing the test by max_diff > VIS_DET_TEMP_DIFF.

Scanner and Flip Mirror Error Checks

The quality checks for the scanners and flip mirrors will utilise the encoder positions for each data sample provided in the scan ISPs. The SCAN mirrors and Flip Mirror encoder positions are frozen on every PIX10SYNC occurrence. The SUE will produce a data packet every PIX10SYNC period containing the positions acquired (at the beginning of) two PIX10SYNC periods before. See Figure 5-8 below.

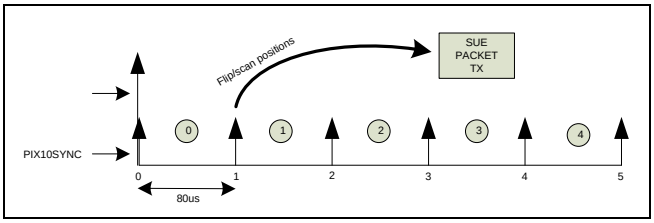

Figure 5-8

The error checks assume that the scanners and flip mirrors are controlled in position by the Scan Unit Electronics (SUE) according to a nominal control law [RD-2].

The scanners will follow two ideal position profiles (one for each mirror) synthesised by the SUE (using the PIX10SYNC and SCANSYNC) and starting from two programmable start positions NA_ZERO_POS and OB_ZERO_POS. I.e. the actual positions as given by the encoder values at each SCANSYNC occurrence correspond to the values respectively stored in NA_ZERO_POS and OB_ZERO_POS registers.

The flip mirror performs a complete switch cycle (NA -> OB -> NA -> OB -> NA) in a CYCLESYNC period (600ms). The timing of the flip transitions is programmable by TC by means of four parameters containing the four flip transition times expressed in multiples of PIX10SYNC during a CYCLESYNC period (i.e. 4 numbers in the range 0 to 7339)

Using the encoder positions we can test for

- Noise errors (bearing, encoder noise)
- Deviation from nominal position

Results of the scan and flip mirror error checks are written to the pointing_flags confidence word of the global ADS.

Bit	Text code	Meaning if set	Comment
0	FlipMirrorAbsoluteError	flip mirror absolute error exceeds threshold	
1	FlipMirrorIntegratedError	flip mirror integrated error exceeds threshold	
2	FlipMirrorRMSError	flip mirror RMS error exceeds threshold	
3	ScanMirrorAbsoluteError	scan mirror absolute error exceeds threshold	
4	ScanMirrorIntegratedError	scan mirror integrated error exceeds threshold	
5	ScanMirrorRMSError	scan mirror RMS error exceeds threshold	
6	ScanTimeError	Scan time is inconsistent with scan count sequence	
7	Platform_Mode	platform mode	0 if nominal, else 1

Scan Mirror Tests

The basic principle of this test is to compare the actual encoder value against the nominal value used for the control law (or based on a long term average). The input for this test shall be a table of expected scan mirror position versus acquistion number (assuming 80us per Pix10Sync). The outputs of the test are flags for each view (nadir, oblique) defined as follows

- Scan Mirror Absolute Error (per pixel), if set to 1 if the absolute difference between the actual and expected value for the pixel exceeds a threshold value scan_instantaneous_threshold.
- Scan Mirror Integrated Error (per view), is set to 1 if the sum of the Absolute pixel values exceeds scan_total_threshold.
- Scan Mirror RMS Error (per view), is set to 1 if the RMS of the absolute pixel errors exceeds scan_rms_threshold.

The flags are written to pointing flags in the GlobalFlags ADS (ref)

The test is performed over the nadir and oblique views for each SCANSYNC period as follows

```
InstantaneousError = double[TargetLength[iview]];
TotalPositionError = 0;
SumsqPositionError = 0;
NumSamples = 0;

for(i=0, i<TargetLength[iview], i++){
      ExpectedScanValue[i] = (Scan_Scale*(target first acquisition + i) +
      Scan_Offset + 360.0) mod 360;
      InstantaneousError[i] = ScanEncoderValue[i,iview] -
      ExpectedScanValue[i,iview];

      ScanMirrorAbsoluteError[i] = (abs(instantaenousError[i]) >
      InstantaneousThreshold);

      TotalPositionError += InstantaneousError[i];
      SumsqPositonError += PositionError[i,j]*PositionError[i,j];
      NumSamples++;
   }
}
```

Here

Scan_scale = 360.0/3670.0 – degrees per pixel - this is not in the geometry ADF
Scan_offset = Mirror offset angle relative to SCANSYNC for each scanner so that 0º is aligned to the +Y axis – this is provided in the geometry ADF.

```
ScanMirrorIntegratedError = (Abs(TotalPositionError) > TotalThreshold);
```

The result of this test should of course be zero. A non-zero value > 1pixel would indicate that the scan control has not been able to maintain the speed of the mechanism and could indicate a control loop error or mechanism roughness. This is equivalent to the ATSR jitter test except that it is applied only to the view and not the complete scan.

```
AvPositionError = TotalPositionError/NumSamples;
```

```
RmsPositionError = Sqrt(SumsqPositionError/NumSamples –
AvPositionError*AvPositionError);

ScanMirrorRMSError = (RmsPositionError >RMSThreshold);
```

Flip Mirror Tests

The basic principle of this test is similar to the scan mirror test and compares the actual encoder value against the nominal value at each position. Since the flip transition occurs outside the data collection window, this will not be recorded. However, the test should show that the flip mirror is at the expected position and the stability. The outputs of the test are flags for each view (nadir, oblique) defined as follows

- Flip Mirror Absolute Error (per pixel), is set to 1 if the absolute position exceeds TBD arcseconds.
- Flip Mirror Integrated Error (per view), is set to 1 if the average position exceeds TBD arcseconds.
- Flip Mirror RMS Error (per view), is set to 1 if the RMS error exceeds TBD arcseconds.

The flags are written to pointing flags in the GlobalFlags ADS (ref)

The test is performed over the nadir and oblique views for each SCANSYNC period and for each scanner as follows

```
InstantaneousError = double[TargetLength[iview]];
TotalPositionError = 0;
SumsqPositionError = 0;
NumSamples = 0;

for(i=0, i<TargetLength[iview], i++){
      InstantaneousError[i] = FlipEncoderValue[i,iview] –
      Flip_nominal_position[iview];

      FlipMirrorAbsoluteError[i] = (abs(instantaenousError[i]) >
      InstantaneousThreshold);

      TotalPositionError += InstantaneousError[i];
      SumsqPositonError += PositionError[i,j]*PositionError[i,j];
      NumSamples++;
   }
}

FlipMirrorIntegratedError = (Abs(TotalPositionError) > TotalThreshold);
```

The result of this test should of course be zero. A significant non-zero value would indicate that the flip mirror is slowly drifting in position during the scan cycle.

```
AvPositionError = TotalPositionError/NumSamples;
RmsPositionError = Sqrt(SumsqPositionError/NumSamples –
AvPositionError*AvPositionError);
```

FlipMirrorRMSError = (RmsPositionError >RMSThreshold);

Scan Time Inconsistency Check

This checks that the time in the scan time ISP is consistent with the scan count. Here we compare the actual time in the ISP against the expected time in the ISP based on the previous scan time.

```
Expected_time = time(scan-1) + 300ms.
ScanTimeErr = (ISP time stamp ≠ Expected_time ± 80ms);
```

Platform mode Check

The platform mode refers to the pointing guidance mode ("Geodetic pointing with yaw-steering guidance (GDC_YED)") as contained in the NAVATT packets (see section 2.7 of RD-14) which is given once every second. Therefore, the pointing mode needs to be replicated for each scan and then mapped onto the image grids during re-gridding.

5.4.3.2 Science Data Processing (Stage 6)

This stage of processing extracts the detector signals and any associated variables from the instrument Source Packets.

We assume that the instrument source packets have been read from the Level 0 product and assembled into the data arrays described in Section 5.1.2. (This merely requires that the Level 0 processing steps described in that section are reversed. Then for each ISP type described in Table 5.1 (excluding the Housekeeping ISP), the relevant data is read into memory.

We adopt the following notation for the extracted channel counts

Following Section 5.1.2.1. we designate the content of the source packet of type `j` corresponding to scan number `i` by `content[i][j]`. The detector count corresponding to given pixel will be denoted by

```
C[ch, target; S, p, t, k]
```

where ch is an index to the channel, target represents the target type (Table 5-3), and the remaining indexing indexing is that introduced in Section 4.2.3. The necessary indexing is complex because a given instrument pixel is associated with a given channel, target and detector as well as a particular scan and acquisition.

Then the procedure is as follows.

for each scan `i` $\in$ { `i`; `0` $\leq$ `i` < `n_scan`}

for each ISP type `j` $\in$ { `j`; `j` corresponds to a valid channel and target ID}

```
scansync[i][j] = content[i][j].scansync
validity[i][j] = content[i][j].validity
target_id[i][j] = content[i][j].target_id
target_first_acq[i][j] = content[i][j]. target_first_acq
target_length[i][j] = content[i][j].target_length
```

Extract the pixel counts. The details depend on the channel corresponding to the ISP type.

SLSTR has multiple element detector arrays for each channel as follows

- S1-S3 - 4 detector elements arranged in a column of 4 rows aligned parallel to the ground track
- S4-S6 - 8 detector elements arranged in a matrix of 2 columns by 4 rows, with the long side of the array aligned parallel to the ground track.
- S7-S9/F1-F2 – 2 detector elements arranged in a column of 2 rows aligned parallel to the ground track

For all subsequent processing we need to adopt a relationship between the detector index *k* and the physical arrangement of the detector elements as shown in the diagram below, which represents the projection of the pixels on the ground.

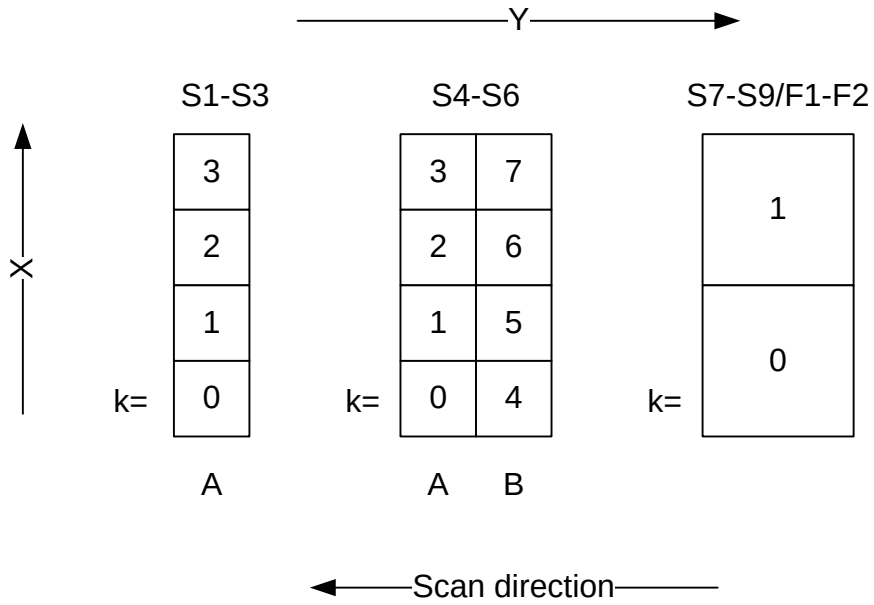

Inconveniently, due to the configuration of the SLSTR FPA and FEE, the readout order of the detectors does not follow this convention, nor are they read out in the same order between channels (IMDD issue 5). Therefore we have to ensure that the detector readings are copied into the correct array element for further processing. The correspondences to the readout order in the ISPs are given by detector pixel indices n[k]provided in the L1b processing configuration ADF.

For the visible channels (S1, S2, S3)

```
C[ch, target_id; S, p, t, k] =
content[i][j].pixel_value[p][t][n[k]];
(((k = 0, 3), t = 0, 1), p = 0, target_length – 1)

For example in the IMDD issue 5 the first pixel in S1 corresponds to
k = 0
```

For the SWIR channels (S4, S5, S6)

```
C[ch, target_id; S, p, t, k] =
content[i][j].pixel_value[p][t][n[k]]; (((k = 0, 7), t = 0, 1), p =
0, target_length – 1)

For example in the IMDD issue 5 the first pixel in S5 corresponds to
k = 7, the last corresponds to k = 0
```

For the thermal infra-red and fire channels (S7, S8, S9, F1, F2)

```
C[ch, target_id; S, p, k] = content[i][j].pixel_value[p][n[k]];
((k = 0, 1), p = 0, target_length – 1)

For example in IMDD imdd issue 5 the first pixel in S7 corresponds
to k = 0
```

5.4.3.2.1 Correct for Signal Channel Nonlinearity

This section deals with how to adjust the signal channel counts for non-linearity.

5.4.3.2.1.1 Theoretical Background

Non-linearity is defined as the relative difference between the actual response and the linear approximation based on calibration at two different signal levels, such that

$$NL = (P_m - P)/P \qquad \text{eq 5.4-9}$$

Where P is the incident optical power and Pm is the measured signal.

So NL is dependent on input power. Non-linearity can be expressed in terms of the signal channel output V, so

$$NL(V;V_c) = \frac{g(V_c)V}{g(V)V_c} - 1 \qquad \text{eq 5.4-10}$$

Where V is the output at which NL is evaluated, Vc is the output at which the detector is calibrated, and P = g(V) is the conversion function, relates to the input power at output V (Yang 1994).

Assuming that the detector non-linearity is of a few percent, the nonlinearity can be referenced from one calibration point V'_C to another calibration point V_C:

$$NL(V;V'_c) = NL(V;V_c) - NL(V'_c;V_c) \qquad \text{eq 5.4-11}$$

This allows us to evaluate the NL of a detector by assuming a dummy calibration point and later translate this to the real calibration point which can be set to zero.

Assuming that the non-linearity is small, the response function of the signal channel can be approximated by a polynomial such that

$$g(V) = \sum_{k=1}^{n} b_k V^k \qquad \text{eq 5.4-12}$$

Assuming that the dark signal is adjusted to zero, the non-linearity has the form

$$NL(V;V_c) = \sum_{k=2}^{n} b_k \left(V^{k-1} - V_c^{k-1}\right) \qquad \text{eq 5.4-13}$$

For SLSTR, the linearity of the VIS and SWIR detectors is expected to be very good with <1% nonlinearity. However, the ROICs for the S4-S7 & F1 channels are expected to show ~8% non-linearity. For the TIR channels, the main cause of non-linearity is due to Auger recombination in the detector material and is expected to be ~5% over the dynamic range.

Since the non-linearity for SLSTR is primarily a function of the output voltage of the DU, we need to consider the signal channel processing through to obtain digital counts C. Figure 1 shows the schematics of the front-end-electronics for each of the SLSTR signal channels [from S3-RP-GA-SL-00026 issue 4]. There are three different typologies for each channel group (Figure 5-9).

- S1-S3 – VIS-NIR channels consists of a TIA offset adjustment, filter instead of integration stage, sample and hold, MUX and gain adjustment before the ADC
- S4-S7 & F1 – SWIR-MIR channels consist of integration on the ROIC of the detector, differential amplifier, offset adjustment and gain before the ADC.
- S8-S9 & F2 – TIR channels consist of a preamplifier, offset adjustment, gain, integrator and MUX before the ADC. The F2 fire channel is implemented in the S8 chain with a common gain amplifier followed by two separate chains of gain and integration.

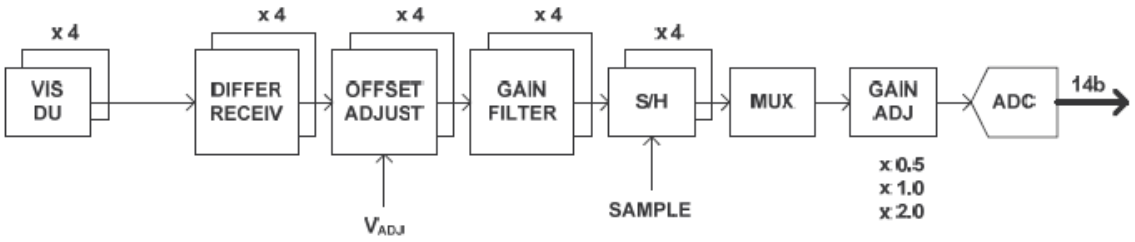

a) VIS-NIR S1-S3

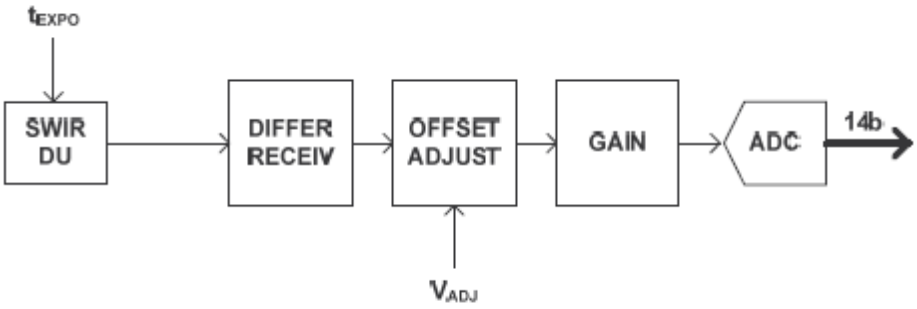

b) SWIR-MIR S4-S7, F1

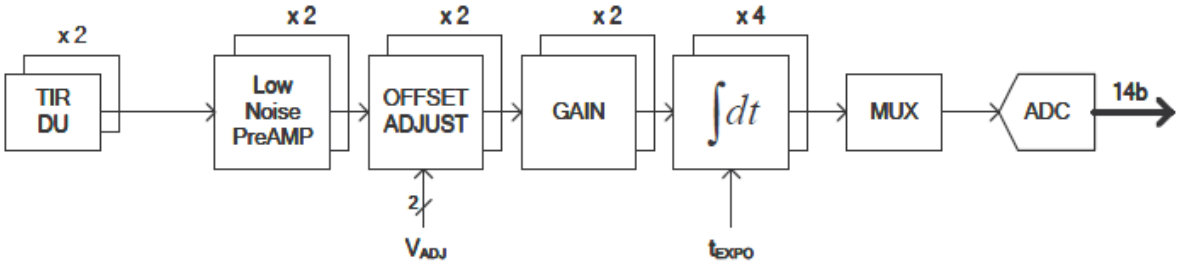

c) TIR S8-S9, F2

Figure 5-9:FEE schematics for a) S1-S3, b) S4-S7 & F1 and c) S8-S9 & F2 channels.

The voltage from the front-end-electronics (fee) at the input to the ADC is given by

$$V_{fee} = (V_{det} + V_{offset})xGain \qquad \text{eq 5.4-14}$$

Where

Voffset = is the adjustable voltage provided in the ancillary data packet.

Vdet = is the output voltage of the detector

Gain = is the electronic gain of the signal channel which is assumed to be fixed. For S1-S3 there is an additional commandable gain adjustment of x0.5 or x1.0.

We assume that the FEE non-linearity is negligible and the ADC is highly linear so that the signal channel counts C is directly proportional to V¬fee. From the above we can see that there are two components of the signal counts

$$C = C_{det} + C_{offset} \qquad \text{eq 5.4-15}$$

The offset voltage is intended to maintain the dynamic range of the signal channels. For the VIS-SWIR channels this is to ensure that there is always a positive count for the zero radiance signals which is essential for the radiometric calibration. The non-linearity of the instrument response will be characterised on ground to produce a look-up table of non-linearity vs. Cdet. The corrected signal should then be

$$C_{corrected} = C_{det}/(NL(C_{det})+1) + C_{offset} \qquad \text{eq 5.4-16}$$

5.4.3.2.1.2 Implementation

The correction for non-linearity is performed as follows:

For each scan obtain convert the adjustable offset, V_{offset} from the housekeeping ISP to obtain C_{offset}[ch,S] using the 'adjustable offset to counts' LUT contained in the Thermal Infrared and Visible characterisation dataset ADFs. Note that in the implementation, for a given value V_{offset}, the value of C_{offset} is relative to the value at launch. So if V_{offset} is the launch value, C_{offset} remains null. Linear interpolation should be used to obtain the intermediate values. If the housekeeping ISP is not present for a scan, then the 'no_parameters' flag shall be set and the detector counts remain uncorrected.

For all valid ISPs for each channel, target and pixel in each scan; convert the recorded counts to detector counts.

$$C_{det}[ch, target\_id, S, p, t, k] = C[ch, target\_id, S, p, t, k] - Coffset[ch, S, t, k]$$

Obtain the appropriate non-linearity correction factor, NL, for C_{det} using the non-linearity LUT for that channel by linear interpolation. The default value for non-linearity is 1.0 (i.e. linear).

Note for S1-S3 there is an adjustable gain setting (nominally x0.5 or x1) after the main gain setting. To account for this the recorded counts should be divided by the gain so that

C = C/Gain where Gain = Gain_S1, Gain_S2 or Gain_S3 from the converted ancillary data (byte 460 of the ancillary packet).

Where Cdet > DetectorCount_first_value and Cdet <DetectorCount_last_value apply the non-linearity correction to Cdet to obtain corrected signal counts

$$C_{corrected}[ch, target\_id, S, p, t, k] = C_{det}[ch, target\_id, S, p, t, k] / Nonlinearity[C_{det}, ch, t, k] + C_{offset}[ch, S, t, k]$$

The parameters, DetectorCount_first_value and DetectorCount_last_value are the valid range over which the non-linearity is characterised. If Cdet falls outside this range NL shall be set to the default value, i.e. no correction is applied.

NOTE:

For S4-S7 there is an adjustable bias setting, and for S4-S9 the integration time can be adjusted. It is understood that, although these settings are adjustable, the flight settings will be those used for pre-launch calibration testing. The non-linearity ADF tables will be based on these settings. Any adjustment in flight will invalidate the ADF table and new tables may be required to compensate for the change in characteristics.

5.4.3.2.2 NAVATT Packet processing

The NAVATT data set is included in the Level 0 product. It comprises an XML header and two binary files; an annotations file, and a file of NAVATT Source Packets. In normal operation NAVATT packets are generated at a 1 Hz rate and comprise satellite position and attitude information sampled at intervals of 1 second, together with time correlation information.

NAVATT packet processing comprises unpacking each ISP into an element of an indexed data structure containing the orbit and attitude data for each sample.

The data fields to be unpacked are shown in the following table.

Field #	Field content
1	GPS time
2	OBT
3	Time correlation validity flag
4	Time of NAVATT data samples
5	Satellite X co-ordinate
6	Satellite Y Co-ordinate
7	Satellite Z co-ordinate
8	Satellite X velocity
9	Satellite Y velocity
10	Satellite Z velocity
11	Attitude Quaternion #1
12	Attitude Quaternion #2
13	Attitude Quaternion #3
14	Attitude Quaternion # 4
15	Attitude Quaternion Difference (Est. – Target) #1
16	Attitude Quaternion Difference (Est. – Target) #2
17	Attitude Quaternion Difference (Est. – Target) #3
18	Attitude Quaternion Difference (Est. – Target) #4
19	Pointing Mode
20	Manoeuvre Flag
21	GNSS Status Flag
22	Orbit Revolution Number
23	Orbit position angle (OOP) – unit 360/2^32 degrees.

These data may be used as input to the time correlation process and to the CFI calls for orbit and target positioning. Note that because of the possibility missing or invalid data, (as evidenced by the presence of validity flags) additional processing is required at this stage to interpolate any missing elements. This processing should be common to the SLSTR and OLCI processing.

5.4.3.3 Infra-red channel calibration

The calculation of the calibration parameters involves determining of the slope and offset for each channel, detector element, pixel parity and each of the nadir and oblique views separately, from the unpacked and validated data in the processed telemetry source packets. It averages the necessary values over the number of packets in a 'calibration interval'; this is a short interval, of the order of 10 source packets. The calibration parameters so derived are then used to calibrate all the packets in the calibration interval.

In each scan cycle the two black bodies are each viewed once each through each view optics chain (nadir and oblique). It follows that the minimum possible length of a calibration period will be one scan cycle (CYCLESYNC interval), and in practice a calibration interval must be an integer number of scan cycles. The length of the calibration interval will be specified in the Level 1b Processor Configuration Anciliary Data Product. If the scans are numbered by S, and if the origin of S is defined so that the first scan of a scan cycle is denoted by an even value of S, then S/2 is an index to the scan cycles. We denote the first and last scans of a calibration interval by S_1, S_2. Note that while in general the calibration interval is of a fixed length, it is possible that the gain or offset values for the channel may change for some S in $S_1 < S < S_2$; this condition should be checked, and if it arises, the value of S2 should be reset to the scan number of the last scan to which the old values applied.

It is stated in section 5.4.3.2 that the counts from the TIR ISPs use the following notation:

C(ch, target_id; S, p, k)

Where ch denotes the channel (S7-S9, F1-2), the target_id denotes the target viewed as defined in table 5-3, S is the scan count, p is the pixel (0<p<target_length-1) and k is the detector element (k=0 or 1 for the TIR).

When calibrating, the parity of the pixels need to be distinguished. In the case of the TIR channels, the odd and even pixels occur every other pixel acquisition and therefore the counts from the instrument can be represented as follows:

C(ch, target_id; S, px, t, k)= C(ch, target_id; S, p, k)

For the IR channels we use t to denote the pixel parity. Where if p is even, t =0 to denote an even pixel, and if p is odd, t=1 to denote an odd pixel. In this case, px is used to represent the pixel acquisitions of each parity and the size of px will be half the target length for that particular target.

The following five steps are applied to all packets in a calibration period for all valid pixels.

Step 1. Derive mean BB temperatures.

The weighted mean thermometer values for each black body (BB) are calculated for both hot and cold black bodies, from all valid values from one packet. This is repeated for all packets in the calibration period. The component means are summed, and a single mean is derived for each BB over the calibration period. Note that there are two sets of average temperatures, one for nadir and the other for the oblique view scanners. This is because the scanners view different parts of the blackbody bases and the weighting has to account for non-uniform gradients across the base.

The weighted mean temperatures, $T_{BB1,Nadir}$ $T_{BB2,Nadir,}$ $T_{BB1,Oblique}$ and $T_{BB2,Oblique}$ are calculated using the equations in Section 5.4.3.1.7.

The mean background (fore-optics) temperature, T_{inst} is also derived from valid data over the same period.

Step 2. Convert the mean BB temperatures to radiance.

Convert each of the weighted mean PRT temperatures for each BB to a radiance value for each IR channel. This is achieved by means of a look up table converting temperature to radiance, with one look up table for each IR channel. The radiance for each black body $L_{BB1}(ch)$ and $L_{BB2}(ch)$ is then a function of channel ch.

The mean instrument temperature is also converted to radiance for each of the TIR channels. $L_{inst}(ch)$.

The look-up tables are derived by integrating the Planck function over the channel filter profile for each channel. Conversion is likely to be considerably more efficient if the data are supplied at sufficiently close enough intervals to allow linear interpolation between points, rather than having fewer data points and relying on polynomial interpolation.

Step 3. Correct the BB radiance values.

Each black body radiance value is now corrected corrected to derive the true mean black body radiance L_true, using the mean background radiance L_{inst} derived in step 2, together with emissivity constants $\varepsilon_{BB1}(ch)$, and $\varepsilon_{BB2}(ch)$.

$$L\_true,_{BB1}(ch) = \varepsilon_{BB1}(ch)\, L_{BB1}(ch) + (1- \varepsilon_{BB1}(ch))\, L_{inst}(ch) \qquad \text{eq 5.4-17}$$

$$L\_true,_{BB2}(ch) = \varepsilon_{BB2}(ch)\, L_{BB2}(ch) + (1- \varepsilon_{BB2}(ch))\, L_{inst}(ch) \qquad \text{eq 5.4-18}$$

Step 4. Derive the mean BB pixel count for each BB over the calibration period.

The mean count values are calculated for odd and even pixels, for both BB1 and BB2, and for all channels and detector elements, from all valid BB pixels in the calibration period. First, the mean (odd and even) pixel count for each channel is derived from the valid BB pixel data in each packet. This is repeated for all packets in the calibration period, and the component means are summed. From this sum of means, a single mean is derived to give a mean BB pixel count over the calibration period, for odd and even pixels, for each BB, for each detector element and for each IR channel.

The pixel sums are calculated independently for each channel, based on the Instrument Source Packets referring to the black body targets. For each channel there are four such ISPs, corresponding to target IDs as follows [RD-6].

Black Body	Nadir view scan	Oblique view scan
BB1	B0	B1
BB2	C0	C1

Table: Target ID (hexadecimal) corresponding to each black body and view combination, from Reference [RD-6].

Denote the black body pixel counts from the relevant ISP by C_{bb}(ch, target_id, S, px, t, k), where target_ID represents the target ID of the black bodies (as in the table above), *s* the scan cycle, pa is the pixel parity, px is the pixel (*px*0 < px < px1, px0 = *target_first_acquisition, px1 = target_first_aquisition target_length for each target id*) is an index to the pixel samples for a given detector, and *k* denotes the detector. (For the thermal and fire channels there are of course two detector elements, and k = 0, 1)

Then the mean channel count for the target denoted by ID and detector *k* is

$$\overline{C}_{bb}(ch,target\_id,t,k) = \frac{1}{N}\sum_{s=s1}^{s2} valid(s) \sum_{px=px0}^{px1} C_{bb}(ch,target\_id,S,px,t,k) \qquad \text{eq 5.4-19}$$

where N is the number of samples that contribute to the sum.

The mean count should also be calculated for the cold black body for the solar channels, to provide the calibration offset for these channels.

It will be necessary to determine from the telemetry which of BB1 and BB2 is the cold and which the hot black body.

Step 5. Calculate the gains and offsets from BB counts and BB radiance.

Derive the calibration_slope and the offset for the calibration period for nadir and oblique views, using:

$$slope_{IR}\{ch,view,t,k\} = \frac{L\_true_{BB1}(ch) - L\_true_{BB2}(ch)}{\overline{C}_{bb}\{ch,ID_1,t,k\} - \overline{C}_{bb}\{ch,ID_2,t,k\}} \qquad \text{eq 5.4-20}$$

$$offset_{IR}\{ch,view,t,k\} = \frac{L\_true_{BB1}(ch)\overline{C}_{bb}\{ch,ID_2,t,k\} - L\_true_{BB2}(ch)\overline{C}_{bb}\{ch,ID_1,t,k\}}{\overline{C}_{bb}\{ch,ID_2,t,k\} - \overline{C}_{bb}\{ch,ID_1,t,k\}} \qquad \text{eq 5.4-21}$$

where ID_1 = B0 or B1 for nadir or oblique views respectively
ID_2 = C0 or C1 for nadir or oblique views respectively.

Note: If the hot and cold blackbody counts are identical then a divide by zero condition will occur. If so set the slope value to Fill_value and

exception{ch, view, S, px, t, k} = 64 (no_parameters)

Step-6 Calculate the radiometric noise from the blackbody signals

First we compute the signal channel noise σC_{bb}(ch,target_ID, pa, k), which is taken as the standard deviation of the detector counts C.

Calculate the mean detector counts measured over the calibration period:

$$C\{ch, t\arg et\_ID, px, t, k\} = \frac{1}{N}\sum_{s=s1}^{s2} C\{ch, target\_ID, s, px, t, k\} \qquad \text{eq 5.4-22}$$

Where N is the total number of valid scans that contribute to the sum.

Then the signal noise is calculated as follows:

$$\sigma C_{bb}\{ch, target\_ID, t, k\} = \left(\frac{1}{n-1} \sum_{px=px0}^{px1} \left(C\{ch, target\_ID, px, t, k\} - \overline{C}_{bb}\{ch, target\_ID, t, k\} \right)^2 \right)^{1/2} \qquad \text{eq 5.4-23}$$

where

target_ID is B0, B1, C0 or C1
C_{bb} is the mean blackbody pixel count calculated in step 4.
n is the number of pixels summed

We then compute the differential of radiance wrt temperature, $\partial L/\partial T$ at each blackbody temperature T_{bb} using the temperature to radiance look-up table (as in step 2) so that

$$\left. \frac{\partial L(ch, target\_ID)}{\partial T(target\_ID)} \right|_{Tbbx} = \frac{L(ch, T_{bbx} + 0.1) - L(ch, T_{bbx})}{0.1} \qquad \text{eq 5.4-24}$$

When x=1, the target_ID=B0 or B1 for BB1
x=2, the target ID=C0 or C1 for BB2.

For the infrared channels the instrument noise is expressed as the noise equivalent brightness temperature difference (NEDT) for each black body, and an absolute function is applied to ensure that the noise is always a positive number

$$dT_{BB\{ch, target_{ID}, t, k\}} = abs(slope_{IR}\{ch, view, t, k\} \times \sigma C_{bb}\{ch, target_{ID}, t, k\} \left(\frac{\partial L(ch, target_{ID})}{\partial T(target_{ID})} \Big|_{T_{bb}} \right)^{-1}) \qquad \text{eq 5.4-25}$$

Where for view = nadir, target_ID=B0 or C0 for BB1 and BB2 respectively

for view=oblique, target_ID=B1 or C1 for BB1 and BB2 respectively.

As with step 4, NEDT values are calculated for odd and even pixels, for both hot and cold black bodies, and for all IR channels and detector elements, from all valid BB pixels in the calibration period.

5.4.3.4 Solar channel calibration

The solar channel gain parameter is derived from the pixel counts over the visible calibration target (the VISCAL unit) during the period when it is illuminated by the sun, and the illumination level is constant.
The illumination period is determined and the average and standard deviation of all valid pixels from the VISCAL unit for all scans during the calibration period so determined are calculated. A similar mean and standard deviation are calculated for all valid pixels from a selected black body, but over the entire orbit. The latter defines the dark signal. This is done for each channel to be calibrated.

It is stated in section 5.4.3.2 that the counts from the VIS and SWIR ISPs use the following notation:

C{ch, target_id, S, p, t, k}

Where ch denotes the channel (S1-S6), the target_id denotes the target viewed as defined in table 5-3, S is the scan count, p is the pixel (0<p<target_length-1), k is the detector element (k=0 -3 for VIS, k=0-7 for SWIR) and t defines the acquisition cycle (which is equivalent to parity).

When calibrating, the parity of the pixels need to be distinguished. In the case of the VIS and SWIR channels, as there are two acquisition cycles in PIX10SYNC period, the parity alternates so there will be an odd and even pixel for each cycle.

so

C{ch, target_id, S, px, t, k}= C{ch, target_id, S, p, t, k }

Where t indexs the acquisition cycle of the pixel. t = 0 for 1st PIX05SYNC acquisition and t = 1 for 2nd PIX05SYNC acquisition. Here px = p is the pixel number as defined by the PIX10SYNC period.

This section describes the process for extracting the calibration data for the SLSTR visible channels using the on-board calibration system.

Step 1. Select window around VISCAL illumination period.

Calculate the time when the VISCAL is under full solar illumination. This time is denoted by calibration_time and expressed in days, as given in the formula below.

```
calibration_time = ascending_node_time + (orbit_period*
(270-solar_declination_angle)/360 + time_offset)/86400.
```

where

ascending_node_time is the ascending node crossing time

orbit_period is the Sentinel-3 orbit period ~100 minutes

time_offset is the period between the time when the VISCAL is fully illuminated and the time that Sentinel-3 crosses the terminator, ~ 4.8 minutes. (The time of full illumination occurs after the terminator (day-night boundary) crossing.)

solar_declination_angle is the solar declination angle

solar_declination_angle =

```
   (0.006918 - 0.399912*cos(day_angle) +
```

```
        0.070257*sin(day_angle) -
        0.006758*cos(2*day_angle) +
        0.000907*sin(2*day_angle) -
        0.002697*cos(3*day_angle) +
        0.00148*sin(3*day_angle)) * 180/π                    eq 5.4-27
```

and

day_angle = 2*π*(day_of_year-1)/365.24 eq 5.4-28

is the day angle for the nth day of the year (Iqbal 1983) where the day of the year is defined as:
day_of_year = (Days since 01-Jan-2000) mod 365.24

To ensure that all the data for the VISCAL is captured when illuminated by the Sun, a window of ±5 minutes around calibration_time should be used. Thus

t_start = calibration_time - window_half_width_in_min/1440 eq 5.4-29

t_end = calibration_time + window_half_width_in_min/1440 eq 5.4-30

where t_start and t_end are expressed in days, and where

window_half_width_in_min = TBD eq 5.4-31

1440=number of minutes in a day eq 5.4-32

Step 2. Process the raw data for the time window between t_start and t_end.

Calculation of solar calibration parameters can only be done if the window centred on the calibration time computed in Step 1 falls within the product limits. Although this should be true for consolidated data, if NRT data is being processed it is possible that the start or end of the Level 0 data will fall within the VISCAL illumination period. In this case it may not be possible to derive a valid visible channel calibration. In particular,

if t_start is earlier than the time of the first scan it may not be possible to generate a valid VISCAL packet, and VISCAL processing should be abandoned.

Otherwise, and provided there are at least 34 TBD scans present in the period between the start of the VISCAL window (t_start) and the end of the Level 0 data process the raw data to extract the pixel counts and instrument telemetry as follows.

[Implementation note:
The algorithm as defined here does not cater for the possibility of a null or invalid scan falling within the time window. In the present prototype implementation, such scans are omitted entirely from the VISCAL processing. The valid scans that fall within the time window determined in Step 1 are copied to a scratch file, which is then re-read and processed as in the following steps.

Experience suggests that such invalid scans are rare, and the omission of one or two sporadic scans (say for a CRC failure) will not significantly bias the algorithm, but the presence of a data gap might lead to an erroneous calibration that would not be recognized as such.
If the algorithm following is applied to a block of scans including invalid scans, the question of how to interpret the invalid monitor count will arise. If the invalid monitor count were set to zero, the effect of a single missing scan would be small in most cases, but the behaviour of the algorithm in the presence of the data gap is not currently specified.]

Step 3. Find period within the time window (t start and t_end) when the smoothed VISCAL monitor is above the specified threshold

In AATSR, monitoring of the VISCAL unit was performed using a photodiode whereas for SLSTR the pixel counts from one of the channels will be used to monitor the brightness of VISCAL. By default, the monitoring channel will be the 0.87μm channel, although there should be flexibility for this to be altered and this is allowed for by including the parameter detection_channel in the SLSTR specific auxiliary data file. The detector element to use for monitoring is detection_element in the SLSTR specific auxiliary data file.

Define monitor_count[view; s] as average counts from 0.87 (or otherwise) channel averaged over all pixels as a function of scan cycle s.

Here, we find the period of time when the monitor channel counts are above a certain threshold value (monitor_threshold) to ensure the VISCAL is in full solar illumination. The monitor_threshold is equivalent to the detection_threshold in the auxiliary data file.

Several tests are performed during this process resulting in confidence flags `found_start[view]` and `found_end[view]` to indicate valid VISCAL start and end data has been found.

The indices of the first and last scans respectively in the time window identified in step1 are denoted by `first_s[view]` and `last_s.[view]`

If *`last_s`* `[view]` is the index of the last scan in the Level 0 product being processed, so that end of data falls within the time window, it may not be possible to generate valid VISCAL parameters. The tests below involving *`last_s`* `[view]` allow for this case.

Initialise flags:

```
found_start[view]    = FALSE
found_end[view]    = FALSE
```

If there are fewer than detection_scan_threshold scans present in the period between the start of the VISCAL window and the end of the Level 0 data (this situation might arise for NRT data) an initial value of the smoothed monitor count, mon1, cannot be derived. In this case a valid VISCAL product cannot be generated, and solar calibration parameter processing should be abandoned.

If last_s – first_s < n_scan_min then abandon.

Otherwise, we smooth the monitor count data measured between first_s and last_s in order to find the correct centroid of the illumination.

Let the smoothing interval be sm_int

```
sm_int = 1
```

The index of the first scan to be processed is not first_s but s0, where

```
s0 = (first_s + sm_int)
```

Calculate a smoothed monitor count mon1 for the first sample where the centre of the interval is given more weighting:

```
mon1 = (monitor_count[s-sm_int] + 2 * monitor_count[s] +
monitor_count[s+sm_int])/4.0
```

where s is greater than or equal to s0

If mon1 > monitor_threshold, it may not be possible to derive a valid centroid, and processing should be abandoned.
Otherwise do the following while statements so that we find the value of s when mon1>monitor_threshold:

```
while mon1 < monitor_threshold and s0 < s < (last_s - sm_int)
s = s + 1
mon1 = (monitor_count[s-sm_int] + 2 * monitor_count[s] +
monitor_count[s+sm_int])/4.0
end while
```

When the while loop ends, it defines the first value of s of the scan cycles for which the smoothed monitor count exceeds the threshold. We also find the source_packet_ut_time, the UTC time of packet s.

```
found_start = TRUE
s1 = s                          (start of monitor window)
ut1 = source_packet_ut_time(s) (monitor window start time)
```

Note that s will correspond to the index of the first sample of a block of 8. The next loop can skip in increments of sm_int.

```
while mon1 ≥ monitor_threshold and s ≤ (last_s - 2*sm_int)
      s = s + sm_int
      mon1 = (monitor_count[s-sm_int] + 2 * monitor_count[s] +
              monitor_count[s+sm_int])/4.0
end while
```

If mon1 < monitor_threshold, the while loop has terminated because of the condition on last_s, and it may not be possible to define a valid centroid, because there is no more data in the monitor time window. This case may arise if the end of the Level 0 product falls within the time window. In this case a valid VISCAL slope cannot be generated, and processing should be abandoned.

Otherwise, the last scan cycle for which the smoothed monitor count exceeds the threshold is:

```
found_end = TRUE
s2 = (s - sm_int)
ut2 = source_packet_ut_time(s) (monitor window end time)
```

Note. This is to be sure that the data used corresponds to the time when the VISCAL is being illuminated by the Sun and not in darkness.

Step 4. Find period of full solar illumination

Now calculate the centroid of the monitor count values between s1 and s2.

```
sum0 = 0.0 d0
sum1 = 0.0 d0
for s = s1, s2, sm_int do
      sum0 = sum0 + monitor_count[s]
      sum1 = sum1 + s * monitor_count[s]
end for
mean_s = integer part of [sum1/sum0]
```

Define the start of the calibration period for the signal channels as being *calibration_window_diff1* scans before the first moment of the of the monitor signal.

```
n1 = mean_s - calibration_window_diff1
```

Define the end of the calibration period for the signal channels as being *calibration_window_diff2* scans after the first moment of the monitor signal.

```
n2 = mean_s + calibration_window_diff2
```

The values n1 and n2 determined above define the limits of the calibration period for the following steps. Thus the length of the calibration window is

calibration_window_diff1 + calibration_window_diff2 + 1 samples.

Calculate an estimate of the mid-point of the monitor window

```
mid_UT_time = (ut1 + ut2)/2.
```

eq 5.4-33

Step 5. Average Pixel Counts over Calibration Period.

The next stage is to calculate the average and standard deviations of the VISCAL counts over the calibration period defined in the previous step and black body counts over the full orbit, as for the

infrared calibration. The cold black body is used in this case to determine the visible calibration coefficient.

Note that at this point we expect that n1 ≥ first_s and n2 ≤ last_s otherwise this step cannot be carried out. In this situation (which can only arise in the event of a significant gap in the data) a valid VISCAL parameter cannot be generated, and Steps 5 to 7 should be abandoned. Otherwise:

Derive the average pixel count and standard deviation for all channels and for all scans which see full illumination as follows:

$$\overline{C}_{viscal}(ch,view,t,k) = \frac{1}{M}\sum_{px=m1}^{m2}\frac{1}{N}\sum_{s=n1}^{n2}C(ch,target\_ID,S,p,t,k) \qquad \text{eq 5.4-34}$$

Where target_ID=D0h when view=nadir and target_ID=D1h when view=oblique and pa indexes the acquisition cycle of the 05PIXSYNC channels.

Identify which of the black bodies is the cold black body and get the average counts as a function of channel (where only S1-S6 are calculated), parity pa, detector element k and nadir and oblique view.

If $T_{BB1}<T_{BB2}$ then

$T_{BBC}=T_{BB1}$ and
Target_IDc = $B0_h$ for view = nadir
Target_IDc = $B1_h$ for view = oblique

else

$T_{BBC}=T_{BB2}$ and
Target_IDc = $C0_h$ for view = nadir
Target_IDc = $C1_h$ for view = oblique

$$\overline{C}_{bbc}(ch,view,t,k) = \frac{1}{M}\sum_{px=m1}^{m2}\frac{1}{N}\sum_{s=s1}^{s2}C(ch,target\_IDc,S,p,t,k) \qquad \text{eq 5.4-35}$$

where

m_1 and m_2 are the start and stop pixels for the view;

M is total the number of pixels used in the view

n1 and n2 are the start and stop scans of the calibration window,

s1 and s2 are the start and stop scans of the dark signal calibration window

and

N is the number of valid scans in the calibration window between n1 and n2 (or s1 and s2) inclusive that contribute to the calibration.

Step 6. Calculate Calibration slope

For each channel *ch*, the calibration slope for the solar channels is then determined using

$$slope_{sol}(ch,view,t,k) = \frac{Reflectance\_factor(ch,k) \times Gain(ch)}{\overline{C}_{viscal}(ch,view,t,k) - \overline{C}_{bbc}(ch,view,t,k)} \qquad \text{eq 5.4-36}$$

where:

Gain[ch] is the instrument gain setting for channel *ch – for SLSTR there are three coarse gain settings of x0.5, x1 and x2 with the default being x1.*

Reflectance_factor[*ch, k*] is the reflectance of the VISCAL diffuser at the channel wavelength; and

C_{viscal} *is the average pixel count from the VISCAL sytem,*

C_{bbc} is the average pixel count from the cold black body previously determined.

This assumes a linear relationship between detector counts and source reflectance. If a non-linear correction has been determined for the channel during pre-launch characterisation, a correction is applied to the detector voltages before the entire calibration process is started and so the assumption of linear calibration will always be true.

Note: If $C_{viscal} = C_{bbc}$ then a divide by zero condition will occur. If so set the slope value to Fill_value and

exception{ch, view, S, px, t, k} = 64 (no_parameters)

Step 8. Reflectance to radiance conversion parameter

The seasonally adjusted solar irradiance, weighted by the channel filter profile, is also calculated for each solar channel to enable the conversion from to reflectance to radiance (Section 3.5.3.8) is also calculated.

*solar_irradiance[ch, view, k] = mean_solar_irradiance[ch, view, k]**

*(1.000110+0.034221*cos(day_angle)+0.001280*sin(day_angle)*

*+ 0.000719*cos(2*day_angle)+0.000077*sin(2*day_angle))* eq 5.4-37

where

day_angle = 2*π*(day_of_year-1)/365.24 eq 5.4-38

day_of_year = (Days since 01-Jan-2000) mod 365.24 eq 5.4-39

and where the values of *mean_solar_irradiance* are taken from the anciliary file of configuration data. We can also calculate the VISCAL radiance, L_viscal

L_viscal(ch , view,k) = Reflectance factor(ch,view,k) x solar irradiance(ch,view,k) / π eq 5.4-40

For the VIS-SWIR channels L_BB = 0.0 since by definition the blackbodies are assumed to be completely dark.

Step 9. Calculation of noise

Finally we compute the signal channel noise of the VISCAL signal σC_{viscal}, which is taken as the standard deviation of the detector counts for the VISCAL during the illumination period and is defined by

$$\sigma C_{viscal}(ch,view,t,k) = \left(\frac{1}{M} \sum_{px=m1}^{m2} \frac{1}{N} \sum_{s=n1}^{s=n2} (C_{viscal}(ch,view,s,p,t,k) - \overline{C}_{viscal}(ch,view,t,k))^2 \right)^{1/2} \quad \text{eq 5.4-41}$$

Where

target_ID=D0h when view=nadir and target_ID=D1h when view=oblique

C_{VISCAL} is the count for channel ch (S1-S6), pixel *px of parity pa, detector element k and view*,

and $\overline{C}_{VISCAL}$ is the mean VISCAL pixel count calculated in step 4.

$$\sigma C_{bbc}(ch,view,t,k) = \left(\frac{1}{M} \sum_{px=m1}^{m2} \frac{1}{N} \sum_{s=s1}^{s=s2} C\ (ch,target\_IDc,S,p,t,k)^2 - (\frac{1}{M} \sum_{px=m1}^{m2} \frac{1}{N} \sum_{s=ns}^{s=s2} C\ (ch,target\_IDc,S,p,t,k))^2 \right)^{1/2} \quad \text{eq 5.4-42}$$

Where target_IDc relates to the target ID of the cold black body defined earlier, in the appropriate view.

$$dL\_viscal(ch,view,t,k) = \frac{\sigma C_{viscal}(ch,view,t,k) * slope_{sol}(ch,view,t,k) * solar\_irradiance(ch)}{\pi} \quad \text{eq 5.4-43}$$

$$dL\_bbc(ch,view,t,k) = \frac{\sigma C_{bbc}(ch,view,t,k) * slope_{sol}(ch,view,t,k) * solar\_irradiance(ch)}{\pi}$$

eq 5.4-44

As for the IR channels, an absolute function should be applied to the noise values for each VIS channel in order to remove the sign.

The values are calculated for odd and even pixels for channels S1 to S6, from all valid VISCAL pixels in the illumination period. Note that the noise values for the cold blackbody should be computed for the full orbit as for the TIR channels.

Step 10. Average Photodiode Signal over calibration window.

The VISCAL system includes a photodiode to monitor the illumination of the diffuser. The parameter is contained in the housekeeping ISP as SUE_TM_VISCAL.

Derive the average photodiode signal and standard deviation for all channels and for all scans which see full illumination as follows:

$$Photodiode\_mean = \frac{1}{N}\sum_{s=n1}^{n2} SUE\_TM\_VISCAL(S)$$

eq 5.4-45

and

$$Photodiode\_SD = \left(\frac{1}{N}\sum_{s=n1}^{s=n2}(SUE\_TM\_VISCAL(S) - Photodiode\_mean)^2\right)^{1/2}$$

eq 5.4-46

5.5 LEVEL 1B PROCESSING

This section describes the processing at Level 1b, including the calibration of the instrument pixels, the re-sampling of the L1b data onto a suitable image grid, and the processing that relates to the regridded data.

The description follows the AATSR practice in which the specified image grid is related to the satellite ground track and instrument swath. Note also that the AATSR grid used equal time interval sampling in the along track direction; that is, although the grid was sampled at 1 km in the across-track direction, in the along-track direction the sampling interval was equal to the distance moved in one instrument scan, which varies around the orbit. If alternative sampling were proposed, then modifications to the scheme would be required.

Again following AATSR practice, we have included land/sea flagging and cloud clearing as processes following regridding.

5.5.1 Algorithm Input

5.5.1.1 Level 1a Data

5.5.1.2 Auxiliary Data

The following auxiliary input data set is required by the signal channel calibration processing stage:

- SLSTR Calibration Data File: defines radiance to temperature look-up tables and non-linearity correction tables for the SWIR channels where required.

The following auxiliary input data sets are required by this cloud clearing processing stage:

- Land-Sea Mask Data File.
- Cloud LUT Data File: contains look-up tables used by the cloud clearing tests.

Fuller details of the contents of these files are given in reference [RD-1] Annex A.

5.5.2 Processing Objective

5.5.2.1 Signal Calibration (Stage 17)

Uncalibrated scan pixels are calibrated using calibration coefficients derived earlier. Pixel calibration uses these calibration coefficients to convert the pixel data to brightness temperature, in the case of the infra-red channels, or to radiance in the case of the visible and near-visible channels.

5.5.2.2 Time Domain Integration (Stage 18)

In order to provide resolutions of 500 m in the short-wave channels, the design of the current FPA for these channels incorporates a 2 by 4 array of detectors, the long edge being aligned in the along-track direction. As a consequence, the swath is effectively scanned twice in the across-track direction, once by each column of the detector array.

An option selected via a processing switch in the L1b processing configuration is to provide an average of the A and B samples with the aim of improving the signal to noise ratio. Note that at the swath edge the pixels of the resultant averaged image will be distorted, but the individual plnes will be retained to support level 1c processing. This step follows signal calibration so that the averaging is applied to calibrated reflectances. This is because the calibrations of the detectors in the two columns may differ.

5.5.2.3 Regrid Pixels (Stage 19)

Calibrated AATSR pixels are regridded into co-located oblique and nadir images, onto a 1 km grid using the pixel positions derived previously. The process used in (A)ATSR processing has migrated instrument pixels to the nearest grid point. This is an input-driven process, in the sense that the process loops over input pixels, and is a highly efficient process in computational terms, but it has been suggested that an output-driven process (looping over image pixels) would present advantages. If such an algorithm were adopted, the next process (cosmetic fill) would not be required.

5.5.2.4 Cosmetic Fill (Stage 20)

Cosmetic filling of nadir/oblique view images is performed, to fill missing image pixels.

5.5.2.5 Image Pixel Positions (Stage 21)

Linear interpolation is performed to determine the latitude and longitude coordinates of the grid pixels for use in the subsequent stages.

5.5.2.6 Determine Land-Sea Flag (Stage 22)

Given the image pixel latitude and longitude, the surface type for each instrument pixel is derived using the land/sea flagging algorithm.

5.5.2.7 Cloud clearing (Stage 23)

The cloud-clearing algorithms are used to identify image pixels as cloudy or cloud-free. Baseline AATSR processing uses nine independent tests based on the AATSR suite of channels, and has recently been expanded by the addition of a new visible channel test. The additional channels proposed for SLSTR will permit additional tests yet to be specified.

5.5.2.8 Meteo annotations (stage 24)

Algorithm Inputs
Level 1b data

- Pixel geo-referencing data: geographic location, viewing and illumination geometry.

Meteorological data are provided by models, as a global prediction of a future situation (hereafter called global forecast) as well as a global view of a past situation, consolidated with observation data such as in situ measurements and remote sensing data (global analysis). These forecasts and analysis are provided by meteo centres like the ECMWF at regular time sampling, typically every 6 hours, spatially sampled on regular geographic grids.
The best available quality level shall be selected at the time of processing, i.e. forecast for NRT and analysis for NTC.

Since the time sampling of meteo files do not match the Sentinel-3 acquisition, temporal interpolation is required and meteo files shall be available at the two closest time samples. Some of the fields require values before and after the nominal time in 6 hourly intervals for the diurnal thermocline modelling and so 5 values are required per analysis time i.e. -18, -12, -6, 0, +6hrs.

Algorithm outputs
The main outputs of this processing step are the annotations to Level 1b products corresponding to meteorological data estimated at the subset of the product pixels. Acquisition geometry, i.e. illumination and viewing angles, are also provided.
Global per product quality flags are generated to indicate the level of quality of the input files (forecast or analysis) and the availability of the appropriate meteo time samples.

5.5.3 Mathematical Description

5.5.3.1 Calibration of Pixel Data

For each channel and for each instrument pixel, the raw pixel counts is converted to brightness temperature (for the thermal and fire channels) or to reflectance (for the solar channels) by the application of the calibration relationship. In all cases a linear relationship is assumed between measured count and either radiance or reflectance as appropriate. For the thermal channels, any non-linearity correction required is included in the radiance to temperature LUTs.

The pixel counts have already been unpacked into a structure and corrected for non-linearity as described in section 5.4.3.3 as

C{ch, target_id, S, px, t, k}

As we only need the nadir and oblique Earth targets the counts can be represented by the following:

C_{scene}{ch, view, S, px, t, k}

where view = nadir if target_id is A0hex, and view=oblique if target_is is A1hex.

Every scan is calibrated, using the set of slope and offset values that were calculated closest in time to the scene scan. The slopes and offsets previously determined were for calibration period measured between scans S1 and S2. The slope and offset values are now represented as a function of scan count S where it is assumed the slopes and offset calculated between S1 and S2 are copied into the array for all S where S1≤S≤S2.

Slope{ch,view, S,t,k}
Offset{ch,view, S,t,k}

For channels S1-S6 the $slope_{sol}$ parameter is used, for channels S7-S9 and F1-2, the $slope_{IR}$ and $offset_{IR}$ parameters are used.

The calibration is performed for all pixels px of each parity, where the pixels relate to the nadir or oblique targets. Note for the solar irradiance channels, the pixel parity is identical to the acquisition sequence.

For each view pixel and for each detector we have a corresponding exception byte that is copied to the MDS. The definition of the exception byte is given in SY-4 and is reproduced as follows.

Bit Number	Text Code	Description
0	ISP_absent	ISP absent
1	pixel_absent	Pixel absent
2	not_decompressed	Not decompressed
3	no_signal	No signal in channel
4	saturation	Saturation in channel
5	invalid_radiance	Derived radiance outside calibration

6	no_parameters	Calibration parameters unavailable
7	unfilled_pixel	Unfilled pixel

Table 5-5 Exception byte contents and meaning

The exception words for each channel and pixel are initialised at the start of the processing as follows.

exception{ch, view, S, px, t, k} = 0;

Also if for a given view or scan S, if no ISP is present then

exception{ch, view, S, px, t, k} = 1; (ISP_absent)

Step 5.5.1 Calibrate infra red channels

For each scan of each view and for each infra-red channel ch = S7, S8, S9, F1 and F2 and detector element all the pixels of the scan are calibrated as follows.

If C{ch, S, px, t, k, view } > 0 and
(slope$_{IR}${ch, view, S, t, k} > 100000 or
offset$_{IR}${ch, view, S, t, k} > 100000)

then the pixel is valid but there is no valid calibration for pixels of the specified parity on the scan. Set the calibrated pixel value to the _FillValue and the corresponding exception value:

BT_{scene}{ch,view, S,px,t,k} = -32768

exception{ch, view, S, px, t, k} = 64 (no_parameters)

If C{ch, view; s, p_v} ≤ 0 then the channel count value is invalid; set value to _FillValue and the corresponding exceptional value

BT_{scene}{ch,view, S,px,t,k}= -32768

exception{ch,view, S, px, t, k} = 4 (No signal in channel)

If C{ch, view; s, p_v} ≥65535 then the channel count value is invalid; set value to _FillValue and the corresponding exceptional value

BT_{scene}{ch,view, S,px,t,k}= -32768

exception{ch,view, S, px, t, k} = 16 (saturation)

Otherwise the pixel count is converted to a radiance

L_{scene}{ch,view, S,px, t, k}= C_{scene}{ch, view, S, px, t, k}*slope$_{IR}${ch, view, S, t, k} +offset$_{IR}${ch, view, S, t, k}

eq 5.5-1

Finally, the radiance L_{Scene} is converted to BT by linear interpolation in the LUT. The LUT consists of radiance L_{LUT} and brightness temperature BT_{LUT}

If the radiance L_{Scene} lies within the range of the first_value and last_value of the appropriate table relavent to each channel, i.e. if

$$\text{first\_value(ch)} \leq L_{scene}\{ch, view, S, px, t, k\} < \text{last\_value(ch)}, \quad \text{eq 5.5-2}$$

find the index g such that

$$L_{LUT}\{q\} \leq L_{scene}\{ch,view,S,px, t, k\} < L_{LUT}\{q+1\}$$

where radiance{g} symbolises the radiance to which the gth tabular brightness temperature corresponds, which is first_value(ch) + g * increment(ch):

$$\text{scale} = (L - \text{first\_value(ch)})/\text{interval(ch)}$$
$$g = \text{integer part of (scale)} \quad \text{eq 5.5-3}$$

Then

$$BT_{scene}\{ch, view, S, px, t, k\} = \text{nearest integer to}$$
$$(100 * (BT_{LUT}\{ch, g\} + \{BT_{LUT}\{ch, g+1\} - BT_{LUT}\{ch, g\}\} * (\text{scale} - g)) \quad \text{eq 5.5-4}$$

(where the factor of 100 converts the units to 0.01 K).

If the scene BT_{Scene} lies outside the range of the table as defined in the Thermal Infrared characterisation dataset ADFs, the calibrated pixel value is set to the Fill Value and the corresponding exceptional value is set:

$$BT_{scene}\{ch, view, S, px, t, k\} = -32768$$
$$\text{exception}\{ch, view, S, px, t, k\} = 32 \text{ (Pixel radiance outside calibration)} \quad \text{eq 5.5-5}$$

Step 5.5.2 Calibrate fire channels

Fire channels will use the same algorithm as for the TIR channels.

Step 5.5.3 Calibrate visible and SWIR channels to reflectance

In this section the visible and SWIR channels are calibrated into a quantity referred to as 'reflectance' and this is subsequently used in the the cloud test in section 5.5.3.7. It should be noted however, that the term reflectance does not strictly apply to R_{scene} derived below as the cosine of the illumination direction is no corrected for.

For each scan and for each short-wave infrared and visible channel ch =S1-S6 all the pixels of the scan are calibrated as follows.

$$\text{If } C_{scene}\{ch,view,S, px, t, k\} > 0 \text{ and}$$
$$(slope_{sol}\{ch, view, S, t, k\} > 100000) \quad \text{eq 5.5-6}$$

then the pixel is valid but there is no valid calibration for pixels of the specified parity on the scan. Set the calibrated pixe l value to the Fill Value and set the corresponding exceptional value:

$$R_{scene}\{ch, view, S, px, t, k\} = -32768$$

$$\text{exception}\{ch, view, S, px, t, k\} = 64 \text{ (no\_parameters)}$$

eq 5.5-7

If C{ ch, view, S, px, t, k } ≤ 0 then the channel count value is invalid; Set the calibrated pixel value to _FillValue and set the corresponding exceptional value:

R_{scene}{ch, view, S, px, t, k} = -32768

exception{ch, view, S, px, t, k} = 4 (No signal in channel)

eq 5.5-8

If C{ch, view; s, p_v} ≥65535 then the channel count value is invalid; set value to _FillValue and the corresponding exceptional value

R_{scene}{ch,view, S,px,t,k}= -32768

exception{ch,view, S, px, t, k} = 16 (saturation)

eq 5.5-9

Otherwise the pixel count is converted to a reflectance using the slope and dark counts from the cold black body previously determined.

R_{scene}{ch, view, S, px, t, k} = (C_{scene}{ch, view, S, px, t, k} - $\overline{C}_{bbc}\{ch, view, S, t, k\}$) / Gain (ch)*$slope_{sol}${ch, view, t, k} eq 5.5-10

Note: The cold blackbody counts C_{bbc} are computed for the full orbit in the same way as for the TIR channels.

For S1-S3 there is an adjustable gain setting (nominally x0.5, x1 and x2) after the main gain setting. Otherwise Gain(ch) = 1.0.

If the scene reflectance, R_{scene} lies outside the range of the table as defined in the Visible and shortwave infrared characterisation dataset ADFs, the calibrated pixel value is set to the Fill Value and the corresponding exceptional value is set such that:

R_{scene}= -32768
Exception = 32 (Pixel radiance outside calibration) eq 5.5-11

Conversion to top-of-atmosphere radiance is performed after the cloud tests as these are based on reflectance values. The algorithm is described in section 5.5.3.10.

5.5.3.2 Apply Vicarious Calibration Correction

It is assumed that the components of the VISCAL system do not drift after the pre-launch calibration. Although every effort is made during the design and manufacture to minimise degradation due to exposure to UV, in practice, it is known that the optical components will degrade during the lifetime of the mission as experienced with ATSR-2 and AATSR. On-board monitoring of the diffuser is limited to a broad band photodiode monitor that is primarily used for detecting the illumination by the Sun, but is not intended for use in calibration. Space and mass constraints in SLSTR do not permit a second diffuser as used for OLCI.

Procedures for determining long term calibration drifts and establishing relative biases with other sensors in the VIS-SWIR range have been established for AATSR and OLCI. To implement these factors in the L1b processing, the approach recommended for SLSTR that is now being adopted for AATSR is to provide the vicarious calibration corrections via a separate ADF. This is to ensure full traceability and reversibility of the process. In the case of AATSR, the data consisted of a drift correction factor D for each channel for each day of the mission. The ADF is updated when new data become available. For the ongoing processing it is intended to include a correction factor extrapolated from the existing drift corrections.

For the purposes of this document we will assume that the vicarious calibration correction factors are available in an ADF provided by ESA in the format described in SY-4. These could be based on actual measurements or a model. The source of these data and the calibration procedure used to derive the factors shall be provided in the ADF.

For each channel and each view read the vicarious calibration factor and uncertainty for the corresponding date and time in the drift table. Here we assume that the calibration drift is common to all detectors of the same channel and view.

The default value for cal_factor shall be set to 1.0, i.e. the calibration is set to the pre-flight values.

Apply correction factor to solar channels as follows

If(Rscene ≠ Fill Value)

R_{scene}{ch,view,S,p,t,k} *= cal_factor(ch,view) eq 5.5-12

5.5.3.3 Processing of SWIR channels

As described earlier in section 5.4.3.2 the SWIR channels of SLSTR use arrays of 8 detector elements arranged in a matrix of 2 columns by 4 rows, with the long side of the array aligned parallel to the ground track. It follows that the swath is effectively scanned twice in the across-track direction; if the detector columns are designated A and B, then the swath is scanned at 0.5 km nominal resolution by each of the A and B columns independently.

For each of the SWIR channels ch = S4, S5, S6 we have a calibrated reflectance

$$R_{scene}\{ch,view,S,p,t,k\}.$$

The detector elements have been re-ordered as shown in the diagram below according to the projection of the pixels on the ground.

	A	B
j=3	3	7

2	2	6
1	1	5
0	0	4
i =	0	1

In the diagram the two-dimensional array of detectors is indexed by *i* and *j*. Where

i = column(*k*) = integer part of [*k*/4];
j = row(*k*) = *k* - 4*i*

Therefore
k = 4*i* + *j*.

We assume that the X and Y co-ordinates increase in the directions of increasing column (*i*) and row (*j*) index

For each channel and target we can segregate this into two arrays corresponding to the images sampled by the two columns of detectors A (*i* = 0) and B (*i* = 1)

$$R_A(S,p',j) = R\{ch,target;S,p',k=j\}$$
$$R_B(S,p',j) = R\{ch,target;S,p',k=j+4\}$$ eq 5.5-13

Here we have introduced the notation

$$p' = 2p + t; \quad (0 \le p' < 2n_t - 1)$$ eq 5.5-14

*which i*s essentially the index to the PIX05SYNC such that

$$R\{ch,target;S,p',k\} = R\{ch,target;S,p,t,k\}$$ eq 5.5-15

where

$$p' = \text{intpt}(p/2);$$
$$t = 2p - p'$$ eq 5.5-16

5.5.3.3.1 Generating the TDI image

The objective of the present stage is to produce a combined 'TDI' image by adding the two images such that their positions are aligned in the centre of the swath. The resultant combined image will then have a lower signal to noise ratio than the A and B images taken separately. To include the 'TDI' image and processing in the Level-1b product may be selected as an option in the processor configuration.

If 'TDI' processing is selected, the combined 'TDI' image, which we will denote by R_C, is obtained by adding the two subsets by columns, with the appropriate offset to align the pixels in the centre of the swath. The correct indexing is obtained by considering the X co-ordinates corresponding to each of the pixel positions.

Consider the ground projection of the pixels. Let the X co-ordinate of the centre of the 0.5 km pixel indexed by {*S*, *p*', *k*} be X(*p*', *i*); we assume that it is essentially independent of scan index *S* and

detector row *j* in the centre of the swath (although this will not be true elsewhere). In the nadir view, the relationship between the columns of detectors means that, again in the centre of the swath,

$$X(p',1) = X(p'+1,0). \qquad \text{eq 5.5-17}$$

The X co-ordinates associated with elements of R_A and R_B are respectively

$$X_A(S,p',j) = X(p',0)$$
$$X_B(S,p',j) = X(p',1) = X_A(s,p'+1,j) \qquad \text{eq 5.5-18}$$
$$(0 \le p' < 2n_t - 1)$$

The arrays must therefore be added so that

$$R_C(S,p'_C j) = \left(R_A(S,p'_A,j) + R_B(S,p'_B,j)\right)/2 \qquad \text{eq 5.5-19}$$

where $p'_B = p'_A + TDI\_Direction(iView)$ and TDI_Direction = -1 or +1 depending on the ground track orientation of the SWIR detectors and the scan direction. Note that this will be different for Nadir and Oblique views.

The algorithm for the nadir view image is thus:

$$R_C(S,p'_C,j) = R_A(S,p'_C,j) \text{ if } p'_C = 0 \qquad \text{eq 5.5-20}$$
$$R_C(S,p'_C,j) = \left(R_A(S,p'_C,j) + R_B(S,p'_C-1,j)\right)/2 \text{ if } 1 \le p'_C \le 2n_t - 1 \qquad \text{eq 5.5-21}$$
$$R_C(S,p'_C,j) = R_B(S,p'_C-1,j) \text{ if } p'_C = 2n_t \qquad \text{eq 5.5-22}$$

In order to regrid the arrays R_C, it is necessary to generate the corresponding weighted pixel *x* and *y* co-ordinates. The same equations are used, but with nadir_x_coordinate and nadir_y_coordinate substituted for the corresponding R.

In the along-track view the relationship between of the detector columns relative to increasing *p* is reversed. X(*p*) decreases with increasing *p*, and the B column trails the A column. Therefore the relationship between the two columns is

$$X_B(S,p',j) = X(p',1) = X_A(s,p'-1,j) \qquad \text{eq 5.5-23}$$

The algorithm for the along-track view then becomes

$$R_C(S,p'_C,j) = R_B(S,p'_C,j) \text{ if } p'_C = 0 \qquad \text{eq 5.5-24}$$
$$R_C(S,p'_C,j) = \left(R_B(S,p'_C,j) + R_A(S,p'_C-1,j)\right)/2 \text{ if } 1 \le p'_C \le 2n_t - 1 \qquad \text{eq 5.5-25}$$
$$R_C(S,p'_C,j) = R_A(S,p'_C-1,j) \text{ if } p'_C = 2n_t - 1 \qquad \text{eq 5.5-26}$$

In order to regrid the arrays R_C, it is necessary to generate the corresponding weighted pixel *x* and *y* co-ordinates. The same equations are used, but with nadir_x_coordinate and nadir_y_coordinate substituted for the corresponding R.

5.5.3.4 Regrid pixels

The basic concept of this procedure is to remap the measured nadir and oblique instrument pixels from their positions on the curved instrument scans to a uniform grid of points in the common quasi-Cartesian co-ordinate system described in section 4.4.3. The procedure uses a modified nearest neighbour type of algorithm.

There are two image grids onto which the measurement pixels should be regridded: a 1km grid and a 0.5km grid. Each channel of each view must be regridded separately. Here we outline the approach that is adopted for a single combination of channel and view.

The starting point for a given channel/view is a set of brightness temperature or reflectance values, sampled on an instrument grid which reflects the curved scanning geometry of the SLSTR instrument, together with the X and Y co-ordinates of these instrument pixels in the image co-ordinate system.

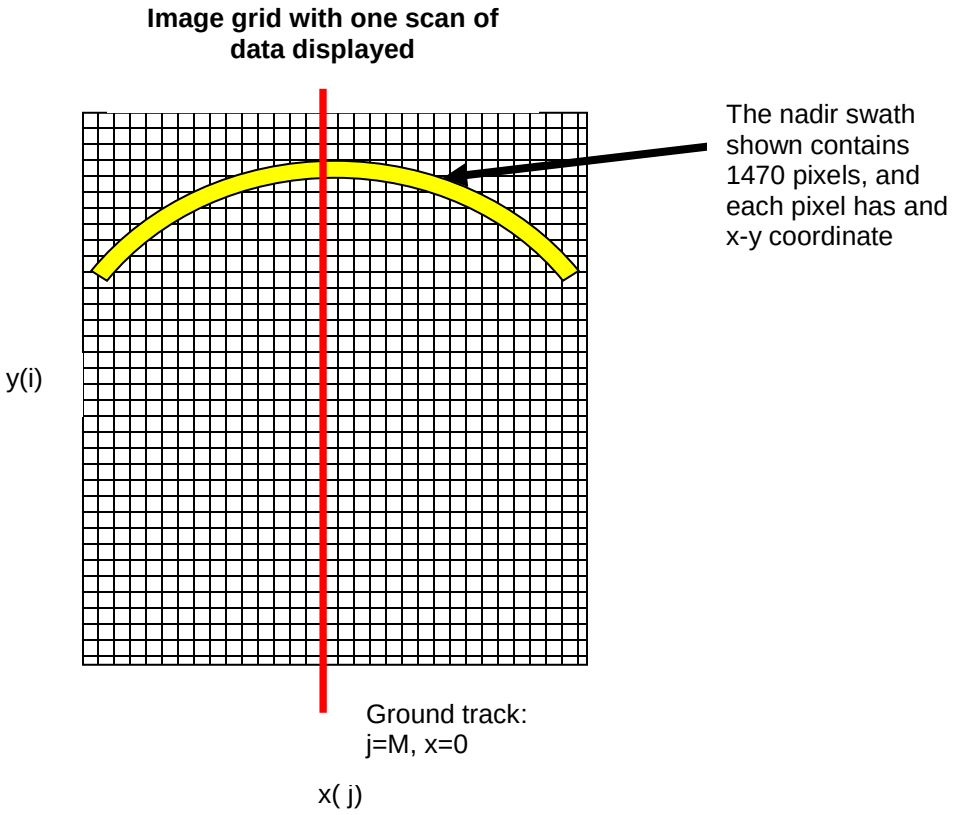

Figure 5-10

The aim of the regridding algorithm is to resample this set of instrument pixels onto a uniform rectangular grid of points in X and Y. Here X is the acrosstrack co-ordinate and Y is the along track co-ordinate.

We adopt the convention that the image grid is indexed by i, j, where the index i is an along-track index (to the rows of the image array) and j is the across-track index (to the columns). This can seem confusing, because i maps to Y and j to X, but it is consistent with the usual convention for indexing arrays, where A[i,j] represents an array indexed by rows (i) and columns (j).

The image is assumed to comprise N columns, indexed j = 0 to N - 1. The columns are equally sampled in X at interval dX. so that there is a linear relationship between X and j, which may be written as

$$X(j) = (j - M)dX. \qquad \text{eq 5.5-27}$$

where M is a constant such that the column indexed by j = M has X = 0 and so corresponds to the nominal ground track, since the definition of X states that X = 0 on the ground track. The nominal swath width is NdX. For the thermal channels, dX = 1 km, for the solar channels dX = 0.5 km.

In the along-track dimension the situation is more complicated, because, following AATSR practice, equal time sampling has been adopted. This means that the sampling interval in Y is given by

$$dY = vdT, \qquad \text{eq 5.5-28}$$

where v is the ground track velocity of the satellite, and dT is the appropriate fraction of the scan (SCANSYNC) period. That is, dT = SCANSYNC / K, where K is the number of detector rows for the channel. The ground trace velocity of the satellite varies around the orbit, so the spatial sampling interval dY also varies and we cannot assume a linear relationship between Y and the index i. Locally however the relationship is linear to a close approximation. If Y(i) is the Y co-ordinate of the row of samples indexed by i, we can write

$$Y(i + k) = Y(i) + kdY \qquad \text{eq 5.5-29}$$

where dY is locally constant, and is approximately equal to dX.

The set of points [i, j] whose co-ordinates are [X(j), Y(i)] for all valid i and j defines the sampling grid. Consider the rectangle whose corners are at the four points [X(j), Y(i)], [X(j), Y(i+1)], [X(j+1), Y(i+1)], [X(j+1), Y(i)]; this is a small rectangular area of approximate side 1 km (thermal channels) or 0.5 km (solar channels), and can be taken to define the image pixel at grid point [j, i]. The centre of this area is at [X(j) + 0.5dX, Y(i) + 0.5dY], and the set of points [X(j) + 0.5dX, Y(i) + 0.5dY] form the grid of pixel centres, displaced relative to the grid of corner points [X(j), Y(i)] by the vector [0.5dX, 0.5dY].

Relationship between the image grids

As noted above, there are two image grids, at nominal sampling intervals of 1.0 and 0.5 km for the thermal / fire and solar channels respectively. In order to distinguish between the two, let us adopt the notation that the 1.0 km grid is indexed by [i_{10}, j_{10}], and the 0.5 km grid by [i_{05}, j_{05}]. Note that as before i is the along-track and j is the across-track index.

The 1.0 km image grid therefore consists of the set of points having co-ordinates

$$X[i_{10}, j_{10}], Y[i_{10}, j_{10}] \qquad \text{eq 5.5-30}$$

where

$$X[i_{10}, j_{10}] = (j_{10} - M)dX \qquad \text{eq 5.5-31}$$

and

$$Y[i_{10} + 1, j_{10}] = Y[i_{10}, j_{10}] + dY \qquad \text{eq 5.5-32}$$

The 0.5 km grid consists of he set of points having co-ordinates

$$X[i_{05}, j_{05}], Y[i_{05}, j_{05}] \qquad \text{eq 5.5-33}$$

where

$$X[i_{05}, j_{05}] = (j_{05} - M)(dX / 2)$$ eq 5.5-34

and

$$Y[i_{05} = 2i_{10}, j_{05}] = Y[i_{10}, j_{10}]$$ eq 5.5-35

In other words the points of the 1.0 km image grid having the indices $[i_{10}, j_{10}]$ are coincident with the points of the 0.5 km grid having indices

$$i_{05} = 2i_{10}; j_{05} = 2 j_{10}$$ eq 5.5-36

We regard the grid points as defining the lower left corners (not the centres) of the image pixels. (In other words the geometrical instrument pixel [i10, j10] at 1 km resolution includes the four 0.5 km pixels $[2*i_{10}, 2*j_{10}]$, $[2*i_{10}+1, 2*j_{10}]$, $[2*i_{10}, 2*j_{10}+1]$, $[2*i_{10}+1, 2*j_{10}+1]$.)

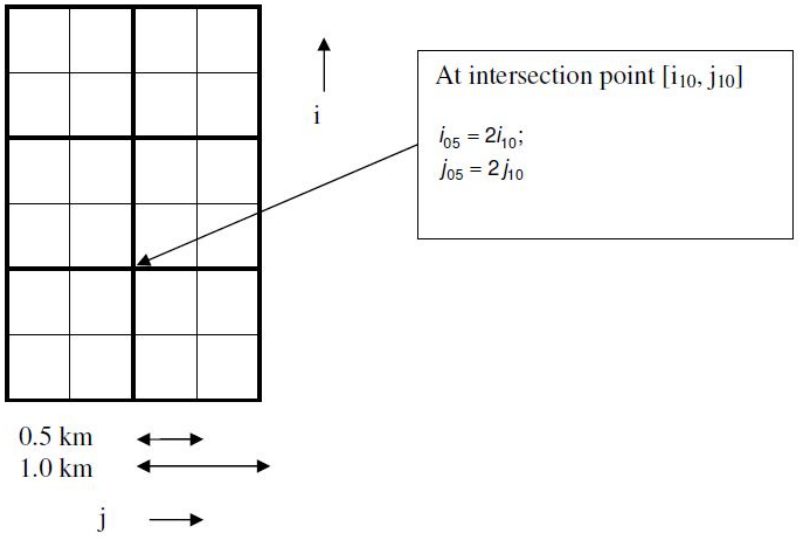

Figure 5-11

Prior processing will have generated input arrays on 4 different instrument grids for each of the two views; the 1 km grid for the 3 thermal and fire channels, 0.5 km A and B grids for the solar channels, and a combined 0.5 km grid for the TDI channels..

The four instrument grids are as follows:

1) *In terms of the notation defined in Section 4.2.3, the thermal and fire channel instrument grid is represented by the set of indices S, p, k = 0, 1, representing scan, pixel and detector number. Alternatively they may be indexed by scan trace and pixel index s, p, which is the approach adopted in Section 5.5.3.3.*

2) *The instrument grid for the A stripe (VIS channels and SWIR) is represented by the index set S, p, t=0, 1, k = 0, …3.*

3) *The instrument grid for the B stripe (SWIR only) by S, p, t=0, 1, k = 4, …7 (assuming the detector indexing illustrated in Section 5.5.3.2 (page 118). Again the ATBD adopts the combined indices s = 4S + row(k), p'= 2p + t. (The prime is then dropped for notational convenience).*

4) *The TDI grid is that defined in Section 5.5.3.2.*

Each channel must be regridded into one of two output grids (at 1 km and 0.5 km resolution, as appropriate). There are two output grids for each view, which differ in that the grid for the solar channels has twice the dimensions of that for the solar thermal channels. The indices i and j refer to the appropriate array, as do the MAX and MIN limits. The 1.0 and 0.5 km image grids are coincident in the sense that alternate samples of the 0.5 km grid coincide with the samples of the 1.0 km grid. In detail, for each view we will have the following:

- *Three thermal and two fire channels, to be resampled from the 1 km instrument grid to the 1 km image grid.*
- *Six 'A stripe' solar channels to be regridded from the 'A stripe' instrument grid to the 0.5 km image grid (assuming that the visible channel detectors correspond to the A stripe).*
- *Three 'B stripe' SWIR channels to be regridded from the 'B stripe' instrument grid to the 0.5 km image grid (again assuming that the visible channel detectors correspond to the A stripe).*
- *Three combined TDI SWIR channels to be regridded from the TDI instrument grid to the 0.5 km image grid.*

In order to retain the link between the regridded pixels and their original positions in the measurement geometry, the original instrument scan, pixel and detector number are retained in an ADS.

Step 5.5.1 Initialize Image Arrays

Initialize the regridded data arrays. This is necessary to ensure (a) that the requirement for cosmetic fill can be recognised; (b) that unfilled pixels can be identified at the conclusion of the regridding and cosmetic fill processes; and (c) that the regridded maximum and minimum temperature variables are initialized.

nadir_fill_state(i, j) = UNFILLED_PIXEL
oblique_fill_state(i, j) = UNFILLED_PIXEL

These are the arrays which will contain the fill state of each pixel after regridding and cosmetic fill. The elements of these arrays may take one of 3 possible values:

NATURAL_PIXEL The pixel has been assigned by the regridding algorithm
COSMETIC_PIXEL The pixel value has been assigned by the cosmetic fill algorithm
UNFILLED_PIXEL Neither the regridding nor cosmetic fill algorithm have assigned a value to this pixel

Unfilled pixels occur because the cosmetic fill algorithm requires that an initially unfilled pixel can only be filled by an adjacent pixel. If a pixel has no naturally filled neighbours, it willremain unfilled. The pixel fill state will eventually appear in the product as an exception flag.

The fill values are used in the global confidence words in table of SY4 and the thermal and visible MDS exception words (see tables below).

Bit Number	Text Code	Description
0	ISP_absent	ISP absent
1	pixel_absent	Pixel absent
2	not_decompressed	Not decompressed
3	no_signal	No signal in channel
4	saturation	Saturation in channel
5	invalid_radiance	Derived radiance outside calibration
6	no_parameters	Calibration parameters unavailable
7	unfilled_pixel	Unfilled pixel

.

Bit	Text code	Meaning if set	Comment
0	coastline	coastline in field of view	
1	ocean	ocean in field of view	
2	tidal	tidal zone in field of view	
3	land	land in field of view	
4	inland_water	inland water in field of view	
5		(spare)	
6		(spare)	
7		(spare)	
8	cosmetic	cosmetic fill pixel	
9	duplicate	duplicate pixel not regridded	
10	day	pixel in daylight	
11	twilight	pixel in twilight	
12	sun_glint	sun glint in pixel	
13	snow	snow	
14	summary_cloud	summary cloud test	
15	summary_pointing	summary pointing	

nadir_min_anc_temps(i, k) = +999.0 (k = 0, 1, ...5)
nadir_max_anc_temps(i, k) = -999.0 (k = 0, 1, ...5)

oblique_min_anc_temps(i, k) = +999.0 (k = 0, 1, ...5)
oblique_max_anc_temps(i, k) = -999.0 (k = 0, 1, ...5)

The above arrays hold the maximum and minimum detector temperatures recorded on the instrument scans that contribute to a given image row.

nadir_packet_invalid(i) = 0
oblique_packet_invalid(i) = 0

Invalidity flags for the source packets contributing to each pixel row.

Also initialise the instrument scan, pixel and detector number to zero for all values of i, j:
nadir_scan_number(i, j) = 0
nadir_pixel_number(i, j) = 0
nadir_detector_number(i, j) = 0

oblique_scan_number(i, j) = 0
oblique_pixel_number(i, j) = 0
oblique_detector_number(i, j) = 0

These arrays are for use by level 1c and 2 processing to show the origin on the instrument grid of each pixel.

For each MDS initialise the exception flags for each channel in each view to FALSE:

exception(i, j) = FALSE; eq 5.5-37
exception_orphan(i, j) = FALSE eq 5.5-38

Step 5.5.2 Regrid Image Pixels, Nadir View

The following steps are implemented for each instrument pixel in the nadir view.

As in section 5.3.3.1, instrument pixels will be identified by the following indices

s	Scan number;
p_n	Absolute pixel number relative to scan sync, nadir scan
p_o	Absolute pixel number relative to scan sync, oblique (inclined) scan
p'_n	Relative pixel number, nadir scan ($0 \le p'_n <$ MAX_NADIR_PIXELS)
p'_o	Relative pixel number, oblique (inclined) scan ($0 \le p'_a <$ MAX_OBLIQUE_PIXELS)
k	Detector element index. k = 0, 1 for the thermal channels, 0, … 3 for the VIS-NIR channels , 0-7 for the SWIR channels.

Note that the regridding is performed using absolute pixel number which is an internal processing parameter. The output measurement dataset on the instrument grid is indexed by relative pixel position. Conversion to absolute pixel position is possible using the 'add_offset' attribute.

In Section 5.3.3.10 the *x* and *y* co-ordinates of each instrument pixel on the instrument tie point grid were determined. We introduce the following notation

- *nadir_x_coords(s, p_n, k)*, *nadir_y_coords(s, p_n, k)* for the x and y co-ordinates respectively of the nadir pixel identified by indices, s, p_n, k.
- *MIN_NADIR_X*, *MAX_NADIR_X* to denote the lower and upper limits of the nadir image in *x* units.
- *scale*, which takes the value 1 for the thermal channels and 2 for the solar channels (it is the reciprocal of the nominal resolution, in km.)
- FIRST_<VIEW>_PIXEL_NUMBER is the first pixel number in the earth view ISPs.

The first pixel number of the solar and SWIR channels will be twice that of the FIRST_<VIEW>_PIXEL_NUMBER, and therefore the *scale* factor is used to account for this in the algorithms.

For each scan *S* the channels are processed as follows:

For each nadir pixel on the instrument tie point grid, for all applicable values of *k*, in the nadir scan S for which

nadir_x_coords(s, p_n, k) ≥ *MIN_NADIR_X* and eq 5.5-39

nadir_x_coords(s, p_n, k) < MAX_NADIR_X, eq 5.5-40

the regridding indices are calculated. Find the row index *ig* on the geolocation grid such that

track_y(ig + K) ≤ *nadir_y_coords*(s, p_n, *k*) < *track_y(ig + K + 1)*

is found where *track_y*, *K* are defined in Section 5.3.3.10.

Obtain the along track distance between geolocation grid rows

$$\Delta y = (track\_y(ig + K + 1) - track\_y(ig + K)) \quad \text{eq 5.5-41}$$

Compute the along track distance between the image pixel and geolocation grid.

$$\delta y = scale\,(nadir\_y\_coords(s, p_n, k_n) - track\_y(ig + K))/\Delta y \quad \text{eq 5.5-42}$$

Obtain the image grid row for the pixel.

$$i' = \text{integer part of } (\delta y) \quad \text{eq 5.5-43}$$

$$i = scale \cdot ig + i' \quad \text{eq 5.5-44}$$

Note that there are twice as many image rows for the VIS-SWIR channels as the TIR channels. *i'* should be 0 or 1 for the TIR channels and 0 - 3 for the VIS-SWIR channels.

Now obtain the image column index jg on the geolocation grid.

$$\delta x = scale(nadir\_x\_coords(s, p_n, k) - MIN\_NADIR\_X) \quad \text{eq 5.5-45}$$

$$j = \text{FIX}(\delta x) \quad \text{eq 5.5-46}$$

If *i or j* is negative, the pixel is outside the image bounds. This should not be an issue provided that the image and scan tie point grids are sized to be larger than the measurement grid.

Step 5.5.2.4 Regrid nadir pixels

Save the instrument scan, pixel and detector number for the regridded image point in the nadir view:

nadir_scan_number(*i*, *j*) = S_n eq 5.5-47
nadir_pixel_number(*i*, j) = scale.p_n eq 5.5-48
nadir_detector_number(i,j) = k eq 5.5-49

Note at this stage the absolute scan and pixel numbers are retained to allow regridding of all parameters. For the output stage only the relative scan and pixel numbers contained within the ISP are retained.

Finally the calibrated nadir channel data and exception flags for each channel are copied to the regridded data arrays. In the following, the index *ch* refers to the channel. *I* refers to the calibrated intensity (Temperature or reflectance, as appropriate) of the destination channel. B*T* and *R* refer to the calibrated brightness temperature or radiance, as appropriate, of the instrument pixel channels.

The fill_state is initially set as UNFILLED_PIXEL and subsequently set as NATURAL_PIXEL during successful regridding. During regridding, if a pixel on the image grid does not have it's fill_state set as UNFILLED PIXEL, the image pixel has already been filled and the source pixel becomes an *orphan pixel*. The *duplicate_pixel* flag within the confidence word of the appropriate image grid is set and the orphan pixels and their coordinates are saved to the orphan dataset, using the indexes i_o and j_o which are incremented each time an orphan is found.

fill_state(*nadir*, *, *) =UNFILLED_PIXEL

For all S and p contained within the earth view ISPs:

For the thermal infra-red channels ch = S7-S9, F1-F2

If fill_state(*nadir*, *i*, *j*) =UNFILLED_PIXEL then

I(ch, nadir; i, j) = BT(ch, nadir; s, p_n,k) eq 5.5-50
exception_flag(ch,nadir, i, j) = Exception(ch, nadir, s, p_n,k)

Else

I_orphan(ch, nadir; i_o, j_o) = BT(ch, nadir; s, p_n,k)
exception_flag_orphan(ch,nadir, i_o, j_o) = Exception(ch, nadir, s, p_n,k)

For the (solar) channels ch = S1-S3, an offset of 1 pixel is applied in order to correct for a positional shift between the VIS channles and the SWIR channels

If fill_state(*nadir*, *i*, *j*) =UNFILLED_PIXEL then

I(ch, nadir, i, j) = R(ch, nadir; s, p_n +1,k). eq 5.5-51a
exception_flag(ch,nadir, i, j) = Exception(ch, nadir, s, p_n +1,k)

Else

I_orphan(ch, nadir, i_o, j_o) = R(ch, nadir; s, p_n +1,k).
exception_flag_orphan(ch,nadir, i_o, j_o) = Exception(ch, nadir, s, p_n +1,k)

For the (SWIR) channels ch = S4-S6,

If fill_state(*nadir*, *i*, *j*) =UNFILLED_PIXEL then

I(ch, nadir, i, j) = R(ch, nadir; s, p_n,k). eq 5.5-52b

exception_flag(ch,nadir, i, j) = Exception(ch, nadir, s, p_n,k)

Else

I_orphan(ch, nadir, i_o, j_o) = R(ch, nadir; s, p_n,k).

exception_flag_orphan(ch,nadir, i_o, j_o) = Exception(ch, nadir, s, p_n,k)

For all S and p outside the earth view ISPs
For all channels ch = S1-S9, F1-F2
I(ch,nadir, i, j) = Fill_value eq 5.5-53

Finally the offset of the source pixel from the corner of the regridded pixel is saved for use by the cosmetic fill routine.

x_offset(*nadir*, *i*, *j*) = fractional part of δx eq 5.5-54
y_offset(*nadir*, *i*, *j*) = fractional part of δy eq 5.5-55
fill_state(*nadir*, *i*, *j*) = *NATURAL_PIXEL* eq 5.5-56

Step 5.5.3 Regrid Image Pixels, Oblique View
This process is repeated for the oblique scan as follows.

In Section 5.3.3.10 the *x* and *y* co-ordinates of each instrument pixel on the tie point grid were determined. We introduce the following notation

- *oblique_x_coords(S, po, k)*, *oblique_y_coords(S, po, k)* for the x and y co-ordinates respectively of the oblique pixel identified by indices, *s*, p_a, *k*.
- *MIN_OBLIQUE_X*, *MAX_OBLIQUE_X* to denote the lower and upper limits of the instrument oblique swath in *x* units (provisionally we expect *MIN_OBLIQUE_X* = -384 km, *MAX_OBLIQUE_X* = +384 km.)

For each oblique pixel for all applicable values of *k* in the oblique scan *s* with

oblique_x_coords(S, p_o, k) ≥ MIN_OBLIQUE_X and
oblique_x_coords(S, p_o, k) < MAX_OBLIQUE _X
eq 5.5-57

the regridding process proceeds exactly as before, except that references to oblique view quantities replace those of the equivalent nadir view variables throughout.

Find the row index *ig* on the geolocation grid such that

$$track\_y(ig + K) \le oblique\_y\_coords(S, p_o, k) < track\_y(ig + K + 1) \quad \text{eq 5.5-58}$$

is found where *track_y*, *K* are defined in Section 5.3.3.10.

Obtain the along track distance between geolocation grid rows

$$\Delta y = (track\_y(ig + K + 1) - track\_y(ig + K)) \quad \text{eq 5.5-59}$$

Compute the along track distance between the image pixel and geolocation grid.

$$\delta y = scale(oblique\_y\_coords(S, p_o, k) - track\_y(ig + K))/\Delta y \quad \text{eq 5.5-60}$$

Obtain the image grid row for the pixel.

$$i' = \text{integer part of } (\delta y) \quad \text{eq 5.5-61}$$

$$i = scale \cdot ig + i' \quad \text{eq 5.5-62}$$

Note that there are twice as many image rows for the VIS-SWIR channels as the TIR channels. *i'* should be 0 or 1 for the TIR channels and 0 - 3 for the VIS-SWIR channels.

Now obtain the image column index jg on the geolocation grid.

$$\delta x = scale(oblique\_x\_coords(S, p_o, k) - MIN\_OBLIQUE\_X) \quad \text{eq 5.5-63}$$

$$j = FIX(\delta x) \quad \text{eq 5.5-64}$$

If *i or j* is negative, the pixel is outside the image bounds. This should not be an issue provided that the image and scan tie point grids are sized to be larger than the measurement grid.If *i* is negative, the pixel is outside the image bounds. (As in the nadir case, this should not happen, provided the image bounds are properly chosen, but if it does) set *j* to the next available orphan pixel index and continue, at **Step 5.5.3.4**.

If $i' = 0$ (that is, if the value of *i* corresponds to a granule row), or
this is the first scan to be regridded, or
oblique_scan_number(i_g, j) = 0

Step 5.5.3.4 Regrid oblique pixels

Save the scan and pixel number for the regridded image point in the oblique view:

oblique_scan_number(*i*, *j*) = S_o eq 5.5-65
oblique_pixel_number(*i*, *j*) = scale.p_o eq 5.5-66
oblique_detector_number(i, j) = k eq 5.5-67

Note at this stage the absolute scan and pixel numbers are retained to allow regridding of all parameters. For the output stage only the relative scan and pixel numbers contained within the ISP are retained.

Finally the calibrated oblique view data for each channel are copied to the regridded data arrays in a similar way as for the nadir view data.

fill_state(*oblique*, *, *) =UNFILLED_PIXEL

For all S and p contained within the earth view ISPs

For the thermal infra-red channels ch = S7-S9, F1-F2

If fill_state(oblique,i,j) = UNFILLED_PIXEL

I(ch, oblique, i, j) = BT(ch, oblique, s, p_n,k) eq 5.5-68

exception_flag(ch, oblique , i, j) = Exception(ch, oblique, s, p_n,k)

Else

I_orphan(ch, oblique, i_o, j_o) = BT(ch, oblique, s, p_n,k)

exception_flag_orphan(ch, oblique , i_o, j_o) = Exception(ch, oblique, s, p_n,k)

For the (solar) channels ch = S1-S3, an offset of 1 pixel is applied in order to correct for a positional shift between the VIS channels and the SWIR channels

If fill_state(oblique,i,j) = UNFILLED_PIXEL

I(ch, oblique, i, j) = R(ch, oblique ; s, p_n+1,k). eq 5.5-69a

exception_flag(ch, oblique , i, j) = Exception(ch, oblique, s, p_n+1,k)

Else

I_orphan(ch, oblique, i, j) = R(ch, oblique ; s, p_n+1,k).

exception_flag_orphan(ch, oblique , i, j) = Exception(ch, oblique, s, p_n+1,k)

For the (SWIR) channels ch = S4-S6

If fill_state(oblique,i,j) = UNFILLED_PIXEL

I(ch, oblique, i, j) = R(ch, oblique; s, p_n,k). eq 5.5-70b

exception_flag(ch, oblique, i, j) = Exception(ch, oblique, s, p_n,k)

Else

I_orphan(ch, oblique, i_o, j_o) = R(ch, oblique; s, p_n,k).

exception_flag_orphan(ch, oblique, i_o, j_o) = Exception(ch, oblique, s, p_n,k)

For all S and p outside the earth view ISPs

For all channels ch = S1-S9, F1-F2

I(ch,oblique, i, j) = Fill_value eq 5.5-71

Finally the offset of the source pixel from the corner of the regridded pixel saved for use by the cosmetic fill routine.

x_offset(*oblique*, *i*, *j*) = fractional part of δx eq 5.5-72

y_offset(*oblique*, *i*, *j*) = fractional part of δy eq 5.5-73

Set the fill state for the pixel just regridded:
fill_state(*oblique*, *i*, *j*) = *NATURAL_PIXEL* eq 5.5-74

Step 5.5.4 Regrid Auxiliary Information
Other nadir view information from the source packet is now regridded. This section is based on the functions performed during AATSR processing, and may require modification for the SLSTR instrument following instrument testing.

To regrid the remaining information find the first and last regridded image rows to which the instrument scan contributes. The extreme scan y positions are :-

nadir_y_coords(s, 0) eq 5.5-75
nadir_y_coords(s, number_of_scan_pixels - 1) eq 5.5-76
nadir_y_coords(s, number_of_scan_pixels / 2) eq 5.5-77

Find the minimum and maximum of these positions ymin and ymax. Then find the regridding indices *imin* and *imax* using the method for calculating *i* detailed above. For each scan i = imin, imax do the following:
Test packet_error(s) in turn for the following.

Raw Packet fails basic validation error
Checksum errors
Scan and Flip Mirror Errors

If equality is found the corresponding bit in the global ADS is set.

Next the minimum and maximum values of each of the 6 anciliary temperatures for the current scan are updated when the current values are exceeded by the instrument scan values.
ie for janc = 0 to 5
if anc_unconv(s, janc) > 0 then
    if anc_temp(s, janc) < nadir_min_anc_temps(i, janc) then
        nadir_min_anc_temp(i, janc) = anc_temp(s, janc)
    if anc_temp(s, janc) > nadir_max_anc_temps(i, janc) then
        nadir_max_anc_temp(i, janc) = anc_temp(s, janc)
end if
eq 5.5-78

This process is repeated to obtain the oblique scan information.

5.5.3.5 Cosmetic Fill

This process is carried out on the regridded nadir image (view = nadir) and then on the regridded oblique image (view = oblique), and is illustrated by the figure 5-10 below:

Example of cosmetic fill for 1km image grid.

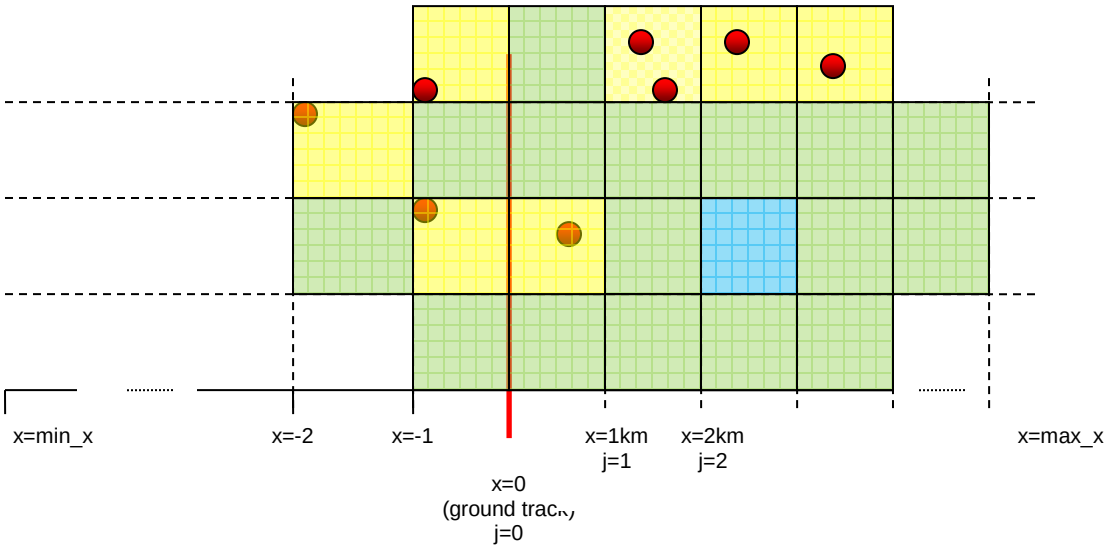

Circles represent the x and y coordinates of the centre of the measurement pixels, xn, yn as previously defined

Image grid square filled with measurement grid data or exception flag. **Naturally filled.**

Image grid square filled with measurement grid data point from the nearest neighbour. **Cosmetically filled.**

Image grid square not filled. **Unfilled pixel.**

Image grid square Naturally filled but there are two measurement pixels contained in the same square. One of these is an **orphan pixel.**

Figure 5-12

Step 5.5.1 Fill Image pixels

For each pixel (i, j) in the regridded image check the fill state flag and if the pixel is unfilled, ie

fill_state(*view*, *i*, *j*) = UNFILLED_PIXEL, eq 5.5-79

an attempt is made to fill it using data from an adjacent pixel as follows.

Examine the 8 regridded pixels adjacent to the unfilled pixel. Each candidate pixel (i_c, j_c) must satisfy the following tests:

1. It is not outside the limits of the swath;
2. It is a naturally filled pixel
   fill_state(*view*, i_c, j_c) = NATURAL_PIXEL
   eq 5.5-80

If no candidate pixels are found then the pixel remains unfilled and the pixel values in every channel are set to the PIXEL_UNFILLED value.

I(ch, v, i, j) = PIXEL_UNFILLED

Set the corresponding exception flag to unfilled pixel accordingly:

exception_flag(ch,view,i,j) = 128 (unfilled pixel) eq 5.5-81

If candidate pixels are found then for each candidate the distance *d* of the source pixel from the centre of the unfilled target pixel is calculated.

$$dx = j_c - j + x\_offset(view, i_c, j_c) - 0.5. \quad \text{eq 5.5-82}$$

$$dy = i_c - i + y\_offset(view, i_c, j_c) - 0.5. \quad \text{eq 5.5-83}$$

$$d = \sqrt{dx^2 + dy^2} \quad \text{eq 5.5-84}$$

The candidate with the smallest distance is selected.

The fill state flag for the target pixel is now set to indicate a cosmetically filled pixel and the pixel values from the selected candidate pixel are copied to the target pixel for all channels *ch*.

fill_state(*view*, *i*, *j*) = COSMETIC_PIXEL. eq 5.5-85

I(ch, v, i, j) = I(ch, v, ic, jc) eq 5.5-86

Set the corresponding exception byte value accordingly:

exception_flag(ch,view,i,j) = 2 (cosmetic fill) eq 5.5-87

Step 5.5.2 Fill Auxiliary Information

Any gaps in the band edge solar angles and band centre solar angles must now be filled. A gap is filled using data from an adjacent valid point along track in the arrays, or if this fails, an adjacent valid point across track is used.

Step 5.5.3 Fill Nadir and Oblique Scan, Pixel and Detector Number Array

In order to permit the array of instrument scan pixel and detector numbers S, P, D to be used during Level 2 processing to time tag averaged product cells, these are also 'cosmetically filled' such that.

S(v, i , j) = S(v, ic, jc)

P(v, i, j) = P(v, ic, jc)

and

D(v, i, j) = D(v, ic, ij) eq 5.5-88

5.5.3.6 Surface classification

The pixel classification is represented as a small number of classification flags, one for each distinct surface type. The classification is performed as follows on the instrument grid:

- Calculate the optical ray corresponding to the centre of the pixel FOV – as described in section 5.3.4
- Calculate the intersection of the ray with the topographic surface of the earth– as described in section 5.3.4. The orbit CFI contains the topography.
- Look up the value of the surface classification map cell containing the intersection point.
- Set classification flags for all surface types detected at the centre of the FOV.
- If several pixel radiances are combined as part of a time domain integration (TDI) algorithm, then the classification flags for the composite pixel are set to the bitwise OR of the flags in the contributing pixels.
- The result of the classification test is regridded to the L1b image grid by the same nearest-neighbour algorithm that is applied to the corresponding pixel radiance - 5.5.3.4 and 5.5.3.5.

The surface classification flags are listed in Table 5-6 below and written to the global flags ADS.

Table 5-6: Surface Classification Flags

Bit	Text code	Meaning if set	Comment
0	coastline	coastline in field of view	
1	ocean	ocean in field of view	
2	tidal	tidal zone in field of view	
3	land	land in field of view	
4	inland_water	inland water in field of view	

5.5.3.6.1 Commentary

No flags will be set for pixels for which do not contain any re-gridded radiances. If required, a default value representing the centre of the L1b pixel can be substituted but, as these pixels cannot be used in subsequent processing, the more obvious approach would be to leave the flags unset, indicating an exception condition.

Separate classifications must be derived for each instrument view, resolution and (for channels S4 – S6) both the “a” and “b” detector “stripes”.

Higher-level products which use combinations of L1b products may need to interpret several classification words. In most cases the correct composite surface classification flags will be the bitwise OR of all contributing pixel surface classification flags.

5.5.3.7 Regrid Solar and view geometry parameters

Solar and view geometry is computed on the instrument tie point grid (5.3.3.8) and need to be regridded using a similar method to the radiometric data after performing the cosmetic filling. These are output on the 16km tie-point grid but an internal variable containing the SZA, SAA at full resolution should be kept to be used at cloud flagging. To obtain the angles for each image pixel we using the same the bilinear interpolation as described in 5.3.3.10. So for each view, scan and pixel we use

S = <view>_scan_number(i,j) eq 5.5-89
P = <view>_pixel_number(i,j) eq 5.5-90

The S and P values for the tie-point grid are a subset of the values used for the full resolution image grids

5.5.3.7.1 Determine if pixel is day, twilight or night

For each pixel, determine whether it is in day, twilight or night and set the appropriate bit in the confidence word. Note that the classification is performed on the instrument grid NOT the image grid.

```
If(solar_zenith_angle(S,p) <= day_threshold_solar_zenith)then
        Confidence_word(s,p) += 2^10

If((solar_zenith_angle(S,p) > day_threshold_solar_zenith) & (solar_zenith_angle(S,p) <=
twilight_threshold)then
        Confidence_word(s,p) += 2^11
```

The processing parameters day_threshold_solar_zenith and twilight_threshold_solar_zenith are provided in the L1b processing configuration ADF. The default values for the thresholds are:

day_threshold_solar_zenith = 90 degrees
twilight_threshold_solar_zenith = 102 degrees (nautical twilight)

Note that the day_threshold_solar_zenith is not the same as the threshold used for the cloud tests.

5.5.3.8 Convert Absolute Scan and Pixel numbers to relative scan and pixel numbers for output grid

Up to this point we have performed all the regridding using absolute scan and pixel numbers. To allow indexing in the output measurement grid we need to convert the scan and pixel numbers to relative values such that

p'_n Relative pixel number, nadir scan ($0 \le p'_n <$ MAX_NADIR_PIXELS)
p'_o Relative pixel number, oblique (inclined) scan ($0 \le p'_a <$ MAX_OBLIQUE_PIXELS)

p = 0, S=0 corresponds to the first pixel on the measurement grid.

For each view the relative pixel number is

$$p'_{view}(i,j) = p_{view}(i,j) - (scale * FIRST\_<view>\_PIXEL\_NUMBER) \quad \text{eq 5.5-91}$$

FIRST_<view>_PIXEL_NUMBER is set as the attribute 'add_offset'. The relative scan number is

$$S'_{view}(i,j) = S_{view}(i,j) - K \quad \text{eq 5.5-92}$$

For all pixels and scans outside the valid range the output S', p' values are set to Fill_values.

If($p'_{view}(i,j) < 0$) and ($p'_{view}(i,j) >=$ MAX_<VIEW>_PIXELS)then
$p'_{view}(i,j)$ = Fill_Value eq 5.5-93

If($S'_{view}(i,j) < 0$) and ($S'_{view}(i,j) >=$ MAX_<VIEW>_SCANS)then
$S'_{view}(i,j)$ = Fill_Value eq 5.5-94

5.5.3.9 Identification of Cloud Affected Pixels

The identification of cloud affected pixels is accomplished by applying in turn a series of tests to the brightness temperature data in the 12, 11 and 3.7 micron channels, and to the reflectance data in the short-wave infra-red visible channels. The pixel is flagged as cloudy if any one of the 'valid' cloud tests indicates the presence of cloud. The condition of a cloud test being 'valid' in order to contribute to the summary_cloud word has been introduced to guard against poorly performing algorithms giving erroneous results in the summary_cloud. A switch in the PCP file is used to indicate which of the cloud tests should be included in the summary_cloud. Note that the results of all cloud tests are still given individually. Table 5-7 below summarises the cloud clearing tests to be applied. All of the tests are of course conditional on the appropriate infra-red or visible channel data being available. The theoretical basis of the majority of these tests is set out in Reference [RD-7]. Most of the tests listed have AATSR heritage, but two are new; these are the 1.375 micron threshold test and the 2.25 micron histogram test, which utilize the new short-wave infra-red channels of SLSTR.

Table 5-7: Cloud Clearing Tests

Test	Comments
gross cloud test	applied to nadir and oblique views separately
thin cirrus test	applied to nadir and oblique views separately
medium/high level cloud test	applied to nadir and oblique views separately
fog/low stratus test	applied to nadir and oblique views separately
11 micron spatial coherence test	applied to nadir and oblique views separately
1.6 micron histogram test	applied to nadir and oblique views separately
11/12 micron nadir/oblique test	uses both views
11/3.7 micron nadir/oblique test	uses both views
infra-red histogram test	applied to nadir and oblique views separately
Visible channel cloud test	applied to nadir and oblique views separately
1.375 micron threshold test	applied to nadir and oblique views separately
2.25 micron histogram test	applied to nadir and oblique views separately
Snow-covered surface test	applied to nadir and oblique views separately

Some of the tests depend on the results from the tests performed previously and hence the order in which they are applied is important. The infrared histogram test is applied after the 1.6 micron and thermal infra-red tests, and only uses those pixels that have not been flagged as cloudy by any of the preceding tests. The 1.6 micron test operates only on pixels not previously flagged as cloudy by the gross cloud test or the thin cirrus and 11 micron spatial coherence tests (the other single view tests that operate on daytime data), and must therefore follow these. The large-scale component of the 11 micron spatial coherence test operates only on pixels that have not been flagged by the gross cloud, thin cirrus, mediun/high level and fog/low stratus tests, and should therefore follow them.

The visible channel cloud test is applied independently of the other tests, and follows the infra-red histogram test; since the visible channel test is currently only applied over land, while the infra-red histogram test is applied only to sea pixels, there is no point in introducing a dependency of the latter on the former, and the visible channel test is therefore applied after the infra-red histogram test.

The two tests using the two new short-wave channels at 1.375 and 2.25 microns are considered untried, and it is therefore not considered prudent to make any of the other tests dependent on them at this stage, although the 2.25 micron test can have the same dependency on other daytime tests as the 1.6 micron test. These therefore follow the other tests.

The snow test is not considered to be a cloud test as such, owing to the difficulty of distinguishing snow-or ice covered surfaces from ice cloud, and it does not contribute to the overall cloud flag. It is therefore applied last.

The tests should be applied in the order in which they appear in Table 5-7. In the following the tests are described in the order in which they are applied, except that the 11 micron spatial coherence test (Section 5.5.3.6.1) appears out of sequence, and should be applied after the fog/low stratus test (Section 5.5.3.6.5) for the reason stated.

The 1.6 micron test and the visible channel test operate on daytime data only. The tests involving the 3.7 micron channel, on the other hand, are only applied to night-time data, because reflected solar radiation may be significant in this channel during the day. Those tests that involve the 11 and 12 micron channels are applicable to both daytime and night-time data. Not all of the tests are implemented over land.
Each test makes use of a look-up table of parameters with which the brightness temperature or reflectance data is compared. Where tests are applied to oblique and nadir view images separately, the parameters may be defined separately for the two cases. More generally, the comparison parameters may depend on the air mass in the line of sight, and this is implemented by allowing the tabular parameters to depend upon the across-track position.

The cloud tests are performed at the native resolution of the detector elements – i.e. for TIR detectors cloud flags are computed at 1km resolution and VIS/SWIR at 0.5km resolution. In detail, the cloud tests are all based on the regridded brightness temperatures or reflectances, which are sampled on a rectangular grid in the cartesian co-ordinates X and Y, where X is the across-track co-ordinate and Y is the along track co-ordinate. For each view there are two grids, at 1 km and 0.5 km resolution, as appropriate, so the grid for the solar channels has twice the dimensions of that for the solar thermal channels. The 1.0 and 0.5 km image grids are coincident in the sense that alternate samples of the 0.5 km grid coincide with the samples of the 1.0 km grid.

We adopt the convention that the grid is indexed by i, j, where the index i is an along-track index (to the rows of the image array) and j is the across-track index (to the columns). With this convention, suppose the thermal image arrays have N colums, indexed j_10 = 0 to N - 1. Then the solar channel

arrays will have 2N columns indexed j_05 = 0, 2N-1. Similarly we can index the arrays in the along-track directionwith i_10 and i_05 for the 1.0 km and 0.5 km channels respectively.

In those cases where a test based on the solar channels uses thermal channel data, the thermal channel value associated with the solar channel pixel at [i_05, j_05] is that indexed by

i_10 = integer part of (i_05/2) eq 5.5-95
j_10 = integer part of (j_05/2) eq 5.5-96

(In other words the geometrical instrument pixel [i_10, j_10] at 1 km resolution includes the four 0.5 km pixels [2*i_10, 2*j_10], [2*i_10+1, 2*j_10], [2*i_10, 2*j_10+1], [2*i_10+1, 2*j_10+1]). The 0.5km grid replicates the 1km cloud tests for each pixel.

In any case where a test based on the thermal channels uses solar channel data, the Logical OR of the 0.5km flags within that 1km pixel are used. Note there is no interpolation.

In general we expect the AATSR cloud tests to be carried over largely unchanged, apart from some changes to the definitions of the processed sub-areas associated with the histogram and spatial coherence tests to account for the wider swaths of SLSTR compared to AATSR. In the particular case of the oblique view, the AATSR forward view tests should carry over essentially unchanged, since these pixels are measured at an essentially constant air mass or (i.e. zenith angle).

In the case of the nadir view, however, the range of air mass values covered by the nadir scan is much wider than with AATSR. Where the auxiliary constants or look-up tables used by the tests depend on air mass in the line of sight, it may therefore be necessary to divide the nadir swath into across-track ranges within which different constants or tables apply. In the central region of the swath (say between -256 and +256 km across-track), the AATSR nadir view auxiliary data sets should apply with only minor changes. At the swath edge, towards -900 km, where the observational incidence angle approaches 55 degrees, the AATSR forward view tables may be more appropriate, while between these ranges an intermediate set of values may be required.

More detailed notes are given under the heading of each test below.

The availability of the new channels at 2.25 and 1.375 microns will permit the implementation of new tests. In the following we propose single channel tests based on the1.6 micron test but using each of the new channels separately.

For the SWIR channels (S4, S5 and S6) the cloud tests can be applied to either A, B or C, the average normalised radiance (reflectance) values. This could be an option in the GPP to select which value to use with the default to be the average pixels.

5.5.3.9.1 Spatial coherence test (11 micron)

The test uses a look-up table containing the following parameters:

SEA_MAX_DEV
LAND_DAY_MAX_DEV
LAND_NIGHT_MAX_DEV
COHERENCE_RESET_THRESH
COH_AREA_SIZE_X
COH_AREA_SIZE_Y
COH_FRACTION_PASSED
COH_ADJ_THRESH_LAND
COH_ADJ_DIF_LAND
CLOUDY_BOX_THRESH

X1
X2

These are not view dependent. The view dependent parameters are:
COH_AREA_DIF
COH_MIN_DIF
COH_AREA_THRESH
with the suffix of either _INT, _NA or _OB to indicate whether it is used with intermediate, nadir or oblique views respectively.

Modifications to the baseline AATSR test: This test actually comprises two tests; the small-scale and the large-scale spatial coherence tests.
In the case of the small-scale test there are no major changes (except that the final overlapping 3 by 3 group is not needed if the swath widths are defined to be multiples of three pixels).
In the case of the large-scale test, there are three view-dependent (i.e. air mass dependent) parameters as identified above. We expect to divide the nadir swath into zones by across-track limits X_1, X_2 such that:
if $-X_1 < X < X_1$ the AATSR nadir view constants are used;
if $X_1 < abs(X) < X_2$, a new intermediate set of values are used;
of $X_2 < abs(X)$, the AATSR forward view constants are used.
The AATSR test tiles the image with sub-areas of COH_AREA_SIZE pixels square, where in practice COH_AREA_SIZE =128. Currently the width of the oblique view is defined to be a multiple of 128 pixels, so this approach can be carried over unchanged. However in the case of the nadir view the definition is not a multiple of 128. it may be appropriate to distinguish between the oblique dimension COH_AREA_SIZE_Y = 128 and the across-track dimension COH_AREA_SIZE_X (< 128 pixels).

The test is performed separately for the nadir and oblique views. The nadir view 12μm and 11μm BT data are used in the nadir view test and the oblique view 12μm and 11μm BT data are used in the oblique view test. In the following, it is assumed that the size of the nadir and oblique swaths are N km, where N will differ for each viewing direction. The across track co-ordinate is x and is indexed by j, the along track co-ordinate is y and is indexed by i. In the equations that follow, the constant M is the pixel number at x=0, the ground track. The figure 5-11 below shows the coordinate used in this test.

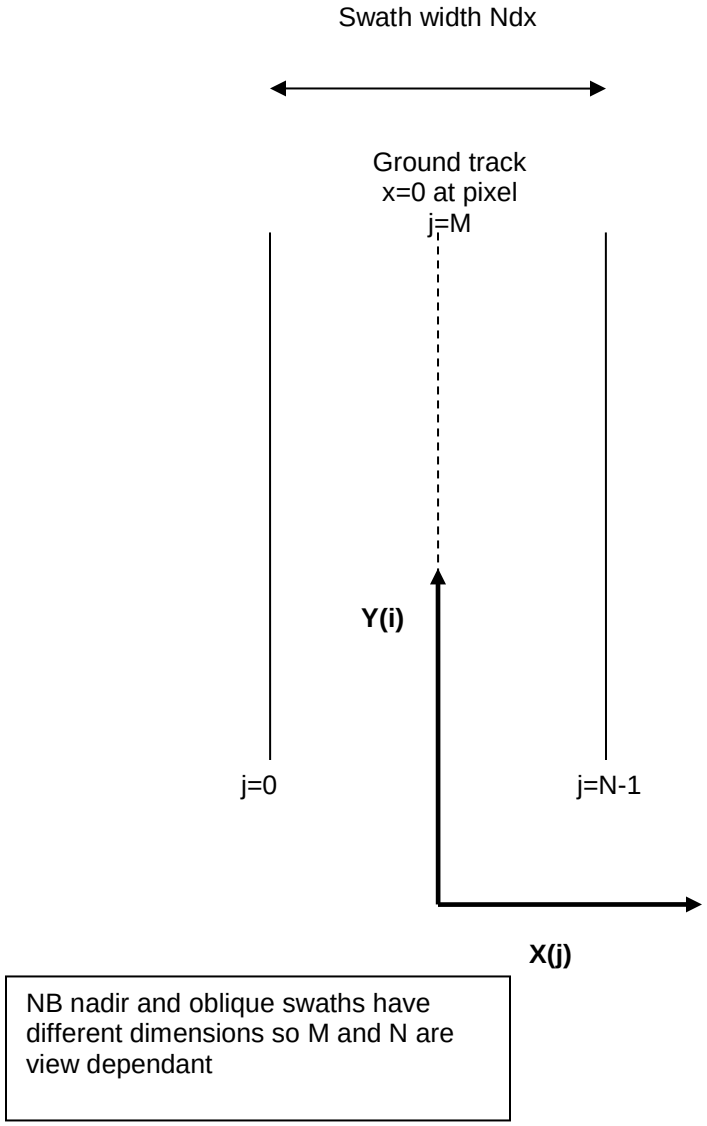

Figure 5-13

The small scale spatial coherence test uses a square array of 3 x 3 pixels and is described below in steps 5.5.3.6.1-1 to 7. The groups are identified by their x_index and y_index and the pixels used in testing a group are in pixel positions - with respect to the satellite ground track corresponding to pixel number M where x=0. The pixel positions of the groups are then given by:

$$[(x\_index*3) - M : (x\_index*3) - M + 2, \quad (y\_index*3) : (y\_index*3) + 2] \qquad \text{eq 5.5-97}$$

If the across track swath width is divisible by 3, then there will be L=swath_width/3 groups. Otherwise, there will be a remainder of swath_width-3L pixels which are not grouped and therefore these will need to use 1 or 2 of the previous pixels to form the final group, giving a total of L+1 groups. Note that the swath width will differ for the nadir and oblique views and therefore there will a different number of groups for each view.

The large scale spatial coherence test uses data from sub-areas of COH_AREA_SIZE_X by COH_AREA_SIZE_Y and is described in steps 5.5.3.6.1-8 to 9. (N.B. The value of COH_AREA_SIZE must be chosen so that it is one of the factors of 512. Its current value is 128 Km.) The sub areas are, similarly to the 3x3 groups above, non-overlapping and congruent.

To determine which of the nadir zones the sub-areas fall into in the case of a sub-area not fallying entirely into one of the zones defined by |X1| or |X2|, we use the parameters of the zone with the greatest overlap. For example, if a zone defined by Xa: Xb, where Xa<X1<Xb

Use the zone –X1 to X1 if (X1-Xa)<(Xb-X1)
Use the zone |X1| to |X2| otherwise.

For each group do Steps 5.5.3.6.1-1 to 5.5.3.6.1-5 inclusive:

Step 5.5.3.6.1-1
Determine solar elevation (90-solar_zenith) at the centre of the across-track band which contains the central pixel of the group.

Transfer the 11μm data for the group being investigated into the 3 x 3 element array ir11

Step 5.5.3.6.1-2
Determine whether the pixels in group are over land or over sea, using the appropriate land flag (confidence word in global flags).

If one or more pixels in a group are over land then set the group_land_flag for the group and store for later use.

If there are 2 or fewer valid pixels proceed to the next group. A valid pixel has the 11 micron brightness temperature > 0 and <view>_fill_state = NATURAL_PIXEL as in step 5.5.3.6.1-3 below.

Step 5.5.3.6.1-3
Calculate the average and the standard deviation of the 11μm brightness temperatures for the valid pixels in the group, excluding cosmetic fill pixels, as follows. Filled pixels are identified by:

<view>*_fill_state(i, j) = NATURAL_PIXEL.* eq 5.5-98

average_11 = (1/n) * Σ *I(ir11, v; i, j)* eq 5.5-99

sigma_11= sqrt((1/(n-1)) * Σ(*I(ir11, v; i, j)*-average_11)^2) eq 5.5-100

where the sums are over the indices (*i, j*), the index of the pixels in the group that satisfy the selection criteria above, and n their total number.
Store the average_11 in average_11_array for later use.

Step 5.5.3.6.1-4
Select the appropriate threshold; if the group is over sea set threshold_sd to SEA_MAX_DEV. If the group is over land (i.e. if group_land_flag is set), inspect the solar elevation angle determined in Step 5.5.3.6.1-1. (Note that cells of mixed surface type are treated here as land cells.)

If solar_elevation > 5°
then
set threshold_sd to the day-time value LAND_DAY_MAX_DEV;
otherwise
set threshold_sd to the night-time value LAND_NIGHT_MAX_DEV.

Step 5.5.3.6.1-5

If sigma_11 > threshold_sd
then
set flag for the group in group_cloud_flag and proceed to the next group.

Step 5.5.3.6.1-6

When all the groups in a view have been processed investigate whether the spatial variation may result from temperature gradients on the surface rather than from cloud. For each group flagged as cloudy (i.e. when group_cloud_flag has been set) in step 5.5.3.6.1-5, do the following:

i) If four or more of the up to 8 surrounding groups are clear (i.e. group_cloud_flag not set) and the group contains more than two valid pixels (as at step (b) above), then proceed to Step ii; otherwise move to the next flagged group.

ii) If the central group is open sea (i.e. group_land_flag not set) and if it is not a border group, calculate the average difference between the 11 and 12 micron channel brightness temperatures for the central (cloudy) group (average_11_12_dif_cloudy) and for those of the surrounding groups that have not been flagged as cloudy (average_11_12_dif_clear)

Specifically,

$$average\_11\_12\_dif\_cloudy = \frac{1}{N_{cloud}} \sum_{i,j} \left(I(ir11, v; i, j) - I(ir12, v; i, j) \right) \qquad \text{eq 5.5-101}$$

where the pixels indexed by *i* and *j* fall within the central cloudy group, are *NATURAL* pixels, and are valid in both channels: $I(ir11, v; i, j) > 0$ and $I(ir12, v; i, j) > 0$. N_{cloud} is the total number of pixels contributing to the sum. Similarly

$$average\_11\_12\_dif\_clear = \frac{1}{N_{clear}} \sum_{i,j} \left(I(ir11, v; i, j) - I(ir12, v; i, j) \right) \qquad \text{eq 5.5-102}$$

where the pixels indexed by *i* and *j* fall within the clear groups, are *NATURAL* pixels, and are valid in both channels: $I(ir11, v; i, j) > 0$ and $I(ir12, v; i, j) > 0$. N_{clear} is the total number of pixels contributing to the sum.

If abs(average_11_12_dif_cloudy - average_11_12_dif_clear) < COHERENCE_RESET_THRESH, eq 5.5-103

then unflag the central group by setting to zero the appropriate element in group_cloud_flag.

Step 5.5.3.6.1-7

Flag all pixels in the cloud-flagged groups (i.e. where group_cloud_flag is set) for which the land flag is not set, as cloudy by setting the small scale cloud flag in each view.

[Note: the objective of the modification above is to effectively disable the spatial coherence test over land without introducing inadvertent side-effects. The cloud flags for each pixel are to be set to group_cloud_flag AND (NOT land). Of course for a given regridded pixel the nadir and oblique view land flags should be the same.]

Step 5.5.3.6.1-8
By using group_land_flag, loop through all the groups in view and flag groups within approximately 6 km of land, as well as all-land groups. A group's flag extended_land_flag(x_index, y_index) is set if

$$\Sigma\Sigma \text{group\_land\_flag}(i, j) > 0 \qquad \text{eq 5.5-104}$$

where the summations are for indices in the ranges of

$$x\_index-3 < u < x\_index + 3 \text{ and} \qquad \text{eq 5.5-105}$$
$$y\_index-3 < v < y\_index + 3 \qquad \text{eq 5.5-106}$$

u and v must also be in the range of 0 to (L+1)., i.e. for groups that overlap the image boundary, the pixels out of range are not counted.

Step 5.5.3.6.1-9
Create arrays used in the large-scale coherence test.

i) Determine the number of sub-arrays(sub_area_nx_v sub_area_ny) across the oblique and nadir views (v=NA or OB). The two views are treated differently in the x direction as the swath widths are different.

$$\text{sub\_area\_nx\_v} = \text{width of swath(nadir or oblique view)} / \text{COH\_AREA\_SIZE\_X} \qquad \text{eq 5.5-107}$$
and
$$\text{sub\_area\_ny} = \text{length of swath} / \text{COH\_AREA\_SIZE\_Y} \qquad \text{eq 5.5-108}$$

ii) Create arrays of size [sub_area_nx_v][sub_area_ny].

Step 5.5.3.6.1-10
For all sub-areas, find the group(s) with the highest average 11μm brightness temperature, and the average (11μm - 12μm) brightness temperature difference(s) of these:

i) Select sub-areas for all combinations of x_index_1_v, y_index_1, where v again denotes the view. The ranges of x_index_1_v and y_index_1 are 0 to (sub_area_nx_v -1 or sub_area_ny - 1).

The groups for sub-area(x_index_1_v, y_index_1) are the array elements average(ix1_v:ix2_v, iy1:iy2) where

$$ix1\_v = \text{INT}((x\_index\_1\_v*coh\_area\_size\_x)/3) \qquad \text{eq 5.5-109}$$

$$ix2\_v = \text{INT}(((x\_index\_1\_v + 1)*coh\_area\_size\_x)/3) - 1 \qquad \text{eq 5.5-110}$$

$$iy1 = \text{INT}((y\_index\_1*coh\_area\_size\_y)/3) \qquad \text{eq 5.5-111}$$

$$iy2 = \text{INT}(((y\_index\_1 + 1)*coh\_area\_size\_y)/3) - 1 \qquad \text{eq 5.5-112}$$

Step (5.5.3.6.1-10i) associates pixel groups with the sub-areas. The set of groups that corresponds to the sub-area indexed by x_index_1_v, y_index_1 comprises those groups whose indices x_index, y_index satisfy

$$(x\_index, y\_index) \in A(x\_index\_1\_v, y\_index\_1), \text{ where}$$

the set of index pairs *A*(x_index_1_v, y_index_1) is formally defined by

A(x_index_1_v, y_index_1) = {(x_index, y_index): ix1_v ≤ x_index ≤ ix2_v; eq 5.5-113

iy1 ≤ y_index ≤ iy2} eq 5.5-114

Since the number of groups is not a multiple of the sub_area_n, the sets *A*(x_index_1_v, y_index_1) do not each contain the same number of groups.

For all sub-areas,

ii) find the highest average 11μm brightness temperature (max_bt_11) and its/their coordinates. Use valid groups only.
'valid' implies that the group satisfies the following conditions:

- its extended_land_flag is not set;
- it has passed the small-scale coherence test; that is, if group_cloud_flag is not set;
- it has not been shown to contain significant cloud by any previous test;
- it contains at least 3 natural pixels having valid 11 micron and 12 micron brightness temperatures; that is, at least 3 NATURAL pixels are available to contribute to the computation of the average (11 micron - 12 micron) brightness temperature difference at j.3) below.

Determine the flag previous_tests(x_index, y_index) as follows:

If cloudy_box_thresh = -1, the value of previous_tests(x_index, y_index) is determined by inspecting only the central pixel of the group:

previous_tests(x_index, y_index) =
(<view>_cloud_state[i][j].gross_test = TRUE or
<view>_cloud_state[i][j].thin_cirrus = TRUE or
<view>_cloud_state[i][j].med_high_cloud = TRUE or
<view>_cloud_state[i][j].fog_low_stratus = TRUE) eq 5.5-115

where *i* is the lesser of (3*y_index + 1, 510) and *j* is the lesser of (3*x_index + 1, 510); *i* and *j* index the central pixel of the group.

If cloudy_box_thresh > 0, the value of previous_tests(x_index, y_index) is determined by inspecting all pixels of the group:

previous_tests(x_index, y_index) = (n_cloudy ≥ cloudy_box_thresh) eq 5.5-116

where n_cloudy is the total number of pixels that fall within the group (x_index, y_index) and for which
(<view>_cloud_state[i][j].gross _test = TRUE or
<view>_cloud_state[i][j]. thin_cirrus = TRUE or
<view>_cloud_state[i][j].med_high_cloud = TRUE or
<view>_cloud_state[i][j].fog_low_stratus = TRUE). eq 5.5-117

The pixels that fall within the group defined by (x_index, y_index) are those whose indices satisfy

$i_0 \le i \le i_0 + 2$, $j_0 \le j \le j_0 + 2$, eq 5.5-118

where i_0 is the smaller of (3*y_index + 1, 509) and j_0 is the smaller of (3*x_index + 1, 509).

Then

max_bt_11 = maximum value of average_11_array(x_index, y_index) eq 5.5-119

over the set of indices (x_index, y_index) $\in A_{valid}$(x_index_1, y_index_1) eq 5.5-120

The set A_{valid}(x_index_1, y_index_1) is the set of indices of VALID groups, and is defined by

A_{valid}(x_index_1, y_index_1) = {x_index, y_index:

(x_index, y_index) $\in A$(x_index_1, y_index_1)
and NOT group_cloud_flag(x_index, y_index)
and NOT extended_land(x_index, y_index)
and NOT previous_test(x_index, y_index)
and (valid_pixel_pairs $\geq$ 3)} eq 5.5-121

where valid_pixel_pairs is the number of pixels in the group defined by (x_index, y_index) for which *<view>_fill_state(i, j) = NATURAL_PIXEL*, and both *I(ir11, v; i, j)* > 0, *I(ir12, v; i, j)* > 0. The set of pixels in the group (x_index, y_index) is as defined above.

Then

sub_area_max_11(x_index_1, y_index_1) = max_bt_11. eq 5.5-122

It is possible that there are no valid groups; A_{valid} is an empty set. In this case sub_area_max_11(x_index_1, y_index_1) and sub_area_dif(x_index_1, y_index_1) should each be set to an exceptional value ($\leq$ 0) to ensure that they are ignored in Step (m) below.

j.3) Calculate the average (11μm - 12μm) brightness temperature difference(s) for the groups with max_bt_11. Use valid pixels only, as in step c).

Use pixels with x coordinates in the range of

max(0, 3*x_max - 1) and min(511, 3*x_max + 1)

and y coordinates in the range of

max(0, 3*y_max - 1) and min(511, 3*y_max + 1)

If a single group had the average 11μm brightness temperature value of max_bt_11 then assign its brightness temperature difference value to sub_area_dif

If more than one group has the same max_bt_11 value then find the highest of differences, and assign this value to sub_area_dif.

This step calculates the average difference between the 11 micron and 12 micron channels for those valid groups for which

average_11_array(x_index, y_index) = max_bt_11 eq 5.5-123

Thus

sub_area_dif(x_index_1, y_index_1) = maximum value of
(11 micron - 12 micron difference) over the groups having
(x_index, y_index) $\in A_{valid}$(x_index_1, y_index_1) and

average_11_array(x_index, y_index) = max_bt_11 eq 5.5-124

Step 5.5.3.6.1-11

k) Set the land_sub_area flag to 1 for all sub-areas in which one or more groups are over or near land i.e, set the flag if

$$\Sigma \text{extended\_land\_flag}(x\_index, y\_index) > 0 \qquad \text{eq 5.5-125}$$

where the sum includes all (x_index, y_index) $\in$ *A*(x_index_1, y_index_1) as defined in step j.

Step 5.5.3.6.1-12

l) Set valid_sub_area_flag to 1 for all sub-areas for which the number of clear sea groups is greater than COH_FRACTION_PASSED of the total number, i.e.

$$\Sigma\ (1-\text{group\_cloud\_flag}(x\_index, y\_index)) * (1-\text{extended\_land\_flag}(x\_index, y\_index)) / (COH\_AREA\_SIZE/3)^{**}2 > COH\_FRACTION\_PASSED, \qquad \text{eq 5.5-126}$$

where the sum includes all (x_index, y_index) $\in$ *A*(x_index_1, y_index_1),

and sub_area_dif(x_index_1, y_index_1) is greater than COH_MIN_DIF.

Step 5.5.3.6.1-13

m) For invalid sub-areas, set the 11μm brightness temperature threshold threshold_11 to 32000 cK i.e. to an an unrealistically high value so that all the sea pixels in these sub-areas are flagged as cloudy and omit Steps (m.1) to (m.7).
For sub-areas that are valid, determine threshold_11 as follows (Steps (m.1) to (m.7)):

m.1) Select the up to 9 sub-areas (valid or not) centred on the one being investigated. These are the sub-areas whose indices fall in the set

$$S(p, q) = \{(x\_index\_1, y\_index\_1):\ 0 \le x\_index\_1 < sub\_area\_n,\ 0 \le y\_index\_1 < sub\_area\_n,\ p-1 \le x\_index\_1 \le p+1,\ q-1 \le y\_index\_1 \le q+1\} \qquad \text{eq 5.5-127}$$

where p, q, $0 \le p < sub\_area\_n$, $0 \le q < sub\_area\_n$, are the indices of the sub-area currently under consideration.

m.2) Set land_in_areas to 1 if one or more of the sub-areas selected has land:

$$land\_in\_areas = (\Sigma land\_sub\_area(x\_index\_1, y\_index\_1))\ ge\ 1$$

where the sum is over index pairs (x_index_1, y_index_1) $\in$ *S*(p, q). eq 5.5-128

Step (m.2) sets the flag land_in_areas if, for any (x_index_1, y_index_1) $\in$ *S*(p, q),
land_sub_area(x_index_1, y_index_1)
is set.

m.3) Find the highest sub_area_dif , bt_dif_max, for valid selected sub-areas.
bt_dif_max = max (sub_area_dif(x_index_1, y_index_1)),
over the set of index pairs (x_index_1, y_index_1) $\in$ *S*(p, q) that identify valid sub-areas.

Notice that at least one sub-area (the central one) must be VALID, so this operation is always possible.

m.4) Select those sub_area_max_11 values for which the corresponding sub_area_dif is within difference_threshold of bt_dif_max, found in step m.3. That is,
sub_area_dif(x_index_1, y_index_1) > bt_dif_max - difference_threshold.
The value of difference_threshold is given by:-
COH_AREA_DIF*(1 + land_in_areas * COH_ADJ_DIF_LAND) eq 5.5-129

m.5) Find the lowest_max_bt of those sub-areas selected in step m.4
lowest_max_bt = minimum of sub_area_max_11(x_index_1, y_index_1)
over the set of index pairs such that (x_index_1, y_index_1) $\in$ *S*(p, q), the sub-area is valid, and sub_area_dif(x_index_1, y_index_1) satisfies the test in step m.4.

m.6) Calculate threshold_11 for the sub-area investigated by decreasing lowest_max_bt by COH_AREA_THRESH + land_in_areas*COH_ADJ_THRESH_LAND.
That is:
threshold_11 = lowest_max_bt - COH_AREA_THRESH
- land_in_areas * COH_ADJ_THRESH_LAND
eq 5.5-130

m.7) If only one valid sub-area was selected at step m.4, and the land_in_area flag is set, lower threshold_11 by 200 cK.

m.8) Flag all sea pixels in the sub-area investigated for those groups for which average_11_array is below threshold_11 by setting the spatial_coh cloud flag in each view.

5.5.3.9.2 Gross cloud test

The test uses a look-up table with values of the threshold tabulated at intervals of 1° of latitude for each view (oblique and nadir), and for each calendar month. The test uses different look-up tables for the land and sea pixels.

Modifications to the AATSR test: The threshold depends on latitude, month and view. As above, we may need to divide the nadir swath into zones by across-track limits X1, X2 such that:
if -X1 < X < X1 the AATSR nadir view constants are used;
if X1 < abs(X) < X2, a new intermediate set of values are used;
of X2 < abs(X), the AATSR forward view constants are used.

a) Derive the month in which the data was collected from the time of the ascending node.

b) Do the gross cloud check for each valid pixel (over both land and sea) in each view (*v* = *n* | *f*) as follows:

b.1) Extract the pixel latitude *image_latitude(i, j)* (in degrees), and convert to an integer *latitude_index* in the range 0 to 180 by adding 90 and taking the integer part.

b.2) Determine threshold *gross_cloud_threshold_x_v (where x denotes land (lnd) or sea and v denotes na, int or ob for the view)* using the latitude index just determined and the month to enter the gross cloud check threshold array for the relevant land/sea and view.

b.3) If the 12μm brightness temp
I(ir12, v; i, j) < *gross_cloud_threshold*,
flag the pixel as cloudy by setting the 12μm gross cloud test flag (gross_test) for each view.

5.5.3.9.3 Thin cirrus test

The test uses a look-up table that defines a threshold THIN_CIRRUS_THRESHOLD[temperature index][across-track band] for the nadir and oblique views separately, for each across-track band, and for values of the brightness temperature index, defined by (T-250) K, from 0 to 60 inclusive. (Note that by symmetry the coefficients for the across-track band i = 0, 1, ...4 are the same as for band 9 - i.) The across track band dimensions are also included in the cloud LUT.

Modifications to the AATSR test:: The index depends on across-track band, so we will need to define a wider set of across-track bands to cover the wider swaths.

It is applied to the oblique (*v = ob*) and nadir (*v = na*) views separately. For each pixel:
a) *Determine the pixel across track band number (band_no) using the across-track pixel number and the band table provided in the cloud LUT.*

across-track band for pixel j = band_table[abs(j)]

b) Determine the brightness temperature index using the 11μm value I(ir11, v; i, j)

bt_index = integer part of (*I(ir11, v; i, j)* - 25000) / 100
if (bt_index > 60 then bt_index = 60
else if (bt_index < 0) then bt_index = 0
end if eq 5.5-131

(Note that brightness temperature values are stored in units of 0.01 K)

c) Calculate the difference

I(ir11, v; i, j) - I(ir12, v; i, j) eq 5.5-132

If this difference is greater than
THIN_CIRRUS_THRESHOLD_v[bt_index][band_no]

for the appropriate view v, flag the pixel as cloudy by setting thin_cirrus cloud.

5.5.3.9.4 Medium/high level cloud test

The test uses a look-up table that defines a threshold MED_HIGH_LEVEL_THRESH[temperature index] for the nadir and oblique views separately, for values of the brightness temperature index, defined by 2*(T-250) K, from 0 to 120 inclusive. The test is applied to the oblique and nadir views separately.

Modifications to the AATSR test: The threshold depends in brightness temperature and view. It therefore may be necessary to divide the nadir swath into zones by across-track limits X1, X2 such that:

if -X1 < X < X1 the AATSR nadir view constants are used;
if X1 < abs(X) < X2, a new intermediate set of values are used;
of X2 < abs(X), the AATSR forward view constants are used.

a) For each scan *i*, retrieve the solar elevation at each end of the scan. Calculate the solar elevation at each end of the scan using 90-solar zenith angle. The test is only performed if these are less than 5°: i.e. if

<view>_ *solar_elevation*(*i,* 0) < 5.0 or eq 5.5-133
<view>_ *solar_elevation*(*i,* max_j) < 5.0, eq 5.5-134

so excluding day-time data. Then for each pixel:

b) Determine threshold med_high_level_thresh[bt_index] for the appropriate view from the table holding the threshold values for this test. The bt_index is calculated from

bt_index = integer part of (*I(ir12, v; i, j)* - 25000) / 50.
if (bt_index > 120 then bt_index = 120
else if (bt_index < 0) then bt_index = 0
end if eq 5.5-135

(Note that brightness temperature values are stored in units of 0.01 K)

c) If the 3.7 and 12 micron brightness temperatures are valid, and the difference

I(ir37, v; i, j) - I(ir12, v; i, j) eq 5.5-136

is greater than MED_HIGH_LEVEL_THRESH[bt_index] for the appropriate view then flag the pixel as cloudy by setting the med_high_cloud flag in the respective view.

5.5.3.9.5 Fog/low stratus test

The test uses a look-up table that defines a threshold FOG_LOW_STRATUS_THRESHOLD[across-track band] for the nadir and oblique views separately, for each across-track band as defined in the cloud LUT. (Note that by symmetry the coefficients for the across-track band i = 0, 1, ...4 are the same as for band 9 - i.)

Modifications to the AATSR test: The threshold depends on across-track band. A wider set of across-track bands will be necessary to cover the wider swath.

Apply the fog/low stratus test as follows:

a) For each image scan *i*, retrieve the solar elevation at each end of the scan. Calculate the solar elevation at each end of the scan using 90-solar zenith angle.The test is only performed if these are less than 5°: i.e. if

<view>_*solar_elevation*(*i,* 0) < 5.0 or eq 5.5-137
<view>_ *solar_elevation*(*i,* max j) < 5.0, eq 5.5-138

so excluding day-time data. Then for each pixel:

b) Determine the pixel across track band number (band_no) using the across-track pixel number and the band table provided in the cloud LUT.

across-track band for pixel j = band_table[abs(j)] eq 5.5-139

c) For each pixel for which a valid 11 micron and 3.7 micron brightness temperature is available, calculate the difference

I(ir11, v; i, j) - I(ir37, v; i, j). eq 5.5-140

If this difference is greater than FOG_LOW_STRATUS_THRESHOLD[band_no] for the appropriate view then flag the pixel as cloudy by setting the cloud flag fog_low_stratus.

5.5.3.9.6 Histogram test (1.6 micron)

The 1.6μm test is applied to sub-arrays of 32 × 32 pixels. It uses the 1.6μm reflectance data from each of the nadir and oblique views.

Modifications to the AATSR test: This is a dynamic threshold test, so to the extent that the parameters do not depend on view, the only issue is the definition of the sub-array size. It is proposed to retain a size of 32 × 32, so the higher resolution results in smaller cells. Provisionally the image size should be a multiple of 32 pixels. However, even if the swath width is not a multiple, the test should still work since the test allows for fewer pixels. This was the case for AATSR. If the number of pixels is minimum_for_histogram then the test currently returns a status of cloudy as the default.

The basis of this test is described by Zavody et al [RD-7]. The test relies on the fact that clouds have a higher reflectivity for short wavelength radiation than the sea (and, often, land). Following AATSR practice, the test is used only for measurements made over the sea, because land surfaces are, in general, much more reflecting than the sea, and show much higher variability in reflectivity. The separation of land and cloud by this test is hence less reliable.

The test uses a dynamic threshold to separate clear from cloudy pixels. Even over water surfaces, it is not possible to parameterize the 1.6-μm signal from a clear sea area accurately by the viewing and incidence angles alone, since, in non-sun-glint conditions, a major source is scattering by atmospheric aerosols, the concentration of which depends on location, wind direction, etc. The threshold value of the signal for clouds is therefore determined dynamically by using the histogram technique as developed by Saunders, 1986.

The basis of the technique is that the 1.6 micron signal is much lower for clear sea areas than for cloudy pixels; moreover for clear sea and for areas of up to about 1000 km^2, the effect of atmospheric variability on the 1.6 μm signal is usually small, while the 1.6 μm signal for cloudy pixels is usually high and highly variable. It follows that if a histogram is formed using the 1.6 μm signal, the clear sea pixels will give rise to a narrow peak at the low end of the histogram, with cloudy pixels distributed over many histogram bins above. The value of the 1.6 μm signal at the peak, if it satisfies the criteria associated with clear pixels, can be used to derive the threshold to be used for the area.

If the area under study is close to the point of specular reflection from the sun - 'sun glint' - then the reflected radiation is high and the area cannot be distinguished from cloud on the relative strength of the signal alone. It is first of all necessary to identify these areas, and this is done by calculating the angle through which the surface would need to be tilted for full specular reflection to occur. If this tilt angle is below a specified threshold then a spatial coherence test, similar to that using the 11 μm brightness temperature values, is used instead of the histogram technique.

Areas adjacent to those where glint occurs are treated specially by the histogram test. The 1.6 μm signal may have a significant gradient with respect to across-track distance even over the relatively small areas used, hence, if such near-glint conditions occur, the spatial gradient in the 1.6 μm values is removed by de-trending the data before the cloud threshold is determined and used on the reflectance data.

Elimination of sun-glint

The test cannot be applied if the pixels are affected by sun-glint, and so it is necessary to identify affected pixels. The test for sun-glint makes use of the solar and viewing angles computed by the geolocation process. Sun-glint will occur in the vicinity of the point at which specular reflection by a horizontal surface would direct incident solar radiation towards the instrument. The criterion for this to occur is that the vector that bisects the angle between the line of sight to the sun from the pixel, and that to the satellite from the pixel is vertical. This vector is in the direction of the normal to a surface

facet that is orientated so as to reflect sunlight towards the instrument; thus if it is close to the vertical, surface facets may be correctly oriented to give specular reflection.

Consider a pixel at latitude φ, longitude λ, and let the solar azimuth and elevation at this point be α_{sun}, ε_{sun}, and the azimuth and elevation of the satellite as seen from the pixel be α_{sat}, ε_{sat}. Then the vectors

$$\mathbf{v}_{sun} = \begin{pmatrix} \cos\alpha_{sun}\cos\varepsilon_{sun} & \sin\alpha_{sun}\cos\varepsilon_{sun} & \sin\varepsilon_{sun} \end{pmatrix} \quad \text{eq 5.5-141}$$

and

$$\mathbf{v}_{sat} = \begin{pmatrix} \cos\alpha_{sat}\cos\varepsilon_{sat} & \sin\alpha_{sat}\cos\varepsilon_{sat} & \sin\varepsilon_{sat} \end{pmatrix} \quad \text{eq 5.5-142}$$

represent the lines of site from the pixel to the sun and to the satellite respectively. A surface facet whose normal bisects these lines of sight would be correctly orientated for specular reflection of sunlight towards the instrument. The vector $\mathbf{v}_{sun} + \mathbf{v}_{sat}$ bisects these two directions, and so if $\mathbf{k}$ is the unit vector in the direction of the local vertical, the tilt angle required for specular reflection is

$$\tau = \arccos\left(\frac{\mathbf{k}.(\mathbf{v}_{sun} + \mathbf{v}_{sat})}{\left|(\mathbf{v}_{sun} + \mathbf{v}_{sat})\right|} \right) \quad \text{eq 5.5-143}$$

The unit vector in the vertical direction $\mathbf{k} = \begin{pmatrix} 0 & 0 & 1 \end{pmatrix}$.

An area is considered to be affected by sunglint if its tilt angle calculated as above is less than 15 degrees. The range of tilt angles between 15 and 23 degrees constitutes the near-glint region, and areas within this range are treated specially by the algorithm.

Overview of algorithm
The auxiliary parameters used in this test are listed in Table 5-8.. Table 5-8 also gives the standard values of these parameters used for AATSR processing, although different values may be appropriate for SLSTR. Apart from the *PEAK_FACTOR* and *SPREAD* parameters, the same parameters are used for both oblique and nadir views.

Table 5-8: Auxiliary parameters used by the 1.6 micron tests

Parameter	***Value***
SPREAD_NA	0.4
SPREAD_OB	0.6
PEAK_FACTOR_NA	4
PEAK_FACTOR_OB	3
MIN_FOR_HISTOGRAM	64
TILT_THRESHOLD	15
THRESHOLD_3	0.07
NEAR_GLINT_RANGE	8.0
MIN_FOR_PASSED	64
SEARCH_RANGE_FOR_PEAK	1.5
TILT_WEIGHT_LIMIT	23
RANGE_WEIGHT_LIMIT	40
TILT_WEIGHT_FACTOR	0.025

MIN_PEAK_VALUE	10
MIN_FOR_DETREND	256
MAX_GLINT_THRESHOLD	90.0

The 1.6 μm test is applied to the nadir and oblique images independently. It is assumed to operate on image segments of 512 image rows, and it is only applied to daytime scenes for which the solar elevation at the centre of the image segment exceeds 5 degrees. For each view the image segment is divided into sub-arrays of 32 by 32 pixels, each representing an area approximately 32 km square and containing a maximum of 1024 valid pixels, and the test is applied to each sub-array in turn.

The sub-area is tested for sunglint. The solar and satellite azimuth and elevation at the centre of the 32 by 32 pixel sub-area are calculated by linear interpolation between the band edge values, and the tilt angle is calculated using (5.5-136) to (5.5.138) If the tilt angle is less than the auxiliary parameter *TILT_THRESHOLD*, sunglint may be present, and the histogram test is not applied. Instead a spatial coherence test is applied as described in a later section. If the tilt angle is less than (*TILT_THRESHOLD* + *NEAR_GLINT_RANGE*), the sub-area falls in the near-glint region

If the sub-area is not affected by sunglint, the histogram of the 1.6 micron reflectance values is generated for the set of valid clear sea pixels in the sub-array. To be included in the histogram a pixel must satisfy all three of the following criteria:

- the 1.6μm reflectivity should be non-negative;
- it should not be a land or a coastline pixel;
- it should not previously have been flagged as cloudy by the gross cloud test, the infra-red spatial coherence test or the thin cirrus test. (These daytime tests precede the 1.6 micron test.)

The units of reflectivity used within the description of this algorithm are assumed to be in percentages ranging from 0 to 100, from AATSR processing heritage and the values given for the LUT parameters in table 5-8 reflect the AATSR processor. If the SLSTR processor uses reflectivities which range from 0 to 1, the LUT parameters should reflect this.

The histogram is generated with a bin size of 0.1% [or 0.001 for stamdard unit reflectance]. If the number of valid pixels contributing to the histogram is less than *MIN_FOR_HISTOGRAM*, these pixels are all flagged as cloudy and processing moves on to the next sub-array. Otherwise, the lower end of the histogram is searched for a valid histogram peak.

The peak is defined by the maximum value, *peak_value*, in the range of bins between *low_interval* and *low_interval* + 15, where *low_interval* is the index of the first non-zero histogram bin. The position of the histogram peak, *peak_interval* is calculated to sub-bin accuracy by fitting a quadratic function to the maximum value and the two adjacent ordinates and finding the position of the maximum of the quadratic; the algebra here is the same as that described below for the infrared histogram test.
If the current sub-array lies outside the near-glint region, the peak is accepted as a valid clear sea peak if the following three conditions are satisfied:

$$peak\_interval - low\_interval < SPREAD \qquad \text{eq 5.5-144}$$

$$peak\_value > MIN\_PEAK\_VALUE \qquad \text{eq 5.5-145}$$

$$peak\_value > (PEAK\_FACTOR + f) \times average\_count \qquad \text{eq 5.5-146}$$

In equation (5.5-141) *average_count* represents the average value of the histogram over the range for which it is non-zero, and *f* is an adjustment factor depending upon the histogram range. The basis

of the latter is described by Zavody et al (2000). The auxiliary parameter *SPREAD* is that (*SPREAD_NA* or *SPREAD_OB*) appropriate to the view.
If the conditions are satisfied, a reflectance threshold is set at the value

$$reflectance\_threshold = peak\_interval + 0.5 \times SPREAD. \quad \text{eq 5.5-147}$$

All valid pixels in the sub-area having a reflectance value greater than *reflectance_ threshold* are flagged as cloudy.

If the conditions are not satisfied, the peak may be cloud-contaminated. In this case all the valid formerly clear sea pixels are flagged as cloudy and processing continues to the next sub-array.
The above is the basic algorithm applied outside near-glint regions. If the current sub-array lies within the near-glint region, the processing is modified. Firstly, the procedure above for determining the threshold is modified, and secondly, the pixel reflectance values are de-trended to remove residual glint reflectance before the threshold is applied.

For near-glint regions, the quantities PEAK_FACTOR and SPREAD in (5.5-141) and (5.5-142) are modified.

A new quantity

$$SPREAD\_ADJUSTED = SPREAD \times (1 + (1 - \tau / TILT\_WEIGHT\_LIMIT)) \quad \text{eq 5.5-148}$$

is derived, and the function

$$g(\tau) = 1 - (TILT\_WEIGHT\_LIMIT - \tau) \times TILT\_WEIGHT\_FACTOR \quad \text{eq 5.5-149}$$

is calculated. Equations (5.5-139) and (5.5-141) are replaced by

$$peak\_interval - low\_interval < SPREAD\_ADJUSTED \quad \text{eq 5.5-150}$$

$$peak\_value > (PEAK\_FACTOR + f) \times g \times average\_count \quad \text{eq 5.5-151}$$

If the three conditions (5.5-146), (5.5-140), (5.5-145) are satisfied, a reflectance threshold is then set as

$$reflectance\_threshold = peak\_interval + 0.5 \times SPREAD\_ADJUSTED. \quad \text{eq 5.5-152}$$

The residual solar glint may lead to erroneous flagging of clear pixels towards the east side of the swath. To compensate for this effect a new histogram is generated after de-trending the data. The across-track reflectance gradient is calculated by fitting a regression line to the plot of reflectance against across-track distance. The data is corrected by subtracting a line of this slope from the reflectance values, and a new histogram is generated from the resulting detrended data. This is tested as before, and a new reflectance threshold derived. If the new histogram peak is valid, all valid pixels in the sub-area having a detrended reflectance value greater than *reflectance_ threshold* are flagged as cloudy. Otherwise a spatial coherence test is attempted.

5.5.3.9.6.1 Spatial coherence test

The sub-array is divided into rectangular groups of 2 pixels in the across-track dimension by 4 pixels oblique. The short dimension of the group aligned in the across-track direction to minimise the effects of across-track gradients of reflectance. The spatial coherence test compares the standard deviation of the reflectance on pixels in the group (omitting cosmetically filled pixels) with a threshold, and flagging those as cloudy that exceed the threshold. The threshold is derived by finding the pixel in the

sub-array that has the highest brightness temperature in the 12 micron channel and finding the standard deviation of the 3 by 3 pixel group centred on this.

5.5.3.9.6.2 Detailed Structure of the Algorithm

The test is performed for the nadir and forward view separately. We define *L* as the size of the sub-array for which the histogram is derived. For each view the following steps are carried out for each non-overlapping *L* by *L* pixel sub-array within the 1.6 micron reflectance image. (The histogram will thus contain a maximum of $L \times L$ pixels.)

1) Verify that the sub-array includes sufficient valid pixels to perform the test. Find the total number of valid pixels; if this is less than *MIN_FOR_HISTOGRAM* then flag all pixels as cloudy, and continue to the next sub-array. In this algorithm 'valid' implies that a pixel satisfies the following conditions:

- it has a valid 1.6μm reflectance value (greater than zero);
- it is not over land or coast;
- it has not been flagged by the gross test or the spatial coherence test or the thin cirrus test.

2) Check for sun glint:

2.1) Use linear interpolation with respect to across-track distance to derive the values of the following solar and viewing angles at the mid-point of the subgroup, using the solar and viewing angles appropriate for the view (as calculated in Section 5.3.3.8: solar elevation angle; satellite elevation angle; satellite azimuth; solar azimuth.

2.2) Calculate the tilt angle τ, the angle by which the sea surface would need to be tilted to give specular reflection, using equations (5.5-136) to (5.5-138) above.

2.3) If the tilt angle $\tau <$ TILT_THRESHOLD then sun glint is deemed to be present. If this condition is satisfied then set a *glint_present* flag.

2.3.1) If *glint_present* is not set then generate a histogram using the 1.6-μm reflectance values with a bin size of 0.1% (i.e. 10 product units), and continue at Step 3.

2.3.2) If *glint_present* is set then set the sunglint flag for the pixels in the sub-array and go to Step 7.

3) Determine the following properties of the histogram:

low_interval the reflectance of the first bin with at least one pixel contributing;
high_interval the reflectance of the last bin with at least one pixel contributing;
hist_range (high_interval - low_interval) + 0.1;

(Note that the units of these quantities are % reflectance; this is related to the histogram bin index by dividing the latter by 10.0.)

peak_box_no the box number at the histogram peak, within the reflectance range of *low_interval* and (*low_interval* + *SEARCH_RANGE_FOR_PEAK*).
peak_value the histogram value at bin *peak_box_no*
average_value the average number of pixels per bin for the histogram, between the reflectance limits of *low_interval* and *high_interval*

By using the three histogram values centred on *peak_box_no*, calculate the accurate peak *peak_interval* position. Fit a quadratic function at the 3 points, and find the abscissa of the function maximum. This, expressed in units of percent, is *peak_interval*.

4) Set the parameter *SPREAD* to *SPREAD_NA* or *SPREAD_OB* according to whether the nadir or the oblique view is selected. Similarly set *PEAK_FACTOR* to *PEAK_FACTOR_NA* or *PEAK_FACTOR_OB* as appropriate. Note: because of the wider nadir swath of SLSTR compared to AATSR it may be necessary that *SPREAD_NA* and/or *PEAK_FACTOR_NA* must be specified as functions of across-track position. This is to be reviewed. This complication does not arise for the oblique view.

Calculate the following:

If *hist_range* < RANGE_WEIGHT_LIMIT then
f = (1.-*PEAK_FACTOR*) × sqrt((*RANGE_WEIGHT_LIMIT* - *hist_range*) / (*RANGE_WEIGHT_LIMIT* - 0.2)))
otherwise
set *f* = 0. eq 5.5-153

If τ < *TILT_WEIGHT_LIMIT* then
g = 1 - (*TILT_WEIGHT_LIMIT* - τ) × *TILT_WEIGHT_FACTOR*,
otherwise
g = 1.0 eq 5.5-154

If tilt ≥ *TILT_WEIGHT_LIMIT*, then
set *SPREAD_ADJUSTED* = *SPREAD*. eq 5.5-155

If tilt < *TILT_WEIGHT_LIMIT*, then
set
SPREAD_ADJUSTED = *SPREAD* × (1.+(*TILT_WEIGHT_LIMIT*-τ)/*TILT_WEIGHT_LIMIT*)
eq 5.5-156

Test whether or not the histogram satisfies the following conditions:
(*peak_interval* - *low_interval*) < *spread_adjusted* eq 5.5-157
peak_value > *(peak_factor +f(hist_range))* × *g(τ)* × *average_value* eq 5.5-158
peak_value > *MIN_PEAK_VALUE* eq 5.5-159

4.1) If all three conditions are satisfied then set the reflectance threshold:
reflectance_threshold = *peak_interval* + *SPREAD_ADJUSTED*/2. eq 5.5-160
Test whether
TILT_THRESHOLD < τ < (*TILT_THRESHOLD* + *NEAR_GLINT_RANGE*) eq 5.5-161
4.1.1) If yes, then the area is in a near-glint region; go to Step 5.
4.1.2) If no, go to Step 6

4.2) If any of the three conditions is not satisfied then test whether the area is in a near-glint region.
4.2.1) If the area is not in a near-glint region, as defined in 4.1 above, then flag all pixels as cloudy and continue to the next sub-array of 32 x 32 pixels.
4.2.2) If the area is in a near-glint region then do calculate
n = 1.5 × *SPREAD_ADJUSTED* eq 5.5-162
Calculate the total number of valid pixels with reflectance values between *low_interval* and *low_interval* + *n* and test whether this number exceeds *MIN_FOR_DETREND*.
4.2.2.1) If yes, set *reflectance_threshold* = *low_interval* + *n* and go to Step 5.
4.2.2.2) If no, go to Step 7 (spatial coherence test on reflectance values).

5) De-trend the reflectance data before applying a threshold as follows:

5.1) Calculate the across-track gradient of reflectance, *gradient*_16 by regressing the reflectance values against their across-track distance, using only pixels having reflectance values less than *reflectance_threshold*.

The gradient is obtained by computing, using valid pixels only,

$a = total\_valid \times \Sigma(x(i) \times ir16(i)) - \Sigma x(i) \times \Sigma ir16(i)$ eq 5.5-163

$b = total\_valid \times \Sigma x(i)^2 - (\Sigma x(i))^2$ eq 5.5-164

where *ir*16 is the 1.6 micron reflectance of the pixel *i* and *x(i)* is its across-track co-ordinate. The summations are for total_valid values for the valid pixels only, and *i* takes the indices of valid pixels determined in step 1.

If *b* is not equal to zero then *gradient*_16 = *a*/*b*, otherwise gradient_16 = 0.

5.2) Correct the reflectance value of each valid pixel using the gradient calculated above:

$detrended\_16(i) = ir16(i) - gradient\_16 \times x(i)$ eq 5.5-165

5.3) Form a new histogram using the detrended reflectances as in step 2.3.1 above.

5.4) Determine *low_interval* and *peak_interval* from the new histogram as in step 3

5.5) If ($peak\_interval - low\_interval \geq SPREAD$ then go to step 7.

5.6) Determine the reflectance threshold appropriate to the de-trended data:

$reflectance\_threshold = peak\_interval + SPREAD/2.$ eq 5.5-166

6) Flag all the pixels with (de-trended, if appropriate) reflectance values greater than *reflectance_threshold* as cloudy, then continue at step 9.

5.5.3.9.6.3 Spatial Coherence Test

7) Calculate the standard deviation threshold for the 1.6 micron spatial coherence test *sd_threshold* in the following way:

7.1) Find the indices of the highest 12-μm brightness temperature among the pixels in the 32 $\times$ 32 array, using only pixels that satisfy the following conditions:

- The pixel satisfies the validity conditions in Step 1;
- its reflectance at 1.6μm is less than *MAX_GLINT_THRESHOLD*
- it has not been cosmetically filled.

7.2) Set *reflectance_at_12um_max* equal to the 1.6μm reflectance value of this pixel (or, if more than one pixel is found, to that with the highest 1.6μm value).

7.3) The standard deviation threshold is given by

$sd\_threshold = reflectance\_at\_12um\_max \times$ THRESHOLD_3 eq 5.5-167

8) Loop through the subgroup by examining the standard deviations of valid pixels from non-overlapping groups of (2 x 4) pixels and flag those whose standard deviation exceeds *sd_threshold*.

8.1) Calculate the standard deviation of 1.6 micron reflectance for the sixteen (2 by 4) pixel groups in horizontal strips of 4 pixels by 32 pixels. (The long side of the 2 by 4 rectangle is in the oblique direction.). Only use valid pixels as re-defined at 7.1 above.

8.1.1) Mark as cloudy those (2 x 4) groups whose standard deviation exceeds *sd_threshold AND* those (2 x 4) groups having more than two valid pixels

8.1.2) If an unmarked (i.e. clear) group lies between two groups marked as cloudy in the strip then mark the group as cloudy.

Repeat these steps for all 8 strips in the 32 by 32 sub-array

8.2) Flag as cloudy all those pixels that are in a group marked as cloudy, and also any pixels with reflectance values at 1.6 microns in excess of *MAX_GLINT_THRESHOLD*.

9) Count the number of clear pixels remaining in the (32 x 32) array. If the total is less than *MIN_FOR_PASSED* then flag these also as cloudy.

5.5.3.9.7 11/12 micron nadir/oblique test

This test is only applied to sea pixels. It uses the auxiliary parameters a0, a1 and 11_12_view_diff_thresh given in the 11/12 micron LUT.

Modifications to the AATSR test: This test is applied only within the across-track swath. The test parameters depend on across-track band, so we must define a wider set of across-track bands to cover the wider swath.

Loop through the pixels in the n_band across-bands of an image (defined in the cloud LUT) and check the relationship between the measured brightness temperature differences for each pixel, using the appropriate parameters and threshold. Use the nadir view 12 micron and 11 micron brightness temperatures and the oblique view 11μ brightness temperatures. For each pixel i, j perform steps (a) to (d) inclusive if

the nadir land flag (*i, j*) (provided in the confidence parameter in global flags) is FALSE and if the brightness temperatures used in Steps (a) and (b) are valid:

a) Derive the nadir view (11μm - 12μm) difference

$dif\_11\_12 = I(ir11, n; i, j) - I(ir12, n; i, j)$ eq 5.5-168

b) Derive the 11μm (nadir-view - oblique-view) differences

$dif\_nv\_fv = I(ir11, n; i, j) - I(ir11, f; i, j)$ eq 5.5-169

c) By using the appropriate coefficients for the band of every pixel, given by equation 5.6.1, compute the expected 11μm (nadir-view - oblique-view) differences, given by

$exp\_dif\_nv\_fv = a0 + a1 * dif\_11\_12$ eq 5.5-170

where

$a0$ = a0(*band_no*); eq 5.5-171

$a1$ = a0(*band_no*) eq 5.5-172

d) Flag those pixels as cloudy for which the difference

abs(*exp_dif_nv_fv* - *dif_nv_fv*) > 11_12_view_diff_thresh eq 5.5-173

by setting the 11_12_view_diff cloud flag.

5.5.3.9.8 11/3.7 micron nadir/oblique test

If night-time and the 3.7μm channel is available, repeat the preceding test, now using the brightness temperatures measured in the 3.7 μm and 11 μm channels with the appropriate parameters and threshold. Use the nadir view 11 μm and 3.7 μm brightness, and the oblique view 3.7 μm brightness temperatures. The test is only applied to sea pixels. This test uses the auxiliary parameters b0, b1, b2 and 37_11_view_diff_thresh provided in the 11/3.7 cloud test LUT.

Modifications to the AATSR test: This test is applied only within the across-track swath. The test parameters depend on across-track band, so we must define a wider set of across-track bands to cover the wider swath.

The test is only applied to pixels on scans for which

nadir_solar_elevation(*i*, 0) < 5.0 and

nadir_solar_elevation(*i*, max j) < 5.0 and

along_track_solar_elevation(*i*, 0) < 5.0 and
along_track_solar_elevation(*i*, max j) < 5.0.

For each scan i for which the above condition is true, and for each pixel j, perform steps (a) to (d) inclusive if

the nadir land flag*(i, j*) is FALSE and if
the brightness temperatures used in Steps (a) and (b) are valid:

a) Derive the nadir view (3.7μm - 11μm) difference

dif_37_11 = I(ir37, n; i, j) - I(ir11, n; i, j) eq 5.5-174

b) Derive the 3.7μm (nadir-view - oblique-view) difference

dif_nv_fv = I(ir37, n; i, j) - I(ir37, f; i, j) eq 5.5-175

c) By using the appropriate coefficients for the band of every pixel, given in the cloud LUT data product, compute the expected 3.7μm (nadir-view - oblique-view) differences, given by

*exp_dif_nv_fv = b0 + b1 * dif_37_11 + b2 * (dif_37_11)**2* eq 5.5-176

where

b0 = b0(*band_no*); eq 5.5-177
b1 = b1(*band_no*); eq 5.5-178
b2 = b3(*band_no*). eq 5.5-179

d) Flag those pixels as cloudy for which the difference

abs(*exp_dif_nv_fv - dif_nv_fv*) > 37_11_view_diff_thresh eq 5.5-180

by setting the 37_11_view_diff cloud flag in the appropriate view.

5.5.3.9.9 Infrared histogram test

The histogram test operates on a 512 by 512 pixel image segment, so the orbit should be divided into image segments of this size; it should be imagined as 'tiled' with 512 row image segments. Note that if at the end of an orbit or for any other reason the data is insufficient to form a complete image segment of 512 rows the histogram can be based on an incomplete image segment. (Because histograms are made up of those pixels which are valid sea pixels, if an image is largely over land, one has an incomplete image anyway.) Provided the number of pixels exceeds MIN_FOR_11_12_HISTOGRAM the test can be applied. It is expected that processing will always include an integer number of granules, so if there is an incomplete image segment at end of data, it will always have at least 32 rows.

Note this test only applies to pixels over sea.

Modifications to the AATSR test: The size of the image segments to tile the views must be modified to HISTOGRAM_AREA_WIDTH by HISTOGRAM_AREA_LENGTH, chosen to fit the wider swaths. For the oblique view, HISTOGRAM_AREA_WIDTH will simply be the entire swath width. The nadir view swath is much wider and should be divided into three regions. A parameter X1 is defined in the cloud LUT and so when -X1 < X < X1, the nadir view parameters should be used. For |X|>X1, the forward view parameters should be used. HISTOGRAM_AREA_LENGTH can be set as 512 for both views.

This is the last of the cloud tests performed and it is applied only to those pixels that have passed all the previous cloud tests. It uses the 11 μm and 12 μm channels, and relies mostly on the following:

1. The difference between brightness temperatures measured in different channels is almost entirely determined by the atmospheric characteristics.

2. The atmospheric variability is usually small over the area of an AATSR image product. It follows that even when strong temperature gradients are present in the sea, the brightness temperature differences form a fairly tight cluster for the clear pixels.

3. Low stratus clouds, the most likely contamination to have escaped detection by the other tests, affect the brightness temperatures differently from the clear atmosphere. There are two effects:

a. The infrared radiation detected originates from a height above sea level and hence the lowest layer of the troposphere is only partially traversed by the radiation. As it is this layer that contains most of the atmospheric water vapour, which is the major source of the difference between the 11 µm and 12 µm brightness temperatures, these differences are reduced over clouds.

b. Low clouds have a slightly higher emissivity in the 12 µm channel than in the 11 µm channel. It follows that the proportion of reflected cold radiation is less for the 12 µm channel as for the 11 µm channel and hence the 12 µm brightness temperature over this type of cloud, compared with the 11 µm brightness temperature, is not as cold as over the clear sea.

The 12 µm brightness temperature is almost always lower than the 11 µm brightness temperature owing to the water vapour absorption. Both the above effects reduce the difference found over clear sea.

4. If the water vapour column amounts are not uniform over an image, and the sea surface temperature is constant, then the lowest brightness temperatures originate from pixels having the highest water vapour loadings and hence the highest (11 µm minus 12 µm) brightness temperature differences. It follows that, in this case, the brightness temperatures and the brightness temperature differences are negatively correlated for clear pixels and positively correlated for cloudy pixels. (N.B. Although this is generally true there are exceptions. A positive correlation in SST with water vapour loading, or lower tropospheric air warmer than the SST, can reduce the correlation or even change its sign.)

The auxiliary parameters used in this test are listed in Table 5-7. They are taken from the auxiliary file of Cloud Look-up Table Data.

Table 5-7: Auxiliary parameters used by the infrared histogram test

MIN_FOR_11_12_HISTOGRAM	100.00
PEAK_FRAC_MIN	0.51
LATITUDE_THRESH	40.0
SECOND_LOW_FRACTION	0.50
HALF_WIDTH_M_NA	0.5
HALF_WIDTH_B_NA	25.0
HALF_WIDTH_M_OB	1.0
HALF_WIDTH_B_OB	15.0
MAX_DIF_AVE_CHAN_1	100.0
MAX_DIF_PEAK_CHAN_1	50.0
RATIO_B	4.0
IR_SPREAD_NA	60.0
IR_SPREAD_OB	80.0
SLOPE_MAX_ALLOWED	10.0
IR_PEAK_MIN	25000.0

5.5.3.9.9.1 Determination of the Difference Threshold

Thus the overall objective of the algorithm is simple, to determine a dynamic threshold against which the brightness temperature differences can be compared to differentiate cloudy from clear pixels. The determination of this threshold is based on the histogram of the distribution of the differences in brightness temperature between the 11 and 12 micron channels. In the presence of undetected cloud, the histogram is expected to be the superposition of two peaks, representing the distribution of the brightness temperature differences of clear sea and of cloudy pixels respectively.

The algorithm attempts to identify the presence of the two peaks, and to identify which one represents clear sea. In the simplest terms, the clear sea pixels should show a narrower and more regular distribution, at a higher brightness temperature difference, than the cloudy pixels. However, the peaks cannot be distinguished by their relative height, since the height of each peak depends on the number of contributing pixels, which is arbitrary and simply reflects the area of clear sea or undetected cloud as appropriate. Moreover, the peaks may overlap.

Therefore the peaks are tested against various criteria to identify a valid peak, that is, a peak that shows the characteristics of the distribution of clear sea pixels. If a valid peak is identified, a threshold is set on its lower edge, and all pixels having a brightness temperature difference less than this threshold are flagged as cloudy.

The procedure involves the following stages.

1 A histogram representing the frequency distribution of the brightness temperature difference ($T_{11} - T_{12}$) is prepared over all the sea pixels that have not been flagged as cloudy by any previous test. At the same time, for each histogram bin, the cumulative brightness temperature in the 12 micron channel is calculated over all the pixels that contribute to each bin.

The histogram is generated of the brightness temperature difference $T_{diff} = (T_{11} - T_{12})$ in the range $-20.0\ K \le T_{diff} < 80.0\ K$ with a bin size $dT = 0.1$ K. If the histogram bins are indexed by k ($0 \le k < 1000$) then the lower limit of bin k corresponds to $T = k \times dT - 20.0$ K. The corresponding histogram value $h(k)$ represents the number of clear sea pixels for which

$$k \times dT - 20.0 \le (T_{11} - T_{12}) < (k + 1) \times dT - 20.0 \qquad \text{eq 5.5-181}$$

The cumulative brightness temperature for bin k is $\Sigma\ T_{12}$, where the sum is over all contributing pixels that fall in bin k.

2 The maximum value of the histogram is found, and its position is taken to represent the principal peak of the histogram. The extent of this peak is determined, and the parameters, height, width and position that describe the peak are calculated.

The maximum of the histogram defines the principal peak, referred to in the following as the major peak, and corresponds to the mode of the frequency distribution. If the bin index corresponding to the maximum is *peak_interval*[MAJOR], then the maximum value is

$$peak\_value[\text{MAJOR}] = h(peak\_interval[\text{MAJOR}]). \qquad \text{eq 5.5-182}$$

The extent of the peak is determined by finding the first local minimum or zero value, whichever is found first, on either side of the peak. The indices of these bins are *lower_limit*[MAJOR] and *higher_limit*[MAJOR].

3 The peak is tested against certain criteria to determine whether or not it is valid, that is, possesses the characteristics likely to represent clear pixels.

The peak is flagged as invalid if it corresponds to a difference value less than zero, that is, *peak_interval*[MAJOR] < 200, unless the absolute latitude at the centre of the image segment exceeds a threshold *LATITUDE_THRESH* (currently set at 40 degrees) or the number of pixels *peak_value*[MAJOR] exceeds a threshold *IR_PEAK_MIN* (currently 25000). Otherwise it is flagged as valid.

If the histogram represents a night-time scene and if the peak has passed the previous tests, so is flagged as valid, a further test is applied to verify that the histogram is not the sum of a clear and a cloudy histogram and hence excessively broad.
Firstly, a more accurate value of the histogram peak is determined, by fitting a quadratic curve to the peak value and the adjacent histogram values on either side. If the histogram peak and its neighbours are

$$h0 = h(peak\_interval[\mathrm{MAJOR}] - 1) \quad \text{eq 5.5-183}$$
$$h1 = h(peak\_interval[\mathrm{MAJOR}]) \quad \text{eq 5.5-184}$$
$$h2 = h(peak\_interval[\mathrm{MAJOR}] + 1), \quad \text{eq 5.5-185}$$

then the quadratic function is

$$h(x) = 0.5x(x\text{-}1)h0 - (x - 1)(x + 1)h1 + 0.5x(x + 1)h2 \quad \text{eq 5.5-186}$$
$$= 0.5x\text{^}2(h0 - 2h1 + h2) + 0.5x(h2 - h0) + h1, \quad \text{eq 5.5-187}$$

where x is a normalised abscissa co-ordinate measured from *peak_interval*. The maximum of this function occurs at

$$x = 0.5(h0 - h2)/(h0 - 2h1 + h2). \quad \text{eq 5.5-188}$$

Thus provided the denominator of this expression is not zero, which can only occur if all three ordinates are the same, improved values of the histogram peak and its position are found. The improved peak value *exact_peak_value* is obtained by evaluating equation () at the value of x given by equation (), while the new position is

$$exact\_peak\_interval = (peak\_interval + x) \quad \text{eq 5.5-189}$$
$$ir11\_ir12\_diff\_at\_peak = (exact\_peak\_interval - 200)*dT \quad \text{eq 5.5-190}$$

Next, the width of the histogram at half-height is computed to sub-bin accuracy by interpolation between the two histogram values bracketing the 50% peak values defined by 0.5* *exact_peak_value* and differencing the abscissae. A half-width threshold is computed from

$$half\_width\_threshold = M \times ir11\_ir12\_diff\_at\_peak + B, \quad \text{eq 5.5-191}$$

where M and B are constants defined in the auxiliary file of cloud LUT data, ATS_CL1_AX. (These constants have different values for the oblique and nadir views.)

The peak is flagged as invalid if

$$half\_width[\mathrm{MAJOR}] > half\_width\_threshold. \quad \text{eq 5.5-192}$$

4 A new histogram is determined by removing the peak just found (the major peak) by setting to zero the histogram values in the open interval between the upper and lower limits of the peak

determined in (2) above. The maximum of the new histogram is found, and its position defines the secondary (or minor) peak. This is tested and flagged in the same way as the major peak.

The new maximum represents the largest secondary peak, and will be designated the minor peak in the following. The same validity tests are applied to it as are described above for the major peak.

5 The two peaks are now further tested in relation to one another. These tests may result in a hitherto valid peak being flagged as invalid. In detail the tests are as set out in the detailed description of the algorithm below, but the main new element here is to use the averaged 12 micron brightness temperatures in the peak to refine the discrimination; if the mean brightness temperature for the rightmost peak exceeds that for the other by more than a threshold *MAX_DIF_PEAK_CHAN*_1, the left-hand peak is flagged as invalid. At the same time, if the peaks overlap, the upper limit of the left-most peak is refined by extrapolation, and the lower limit of the rightmost peak (which may for the basis of the threshold determination) is then adjusted upwards to match the extrapolated limit. (This makes for a more conservative detection.)

6 The difference threshold is now set. If only one peak is valid, the difference threshold is set to the lower limit of the valid peak. If both peaks are flagged as valid, that at the lower abscissa is selected and its lower limit is used. If neither peak is valid, all pixels are flagged as cloudy.

7 The correlation property described in paragraph 4 following section (5.5.3.7.9) above is used to validate and, in the case of night-time scenes, refine the threshold just derived. The average 12 micron brightness temperature associated with each histogram box is calculated, using

$$Tmean(k) = \text{sigma } (T_{12})/h(k), \qquad \text{eq 5.5-193}$$

where the sum is over all pixels contributing to box *k*. (The calculation uses the histogram associated with the chosen peak; thus if the minor peak was valid and selected, the histogram after removal of the major peak is used.) The histogram bin corresponding to the maximum brightness temperature is identified, and the slope of the averaged brightness temperature with Bt difference is computed. If this slope exceeds a value *SLOPE_MAX_ALLOWED*, all pixels are flagged as cloudy.

If the histogram represents a night time scene, the average 12 micron BT are used to refine the threshold just derived. If the position of the chosen histogram peak is to the right of the BT maximum, the threshold is increased until the histogram value at the threshold exceeds a given fraction (1/RATIO_B) of that at the position of the maximum BT. If the position of the chosen histogram peak is to the left of the BT maximum, the threshold is increased until either the histogram peak is reached, or a bin is found at which the 12 micron average exceeds the highest average BT less *MAX_DIF_AVE_CHAN* - 1 and the slope is lower than *SLOPE_MAX_ALLOWED*.

Finally, all so far clear sea pixels having a brightness temperature difference less than the threshold are flagged as cloudy. If the number of clear pixels that remain is less than the threshold MIN_FOR_11_12_HISTOGRAM, these pixels are also flagged as cloudy.

The detailed algorithm follows.

a) The following steps (b) to (m) are applied to the nadir and oblique views separately. Some of the cloud detection parameters provided in the auxiliary file of Cloud Look-up Table Data differ for the two views, and where applicable those appropriate to the view being processed should be used.

b) The 11um minus 12um brightness temperature differences ($T_{11} - T_{12}$) are calculated for those pixels that have not been flagged by any of the previous cloud tests and are not over land. The histogram of these differences is generated with a bin size of 0.1 K. For each histogram bin the

cumulative brightness temperature in the 12 micron channel is calculated for all the pixels that contribute to each bin.

c) If the number of pixels contributing to the histogram is less than the auxiliary value *MIN_FOR_11_12_HISTOGRAM*, all the pixels are flagged as cloud no further processing is applied to this view. (If the scene is less than 512 rows in length, the above threshold is scaled in proportion.)

d) The position of the histogram peak, and the histogram value at the peak, are determined. If possible, the position of the peak of the distribution is derived to sub-box accuracy by fitting a quadratic function to the histogram values at the peak and in the two adjacent boxes, and computing the position and ordinate of the maximum of the quadratic. The peak determined at this step will be termed in the following the major peak.

e) The extent of the peak is determined by finding the position of a local minimum or of an empty histogram box on each side of the peak.

> e.1) Starting at the histogram peak and working to the left, inspect each histogram bin until either a bin value of zero or a local minimum lower than peak_frac_min times the peak value is found.
>
> e.2) Check if possible that the trough found is genuine by testing that the histogram value at the local minimum found in e.1 is greater than 10% of the peak value and that the value in the second bin from the minimum in the direction away from the peak is not lower than the local minimum value. If neither of these conditions is true then the search is continued as in e.1. (This step is done only once.)
>
> e.3) The higher limit is found in a similar way but working to the right of the peak (to higher bin numbers).

Note: It is possible, although unlikely, that an upper or lower limit cannot be found at this step. In this case the present implementation will terminate the processing if the current view here.

f) If the number of pixels contributing to the histogram peak is less than the auxiliary value *IR_PEAK_MIN*, the brightness temperature difference at the histogram peak is less than zero, and the absolute latitude of the image centre is greater than 40 degrees, then the peak is flagged as INVALID. If any of these three conditions do not apply, the peak is flagged as VALID.

Note: the current value of IR_PEAK_MIN is 25000. If the peak value of the histogram is greater than this, the peak will be flagged as VALID.

g) The average 12um brightness temperature for the pixels that fall in the histogram bin containing the most pixels (the histogram peak) is computed from the cumulative sum calculated at step (b).

h) If the major peak is VALID, and the solar elevation at the centre of the scene is less than 5 degrees, so that the histogram represents a night-time scene, the following tests are applied to verify that the histogram is not the sum of a clear and a cloudy histogram and hence excessively broad.

> h.1) The width of the histogram at half-height is computed to sub-box accuracy by interpolation, using the two values bracketing the 50% peak values.
>
> h.2) A half-width threshold is calculated from the auxiliary parameters appropriate to the view. These parameters define the threshold as a linear function of the (11um - 12um) difference value at the histogram peak.

h.3) If the half width found at (h.1) exceeds than half-width threshold from (h.2) the peak is flagged INVALID.

i) A new histogram is generated by setting to zero the histogram values in the open interval between the upper and lower limits of the major peak. The peak of this histogram, which is a secondary peak of the original histogram, and which in the following will be called the minor peak, is found and tested for validity as follows. If the number of pixels contributing to the new histogram is less than threshold used in Step (c), the minor peak is flagged as INVALID. Otherwise:

i.1) Steps (d) to (h) are repeated to determine the position of the minor peak and its limits.
If the histogram peak is at a difference value less than zero, and the (absolute) latitude of the image centre is greater than 40 degrees, then flag the minor peak as INVALID.

i.2) The minor peak is flagged as INVALID if any of the following conditions apply:

i.2.1) The difference between the higher and lower limits is 20 cK or less;

i.2.2) The major peak is highly likely to be cloudy, and the minor peak is not sufficiently distinct from the major peak:
- The box number of the minor peak is at a greater difference value than that of the major peak, AND
- The average 12um BT at the minor peak is greater than that at the major peak by more than threshold *MAX_DIF_PEAK_CHAN*_1, AND
- the lower limit of the minor histogram is less than the higher limit of the major histogram, AND
- the value of the major peak at its higher limit is greater than second_low_fraction times the minor peak

i.2.3) The minor peak is highly likely to be cloudy:
- The box number of the minor peak is smaller than that of the major peak, AND
- The average 12um BT at the minor peak is less than that at the major peak by more than threshold *MAX_DIF_PEAK_CHAN*_1

i.3) It is possible that there are no empty histogram boxes between the minor and major histogram peaks. In this case, if the major peak is likely to be cloudy, an extrapolation is used to find the intersect of the falling edge of the major peak and the *x* axis to refine the limits.

(i.3.1) If the minor histogram is valid and to the right of the major, the higher limit of the major histogram is adjusted by extrapolation:

(i.3.1.1) If the lower limit of the minor histogram is less than the higher limit of the major, then it is reset to the higher limit of the major histogram.

i.3.1.2) If the difference between the box numbers for the major peak and the high interval for the major peak is greater than 3 then extrapolate using the major peak box number and value, and the box number and value of the box at (high interval minus 1). Specifically, define x1, y1 as the histogram mode abscissa and ordinate respectively;

x1 = peak_interval[MAJOR], y1 = peak_value[MAJOR]. eq 5.5-194

Similarly define

x2 = high_interval[MAJOR] – 1, y1 = h[high_interval[MAJOR] – 1].
eq 5.5-195

Then the linearly extrapolated value of x when y = 0 is:

x = x1 + y1(x2 - x1)/(y1 - y2) eq 5.5-196
This is the new value of high_interval[MAJOR].

i.3.1.3) If the difference between the box numbers for the major peak and the high interval for the major peak is not greater than 3 then linearly extrapolate as above but using the major peak box number and value, and the box number and value of the box at high interval.

(i.3.1.4) If the lower limit of the minor histogram is less than the adjusted higher limit of the major, then it is reset to the higher limit of the major histogram, or to the (peak position – 1) if that is smaller.

i.4) If the minor peak is invalid and is to the left of the major histogram then recompute the minor high limit:

(i.4.1) If (high_limit[MINOR] – peak_interval[MINOR]) is greater than 3 histogram bins then re-adjust the minor high limit by linear extrapolation as at Step (i.3.1.2) above using
the values of the histogram mode and the bin second to the left of the old limit

(i.4.2) If (high_limit[MINOR] – peak_interval[MINOR]) is not greater than 3 histogram bins
then re-adjust the minor high limit by LINEAR extrapolation as at Step (i.3.1.2) above using the values of the histogram mode and the bin immediately adjacent to the old limit

(i.4.3) If low_limit[MAJOR] < high_limit[MINOR] then reset low_limit[MAJOR] to the smaller of high_limit[MINOR] or (peak_interval[MAJOR} + peak_interval[MINOR])/2.

(i.5) If the minor peak is to the right of (i.e. at a higher difference value than) the major peak, AND its average 12um brightness temperature is greater by threshold *MAX_DIF_PEAK_CHAN*_1 than that of the major peak, then flag the major peak as *INVALID*.

j) Choose between the lower limits of the major and the minor peaks, if necessary:

If both peaks are *VALID* then choose the lower value.
If there is only one *VALID* peak then choose its lower limit.
If there is no *VALID* peak then flag all pixels as cloudy and exit.

j.1)For the chosen peak, calculate the difference

(peak_interval[CHOSEN] – low_limit[CHOSEN])*bin_size eq 5.5-197

(where bin_size = dT = 0.1 K). If this quantity is greater than the value of ir_spread appropriate to the view, then replace the previous threshold value by

threshold = peak_interval[CHOSEN] – ir_spread[view]/bin_size eq 5.5-198

and omit step (k), otherwise execute step (k).

k) If the lower limit was successfully determined in (i) then check the way the 12um brightness temperature varies with the (11um minus 12um) difference. Under normal conditions, it decreases as the difference increases.

k.1) Average the 12um brightness temperature values for the pixels in each (11um minus 12um) difference histogram box

k.2) Find the (11um minus 12um) difference value that has the highest average 12um brightness temperature.

k.3) Compute the slope of the (average 12um BT) with respect to the (11um minus 12um) difference, at this point.

k.4) If the slope exceeds threshold *SLOPE_MAX_ALLOWED* then flag all pixels as cloudy, and exit.

k.5) At night, use the 12um average BTs to tighten the lower limit, if necessary.

k.5.1) If the peak position from the (11um minus 12um) histogram is at a higher difference value than the difference value from k.2 then, starting with the lower limit calculated above, increase its value until the histogram reaches a certain fraction (1/*RATIO_B*) of the peak value.

k.5.2) If the peak position from the (11um minus 12um) histogram is at a lower difference value than the difference value from k.2 then

k.5.2.1) Generate slopes of delta(12um BT) / delta(11um-12um BT) for each non-empty histogram box

k.5.2.2) Starting with the lower limit calculated above, increase its value until, at lower limit, the (12um average plus threshold *MAX_DIF_AVE_CHAN*_1) value exceeds the highest average 12um brightness temperature determined in (k.2), and the value of the slope here is less than threshold *SLOPE_MAX_ALLOWED*

l) Flag as cloudy all formerly clear pixels with a (11um minus 12um) difference value less than the value of lower limit, determined above.

m) If the number of clear pixels remaining is less than a threshold, then flag all the remaining clear pixels as cloudy.

m.1) Calculate the number of clear) pixels remaining;

m.2) If the total is less than threshold value *MIN_FOR*_11_12_*HISTOGRAM* then flag all clear pixels as cloudy.

5.5.3.9.10 Visible channel cloud test

This test operates on a pixel-by-pixel basis, and applies to daytime pixels only. It is applied to each view separately.
The test makes use of an NDVI-based surface classification from unpublished work at RAL by A.D. Stevens. The classification scheme uses two NDVI-like indices to classify individual pixels on the basis of pre-assigned criteria. The NDVI may be defined as

$$NDVI = (R87 - R67)/(R87+R67), \quad \text{eq 5.5-199}$$

where R87 and R67 are the calibrated reflectances in the 0.87 and 0.67 micron channels respectively. In addition to the conventional NDVI defined above a second index may be defined making use of the 0.55 micron channel reflectance R55:

$$NDI2 = (R67 - R55)/(R67 + R55) \quad \text{eq 5.5-200}$$

If these two indices are calculated for each pixel, the pixel can be plotted on a graph of NDVI versus NDI2. Such a plot defines an NDVI space within which pixels of different surface types form clusters, and by identifying into which cluster a pixel falls, the surface type at the pixel can be determined.

The clusters have been defined by empirically dividing the NDVI space into a series of polygons, each of which represents a particular surface type. Figure 5-12 shows this subdivision. The classification defines 12 surface types (numbered 0 to 11). Note that the figure shows, in the centre, a pure cloud type (Type 3) together with 4 mixed types incorporating some cloud (Types 1, 2 9 and 10).

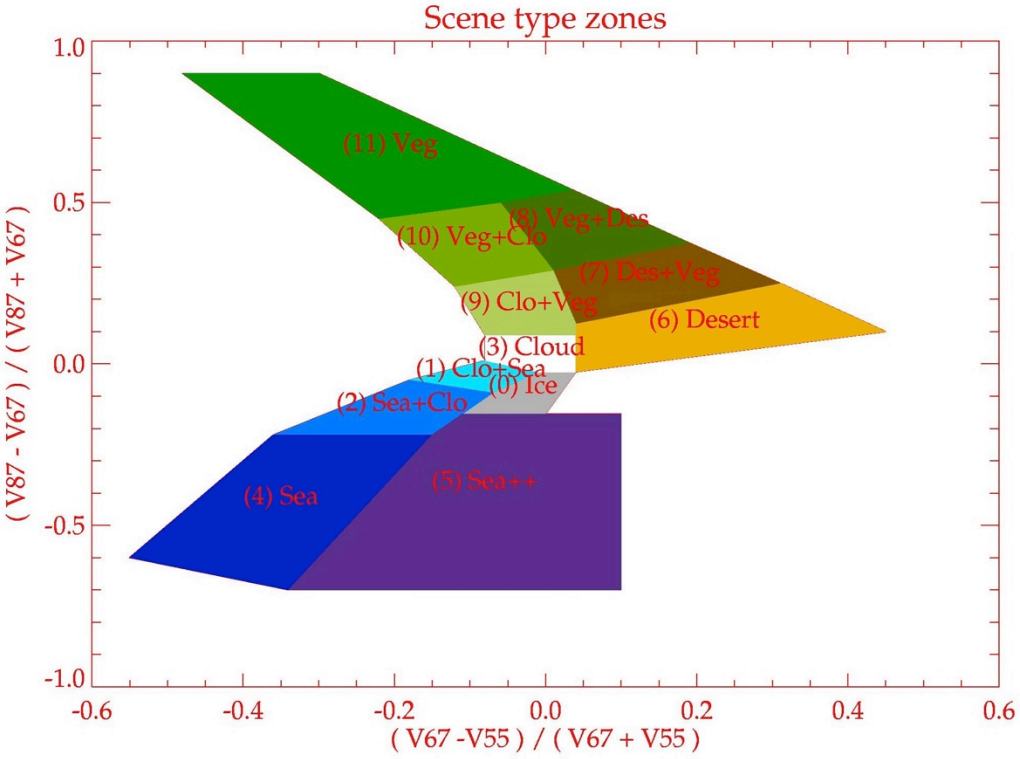

Figure 5-14 Surface type zones according to the classification discussed in the text.

Thus the test proceeds by calculating both indices for each valid pixel and determining the polygonal zone into which it falls. The cloud flag is then set if the pixel falls into one of the zones designated cloudy. The polygonal zones are defined by the co-ordinates [NDVI, NDV2] of its vertices.

Auxiliary parameters used by the visible channel cloud test are defined in the general parameters, zone vertices and zone definitions table in RD-11. These provide the information on the positions of the zones. There is provision for one set of vertices for each of 3 air mass ranges (v=na, int, ob (near-nadir, intermediate, oblique)).

N_SIDES	Number of vertices (or sides) per zone	
N_ZONES	Number of defined zones	
Vertex_index[j_ver]	Vertex index of vertex j_ver	*j_ver* = 0, …,NSIDES - 1
Zone_index[i_zone]	Zone index of zone i_zone	i_zone= 0,..*N_ZONE-1*)
Vetex_id[j_ver, i_zone]	Vertex identifier	*j_ver* = 0, …,NSIDES – 1, i_zone= 0,..*N_ZONE-1*)
X_v[j_ver, i_zone]	X co-ordinate of vertex j_ver in zone i_zone	*j_ver* = 0, …,NSIDES – 1 i_zone= 0,..*N_ZONE-1*)
Y_v[j_ver, i_zone]	Y co-ordinate of vertex j_ver in zone i_zone	*j_ver* = 0, …,NSIDES – 1 i_zone= 0,..*N_ZONE-1*)

Modifications to the AATSR test: This is a single pixel test based on a surface classification. In AATSR processing the same classification LUT is used for both oblique and nadir views, so to this extent the test can be carried over unchanged. In principle slightly different tables could be used for the nadir and inclined view, and if this idea were adopted, we might also divide the nadir swath into zones as above by across-track limits X_1, X_2 such that:

if $-X_1 < X < X_1$ the AATSR nadir view definitions are used;
if $X_1 < \text{abs}(X) < X_2$, an intermediate set of definitions are used;
of $X_2 < \text{abs}(X)$, the inclined view definitions are used.

The following steps are applied for each view ($v = n \mid f$).

For each scan *i*, retrieve the solar elevation at each end of the scan. The test is only performed if these are not less than 5°: i.e. if

<view>_ *solar_elevation*(*i,* 0) ≥ 5.0 or eq 5.5-201
<view>_ *solar_elevation*(*i,* max j) ≥ 5.0, eq 5.5-202

so excluding night-time data.

For each day-time pixel *j* identified above for which the visible channel reflectance values are valid, i.e. for which *I(ch, v; i, j)* > 0 for *ch* = *v*870, *v*670, *v*555 calculate the normalised difference indices as follows:

$$NDVI = (I(v870, v; i, j) - I(v670, v; i, j))/(I(v870, v; i, j) + I(v670, v; i, j)) \quad \text{eq 5.5-203}$$
$$NDI2 = (I(v670, v; i, j) - I(v555, v; i, j))/(I(v670, v; i, j) + I(v555, v; i, j)) \quad \text{eq 5.5-204}$$

Perform the following procedure to identify within which cluster defined by *NDVI* and *NDV2* the pixel falls.

For each zone *i_zone* = 0, *N_ZONE* – 1

Extract array of vertices:

Vertex[*j_ver*] = *vertex_id*[*j_ver*, *i_zone*], *j_ver* = 0, N_SIDES-1 eq 5.5-205

Define arrays (X_ar, Y_ar) of dimension N_SIDES + 1 and extract the vertex co-ordinates into them:

For each vertex j_ver= 0, N_SIDES – 1
X_ar[*k*] = X(*k*) eq 5.5-206
Y_ar[*k*] = Y(*k*) eq 5.5-207
End for

X_ar[*N_SIDES*] = *X*[0] eq 5.5-208
Y_ar[*N_SIDES*] = *Y*[0] eq 5.5-209

Identify whether the point *PX*, *PY* lies within this zone.

FLAG = *TRUE* eq 5.5-210
PX = *NDI*2 eq 5.5-211
PY = *NDVI* eq 5.5-212

For *k* = 0, *N_SIDES* – 1
SX = *X_ar*[j_ver+ 1] – *X*[*j_ver*] eq 5.5-213
SY = *Y_ar*[*k*j_ver+ 1] – *Y*[*j_ver*] eq 5.5-214
QX = *PX* – *X*[*j_ver*] eq 5.5-215
QY = *PY* – *Y*[*j_ver*] eq 5.5-216

Calculate the vector cross product Q × S:
ZZ = (*QX* × *SY* – *QY* × *SX*) eq 5.5-217
FLAG = *FLAG* AND (*ZZ* ≥ 0) eq 5.5-218
If *FLAG* = *FALSE* then exit loop; the point is not in this zone
End for
If *FLAG* = *TRUE*, exit loop ; we have found the zone
End for

The table of zones will only contain those regions that are associated with cloud. Thus the value of *FLAG* at this point tells whether or not the pixel is cloudy.

If *FLAG* = *TRUE* and the pixel is a land pixel for which the land flag (provided by the confidence parameter in the global flags) is set then flag the pixel as cloudy by setting the cloud flag vis_test for each view.

(Implementation note: although this algorithm in theory works over sea as well as land, use over sea is disabled for the time being. This is done in this step rather than by applying the test as a whole to land pixels only so that it can be easily enabled for sea pixels if desired at some time in the future.)

5.5.3.9.11 1.375 micron threshold test

It is proposed that a simple test based on the new 1.375 micron channel be used to detect cirrus cloud. The present test is based on a fixed reflectance threshold, similar to that defined for MODIS [RD-12.

This is a threshold test applied on a pixel by pixel basis to the 1.375 micron channel data. The physical basis of the test is that water vapour absorption in this band is very strong, so that if the atmosphere contains more than about 1 cm of total precipitable water in a column, no radiation from the surface will reach the satellite. Except in the driest regions therefore, any signal received in this channel will be the result of reflection or scattering by cloud. The basic test is then that if the observed reflectance exceeds a threshold (corrected for solar incidence angle), cloud is flagged.

The test is only applicable to daytime pixels, which for consistency with other tests are defined by a solar elevation exceeding 5 degrees, but it is valid over both land and sea. It is not applied if the surface elevation exceeds 2000 m, where precipitable water may be low, and it may be invalid in polar regions for the same reason.

The following steps are applied for each view (*v = nadir (NA)* | *oblique (OB)*).

Retrieve the threshold for the view v, R137_THRESHOLD_v from the auxiliary data file of cloud look-up table values.

For each scan *i*, retrieve the solar elevation at each end of the scan, as in Section 5.5.3.7.11 above. The test is only performed if these are not less than 5°, so excluding night-time data.

A linear interpolation may be used to determine the solar elevation at intermediate points, again as in Section 5.5.3.7.11 above. Denote this by *sol_elev*.

Extract the surface elevation. Only proceed with the test if the solar elevation exceeds 5 degrees and the elevation is less than 2000 m.

The solar zenith angle in radians is

$$z = \pi(90 - sol\_elev)/180.0. \qquad \text{eq 5.5-219}$$

The calibrated reflectance at 1.37 microns, corrected to normal solar incidence, is then

$$R137 = (I(v137, v; i, j) * sec(z) \qquad \text{eq 5.5-220}$$

If *(R137 > R137_THRESHOLD),* the pixel is considered cloudy. Flag the pixel accordingly using the thresh_test cloud word.

Note: although the test is described here with a fixed threshold, it may be necessary to provide a look-up table of threshold values as functions of solar zenith and viewing angles pending further study.

5.5.3.9.12 2.25 micron histogram test

It is proposed that a dynamic threshold test similar to the 1.6 micron test but using the 2.25 micron pixel may be defined. The test is performed as above, but substituting the calibrated reflectance in the 2.25 micron channel, along with a different dedicated look-up table of parameters.

5.5.3.9.13 Snow-covered surface test

This test operates on a pixel-by-pixel basis, and applies to daytime pixels only. It is applied to each view separately.

Modifications to the AATSR test: This test can be carried over unchanged. It is not strictly a cloud test, and the result is not masked into the overall cloud flag. Note that MODIS experience suggests that it may be unreliable at high incidence angles.

The following steps are applied for each view ($v = n \mid f$).

For each scan i, retrieve the solar elevation at each end of the scan. The test is only performed if these are not less than 5°: i.e. if

<view>_ solar_elevation(i, 0) ≥ 5.0 or eq 5.5-221

<view>_band_centre_solar_elevation(i, max j) ≥ 5.0, eq 5.5-222

so excluding night-time data.

For each day-time pixel j identified in step (5.22.3-114) above for which the 1.6, 0.87 and 0.55 micron channel reflectance values are valid, i.e. for which $I(ch, v; i, j) > 0$ for $ch = v16, v870, v555$ calculate the normalised difference snow index $NDSI$ as follows:

$$NDSI = (I(v555, v; i, j) - I(v16, v; i, j))/(I(v555, v; i, j) + I(v16, v; i, j)) \quad \text{eq 5.5-223}$$

The across-track band number for each pixel in the regridded image is given by

$$band(j) = 0 \text{ IF } j < 6 \quad \text{eq 5.5-224}$$

$$band(j) = \text{integer part of } (j - 6) / 50 \text{ IF } 6 \leq j < 506 \quad \text{eq 5.5-225}$$

$$band(j) = 9 \text{ IF } j \geq 506 \quad \text{eq 5.5-226}$$

where j is the pixel across track index.

A linear interpolation may be used to determine the solar elevation.

$$w = float(j - 6)/50.0 - band(j) \quad \text{eq 5.5-227}$$

$$sol\_elev = (1.0 - w) * nadir\_band\_edge\_solar\_elevation(i, band(j)) + w \times nadir\_band\_edge\_solar\_elevation(i, band(j) + 1) \quad \text{eq 5.5-228}$$

The solar zenith angle in radians is

$$z = \pi(90 - sol\_elev)/180.0. \quad \text{eq 5.5-229}$$

The calibrated reflectance at 0.87 microns, corrected to normal solar incidence, is then

$$R87 = (I(v870, v; i, j) * sec(z) \quad \text{eq 5.5-230}$$

Extract the 11 micron brightness temperature:

$$T11 = I(ir11, v; i, j) \quad \text{eq 5.5-231}$$

Convert the units of the NDSI threshold:

$$NDSI\_THRESH = NDSI\_THRESH / 10000. \quad \text{eq 5.5-232}$$

If *T11* < *T11_THRESH* and *(R87* > *R87_THRESH* and *NDSI* > *NDSI_THRESH),* the pixel is considered snow-covered.

5.5.3.10 Convert Solar Channel Reflectances to Radiance

So far all processing relating to the S1 to S6 channels has been carried out using calibrated reflectances. It is necessary at the output stage to convert all such reflectance values to radiance by multiplication by the appropriate scaling factors representing the solar irradiance.

Suppose the solar irradiance at wavelength λ is $E_0(\lambda)$, such that the radiant flux from the sun falling normally on an area dA in wavelength range $d\lambda$ is

$$d\phi = E_0(\lambda) dA d\lambda \qquad \text{eq 5.5-233}$$

During calibration, the scene pixels in the solar channels are in effect compared with the reflected energy from a diffuser of known reflectance R_0, normally illuminated by the sun. The energy reflected from the diffuser into solid angle $d\Omega$ is then

$$d\phi = R_0 E_0 dA d\lambda d\Omega / \pi \qquad \text{eq 5.5-234}$$

The equivalent spectral radiance L_0 is $\frac{1}{\pi} R_0 E_0(\lambda)$. Thus if a the calibrated reflectance of a pixel is R, the equivalent spectral radiance at the detector is $\frac{1}{\pi} R_{scene} E_0(\lambda)$. In practice what us measured by SLSTR is the integral of this quantity over the spectral profile of the channel $sp(\lambda)$. It follows that the calibrated quantity is the mean spectral radiance defined by

$$\frac{R_{scene}}{\pi} \int E_0(\lambda) sp(\lambda) d\lambda \Big/ \int sp(\lambda) d\lambda \qquad \text{eq 5.5-235}$$

.
We define

$$E_{0,\lambda} = \int E_0(\lambda) sp(\lambda) d\lambda \Big/ \int sp(\lambda) d\lambda \qquad \text{eq 5.5-236}$$

to be the solar irradiance weighted by the SLSTR instrument passband. It is noted that $E_{0,\lambda}$ is a function of view and detector number. Then the conversion from the 'reflectance' computed in step 5.5.3 of section 5.4.3.4 to radiance for a given pixel is simply

$$L_{scene} = R_{scene} E_{0,\lambda} / \pi \qquad \text{eq 5.5-237}$$

where R_{scene} is the calibrated reflectance of the channel. The seasonally adjusted values of $E_{0,\lambda}$ for each SLSTR channel are output from the visible calibration algorithm (section 5.4.3.4).

5.5.3.11 Meteo annotations

Models do not in general provide parameter data sets contemporary and co-located with the SLSTR samples. Then spatial interpolations are necessary. Temporal interpolation is not performed but rather the nearest available data to the acquisition time are used.

The selection of the input meteo dataset is performed as follows

1. Test of the availability of meteorological data at a time preceding and following the mid-exposure product time.
2. Evaluation of the confidence in the temporal interpolation of meteo data. For this purpose a Product Confidence Data (PCD) is set according to the length *n* of the time interval, separating the two meteo data files, relative to a reference length N_{ref} (corresponding to the usual meteo time sampling, of 6 hours). For example, the formula used to compute this PCD could be:

$$PCD_{meteo\_temporal\_interpolation} = \left[\text{int}(n) / N_{ref} \right] - 1 \qquad \text{eq 5.5-238}$$

Once the nearest ECMWF dataset has been selected, a bi-linear interpolation is applied to this grid, in order to compute meteo data on the tie points grid chosen, following these steps:

1. coordinates of the 4 environment spatial grid nodes enclosing each tie point are computed,
2. meteo parameters are extracted at these 4 grid points,
3. their values are spatially interpolated at the tie point location by a bi-linear method

Finally, re-sampled meteo data are copied in the product annotation.

If any of the required meteo fields are not present in the ECMWF time frames immediately before and after the product time, then a fill value shall be used.

5.5.3.12 Summary Quality Annotations

The quality information required for the summary quality ADS is taken from the quality structure defined in section 5.1.2.1 where it is indexed by scan count and ISP type. The quality flags must be first regridded onto the image grid so that the quality information is indexed by image row. For each of the quality indicators, the numbers of failed flags are counted over segments of 512 image rows. There will be *n_seg* summary quality flags per image. The summary quality information is found as a function of PCAT, view and scene for each ISP type by using the PCAT and target_id codes.

5.5.3.13 InfraRed Internal Stray Light Correcton

An algorithm for providing an empirical correction for internal stray light sources is provided in RD-15

APPENDIX A – BREAKPOINT TABLE

The following data shall be used as breakpoints in the testing of the Level 1b process. The final column indicates the accuracy with which the data should be verified against the output of the reference processor. Note that the Parameter Identifiers in the first column are historical, and should be updated to provide an unambiguous cross-reference to the DPM [RD-16].

Note: In the table, 'Generally exact' relates to flags or quantities of type integer, and indicates that test results should agree exactly with the reference processor in the majority of cases, but that a small number of discrepancies may acceptable owing to differences in machine precision.

Similar verification accuracies apply to the Level 1B Product Measurement Data sets. The relevant verification accuracies are:

Brightness temperature parameters	0.01 K
Visible Channel reflectances	0.01 %
Confidence and Cloud/land flags	Generally exact
GBTR ADS Quantities	As corresponding quantities in Table 3-1.

Table A-1: Breakpoints

Parameter ID	Name	Verification Accuracy
From Stages1 to 5:		
L1B-INT-003	auxilary_data_validation_result[i]	exact
L1B-INT-004	converted_auxiliary_data[i]	dependent upon datum type
L1B-INT-005	unpacked_auxiliary_data[i]	exact
From Stage 6 (Science Data Processing)		
L1B-INT-080	unpacked.pixels.nadir[MAX_NADIR_PIXELS]	exact
L1B-INT-081	unpacked.pixels.along-track[MAX_ALONG-TRACK_PIXELS]	exact
L1B-INT-082	unpacked.pixels.plus_bb[MAX_PXBB_PIXELS]	exact
L1B-INT-083	unpacked.pixels.minus_bb[MAX_MXBB_PIXELS]	exact
L1B-INT-084	unpacked.pixels.viscal[MAX_VISCAL_PIXELS]	exact
From Stage 7 (IR Channel Calibration)		
L1B-INT-006	calibration_invalid[channel]	exact
L1B-INT-010	gain[parity][channel] (channel[.] slope)	1 part in 1e6
L1B-INT-011	offset[parity][channel] (channel[.]intercept)	1 part in 1e6
From Stage 8 (Visible/SWIR Channel Calibration)		
L1B-INT-410 - 438	Visible/SWIR Calibration Product Parameters	dependent upon datum type
From Stage 9 (Satellite Time Calibration)		
L1B-INT-400	source_packet_ut_time(s)	1e-12 days (1 microsecond)
From Stages 12 (Geolocate Pixels), 14 (Interpolate Pixel Positions)		
L1B-INT-060	nadir scan pixel latitude	1 part in 1e6
L1B-INT-061	nadir scan pixel longitude	1 part in 1e6
L1B-INT-062	along-track scan pixel latitude	1 part in 1e6
L1B-INT-063	along-track scan pixel longitude	1 part in 1e6
From Stages 13 (Calculate Pixel x and y co-ordinates), 14 (Interpolate Pixel Positions)		
L1B-INT-064	nadir scan x coordinate (source packet nadir pixel x coords)	1 m
L1B-INT-065	nadir scan y coordinate (source packet nadir pixel y coords)	10 m
L1B-INT-066	along-track scan x coordinate (source packet along-track pixel x coords)	1 m
L1B-INT-067	along-track scan y coordinate (source packet along-track pixel y coords)	10 m
From Stage 18 (Signal Calibration)		

Parameter ID	Name	Verification Accuracy
L1B-INT-087	calibrated.pixels.nadir[MAX_NADIR_PIXELS], infra-red /fire channels	0.01K
L1B-INT-088	calibrated.pixels.inclined[MAX_ALONG_TRACK_PIXELS], infra-red/fire channels	0.01K
L1B-INT-089	calibrated.pixels.nadir[MAX_NADIR_PIXELS], visible/SWIR channels	0.01%
L1B-INT-090	calibrated.pixels.inclined[MAX_ ALONG_TRACK _PIXELS], visible/SWIR channels	0.01%
From Stage 15 (Solar and Viewing Angles)		
L1B-INT-120 - 127	nadir_band_edge_<solar and viewing angles>	1 part in 1e6
L1B-INT-140 - 147	along_track_band_edge_<solar and viewing angles>	1 part in 1e6
From Stage 19 (Regrid Pixels).		
L1B-INT-101	regridded nadir ir12 Brightness Temp.	0.01K
L1B-INT-102	regridded nadir ir11 Brightness Temp.	0.01K
L1B-INT-103	regridded nadir ir37 Brightness Temp.	0.01K
L1B-INT-102A	regridded nadir ir11 Fire Channel Brightness Temp.	0.01K
L1B-INT-103A	regridded nadir ir37 Fire Channel Brightness Temp.	0.01K
L1B-INT-104	regridded nadir v2.25 Reflectance	0.01%
L1B-INT-104A	regridded nadir v1.6 Reflectance	0.01%
L1B-INT-104B	regridded nadir v1.375 Reflectance	0.01%
L1B-INT-105	regridded nadir v870 Reflectance	0.01%
L1B-INT-106	regridded nadir v670 Reflectance	0.01%
L1B-INT-107	regridded nadir v555 Reflectance	0.01%
L1B-INT-108	nadir x offset(i, j)	5 m
L1B-INT-109	nadir y offset(i, j)	5 m
L1B-INT-111	regridded along-track ir12 Brightness Temp.	0.01K
L1B-INT-112	regridded along-track ir11 Brightness Temp.	0.01K
L1B-INT-113	regridded along-track ir37 Brightness Temp.	0.01K
L1B-INT-112A	regridded along-track ir11 Fire Channel Brightness Temp.	0.01K
L1B-INT-113A	regridded along-track ir37 Fire Channel Brightness Temp.	0.01K
L1B-INT-114	regridded along-track v2.25 Reflectance	0.01%
L1B-INT-114A	regridded along-track v1.6 Reflectance	0.01%
L1B-INT-114B	regridded along-track v1.375 Reflectance	0.01%
L1B-INT-115	regridded along-track v870 Reflectance	0.01%
L1B-INT-116	regridded along-track v670 Reflectance	0.01%
L1B-INT-117	regridded along-track v555 Reflectance	0.01%
L1B-INT-118	along-track x offset(i, j)	5 m
L1B-INT-119	along-track y offset(i, j)	5 m
L1B-INT-134	nadir view instrument scan number	Generally exact (See note)
L1B-INT-135	nadir view instrument pixel number	Generally exact (See note)
L1B-INT-154	along-track view instrument scan number	Generally exact (See note)
L1B-INT-155	along-track view instrument pixel number	Generally exact (See note)
From Stage 20 (Cosmetic Fill)		
L1B-INT-100	nadir fill state(i, j)	Generally exact (See note)
L1B-INT-110	along-track fill state(i, j)	Generally exact (See note)
From Stage 21 (Determine Image Pixel Positions)		
L1B-INT-160	image_latitude(i, j)	1 part in 1e6
L1B-INT-161	image_longitude(i, j)	1 part in 1e6
From Stage 22 (Determine Land/Sea Flag)		
L1B-INT-232	nadir land flag	Generally exact (See note)
L1B-INT-248	along-track land flag	Generally exact (See note)
From Stage 23 (Cloud Clearing)		
L1B-INT-233 - 244	nadir cloud flags	Generally exact (See note)
L1B-INT-249 - 260	along-track cloud flags	Generally exact (See note)

End of Document